



THE UNIVERSITY *of* EDINBURGH

This thesis has been submitted in fulfilment of the requirements for a postgraduate degree (e.g. PhD, MPhil, DClinPsychol) at the University of Edinburgh. Please note the following terms and conditions of use:

This work is protected by copyright and other intellectual property rights, which are retained by the thesis author, unless otherwise stated.

A copy can be downloaded for personal non-commercial research or study, without prior permission or charge.

This thesis cannot be reproduced or quoted extensively from without first obtaining permission in writing from the author.

The content must not be changed in any way or sold commercially in any format or medium without the formal permission of the author.

When referring to this work, full bibliographic details including the author, title, awarding institution and date of the thesis must be given.



Exploration of the Catalytic Use of Alkali Metal Bases

Thesis Submitted in Accordance with the Requirement of The University of
Edinburgh for the Degree of Doctor of Philosophy

By

Wei Bao

Supervisor: Dr. Uwe Schneider

EaSTCHEM, School of Chemistry

College of Science and Engineering

The University of Edinburgh

Aug 2017

DECLARATION

I, Wei Bao, hereby declare that, except where specific reference is made to other resources, the work presented in this thesis is the original work of my own research since the start of my PhD degree in October 2012. This thesis has been composed by myself and has not been submitted, in whole or part, for any other degree, diploma or other qualification.

ACKNOWLEDGEMENTS

First, I would like to thank my parents for all the support.

I would also like to thank my supervisor, Dr Uwe Schneider, for giving me the opportunity to work in the Schneider group, which allows me to develop my skills and knowledge for science in the pursuit of my Ph.D. degree.

I would also like to thank my funding sponsor – Eli Lilly – for the supporting of my tuition fees and living cost in my four-year's Ph.D. study.

Thank you to all of the students in the Schneider group for a great scientific research environment and learning experience in my Ph.D. study. Bo, Xun, Hanno, Jonathan, Alex, and Peter, it has been great knowing all of you.

Thank you also to the analytical department in School of Chemistry, University of Edinburgh for providing a smooth and high quality services to our researchers. These include, Lorna and Juraj from NMR service, and Alan Taylor from Mass Spectrometry.

Table of Contents

DECLARATION	2
ACKNOWLEDGEMENTS	3
Table of Contents	4
Abbreviations	7
Abstract	9
General Introduction.....	10
Introduction	12
<i>Electrophilic Allylation via C–H Bond Activation</i>	<i>12</i>
C–H Bond Activation Catalysed by Palladium(II)	12
C–H Bond Activation Catalysed by Copper	15
C–H Bond Activation Catalysed by Iron	16
<i>Nucleophilic Allylation via C–X Bond Activation</i>	<i>16</i>
Reductive Umpolung of Electrophilic Allyl–Pd Species: C–O Bond Activation	17
Use of σ -Donor Ligands: C–Sn Bond Activation.....	17
Use of σ -Donor Ligands: C–Si Bond Activation.....	18
Use of σ -Donor Ligands or Low-Valent Metal Species: C–B Bond Activation.....	18
<i>Nucleophilic Allylation via C–H Bond Activation</i>	<i>20</i>
<i>Imine Allylation</i>	<i>21</i>
Grignard-Type and Barbier-Type Allylations.....	21
Asymmetric Imino-ene Reactions.....	23
Use of Allyl Silicon and Allyl Tin Reagents	23
Use of Allyl Boron Reagents.....	24
Umpolung-Type Imine Allylation	25
<i>Catalytic Use of Alkali Metal Amides in Organic Synthesis.....</i>	<i>27</i>
Hydroamination.....	27
Brønsted Base Catalysis.....	27
Redox Chemistry	31
Lewis Base Catalysis.....	32
Aims	33
1 Allylic C(sp³)–H Bond Activation of Alkenes Triggered by a Sodium Amide.....	34

1.1	<i>Allylic C(sp³)-H Bond Activation of Fluorinated Pro-Nucleophiles</i>	34
1.1.1	<i>Attempted Syntheses of Fluorinated Pro-Nucleophiles</i>	34
1.1.2	<i>Preliminary Catalysis Results Using Allyl Perfluorobenzene</i>	36
1.2	<i>Alkali Metal Amide-Catalysed Allylic C(sp³)-H Bond Activation</i>	41
1.2.1	<i>Influence of the N-Protecting Group</i>	42
1.2.2	<i>Solvent Screening</i>	42
1.2.3	<i>Screening of Metal-Brønsted Bases</i>	43
1.2.4	<i>Screening of Metal-Free Organic Brønsted Bases</i>	47
1.2.5	<i>Substrate Scope for Imines</i>	48
1.2.6	<i>Other Aromatic Allyl Pro-Nucleophiles</i>	50
1.2.7	<i>Use of a Skipped Diene as Pro-Nucleophile</i>	52
1.2.8	<i>Unsuccessful Pro-Nucleophiles</i>	54
1.2.9	<i>Investigations into the Reaction Mechanism</i>	56
1.2.10	<i>Preliminary Kinetic Study</i>	59
1.2.11	<i>Toward an Asymmetric C-C Bond Formation</i>	61
1.2.12	<i>'Functionalised' C-C Bond Formation</i>	73
	Use of Allyl Silicon Reagents	73
	Use of an Allyl Boron Reagent	74
	Use of an Allyl Tin Reagent	77
	Use of Allyl Sulfur Reagents	77
1.2.13	<i>Attempted Brønsted Base Activation of PhCF₂H</i>	80
Conclusion		84
2	Catalytic Use of an Alkali Metal-Lewis Base in Catalytic Difluoromethylation	85
2.1	<i>Introduction</i>	85
	Nucleophilic Difluoromethylation	85
	Electrophilic Difluoromethylation	88
2.2	<i>Alkali Metal-Base-Catalysed C^F-Si Bond Activation</i>	89
	Brønsted Base (BB) or Lewis Base (LB) Activation?	89
	Optimisation of Reaction Conditions for the Use of DMF as Electrophile	92
	Optimisation of Reaction Conditions for the Use of NMP as Electrophile	93
	Hypervalent Silicon Species and their Application in Organofluorine Chemistry	94

α,β -Unsaturated Amides as Potential Electrophiles	96
Substrate Scope	98
Conclusion	101
Future Work	102
3 Experimental.....	104
3.1 General Experimental	104
3.2 General Procedures.....	106
GP-I: Preparation of Aldimines	106
GP-II: Preparation of Ketimines	106
GP-III: Sodium Amide-Catalysed Imine Allylation	106
GP-IV: Imine Allylation – Portionwise Addition	106
GP-V: Preparation of 10a	107
GP-VI: Preparation of 10b	107
GP-VII: Preparation of 10c and Imine Allylation Catalysed by 10c	107
GP-VIII: Preliminary Kinetic Study	108
GP-IX: Imine Allylation Using Functionalised Allyl Reagents.....	108
GP-X: Isomerisation of Functionalised Allyl Reagents.....	108
GP-XI: Catalytic Asymmetric Imine Allylation	109
GP-XII: Catalytic Difluoromethylation of Amides and Lactams	109
GP-XIII: One-Pot Sequence Difluoromethylation/Allylation	109
3.3 NMR Data of Prepared Compounds.....	111
Preparation of an Alkene	111
Preparation of Aldimines	111
Preparation of Ketimines	120
Preparation of Homoallylic Amines	123
Preparation of Dehydroaminated Products	152
Preparation of Functionalised Internal Alkenes	153
Detection of Reaction Intermediates	155
Attempted Asymmetric Catalysis	156
Catalytic Difluoromethylation of Amides and Lactams	157
References	163

Abbreviations

AAA	asymmetric allylic alkylation	<i>ee</i>	enantiomeric excess
Å	angstrom	EI	electron ionisation
Ac	acetyl	EPSP	excitatory postsynaptic potential
acac	acetylacetonate	ESI	electron spray ionisation
Ar	aryl	equiv	equivalent
aq	aqueous	Et	ethyl
BA	Brønsted acid	EWG	electron withdrawing group
BB	Brønsted base	Flu	fluorene
Bn	benzyl	h	hour
Boc	<i>tert</i> -butoxycarbonyl	het	hetro
BOX	bisoxazoline	HPLC	high-performance chromatography liquid
BQ	benzoquinone	HQ	hydroquinone
^t Bu	<i>tert</i> -butyl	HRMS	high resolution mass spectrometry
br	broad	Hz	hertz
BTF	trifluorotoluene	ⁱ Pr	<i>iso</i> -propyl
cat	catalyst	IR	infra red
χ	electronegativity	κ	denticity
conc	concentration	L	ligand
conv	conversion	LA	Lewis acid
COD	cyclooctadiene	LB	Lewis base
°C	degrees celsius	Mes	mesityl
d	doublet <i>or</i> day	μ L	microliter
DBU	1,8-diazabicyclo[5.4.0]undec-7-ene	m	mol per liter [molarity]
DCM	dichloromethane	m	multiplet
DCE	dichloroethane	Me	methyl
DDQ	2,3-dichloro-5,6-dicyano- <i>p</i> -benzoquinone	mg	milligram
DFT	density functional theory	μ L	microliter
DIBALH	diisobutylaluminium hydride	min	minute
DIPEA	<i>N,N</i> -diisopropylethylamine [= Hünig's base]	MO	molecule orbital
dipp	diisopropylphenyl	mp	melting point
DMAc	dimethylacetamide	Ms	mesyl
DMBQ	2,6-dimethylbenzoquinone	MS	mass spectrometry <i>or</i> molecule sieve
DME	dimethoxyethane	<i>m/z</i>	mass to charge ratio
DMF	dimethylformamide	ND	not determined
DMSO	dimethylsulfoxide	nm	nanometer
<i>dr</i>	diastereometric ratio	NHC	<i>N</i> -heterocyclic carbene
DMPU	<i>N,N</i> '-dimethylpropylene urea	NMP	<i>N</i> -methyl-2-pyrrolidone
ϵ	dielectric constant	NR	no reaction
<i>E</i>	electrophile	Ns	nitrobenzenesulfonyl [nosyl]
EDG	electron donating group	OA	oxidative addition

OTf	trifluoromethanesulfonate
pent	pentyl
PE	petroleum ether
PG	protecting group
ph	phenyl
pK _a	logarithmic acid dissociation constant
py	pyridyl
pin	pinacol
PMTDA	<i>N,N,N',N'',N'''</i> -pentamethyldiethylenetriamine
py	pyridyl
PMP	<i>p</i> -methoxy-phenyl
ppm	parts per million
PTLC	preparative thin layer chromatography
q	quartet
RE	reductive elimination
rt	room temperature
s	singlet
t	time <i>or</i> triplet
T	temperature
t _R	retention time
TASF	tris(dimethylamino)sulfonium difluorotrimethylsilicate
TBAF	tetra- <i>n</i> -butylammonium fluoride
TBME	methyl <i>tert</i> -butyl ether
TBS	<i>tert</i> -butyldimethylsilyl
THF	tetrahydrofuran
TIPS	triisopropylsilyl
TMEDA	<i>N,N,N',N'</i> -tetramethylethylenediamine
TMP	tetramethylpiperidide
TMS	trimethylsilyl <i>or</i> tetramethyl silane
<i>tol</i> -BINAP	2,2'-bis(di- <i>p</i> -tolylphosphino)-1,1'-binaphthyl
TRIP	3,3'-bis(2,4,6-tri- <i>iso</i> -propylphenyl)-2,2'-binaphtholate
Ts	<i>para</i> -toluenesulfonyl [tosyl]
TS	transition state
TON	turn over number
Xantphos	4,5-bis(diphenylphosphino)-9,9-dimethylxanthene
v/v	volume/volume
UV	ultraviolet
ν	wave number
η	hapticity
[18]c-6	18-crown-6 [1,4,7,10,13,16-hexaoxacyclooctadecane]

Abstract

This PhD thesis project was concerned with the use of alkali metal amide Brønsted bases and alkali metal alkoxide Lewis bases in (asymmetric) catalysis. The first chapter deals with formal allylic C(sp³)-H bond activation of aromatic and functionalized alkenes for subsequent C-C and C-H bond formations. The second chapter is focused on C(sp³)-Si bond activation of fluorinated pro-nucleophiles in view of C-C bond formations. In the first chapter, a screening of various metal amides, hydrides, and alkyl reagents resulted in the observation that alkali metal amides were effective Brønsted bases to trigger allylic C(sp³)-H bond activation of aromatic alkenes at room temperature. Sodium hexamethyldisilazide was found to be most efficient compared with other s-, p-, d-, and f-block metal amides. This unique transition metal-free methodology was exploited to activate a variety of alkene pro-nucleophiles, which were shown to undergo γ -selective C-C bond formation with various aromatic aldimines as well as one aliphatic substrate. The corresponding homoallylic amine derivatives were obtained in high yields with excellent *E:Z* ratios. The reaction mechanism was investigated and attempts to detect and/or isolate key intermediates were undertaken. Importantly, it was shown that metal-free superbases of the Schwesinger or Verkade type were not apt to catalyse this challenging C-C bond formation. The asymmetric version of this rare sodium amide catalysis has been achieved by using a commercially available enantiopure bisoxazoline ligand (46% *ee*). Subsequently, the catalytic use of sodium and potassium amides was applied to the isomerization of terminal aromatic alkenes to generate the thermodynamically more stable internal olefins in excellent yields with high *E:Z* ratios. Furthermore, functionalized metalloid (B, Si) and metal-free alkenes were found to undergo alkali metal amide-triggered (chemoselective) allylic C(sp³)-H bond activation in view of isomerization and/or C-C bond formation with aldimines. In the second chapter, the catalytic C-Si bond activation of an important difluoromethylation reagent, HCF₂SiMe₃, was investigated. Here, alkali metal alkoxides were shown to be more effective Lewis base triggers than other metal alkoxides or metal-free superbases. This novel method was successfully used to transfer the nucleophilic difluoromethyl fragment to electrophiles such as a variety of amides and lactams, whereas unsaturated amides failed to undergo the intended conjugate C-C bond formation. In this context, it is noted that the α -hydrogen of certain amides was tolerated. This unprecedented catalytic difluoromethylation of unactivated carbonyl electrophiles was achieved using potassium *tert*-butoxide at room temperature, and the corresponding fluorinated 'hemiaminal' products were obtained in high yields.

General Introduction

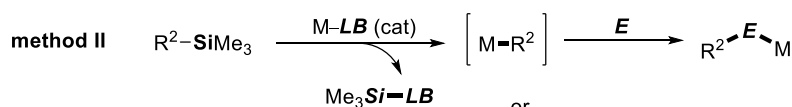
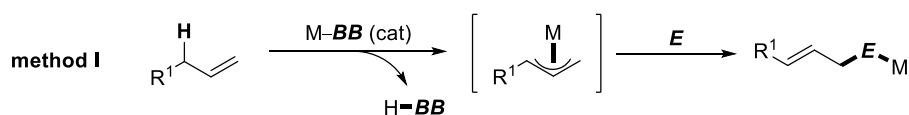
A typical definition of a catalyst and/or catalysis may be as follows: “A catalyst is a substance that increases the rate of a reaction without modifying the overall change of the reaction’s standard Gibbs energy; such process is termed catalysis”.^[1] The catalyst is not consumed in a reaction. Presently, many industrial chemical processes are based on catalytic reactions.^[2, 3] The efficient replacement of classical stoichiometric methodologies by cleaner catalytic alternatives is also promoted by a growing awareness of “green chemistry”.^[4]

The formation of carbon–carbon single bonds is of fundamental importance in organic synthesis.^[5] As a result, there is an increasing number of methods available for various types of C–C bond formation. Among the most useful reagents in this context are organometallic compounds, molecules that contain metal–carbon bonds e.g. metal enolates.^[6, 7] The catalytic formation and use of these reagents may be realised through metal catalysis. Asymmetric C–C bond formation can also be achieved by using this category of reagents to yield single enantiomers in the presence of an enantiopure ligand or anion.^[8, 9] Whereas the organometallic chemistry of transition metals has been well-established in the context of organic synthesis and catalysis, the use of main group metals, especially alkali metals, in catalysis has been lagging far behind.^[10-12]

The electronegativity of C(sp³) is 2.55 (Pauling), whereas the electronegativity of metals is between 0.7 (Cs) and 2.5 (Au).^[13] Consequently, carbon–metal bonds are polarised accordingly: C(δ^-)–M(δ^+). For late d-block metals (groups 8 to 12), the polarity is rather low. This lower polarity of C–M bonds may enable the switch of reactivity of the organometallic compounds; e. g. allyl–palladium complexes may be either electrophilic or nucleophilic by tuning the ligands that coordinate to the Pd centre.^[14] However, it is notable that for s-, p-, and early d-block metals (groups 3 to 7), the ionic character of the C–M bond increases with its polarity.

Our research focused on alkali metals; organic alkali metal compounds can be considered as essentially ionic, and *only* nucleophilic. However, the exact bonding mode may also depend on the ligands and the hybridisation of the carbon atom bonded to the metal. Indeed, the electronegativity of C(sp²) and C(sp) was calculated to be 2.88 and 3.37, respectively.^[15] The high reactivity of the alkali metal–C(sp³) complex contributes directly to its extreme sensitivity to air, water, and a variety of reagents. Thus, it is difficult to study alkali metal–C(sp³) species involved in catalysis. However, the key to make these reagents more controllable would be to stabilise the sp³-hybridised carbanion so that the catalytic formation and regeneration of alkali metal–C(sp³) species would be feasible.

This thesis has introduced two distinct novel catalyses. The first method detailed the use of an alkali metal–Brønsted base (M–BB) catalyst for the generation of an allylic C(sp³)–M species, which was stabilised through conjugation with an (hetero)aromatic moiety (method I; Scheme 1). The second method has dealt with the use of an alkali metal–Lewis base (M–LB) catalyst that was exploited for the activation of the C(sp³)–Si bond of HF₂C–SiMe₃. The formed nucleophilic intermediate was *potentially* stabilised by the –I effect of fluorine, or a hypervalent silicon species (*not detected*; method II; Scheme 1). Moreover, the regeneration of the described species may (partially) rely on autocatalysis, where an intermediate or one of the products are catalytically active.



M = alkali metal

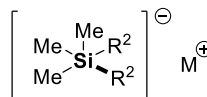
BB = Brønsted base

LB = Lewis base

R¹ = aryl, alkene

R² = fluorinated alkane

E = π-electrophile



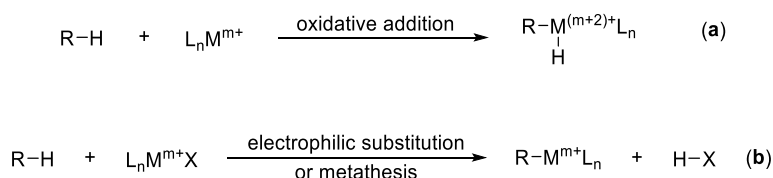
Scheme 1: The two methods developed in this thesis.

It is notable that C–C bond formation can also be achieved by metal-free organocatalysis, which includes Brønsted acid, Brønsted base, Lewis acid, Lewis base, and acid–base dual catalysis.^[16] Enantioselective organocatalysis is also a powerful approach to realise asymmetric C–C bond formation that is complimentary to metal-catalysed reactions.^[17] However, organocatalysis was not discussed intensively in this thesis.

Introduction

Electrophilic Allylation *via* C–H Bond Activation

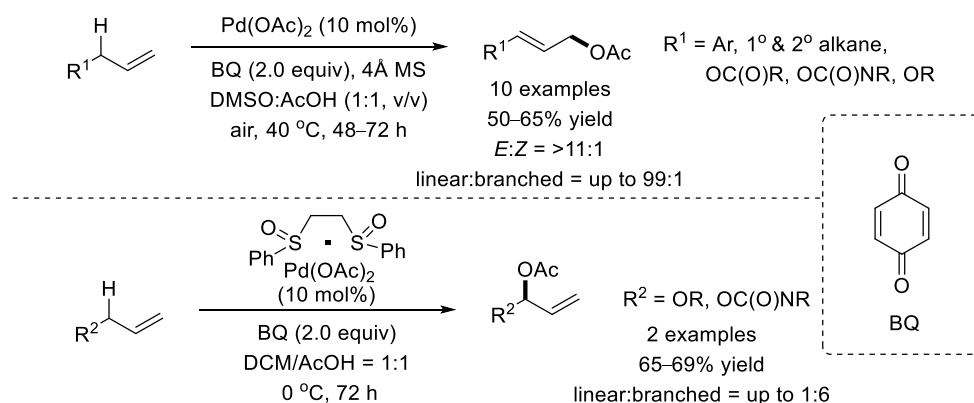
Carbon–hydrogen bond activation followed by further functionalisation could lead to atom and step economy in chemical synthesis. In 1997, a review by Shul'pin and Shilov concluded that a C–H bond splitting promoted by metal complexes could be recognised as a “true” C–H bond activation when a C–M σ -bond was formed.^[18] The cleavage of the C–H bond could be promoted by oxidative addition of a transition metal at its low oxidation state (Equation **a**, Scheme 1). Alternatively, this cleavage can go through electrophilic substitution of a metal complex or metathesis pathway when a metal is not oxidised (Equation **b**, Scheme 1). Pathway **a** turned the hydrogen to a hydride species, while pathway **b** generated a proton which was readily captured by an anionic species X^- . In order to distinguish C–H bond activation *via* pathway **b** from a traditional acid–base reaction, the C–H bond activation relies on a metal complex while an acid–base reaction relies on a sufficient gap of the pK_a values between the conjugate acid of the base and the substrate (acid). Other types of C–H bond activation have been included in the review as well.^[18]



Scheme 1: Mechanisms of a “True” C–H Bond Activation.

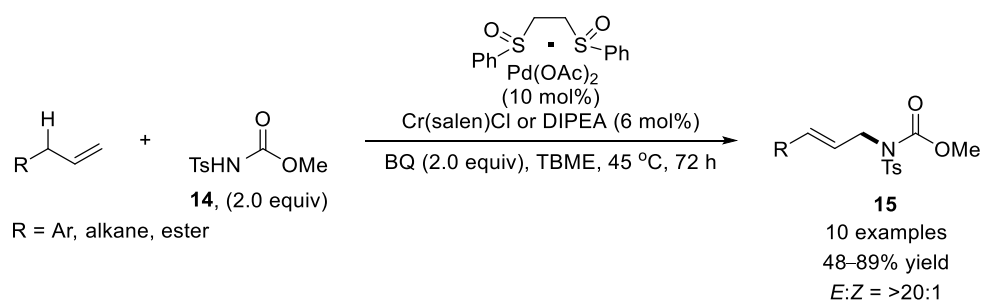
C–H Bond Activation Catalysed by Palladium(II)

Transition metal catalysts have been used to activate both $\text{C}(\text{sp}^2)\text{--H}$ and $\text{C}(\text{sp}^3)\text{--H}$ bonds.^[19, 20] In the context of allylic $\text{C}(\text{sp}^3)\text{--H}$ bond activation of alkenes, White and co-workers reported in 2004 a ligated palladium(II) acetate catalyst to generate an *electrophilic* allyl–palladium intermediate, which underwent C–O bond formation to generate allylic acetates (Scheme 2).^[21] This catalytic system has the interesting feature of delivering either predominantly linear *or* branched products depending on whether DMSO or bis(sulfoxide) ligands are used; a stoichiometric amount of benzoquinone (BQ) was used as an oxidant that functions as well as a π -acceptor ligand. It is noted that the same reaction system predominantly underwent a Wacker oxidation process (Markovnikov oxypalladation/ β -hydride elimination) in the absence of the sulfoxide ligand, thus generating a vinyl acetate.



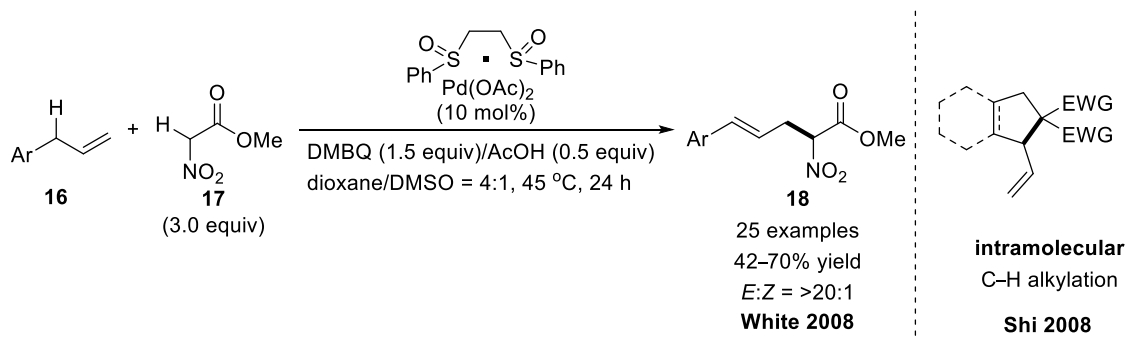
Scheme 2: Regioswitchable C–H Bond Oxidation.

The oxidative C–H bond activation has also been exploited for C–N bond formation (Scheme 3). In 2008 and 2009, two strategies for allylic C–H bond amination were reported by White's group. The first strategy required the use of a Lewis acid co-catalyst [Cr(III)(salen)Cl] to promote the amination, possibly by activating the electrophilic π -allyl–palladium intermediate for the addition of a nucleophile.^[22] The second strategy relied on the use of a Brønsted base to deprotonate and thus activate a tethered pro-nucleophile;^[23] here, while the use of an *endogenous* base [acetate anion of the Pd(II) source] did not work effectively, the addition of an *exogenous* base [external acetate source or *N,N*-diisopropylethylamine (DIPEA)] generated predominantly the corresponding linear products in 48–98% yields with excellent geometric selectivity. Both strategies proceeded through an electrophilic π -allyl–palladium intermediate and required the use of a stoichiometric amount of BQ.



Scheme 3: Lewis Acid- or Brønsted Base-Assisted C–H Amination.

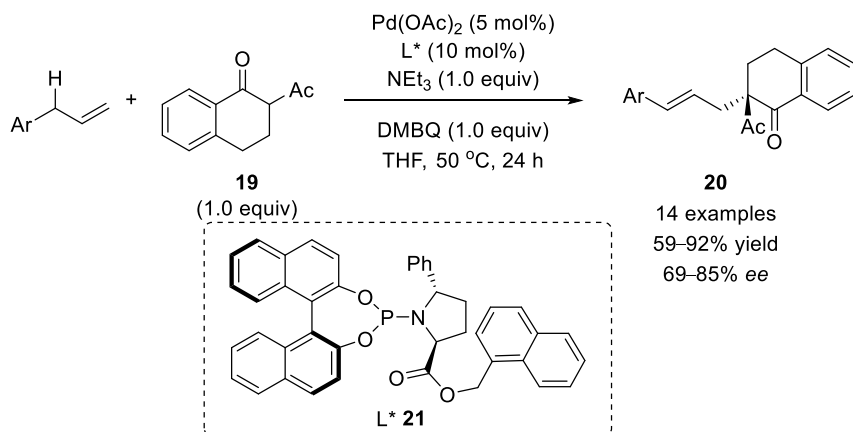
In 2008, the first electrophilic palladium(II)-catalysed allylic C–H bond alkylation was reported independently by Shi (intra/intermolecular) and White (intermolecular), respectively (Scheme 4).^[24, 25] While the intramolecular allylic C–H bond activation proceeded with aliphatic alkenes, the intermolecular version was limited to aromatic olefins **16**. Bis(sulfoxide)/Pd(OAc)₂ was used as the catalyst system; here, a more sterically hindered 2,6-dimethylbenzoquinone (DMBQ) was required as an oxidant. Indeed, it was shown that BQ would undergo conjugate addition with a soft carbon nucleophile, thus preventing the intended allylic C–H bond alkylation. DMSO acted as both a solvent and a ligand to activate the allyl–palladium intermediate, which potentially facilitated the liberation of the acetate anion to deprotonate pro-nucleophile **17**. This combined catalytic system allowed the formation of linear products **18** in 42–70% yields, alongside with excellent geometric selectivity. These direct allylic C–H alkylations omitted the pre-functionalisation step in the traditional Tsuji–Trost reaction, thus allowing the C–C bond formation in an atom-economic fashion.



Scheme 4: Palladium(II)-Catalysed C–H Bond Alkylation.

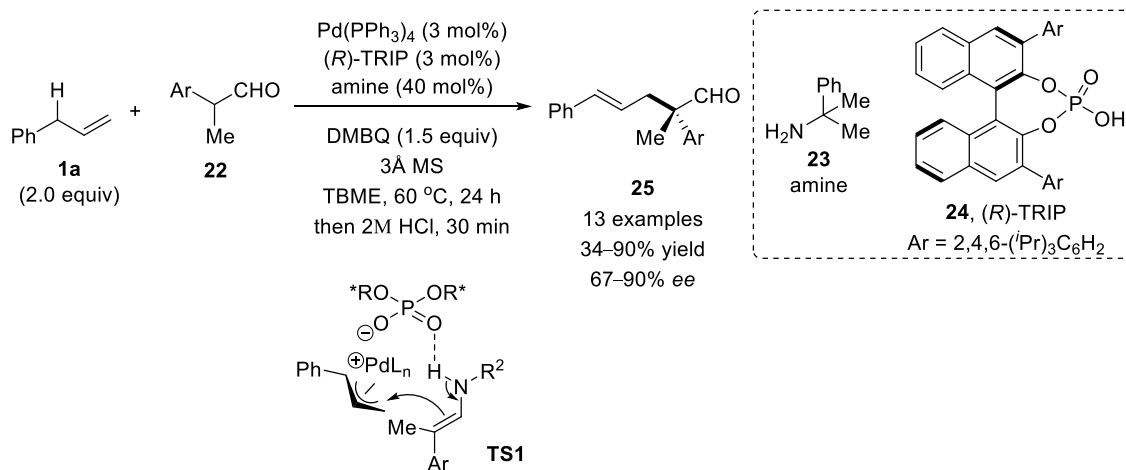
In 2013, *asymmetric* allylic alkylation (AAA) *via* C–H bond activation was developed by Trost *et al.* (Scheme 5).^[26] α -Methyl ketone **19**, bearing a relatively higher pK_a value, was chosen as the pro-nucleophile. In turn, a

stronger base, NEt_3 , was required to generate the nucleophile. Asymmetry was induced using a catalytic amount of enantiopure ligand **L*21**. Here again, DMBQ was used as an oxidant for the catalyst regeneration. Under these conditions, the aromatic allyl functionality was successfully transferred to the final products **20** in 59–92% yields with up to 85% *ee*.



Scheme 5: Palladium(II)-Catalysed Asymmetric C–H Alkylation.

In 2014, another strategy to conduct the AAA reaction through oxidative C–H bond activation was reported by Gong and co-workers using chiral anion **24** (Scheme 6).^[9] An electrophilic π -allyl–palladium phosphate complex was generated *via* oxidative C–H bond activation of allyl benzene (**1a**). In parallel, primary amine **23** reacted with aldehydes **22** to form an imine that tautomerized to the enamine form through the assistance of hydrogen bonding. The allyl–palladium phosphate complex (electrophile) then underwent C–C bond formation with the enamine (nucleophile) through **TS1** to generate optically active imines, which were hydrolyzed to the final aldehyde products **25** in up to 90% yield with up to 90% *ee*.

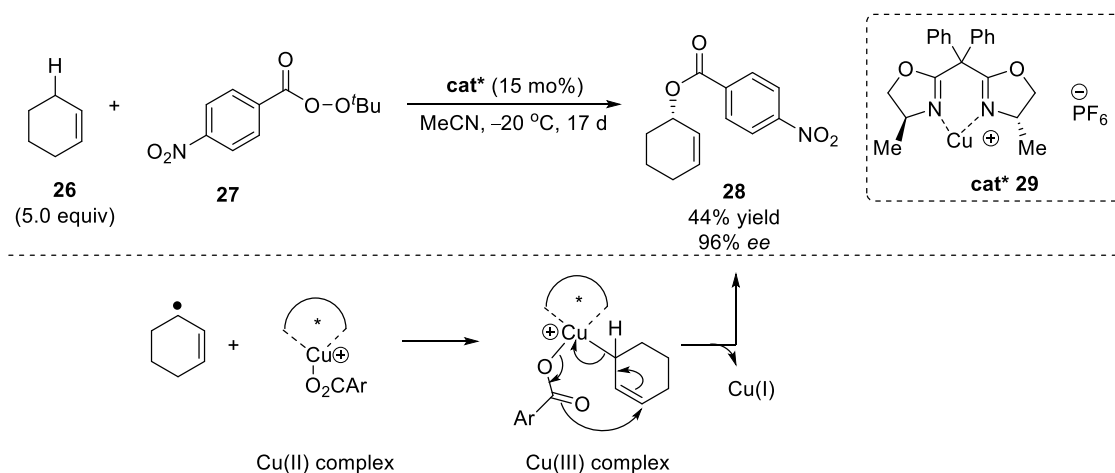


Scheme 6: Palladium-Catalysed Asymmetric C–H Alkylation.

However, it is noted that, apart from electrophilic allylation, a substituted π -allyl–palladium complex can also undergo β -hydride elimination; such process can be used to generate butadienes that can be further reacted in Diels–Alder reactions.^[27]

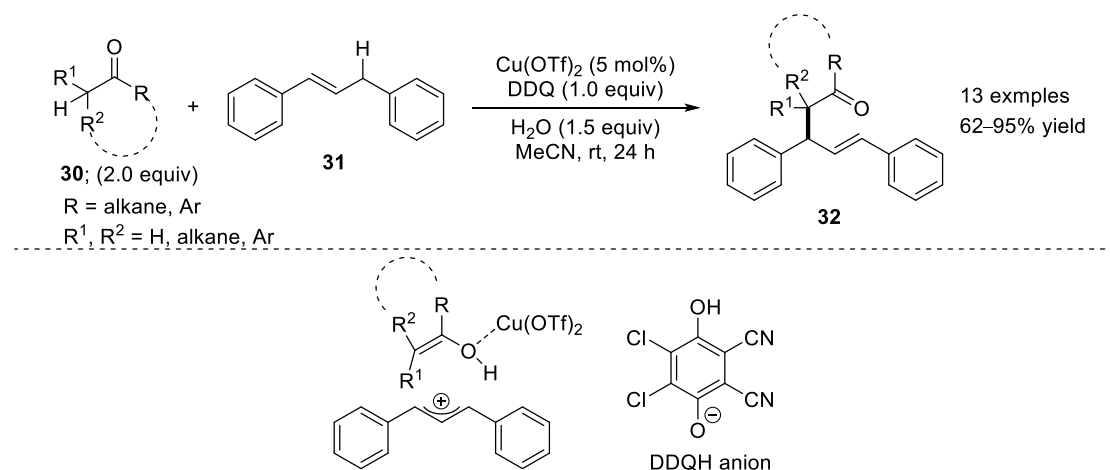
C–H Bond Activation Catalysed by Copper

In addition to palladium, other transition metals have also been used in allylic C(sp³)–H bond activation. Andrus and co-workers reported a C–H bond oxidation between cyclohexene (**26**) and perester **27** catalyzed by enantiopure copper(I)–bisoxazoline complex **cat*** **29** (Scheme 7);^[28] allylic ester **28** was formed with 96% *ee*. The copper catalyst system worked differently compared to palladium catalysts. Instead of forming η^2 - or η^3 -metal complexes with olefins, the complex **29** reacted with perester **27** to form ^tBuOH and a copper(II) acetate complex. Mechanistic studies also revealed that **26** reacted through an allylic radical intermediate by hydrogen atom abstraction (homolysis); the allylic radical reacted then with the less hindered quadrant of the C₂-symmetric copper(II) complex. The generated copper(III) intermediate rearranged to give enantioenriched product **28** with concomitant regeneration of copper(I) complex **29**. Here, perester **27** served as a reactant and an oxidant. The above activation mode falls into “the third type of C–H bond activation” introduced by Shul’pin and Shilov.^[18] Instead of reacting with the olefin, the metal complex reacted with other reagents first (perester) to generate a more reactive species (alkoxide radical). This more reactive species then adds to the olefin independently without the assistance of the metal complex.



Scheme 7: Copper(I)-Catalysed Asymmetric C–H Bond Oxidation.

In 2014, Huang and co-workers reported a copper(II)-catalysed dehydrogenative cross-coupling between the α -C–H bond of ketones and allylic C–H bonds (Scheme 8).^[29]

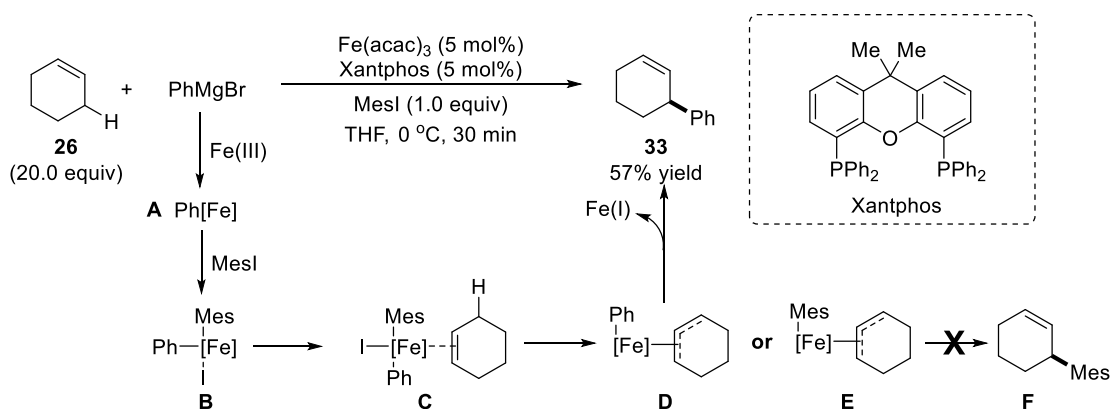


Scheme 8: Copper(II)-Catalysed C–H Bond Alkylation.

A radical-promoted mechanism was involved in the initial stage when alkene **31** reacted with DDQ to form a carbocation and a DDQH anion. Cu(OTf)₂ reacted as a Lewis acid with ketone **30** to form an enol that added to the carbocation, thus generating the intended product **32** in 62–95% yields. The DDQH anion would then obtain the hydrogen from the enol to form DDQH₂. Thus, a stoichiometric amount of DDQ as an oxidant was required for this transformation.

C–H Bond Activation Catalysed by Iron

In 2013, Nakamura *et al.* reported an iron-catalysed arylation of the allylic C(sp³)–H bond of alkenes of type **26** and unactivated alkanes (Scheme 9).^[30] A catalytic amount of Fe(acac)₃ and Xantphos was used as the catalyst system.



Scheme 9: C–H Bond Arylation Catalysed by Iron Species.

The aryl Grignard reagent first reacted with an iron(III) species to generate phenyl–iron intermediate **A**, which was converted to coordinatively unsaturated iron complex **B** via oxidative addition to mesityl iodide. Species **B** coordinated to olefin **26** to generate intermediate **C**, where the aryl groups abstracted the allylic hydrogen to generate allyl–iron species **D** or **E**. Reductive elimination took place selectively from intermediate **D** to form an iron(I) complex and the intended arylation product **33**. Potential by-product **F** derived from allyl–iron intermediate **E** was not observed. The unreactive intermediate **E** was ascribed to the sterically demanding Mes moiety of the oxidant mesityl iodide.

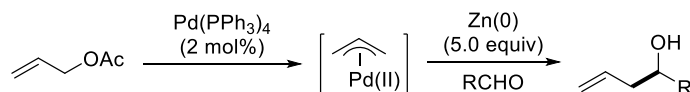
According to all the examples introduced above, a stoichiometric amount of an oxidant was always required in these allylic C(sp³)–H bond activations; an electrophilic allyl–M intermediate was typically involved.

Nucleophilic Allylation via C–X Bond Activation

Electrophilic allyl–palladium species can undergo stoichiometric reductive *umpolung* to generate a nucleophilic allyl–M intermediate.^[14, 31] This reversal of reactivity proceeds via reduction by: using metal(0) or low-valent metal species; transmetalation of the allyl functionality to metals or metalloids with lower electronegativity; a structure change from a π -allyl–palladium to a σ -allyl–palladium complex. However, this strategy *cannot* be achieved by a catalytic *oxidative* C–H bond activation because it precludes a stoichiometric *reductive* *umpolung*.

Reductive Umpolung of Electrophilic Allyl-Pd Species: C–O Bond Activation

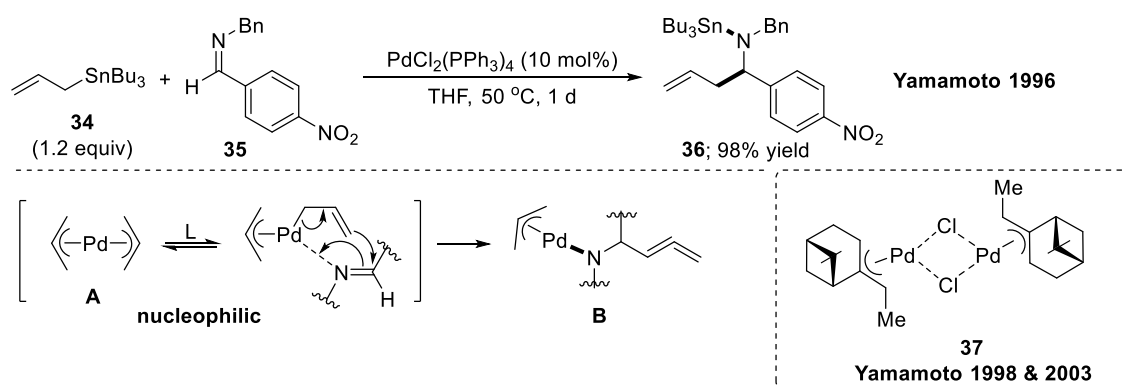
In 1987, Masuyama and co-workers used a stoichiometric amount of Zn(0) as a reductant to reverse the reactivity of electrophilic allyl-palladium species (Scheme 10);^[32] overall, the combined use of a catalytic amount of palladium(0) and a stoichiometric amount of zinc(0) successfully turned allyl acetates to synthons of the corresponding allylic carbanions that added to aldehydes. The same concept was realised by using indium(I) iodide or In(0) as a reducing agent.^[33] However, a stoichiometric amount of waste is generated in these reactions.



Scheme 10: Umpolung of Electrophilic Allyl-Palladium Species by Zinc(0).

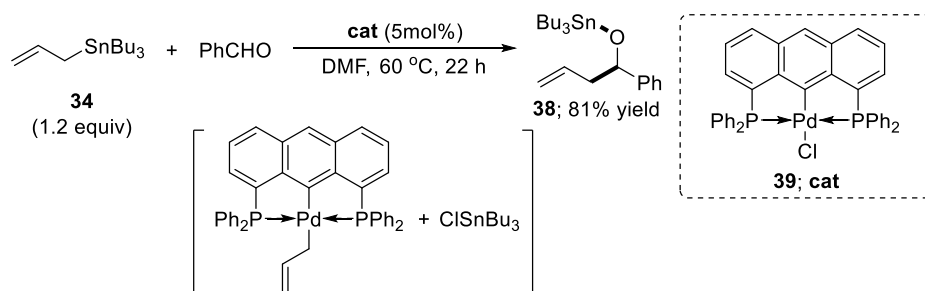
Use of σ -Donor Ligands: C–Sn Bond Activation

In 1996, Yamamoto and co-workers reported a Pd(II)-catalysed nucleophilic addition of allyl stannane **34** to aldehydes and imines, respectively (Scheme 11).^[34] In the case of imines, the palladium complex reacted with **34** twice to generate the symmetrical bis(π -allyl)-Pd complex **A**, which reacted as a nucleophile due to the anionic allyl moieties (σ -donor ligand) and phosphine coordination. The C–C bond formation with imine **35** proceeded *via* a cyclic closed transition state. The generated palladium complex **B** reacted with **34** again to form product **36**, which can be hydrolysed during work-up to form the free amine. The nucleophilic allyl-Pd intermediate **A** can also be generated from allyl chloride or acetate using Pd(0) and hexamethylditin ($\text{Me}_3\text{Sn-SnMe}_3$).^[35] In 1998, the asymmetric version of this reaction was developed using an enantiopure exoethylidene-derived π -allyl-Pd chloride catalyst (**37**; Scheme 11).^[36] Interestingly, the addition of water to the reaction system was shown to enhance the asymmetric induction.^[37]



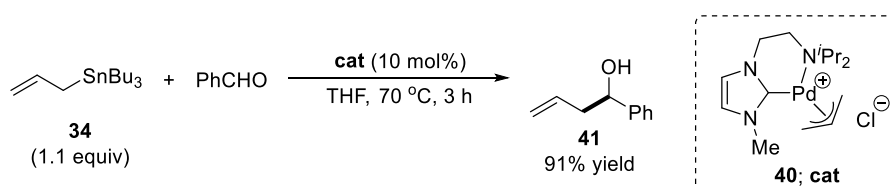
Scheme 11: Allylation of Imines *via* an *In Situ*-Generated Nucleophilic Allyl-Pd Species.

In 2003, Szabó's group reported palladium(II)-pincer complex **39** to catalyse aldehyde allylations (Scheme 12).^[38] The reaction proceeded through a nucleophilic η^1 -allyl-Pd intermediate. Due to the strong κ^3 -coordination of the pincer ligands to the palladium centre, only one coordination centre was available. Thus, the η^1 -allyl-Pd complex was formed and stabilised through hyperconjugation between $\sigma(\text{Pd-C})$ and $\pi^*(\text{C-C})$ molecular orbitals.^[39, 40] The aldehyde was likely to react with this allyl-Pd complex *via* a cyclic closed transition state to form product **38** (prior to hydrolysis). A similar transformation with aldehydes and imines was later reported with a slight modification of the pincer ligand.^[41]



Scheme 12: Palladium(II)–Pincer Complex-Catalysed Aldehyde Allylation.

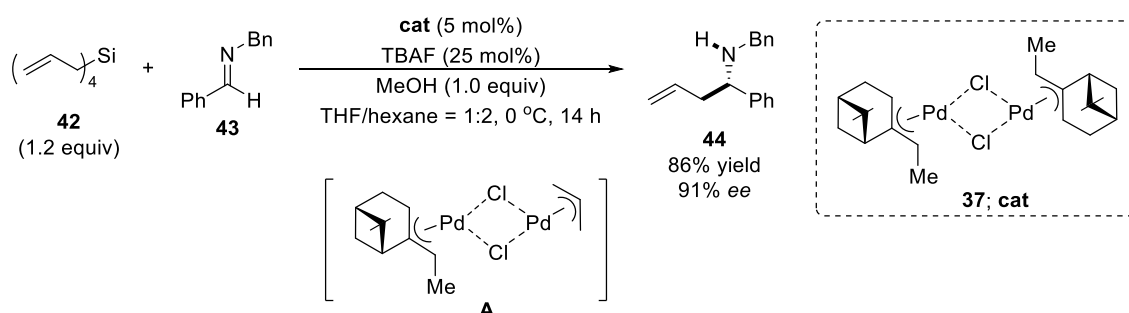
In 2007, Jarvo and co-workers reported a conceptually similar allylation of aldehydes with **34** promoted by a bidentate NHC ligated palladium species (**40**; Scheme 13).^[42] The NHC ligand represents a strong σ -donor ligand, which contributed to the nucleophilicity of **40**. Homoallylic alcohol **41** was formed in 91% yield.



Scheme 13: Palladium(II)–NHC Complex-Catalysed Aldehyde Allylation.

Use of σ -Donor Ligands: C–Si Bond Activation

The so-called *umpolung*-allylation strategy for tin pro-nucleophiles was later extended to the use of silicon pro-nucleophiles. In 2004, Yamamoto *et al.* reported a catalytic imine allylation using allyl silane **42** and bis(π -allyl)–Pd complex **37** (Scheme 14).^[43] TBAF as a sub-stoichiometric additive first reacted with silane **42** to form an anionic allyl equivalent that was transferred to the palladium catalyst *via* anion metathesis. The generated new bis(π -allyl)–palladium complex **A** reacted with **43** in a cyclic closed transition state, followed by protonation with methanol to form product **44** in 86% yield with 91% *ee*; the key for asymmetric induction may be the efficient coordination of the imine to complex **A**. Palladium-free examples using silicon pro-nucleophiles include catalysis with copper(II)^[44] and silver(I) species.^[45]

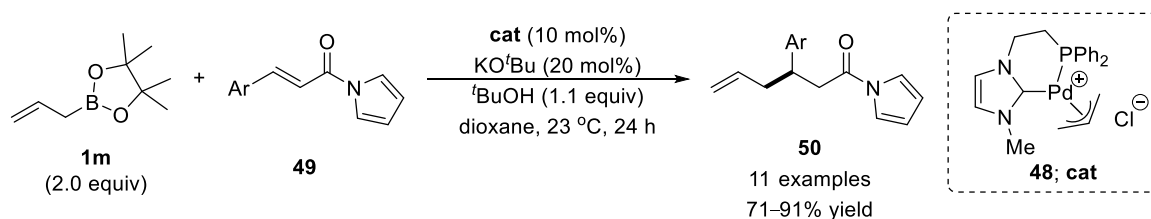


Scheme 14: Pd-Catalysed Allylation Using Silicon-Centered Pro-Nucleophiles.

Use of σ -Donor Ligands or Low-Valent Metal Species: C–B Bond Activation

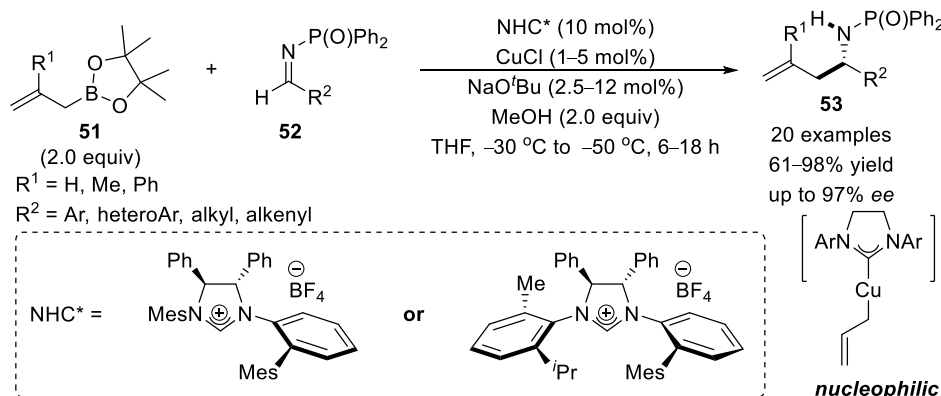
In 2008, Jarvo *et al.* reported the application of the *umpolung*-allylation strategy to the use of boron pro-nucleophile **1m** (Scheme 15).^[46] Bidentate NHC–palladium complex **48** was used as a catalyst in the presence of a sub-stoichiometric amount of a base, KO^tBu, and a stoichiometric amount of ^tBuOH to activate boronic ester

1m. The nucleophilic allyl functionality underwent conjugate addition to α,β -unsaturated *N*-acetylpyrrole **49** to form product **50** in 71–91% yields. This method has been extended as well to the conjugate allylation of alkylidene malononitriles.^[47]



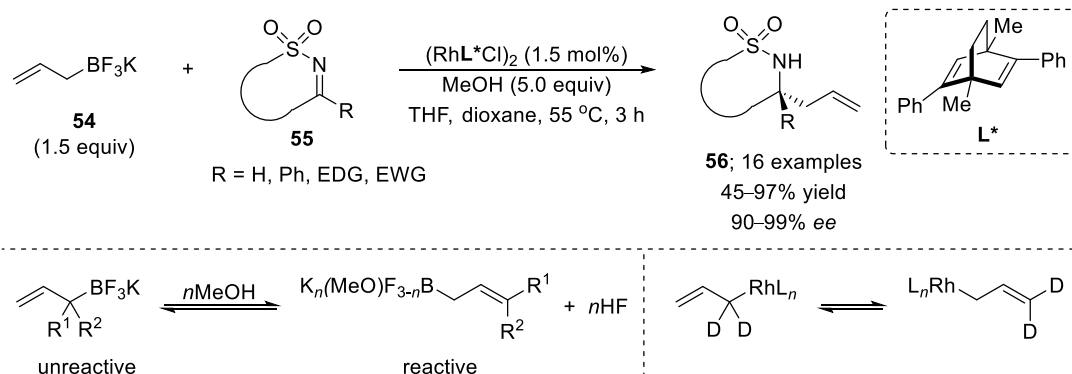
Scheme 15: Pd-Catalysed Allylation Using Boron-Centered Pro-Nucleophiles.

Other transition metals were also used to catalyse nucleophilic allylations with boron pro-nucleophiles. Hoveyda and co-workers reported Cu(I)-catalysed asymmetric allylations of imines **52** using allyl boronic ester **51** (Scheme 16).^[48] In the presence of a chiral NHC ligand, copper chloride reacted with **51** and a sodium alkoxide to generate an NHC–Cu–allyl species, which was driven by the formation of the energetically favourable B–O bond (in the stoichiometric by-product of the B-to-Cu transmetalation). The nucleophilic allyl fragment was transferred to imines **52** to form homoallylic amines **53** in 61–98% yields with up to 97% *ee*. In 2013, this NHC-assisted copper(I)-catalysed allylation methodology has been further applied to CO₂ as electrophile by Duong’s group to synthesise β,γ -unsaturated carboxylic acids.^[49] Apart from aldimines, the Cu(I)-catalysed enantioselective allylation of ketimines was also reported.^[50]



Scheme 16: Cu-Catalysed Allylation Using Boron-Centered Pro-Nucleophiles.

Lam and co-workers reported a rhodium(I)-catalysed enantioselective allylation of cyclic imines using allyl trifluoroborate (**54**; Scheme 17).^[51] This bench-stable reagent may be activated by MeOH to form a more reactive trivalent allyl boron species that transmetalates with a chiral diene–Rh(I) complex. The resulting nucleophilic allyl–rhodium species would add to imines **55** to generate homoallylic amines **56** in 45–97% yields with 90–99% *ee*. One factor to consider in catalytic asymmetric additions to imines is the potential isomerisation of the C=N double bond, which may have a negative impact regarding stereoselectivity.^[52] The use of cyclic imines **55**, in which the C=N double bond is constrained in the *Z* geometry, may rule out such undesired isomerisation.^[53] Mechanistic studies suggested the allylation proceeded *via* the formation of a σ -allyl–rhodium(I) species that may undergo a rapid metallotropic rearrangement.

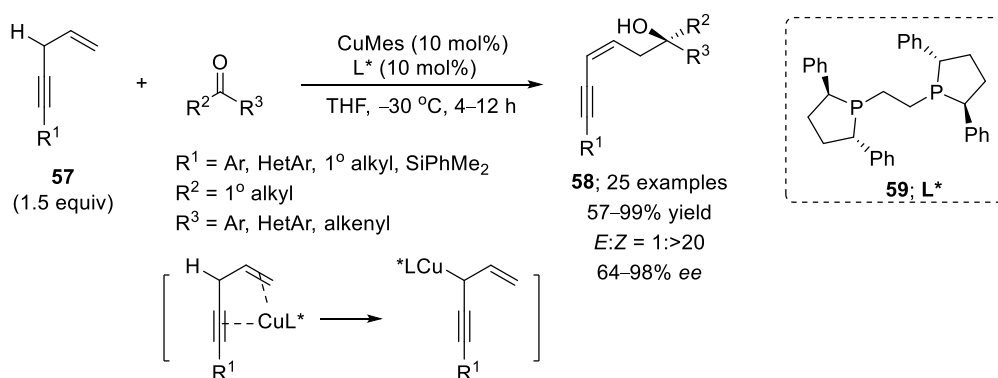


Scheme 17: Rhodium(I)-Catalysed Allylation Using a Boron-Centered Pro-Nucleophile.

In all displayed examples of nucleophilic allylation, C–X bonds had to be activated in order to form a nucleophilic allyl–metal species ($X = O, Sn, Si, B$). Thus, a stoichiometric amount of waste had to be generated in these non-atom-economic reactions.

Nucleophilic Allylation *via* C–H Bond Activation

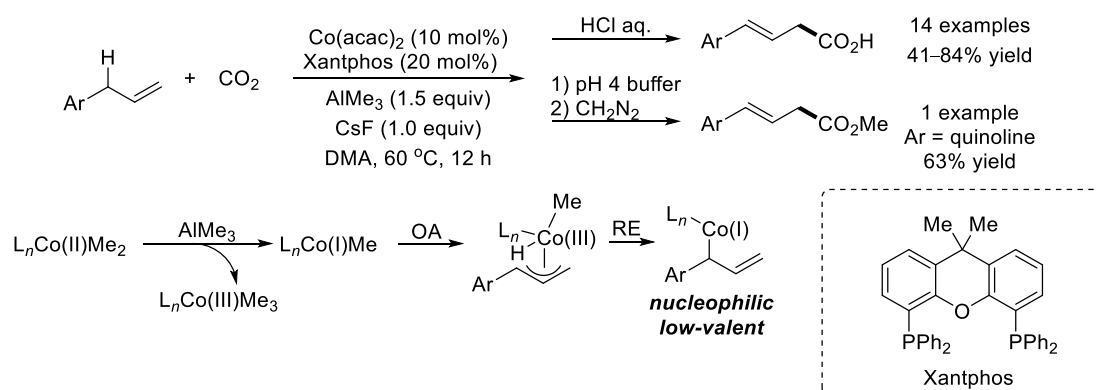
More recently, after the completion of our research,^[54] *transition metal*-catalysed nucleophilic allylation *via* C–H bond activation was developed independently by two Japanese groups. Kanai *et al.* reported a copper(I)-catalysed C(sp³)–H bond activation of enynes for subsequent ketone allylations (Scheme 18).^[55] Pro-nucleophiles **57** contain both a C=C double bond and a C≡C triple bond, which may coordinate to a π -acidic copper(I) centre; such coordination would facilitate the following deprotonation by a Brønsted base (Mes). The generated allyl–copper(I) species would serve as a nucleophile in the addition to ketones. In the presence of enantiopure diphosphine ligand **59**, the reaction proceeded to give the γ -adducts **58** in 57–99% yields with up to 98% *ee*. The *Z*-geometry was observed as the major isomer, which was ascribed to the configuration of the allyl–copper(I) intermediate.



Scheme 18: Copper(I)-Catalysed Nucleophilic C(sp³)–H Bond Allylation with Ketones.

More recently, Mita and Sato *et al.* reported cobalt(II)-catalysed CO₂ allylations using allyl benzene pro-nucleophiles although super-stoichiometric quantities of additives were required (Scheme 19).^[56] The general concept was to generate a low-valent allyl–metal species bearing a potentially nucleophilic character; XantPhos served as a bidentate ligand to coordinate to the cobalt centre. The cobalt(II) catalyst first reacted with AlMe₃ *via* anion metathesis and disproportionation. As a result, a methyl–cobalt(I) and a tris(methyl)–cobalt(III) complexes

were formed. It was proposed that methyl–cobalt(I) would undergo oxidative addition to the alkene to generate an allyl–cobalt(III) complex. The following reductive elimination would lead to the formation of allyl–cobalt(I) and CH₄ as a by-product. The nucleophilic cobalt(I) species would then add with γ -selectivity to CO₂ to give homoallylic acids or, after methylation, methyl esters in 41–84% yields. These two examples constitute pioneering chemistry in the field of transition metal-catalysed C–H bond action.

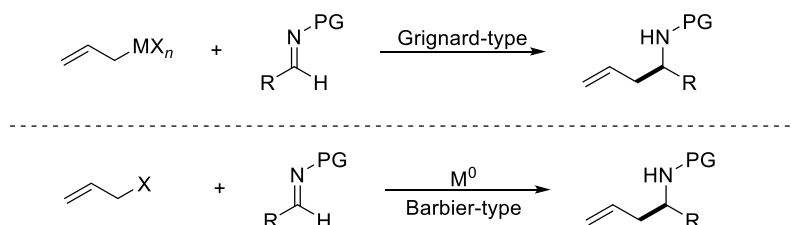


Scheme 19: Cobalt(II)-Catalysed Nucleophilic C(sp³)-H Bond Allylation with CO₂.

Imine Allylation

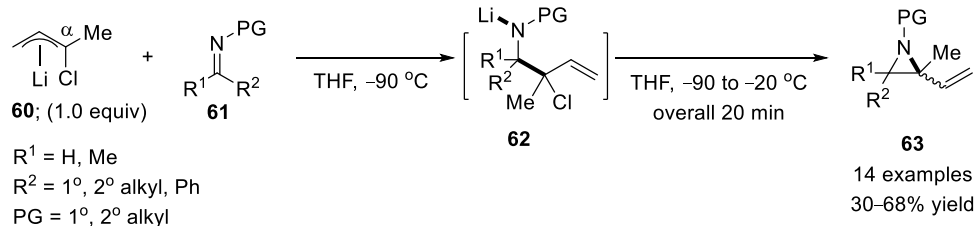
Grignard-Type and Barbier-Type Allylations

Apart from the examples above, traditional imine allylation normally occurred using a stoichiometric amount of an allyl–metal species (Grignard-type), which may be also generated *in situ* from the corresponding halide (Barbier-type; Scheme 20). The use of allyl–metal reagents in this context was summarised in a comprehensive review by Yamamoto and co-workers.^[57] A few selected examples are detailed below.



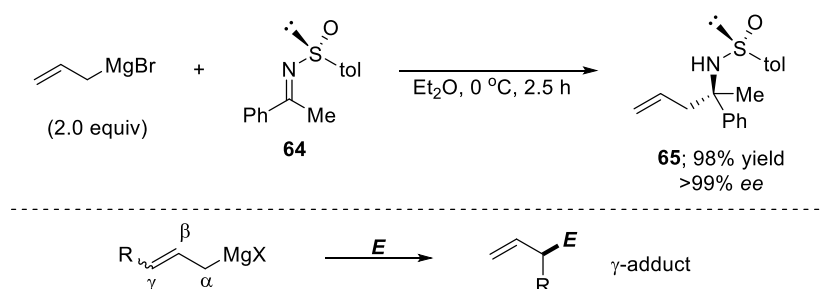
Scheme 20: Grignard-Type and Barbier-Type Imine Allylations.

Allyl–Li compounds were reported as π -allyl species by Schlosser.^[58] Regarding their use in organic synthesis, Mauzé reported a nucleophilic allylation of imines using allyl–Li reagent **60** as early as in 1980 (Scheme 21).^[59] The generated homoallylic lithium amides **62** underwent 3-*exo*-tet cyclisation (favoured according to Baldwin's rules^[60]) to form tetrasubstituted aziridines **63** in 30–68% yields. These relatively low yields might be ascribed to the α -hydrogen of imines **61** where R¹ and/or R² correspond(s) to primary or secondary alkyl substituents. The initial C–C bond formation to give homoallylic amides **62** proceeded with α -selectivity; the chloride then served as a good leaving group in the subsequent aziridine formation. Other applications of using allyl–Li reagents to allylate carbonyl electrophiles can be found in the work by Seyferth.^[61]



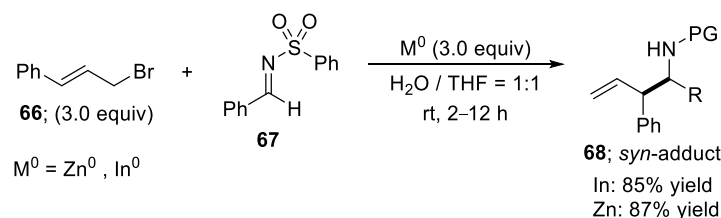
Scheme 21: Allylation of Imines Mediated by an Allyl-Lithium Species.

According to a ^{13}C NMR study by Schlosser, allyl-Mg reagents were reported as σ -allyl species, where the Mg was bond to the less substituted carbon atom.^[58] Allyl-MgBr was reported to allylate Ellman's chiral imine (**64**), thus affording a single enantiomeric homoallylic amine **65** in 98% yield (Scheme 22).^[62] It is noted that allyl-Mg compounds normally add to electrophiles with γ -selectivity.^[63] Other Grignard-type imine allylations, including metals such as Li, Mg, Ba, Ti, Cu, Zn, B, Al, In, and Sn, are summarised in a review by Bloch.^[64]



Scheme 22: Allylation of Ellman's Chiral Imine Mediated by an Allyl-Magnesium Species.

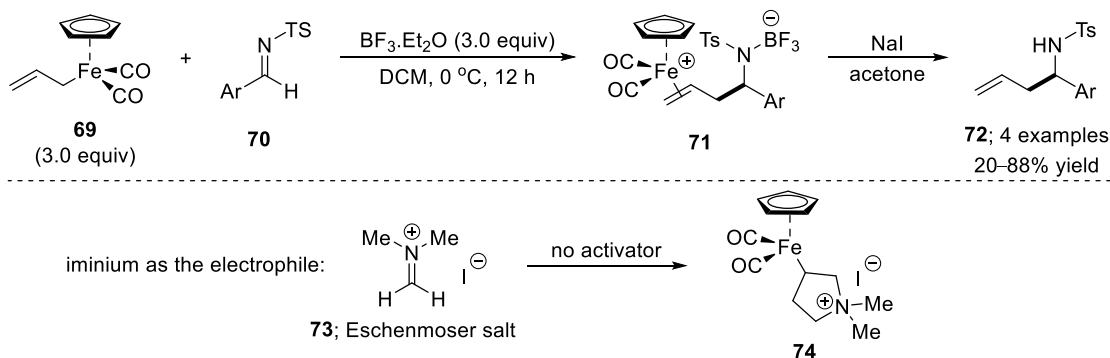
The one-pot Barbier-type allylation of imines include the use of metals such as Mg, Ti, Ta, Cr, Zn, Cd, Al, In, Sn, Bi.^[64] Treating allyl bromide **66** with zinc or indium powder allowed the *in situ* formation of allyl-zinc or allyl-indium reagents that would add to imine **67** through a cyclic closed transition state, as reported by Chan and co-workers (Scheme 23).^[65] It is noted that this Barbier-type transformation can be carried out in aqueous media at room temperature. Regarding the regioselectivity, both metals (zinc and indium) gave the final product with exclusive α -selectivity. In terms of diastereoselectivity, only *syn*-adduct **68** was observed in both cases, which can be explained by a chair-like six-membered transition state where the allyl-metal species was added to the imine with predominant *E*-geometry.



Scheme 23: Barbier-Type Imine Allylation Mediated by Zinc or Indium Powder.

The addition of nucleophilic allyl-iron species **69** to imines **70** required the use of an external Lewis acid in superstoichiometric quantities (Scheme 24).^[66] The formed zwitterionic compounds **71** were typically isolatable yellow salts, which were demetalated by NaI in acetone giving homoallylic amines **72** in 20–88% yields. It is noted that an electron-withdrawing substituent on the imine was critical for a high product yield. Interestingly, when allyl-iron species reacted with the Eschenmoser salt (**73**), the allylated zwitterionic intermediate was not detected;^[67]

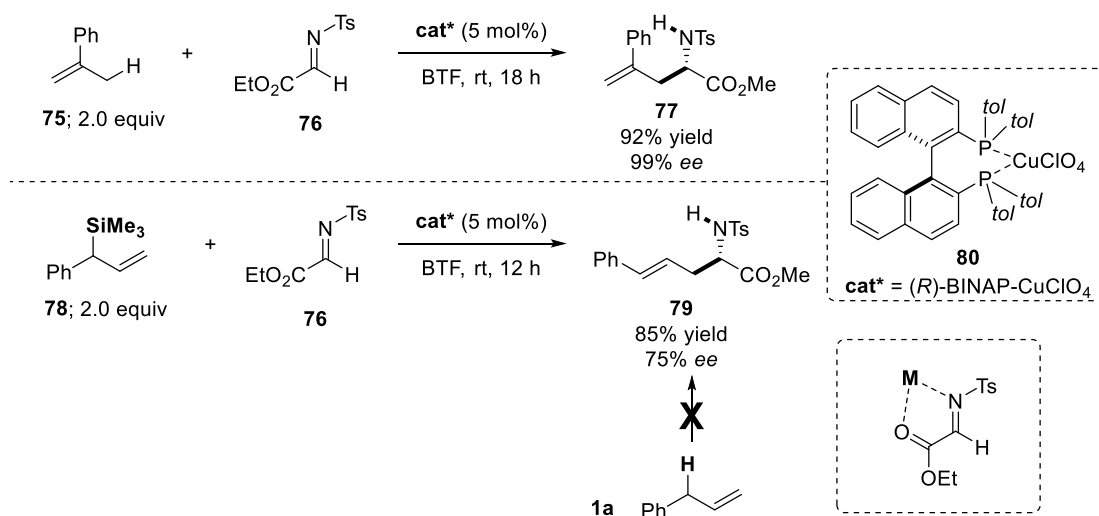
instead, a formal [3+2] cycloaddition was observed to give product **74**. Such reactivity is likely due to the strong electrophilicity of the π -iron complex serving as an electrophile for the subsequent cyclisation.



Scheme 24: Imine Allylation Mediated by an Allyl-Iron Species.

Asymmetric Imino-ene Reactions

Imino-ene reactions allowed the addition of unactivated olefins to imines in the presence of a Lewis acid catalyst.^[68] The first catalytic enantioselective imino-ene reaction was developed by Lectka and co-workers in 1998 using a chiral diphosphine–copper(I) catalyst (**80**; Scheme 25).^[69, 70] The reaction between α -methyl styrene (**75**) and α -imino ester **76** proceeded to give product **77** in 92% yield with 99% *ee*, which may also serve as a precursor for the corresponding α -amino acid. However, it is noted that product **79** –with distinct connectivity relative to **77**– was only accessible using *silylated* allyl benzene **78**.^[71]

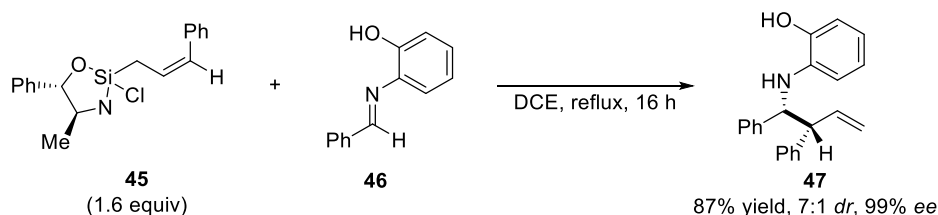


Scheme 25: Asymmetric imino-ene reaction and its silicon analogue.

Use of Allyl Silicon and Allyl Tin Reagents

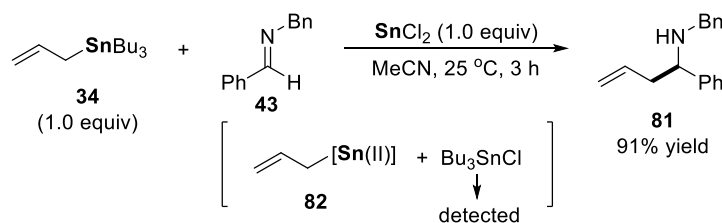
The use of allyl silanes and stannanes as pro-nucleophiles often required the use of an external Lewis acid due to the relatively low reactivity of these reagents (e.g. in the Hosomi–Sakurai reaction^[72]). However, the *activated* allyl silicon reagent **45** was shown to directly allylate *activated* imines of type **46** in the absence of a catalyst under heating conditions (Scheme 26).^[73] The *ortho*-phenol protecting group was proposed to react with the chloride to form HCl, which would protonate the nitrogen atom of the pseudoephedrine auxiliary; this step simulated a

Brønsted acid activation of the allyl silane. The imine nitrogen would then coordinate to the silicon centre to facilitate C–C bond formation to generate product **47** in 87% yield with high diastereoselectivity and 99% *ee*.



Scheme 26: Diastereoselective Imine Cinnamylation using an Enantiopure Allyl Silicon Reagent.

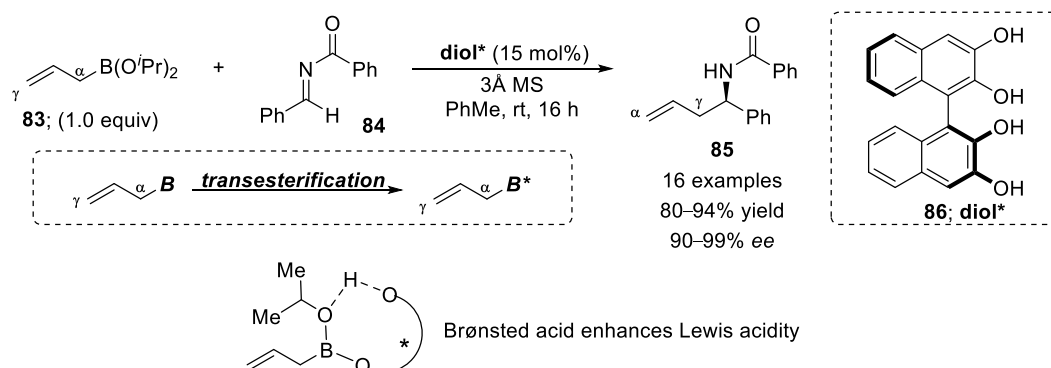
One novel approach to render an allyl stannane more reactive was to transmetalate Sn(IV) to low-valent Sn(II) (Scheme 27).^[74] The reaction between allyl Sn(IV) reagent **34** and aldimine **43** proceeded in the presence of SnCl₂ to generate homoallylic amine **81** in 91% yield; a reaction did not occur in the absence of the Sn(II) trigger. In the absence of an electrophile, treating **34** with SnCl₂ led to the formation of Bu₃SnCl in 92% yield, which strongly suggests the formation of an intermediary allyl tin(II) species (**82**).



Scheme 27: Imine Allylation Mediated by a Sn(II) Species.

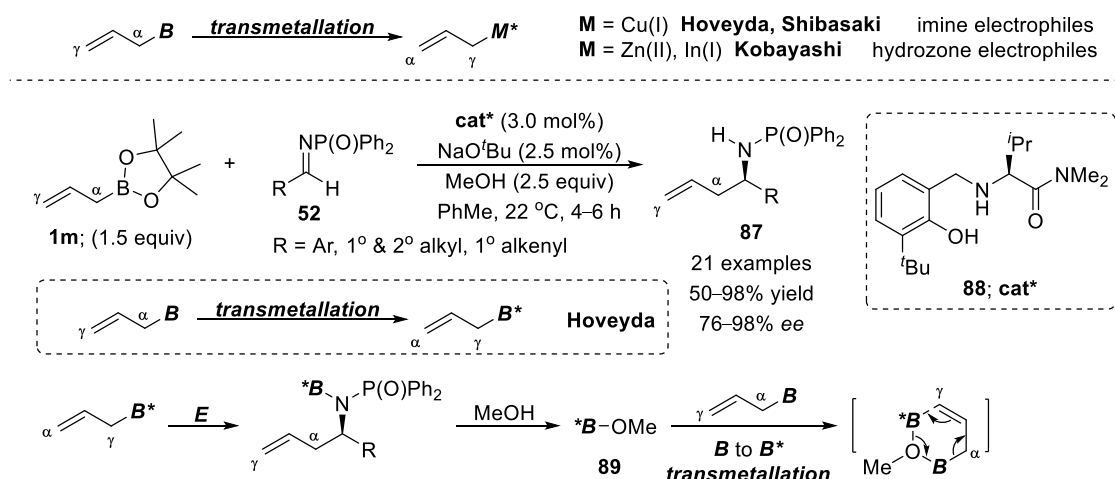
Use of Allyl Boron Reagents

Imine allylation using allyl boronates mediated by transition metals has been discussed in the previous section. Recent advances in the use of allyl boron reagents in organic synthesis were summarised by Szabó and co-workers in 2017.^[75] Unlike aldehyde allylation that may occur directly in apolar solvents, imine allylation was shown to be challenging because a C=N double bond is less polarised than a C=O double bond. In addition, the geometric configuration of the C=N double bond normally favours the *E* geometry, which will lead to a disfavoured 1,3-diaxial interaction in the cyclic six-membered transition state. The idea of using Brønsted acid catalysis to activate allyl boronic esters was realised by Hall^[76] and Antilla.^[77] The electron density at the oxygen atom of a boronic ester would be decreased by a Brønsted acid thus affording a more Lewis acidic boron centre that may be coordinated more easily by a Lewis basic electrophile to ultimately activate the allylic C–B bond. In a similar context, Schaus and co-workers reported asymmetric allylation of imines of type **84** using boron pro-nucleophile **83** catalysed by chiral diol **86** (Scheme 28).^[78] The first step was shown to be a transesterification at boron; only *one* *O*^{*i*}Pr group was replaced based on NMR and ESI–MS studies. The free hydroxy group of **86** may act as an internal Brønsted acid that would enhance the Lewis acidity of the boron centre. The resulting more reactive and chirally modified allyl boronic ester was shown to undergo smooth C–C bond formation to give homoallylic amines of type **85** in 80–94% yields with 90–99% *ee*.



Scheme 28: Chiral Diol-Catalysed Imine Allylation Using an Allyl Boronic Ester.

The transmetalation from boron to a metal would provide a more reactive allyl–metal species; it is noted that the regioselectivity of such reagent may be formally inverted. Kobayashi and co-workers reported zinc(II)- and indium(I)-catalysed allylations of hydrazones.^[79, 80] Both transformations were accomplished with high regio-, diastereo-, and enantioselectivities. Likewise, copper(I) catalysis was reported in this context by Kanai and Shibasaki *et al.* as well as Hoveyda *et al.* (see Scheme 16, page 19).^[48-50] In 2013, Hoveyda’s group reported a boron-to-boron “transmetalation” using an enantiopure aminoalcohol catalyst (Scheme 29).^[81] The first step was shown to be an exchange of the bidentate ligand at boron (**1m**) to replace pinacol by chiral aminoalcohol **88**. The newly formed chirally modified allyl boronic ester was proposed to be more reactive towards imines of type **52**; the C–C bond formation proceeded with exclusive γ -selectivity. Protonation of the homoallylic amide intermediate by MeOH would release chiral boron moiety **89**, which would undergo γ -selective boron-to-boron “transmetalation” with **1m**. The following cycle would repeat this procedure: double γ -selectivity affords overall product **87** with net α -selectivity in 50–98% yields with 76–98% *ee*. In 2016, this work was applied to generate an overall net γ -adduct through the use of a suitable Lewis acid, Zn(OMe)₂.^[82]

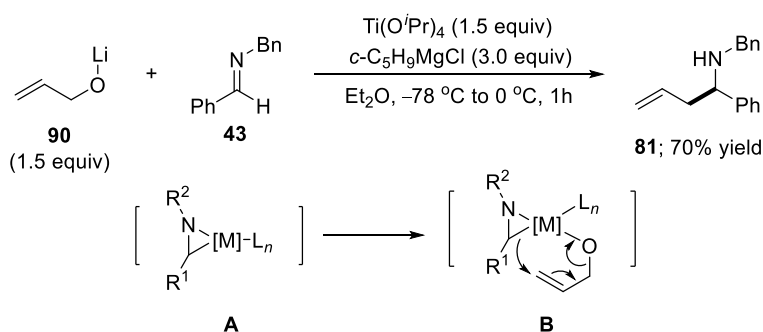


Scheme 29: Swap of Regioselectivity via Boron-to-Boron Transmetalation.

Umpolung-Type Imine Allylation

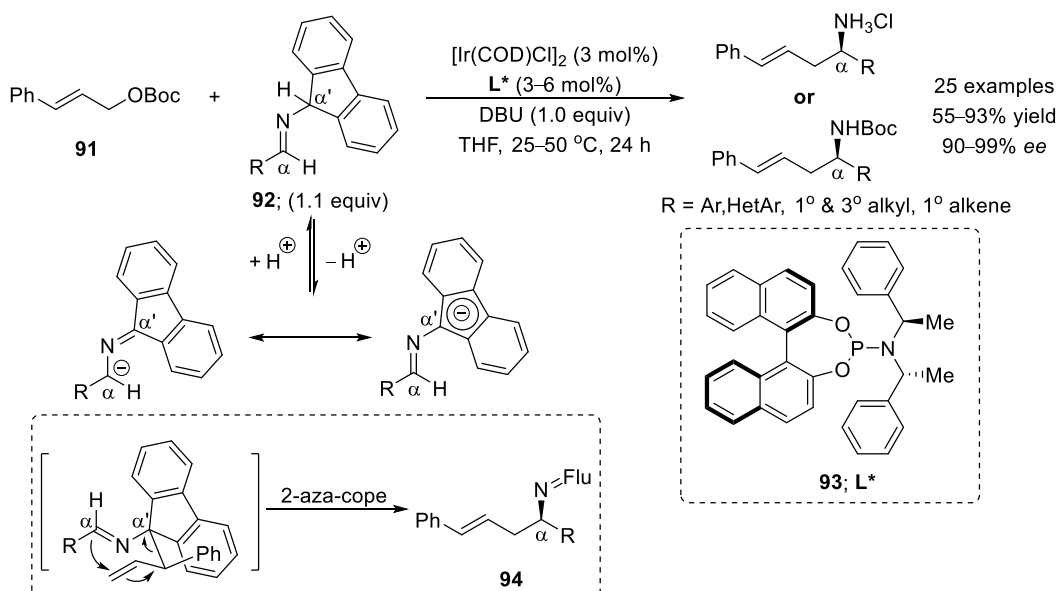
The examples above displayed allylation of imine *electrophiles*. However, *umpolung*-type imine allylation – where imines served as *nucleophiles*– have also been developed; the examples below are specific for an allylation occurring at the carbon atom of the C=N double bond. For instance, a direct coupling between allylic alcohol and imines was reported by Micalizio’s group in 2009 (Scheme 30).^[83] The allylic alcohol was first converted to

lithiated allyl alkoxide **90**. It was assumed that titanium(IV) would insert into the C=N double bond of imine **43** to form intermediate **A**, which then underwent ligand exchange with the lithium alkoxide to form intermediate **B**. A 3,3-metallotropic rearrangement of the latter would form after hydrolysis homoallylic amine **81**.



Scheme 30: Direct Coupling between Allyl Alcohol and an Imine.

In 2016, an *umpolung*-type imine allylation by iridium catalysis was developed by Niu and co-workers (Scheme 31);^[84] *N*-fluorene-protected aldimines of type **92** were used as pro-nucleophiles. The α' -C–H of the protecting group was proposed to be deprotonated by 1,8-diazabicyclo[5.4.0]undec-7-ene (DBU). The formed aza-allyl anion would be stabilised as the negative charge may be delocalised within the fluorene motif (aromatic 14 π -electron system) and at the α -carbon. Allyl carbonate **91** reacted with the iridium complex to generate an electrophilic allyl–Ir species that was trapped in a Tsuji–Trost-type fashion with branched selectivity by the α' -carbon of the aza-allyl anion. A subsequent 2-aza-cope rearrangement afforded the overall α -C-functionalised homoallylic imines of type **94**, and after hydrolysis homoallylic amines in 55–93% yield with 90–99% *ee*; the asymmetric induction was achieved using enantiopure ligand **93**. Other examples of catalytic asymmetric imine allylation were summarized by Yus in 2011.^[85]

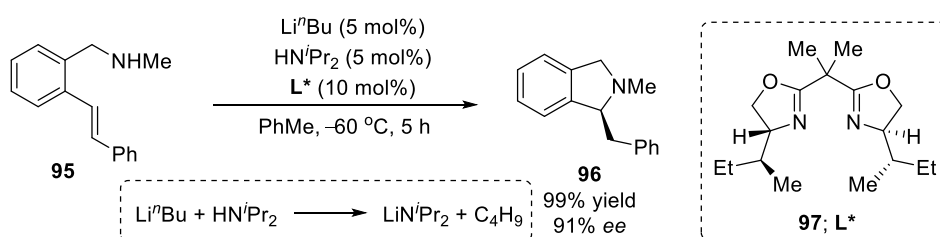


Scheme 31: *Umpolung*-Type Imine Allylation Catalysed by an Iridium Complex.

Catalytic Use of Alkali Metal Amides in Organic Synthesis

Hydroamination

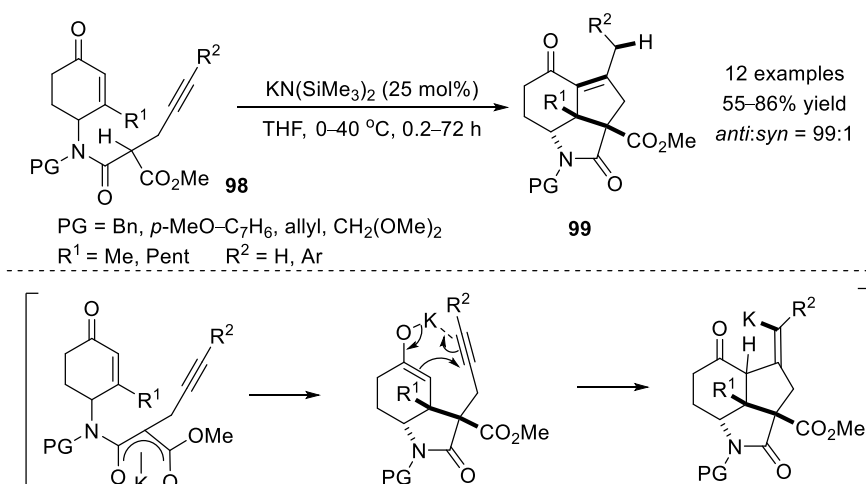
Alkali metal amides were often used in stoichiometric quantities for deprotonation of acidic hydrogens due to their strong Brønsted basicity and weak Lewis basicity. Such amides have been extensively used in catalytic hydroamination.^[86, 87] In 2007, Tomioka and co-workers reported an asymmetric intramolecular hydroamination of substrate **95** catalysed by an *in situ*-generated lithium amide and enantiopure BOX ligand **97** (Scheme 32).^[88] The BOX ligand was shown to activate the lithium amide and to induce asymmetry in the 5-*exo*-trig cyclisation to form product **96** in 99% yield with 91% *ee*. In addition, Hultzsich and co-workers found that a TMEDA-ligated lithium amide or potassium amide was apt to catalyse intermolecular hydroamination.^[89] In both cases, an *anti*-Markovnikov regioselectivity was observed, which stands in contrast to late-transition metal-catalysed hydroamination – with the exception of three examples of rhodium catalysis.^[90-92] The detailed mechanism and pathways to achieve Markovnikov and/or *anti*-Markovnikov regioselectivity in hydroamination was discussed in a recent review by Gooßen and co-workers.^[93]



Scheme 32: Lithium Amide-Catalysed Asymmetric Hydroamination.

Brønsted Base Catalysis

In 2012, Dixon and co-workers reported an elegant cascade cyclisation using a sub-stoichiometric amount of a potassium amide (Scheme 33).^[94]

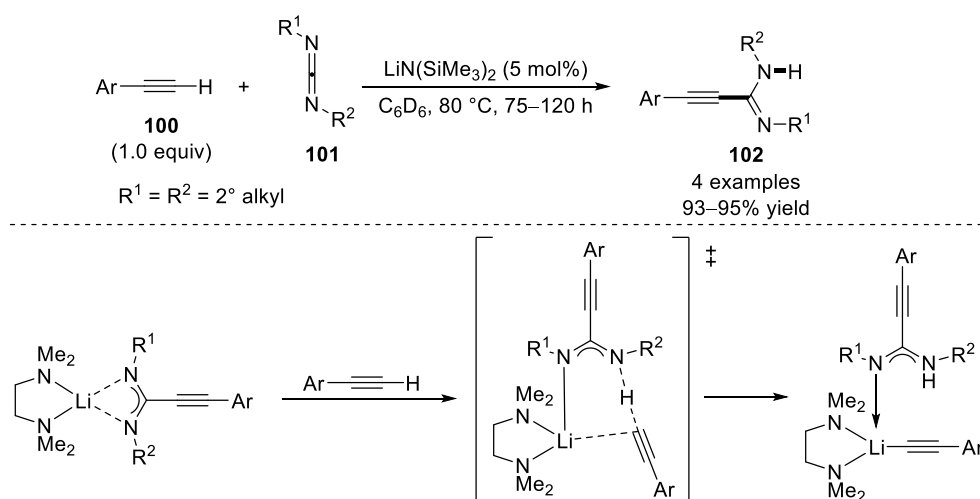


Scheme 33: Potassium Amide-Catalysed Cascade Cyclisation.

After deprotonation of malonamates of type **98** ($\text{pK}_a = 15$ in DMSO),^[95, 96] the generated potassium enolate underwent conjugate addition to the α,β -unsaturated ketone motif, thus forming another potassium enolate. The potassium Lewis acid then potentially coordinated to the $\text{C}\equiv\text{C}$ triple bond, thereby facilitating the enolate addition

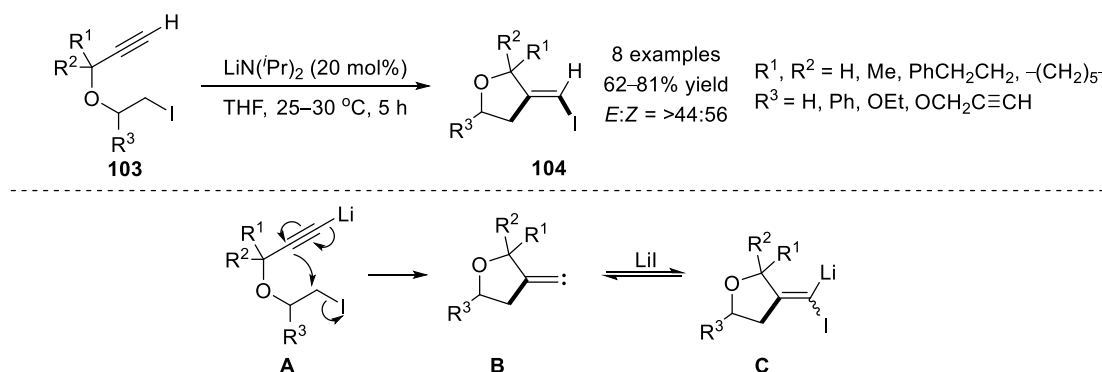
to the alkyne. This 5-*exo*-dig cyclisation resulted in the formation of an vinyl-potassium species that was converted –through proton transfer to the less substituted carbon atom– to products of type **99** in 55–86% yield with exclusive *anti*-selectivity. In 2017, a similar transformation was developed towards a natural product synthesis by Trauner *et al.*, although a stoichiometric amount of KO^tBu was used.^[97]

In 2006, an alkynylation of carbodiimides **101** was reported by Richeson and co-workers to form amidines **102** (Scheme 34);^[98] a lithium amide was used as a Brønsted base to deprotonate terminal aromatic alkynes **100** ($pK_a = 28.8$ in DMSO).^[99] Subsequently, the carbanion added to **101** to give the products in 93–95% yields. It is noted that when the same catalyst was applied to N–H and P–H pro-nucleophiles in N–C bond and P–C bond formations, respectively, a catalytic amount of TMEDA was required to increase the reactivity of the lithium amide. The rate-determining step of this transformation was analysed in 2008.^[100] Both DFT calculations and previous literature examples^[101] have suggested that the carbodiimide could insert into the Li–C bond of the alkynyl nucleophile, which generated the lithiated product in the first cycle. The following regeneration of the Li–C bond relied on a proton transfer step. It was found that lithium had a fairly weak interaction with **100**, originating from the C–H σ -bond rather than the C \equiv C π -bond. Thus, the lithiated alkyne was only formed to a small extent in the transition state. Thus, it was proposed that the proton transfer was rate-limiting.



Scheme 34: Lithium Amide-Catalysed Alkyne Amidination.

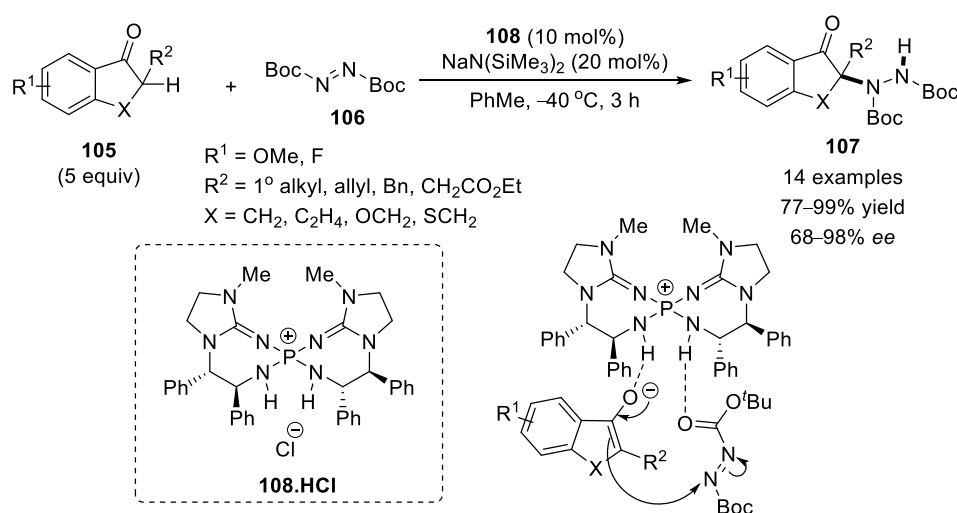
Harada's group reported an LDA-catalysed carbocyclisation of terminal alkynes **103** to give tetrasubstituted furans **104** (Scheme 35).^[102]



Scheme 35: Lithium Amide-Catalysed Cyclisation.

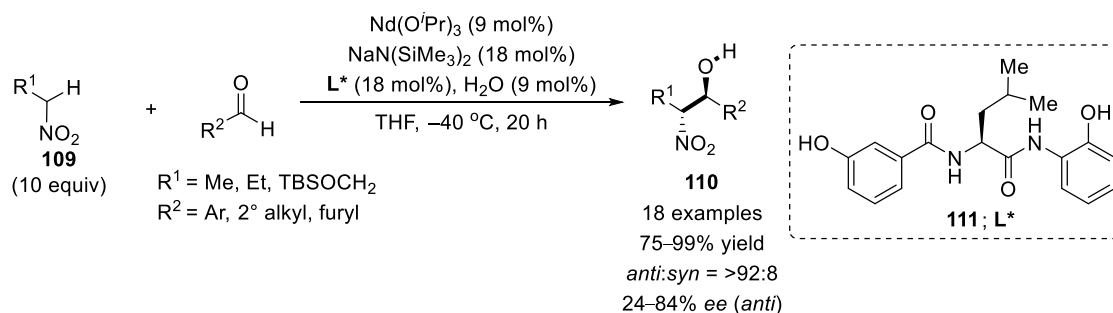
The most acidic hydrogen of **103** ($pK_a \sim 28\text{--}29$ in DMSO)^[99] was deprotonated by LDA to generate intermediate **A**. Next, according to their previous work,^[103] an *exo*-cyclisation occurred to form a cycloalkylidene carbene **B** that could insert into lithium iodide to form carbenoid **C**, which was protonated to form the products **104** in 62–81% yield. It is noted that carbene **B** may also undergo a C–H insertion into pro-nucleophile **103**, thus leading to the formation of a by-product.

Asymmetric organocatalysis has been developed using a sodium amide as co-catalyst; Terada and co-workers reported an enantioselective hydrazination using this Brønsted base for the *in situ* formation of a chiral phosphazene organosuperbase catalyst (Scheme 36).^[104] The active organosuperbase catalyst was generated *in situ* by treating the HCl salt of **108** with $\text{NaN}(\text{SiMe}_3)_2$. The α -hydrogen of ketones of type **105** ($pK_a \sim 20$ in DMSO)^[96] was deprotonated by the organosuperbase. The protonated catalyst then acted as a hydrogen bond donor (N–H bond), which may activate electrophile **106** for C–N bond formation to give products **107** in 77–99% yields with 68–98% *ee*. It is noted that two equivalents of $\text{NaN}(\text{SiMe}_3)_2$ in comparison with the chiral phosphonium pre-catalyst were required to secure high yields *and* to maintain the level of asymmetric induction. The use of lithium and potassium amides led to low yields and low selectivities. In 2016, a slightly modified catalyst system was applied to asymmetric direct-type Mannich reactions by the same group.^[105]



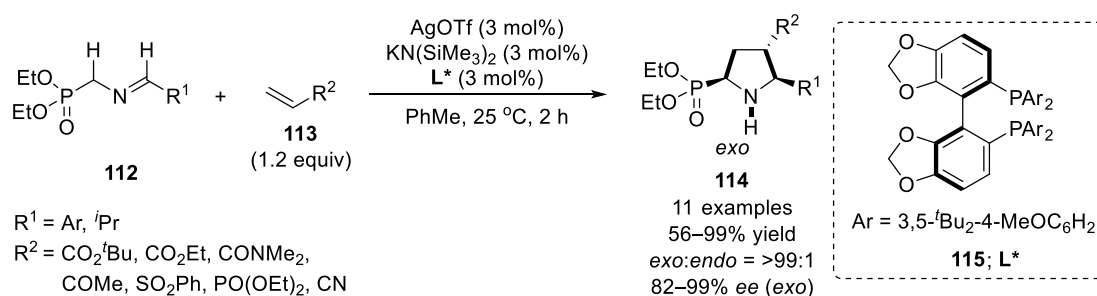
Scheme 36: Sodium Amide Used as a Co-Catalyst in Asymmetric Organocatalysis.

$\text{NaN}(\text{SiMe}_3)_2$ was also used in combination with chiral rare earth metal catalysts in asymmetric Henry reactions by Shibasaki *et al.* (Scheme 37).^[106, 107] In this catalyst system, Na and Nd acted as Lewis acids independently. Pro-nucleophiles of type **109** ($pK_a \sim 17$ in DMSO)^[96] were deprotonated by the Brønsted basic alkoxide (or amide), and subsequently added to aldehydes to form products of type **110** in 75–99% yields with 24–84% *ee* for the predominant *anti*-isomer. The heterobimetallic system was the key for the observed *anti*-selectivity: it was proposed that one metal may coordinate to the electrophile while the other metal may interact with the nitro group to arrange the transition state in an *anti*-periplanar configuration.



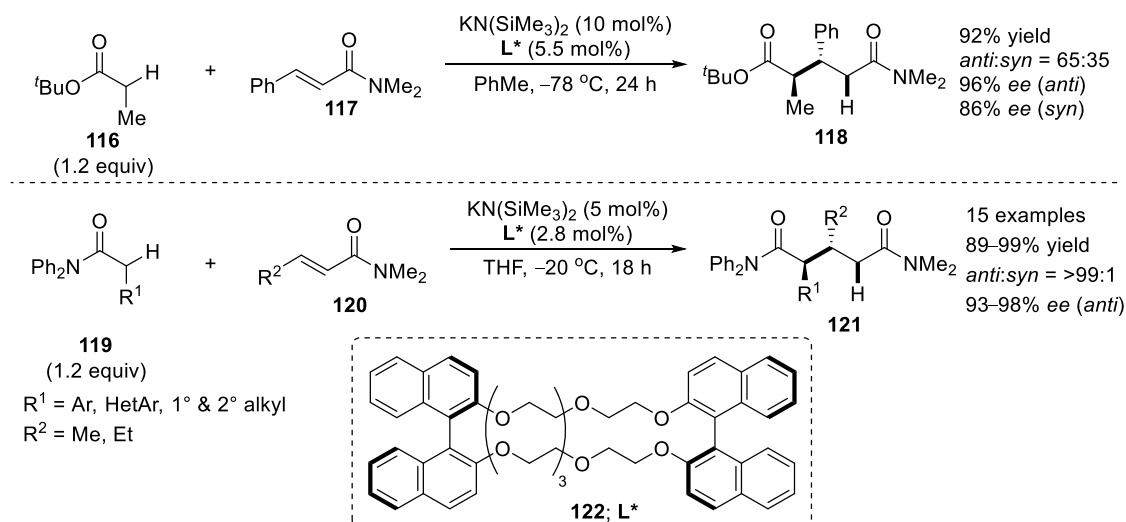
Scheme 37: Sodium Amide Used as a Co-Catalyst in Asymmetric Metal Catalysis.

In addition, Kobayashi and co-workers reported a catalyst system composed of $\text{KN(SiMe}_3)_2$, AgOTf , and chiral diphosphine **115** (Scheme 38).^[108] The *in situ* formed $\text{AgN(SiMe}_3)_2$ was proposed to be activated by **115**^[109] in order to deprotonate Schiff base substrate **112** ($\text{pK}_a \sim 25$ in DMSO).^[110] The generated aza-allyl nucleophile reacted with alkene **113** via a [3+2] cycloaddition to form predominantly *exo*-pyrrolidines **114** in 56–99% yields with 82–99% ee. It is noted that the use of $\text{KN(SiMe}_3)_2$ outperformed its barium analogue and other strong bases; interestingly, a higher loading of KHMDs was shown to decrease the diastereoselectivity. Moreover, $\text{KN(SiMe}_3)_2$ was also used as a co-catalyst in asymmetric copper catalysis by Shibasaki and co-workers.^[111]



Scheme 38: Potassium Amide Used as Co-Catalyst in Asymmetric Silver Amide Catalysis.

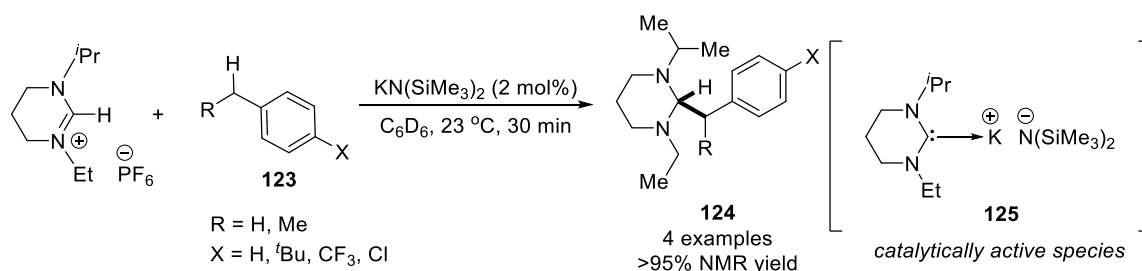
In 2015, Kobayashi and co-workers reported $\text{KN(SiMe}_3)_2$ -catalysed asymmetric conjugate additions (Scheme 39).^[112]



Scheme 39: Potassium Amide-Catalysed Asymmetric Conjugate Additions.

Ester **116** ($pK_a = 31$ in DMSO)^[113] and amides of type **119** ($pK_a = 35$ in DMSO)^[113] were used as pro-nucleophiles in this reaction, bearing rather non-acidic protons. $\text{KN}(\text{SiMe}_3)_2$, complexed by enantiopure crown ether **122**, acted as a Lewis acid–Brønsted base dual catalyst that first deprotonated the pro-nucleophiles to generate the corresponding chirally modified potassium enolate; the latter added to Michael acceptors **117** and **120** to form products **118** and **121**, respectively, in 89–99% yields with up to 98% *ee* for the predominant *anti*-isomer. NMR and MS studies revealed the structure of a chiral crown ether–potassium salt, showing that the crown ether combined with $\text{KN}(\text{SiMe}_3)_2$ in a 1:1 ratio, although a 1:2 ratio was required to achieve high asymmetric induction. The combined catalytic use of $\text{KN}(\text{SiMe}_3)_2$ and chiral ligand **122** was applied to the use of alkyl nitrile pro-nucleophiles by the same group.^[114, 115]

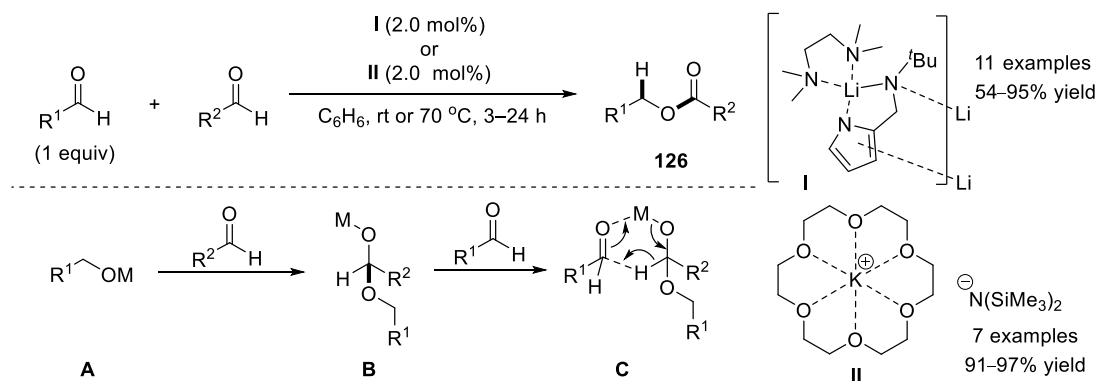
Lloyd-Jones *et al.* reported a carbene insertion into a non-acidic C–H bond using a catalytic amount of $\text{KN}(\text{SiMe}_3)_2$ (Scheme 40).^[116] The *N*-heterocyclic carbene precursor ($pK_a \sim 16$ in DMSO)^[110] was first deprotonated by $\text{KN}(\text{SiMe}_3)_2$ to generate the corresponding free carbene, which was apt to insert into the benzylic C–H bond of toluene derivatives **123** ($pK_a = 42\text{--}44$ in DMSO),^[117] likely by transferring electrons into the C–H σ^* orbital. This insertion was proposed to be facilitated by a highly reactive amide anion in the carbene-ligated potassium amide complex **125**. The reaction rate was strongly dependent on the *para*-substituent X.



Scheme 40: Potassium Amide-Catalysed Carbene Insertion.

Redox Chemistry

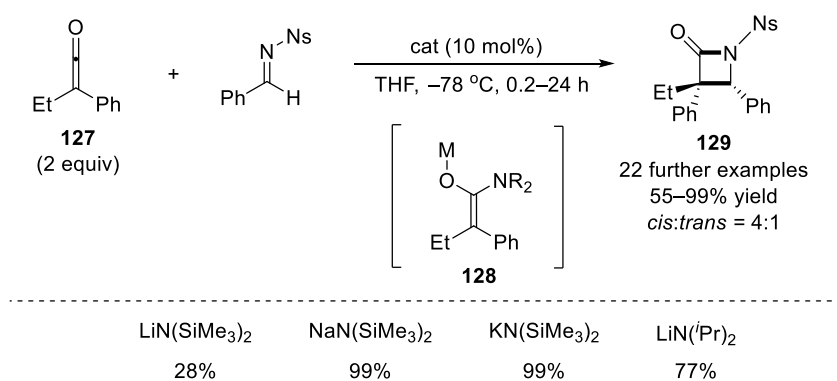
Apart from the Brønsted base catalysis examples above, alkali metal amides have also been used in redox chemistry. The Tishchenko reaction was reported to be catalysed by complexed lithium and potassium amides **I** and **II**, respectively (Scheme 41).^[118, 119] The first step involved the redox reaction between the first aldehyde and metal amide to form primary metal alkoxide **A**, which underwent C–O bond formation with the second aldehyde to form intermediate **B**. The latter reacted with the first aldehyde in a cyclic closed transition state (**L**) to form ester products of type **126**, with regeneration of metal alkoxide **C**.



Scheme 41: Tishchenko Reactions Initiated by Alkali Metal Amides.

Lewis Base Catalysis

Alkali metal amides were also used in Lewis base catalysis. In 2009, Wilhelm and co-workers reported Staudinger reactions between ketenes of type **127** and *N*-nosyl-protected imines (Scheme 42).^[120] The amide added to the electrophilic carbon centre of **127** to form metal enolates of type **128**, which then underwent [2+2] cycloaddition with imines to afford β -lactams of type **129** in 55–99% yields with predominant *cis*-configuration. Another example of alkali metal amide Lewis base catalysis was reported by Itoh and co-workers in C–Si bond formation.^[121]



Scheme 42: Staudinger Reactions Catalysed by Alkali Metal Amides.

Aims

Oxidative allylic C(sp³)–H bond activation often resulted in a high-oxidation state metal–allyl species with an intrinsic *electrophilic* character (Figure 1). Our research aimed at forming a *nucleophilic* allyl–metal species directly *via* C–H bond activation through concerted deprotonation/metalation (anion metathesis). Thus, we sought a single metal Lewis acid–Brønsted base dual catalyst to realise this goal.

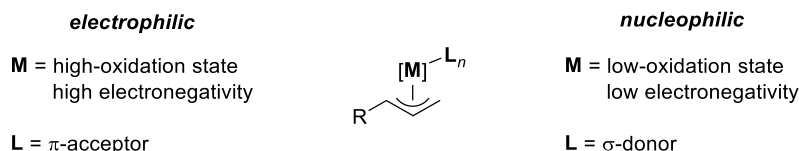
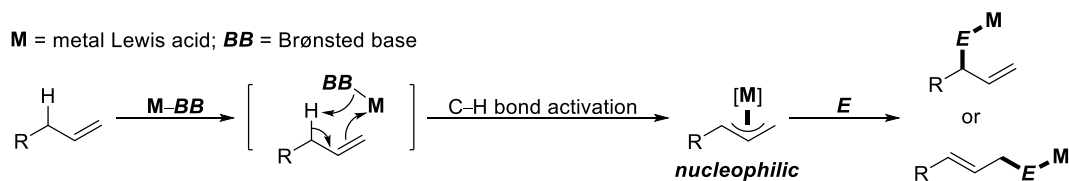


Figure 1: Allyl–Metal Species of Opposite Intrinsic Reactivity.

The Lewis acidic metal may coordinate to the C=C double bond to facilitate the deprotonative C–H bond activation by the Brønsted basic ligand (Scheme 1). This deprotonation/metalation may lead to the formation of a nucleophilic allyl–metal species. Both reactivity and selectivity of such intermediate may be controlled by: the ligand by which the metal centre is coordinated; the substituents at the carbon atom bearing the non-acidic hydrogen; the nature of the reaction solvent; the reaction temperature. This nucleophilic allyl–metal species may be trapped by a neutral electrophile *E*. In the case of π -electrophiles such as carbonyl (C=O) and imine (C=N–PG) compounds, the C–C bond formation would result in the generation of a product-base (alkoxide or amide). If the conjugate acid of that product-base has a similar p*K*_a value compared to the conjugate acid of the Brønsted basic ligand, the Lewis acid–Brønsted base catalyst may be regenerated (catalysis). Alternatively, if the conjugate acid of that product-base has a similar p*K*_a value as the pro-nucleophile (acid), the allyl–metal nucleophile may be regenerated (initiation). The metal choice has been dictated by industrial needs to be “green” first-row transition metals such as iron (Fe), copper (Cu), zinc (Zn), and cheap main group metals. It was anticipated that an asymmetric version of such transformations might be realised through the use of an appropriate enantiopure ligand and/or counteranion; likewise regarding the control of both regio- and diastereoselectivity.



Scheme 1: Deprotonative C–H Bond Activation Through Lewis Acid–Brønsted Base Dual Catalysis.

Fluorinated substrates were of particular interest (Figure 2). Beside the medicinal chemistry interest,^[122] a fluorinated pro-nucleophile may have a lower activation energy and thus a lower p*K*_a value for the allylic C(sp³)–H bond. However, the nucleophilicity of such a fluorinated allyl–metal species may be compromised. A careful selection of both the metal catalyst *and* the electrophile may be a key to balance these two critical points.

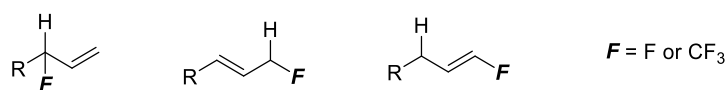
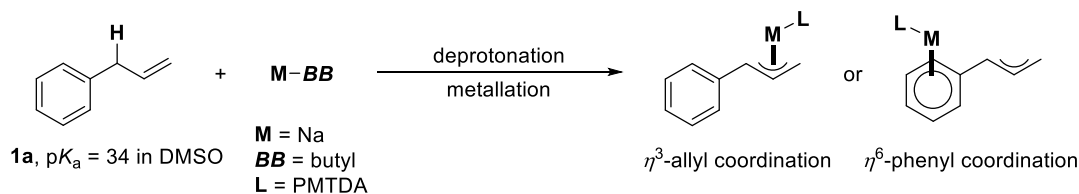


Figure 2: Potential Fluorinated Allylic Pro-Nucleophiles.

1 Allylic C(sp³)–H Bond Activation of Alkenes Triggered by a Sodium Amide

1.1 Allylic C(sp³)–H Bond Activation of Fluorinated Pro-Nucleophiles

The pK_a value of allyl benzene (**1a**) was calculated to be around 34 (in DMSO),^[123] making **1a** a challenging substrate for C–H bond activation. However, once deprotonated the generated metal–carbanion species may be stabilised through metal complexation by the allyl and/or the phenyl moieties. Indeed, the metallated (phenyl)allyl species was reported to exist as either η^3 -allyl or η^6 -phenyl complexes depending on the steric demand of the allyl substituent (Scheme 1).^[124]



Scheme 1: Coordination Modes of a (Ph)Allyl–Metal Species.

In terms of fluorinated allyl benzenes (**1b**, **2–4**), an electron-withdrawing inductive effect (–I effect) may increase the acidity of the allylic hydrogen atom, thus facilitating C–H bond activation (Figure 1). In addition, such an electron-withdrawing substituent may help further to stabilize the generated allyl–metal species.

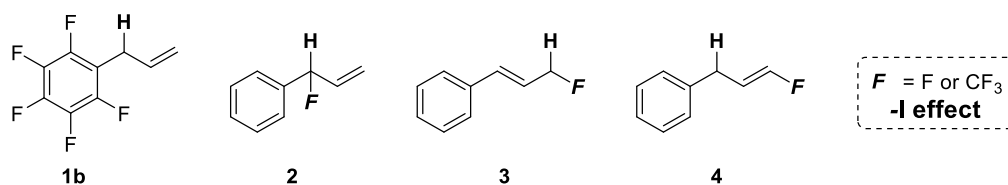
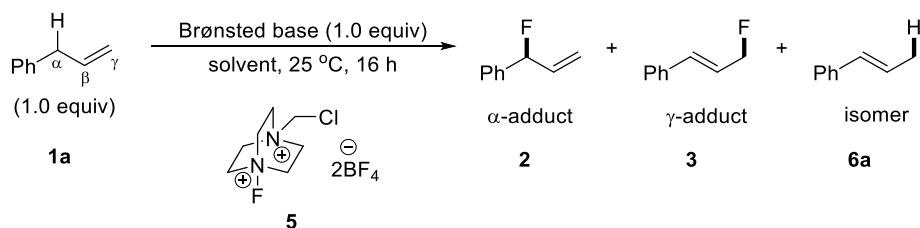


Figure 1: Fluorinated (Phenyl)Allylbenzene.

1.1.1 Attempted Syntheses of Fluorinated Pro-Nucleophiles

Substrates **2** and **3** ($F = F$) are not commercially available; thus, these compounds had to be synthesised. In turn, allyl benzene (**1a**) was treated with a few strong Brønsted bases in the presence of Selectfluor[®] (**5**; 1 equiv) at 25 °C (Table 1). The reaction was carried out in a glove box due to the moisture sensitivity of the Brønsted bases used. Considering the high pK_a values of the conjugate acids of these bases, we anticipated that deprotonation in allylic position may occur to generate the corresponding allyl anion; the latter may then react with Selectfluor[®] (**5**) to generate the intended fluorinated molecule. Due to the amphiphilic nature of the allylic anion, the resulting regioselectivity (α or γ) for the C–F bond formation was anticipated to be controlled by an appropriate choice of base, solvent, and ligand.

Table 1: Attempted Synthesis of Fluorinated Pro-Nucleophiles.

entry	Brønsted base	solvent	conv ^[a] to 6a	<i>E</i> : <i>Z</i>
1	NaH	THF	NR ^[b]	–
2	NaH	DMAc	65	>10:1
3	KH	THF	66	>10:1
4	KH	DMAc	30 ^[c]	ND ^[d]
5	KN(SiMe ₃) ₂	THF	>99	>19:1
6	KN(SiMe ₃) ₂	MeCN	>99	>19:1
7	KN(SiMe ₃) ₂	DMAc	80	>19:1

^[a] The conversions and geometric selectivities were determined by ¹H NMR spectroscopic analysis of a reaction aliquot (without using an internal standard). ^[b] NR = no reaction; the intended products **2** and **3** were not detected – only starting materials were recovered (¹H NMR spectroscopic analysis of a reaction aliquot). ^[c] The conversion was the combined conversion to **6a** and other side-products (¹H NMR spectroscopic analysis of a reaction aliquot). ^[d] ND = not determined; the geometric selectivity was not determined.

A stoichiometric amount of a hydride or amide base was used in a variety of solvents at 25 °C for 16 h; the ¹H NMR spectroscopic analysis of the corresponding reaction aliquots revealed that the intended C–F bond formation did not occur in any of these experiments. The use of NaH in THF gave full recovery of allyl benzene, likely due to the hydride's poor solubility (entry 1). When using a more polar solvent, dimethyl acetamide (DMAc), the terminal alkene substrate underwent isomerisation to give β -methyl styrene (**6a**) predominantly as the *E* isomer (65% conv, *E*:*Z* = >10:1; entry 2). The use of KH in THF gave 66% conversion to **6a** (*E*:*Z* = >10:1; entry 3). When switching the solvent to DMAc, a messy ¹H NMR spectrum was obtained indicating the formation of **6a** (30% conv) and other side-products (entry 4). Next, a potassium amide was used in various solvents. The conversion to **6a** was significantly improved to 80–99% (*E*:*Z* = >19:1; entries 5–7). Regarding the synthesis of **2** and **3**, only catalytic methods at a 0.2 mmol-scale without isolation have been reported.^[125] In the ¹H NMR spectroscopic analysis of our reaction aliquots, the signal of the geometric isomers of the internal alkene product, (*E*)-**6a** (δ = 6.4 ppm and δ = 6.2 ppm, 1H each; dq, J_E = 15.8, 6.8 Hz) and (*Z*)-**6a** (δ = 5.8 ppm, 1H; dq, J_Z = 11.5, 6.8 Hz), were detected and quantified by integration of the corresponding β -hydrogen atom.^[126] None of these signals overlapped with any of the signals from the starting material (allyl benzene; δ = 6.0 ppm).

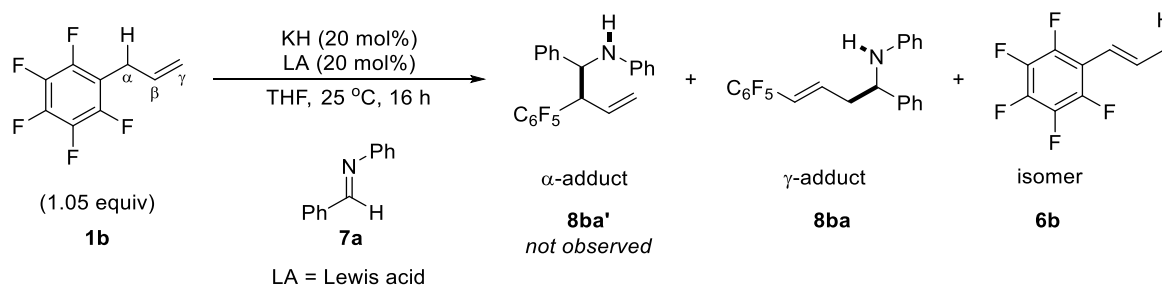
While the C–F bond formation has proved unsuccessful, the isomerisation of allyl benzene (**1a**) *per se* has shown a promising potential for the clean generation of an allyl anion intermediate through the use of an alkali metal amide. The next step was to use this highly nucleophilic species for addition to a suitable carbon electrophile in order to achieve C–C bond formation.

1.1.2 Preliminary Catalysis Results Using Allyl Perfluorobenzene

The Combined use of K–H and Metal Lewis Acids

The commercially available allyl perfluorobenzene (**1b**) was used for the intended Lewis acid–Brønsted base (LA–BB) dual catalysis (Table 2).

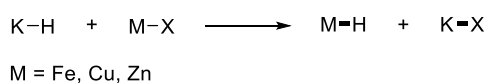
Table 2: Initial Experiments Using K–H in the Absence or Presence of a Metal Lewis Acid (LA).



entry	LA	conv ^[a] to 8ba (%)	conv ^[a] to 6b (%)
1	–	36	27
2	Fe(OTf) ₂	33	26
3	Fe(OTf) ₃	33	30
4	(CuOTf) ₂ •PhMe	NR ^[b]	–
5	Cu(OTf) ₂	NR ^[b]	–
6	Zn(OTf) ₂	33	33

^[a] The conversions and geometric selectivities were determined by ¹H NMR spectroscopic analysis of a reaction aliquot (without using an internal standard). ^[b] NR = no reaction; the intended product **8ba** was not detected – only starting materials were recovered (¹H NMR spectroscopic analysis of a reaction aliquot).

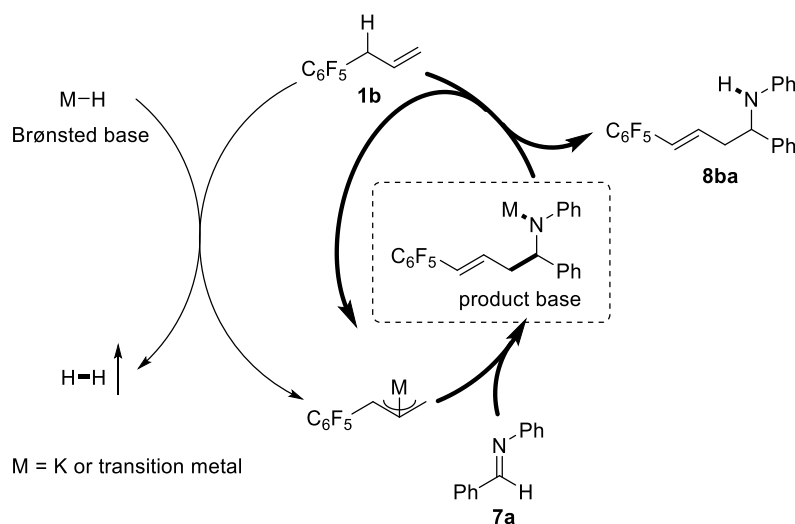
The *N*-Ph-protected aldimine **7a** was selected as electrophile and K–H was used as Brønsted base mediator (20 mol%) in the absence or presence of a first-row transition metal Lewis acid M–X (Fe, Cu, Zn; 20 mol%). It was anticipated that an anion metathesis may generate *in situ* K–X and the corresponding transition metal hydride M–H, which may display a more suitable acid–base dual character (Scheme 2).



Scheme 2: Envisioned Anion Metathesis.

In this scenario, the allylic proton of **1b** would be removed by the metal hydride, and the formed allyl–M nucleophile would add to electrophilic imine **7a**. Fe, Cu, and Zn ions, being stronger Lewis acids than K⁺, were expected to activate the Lewis basic substrate **7a** more effectively in view of the intended C–C bond formation. The model reaction was monitored by ¹H NMR spectroscopic analysis of the corresponding reaction aliquot (Table 2). In all cases, both C–C bond formation between **1b** and **7a** as well as isomerisation of **1b** were detected with the exception of the Cu-containing reaction mixtures (entries 1–6). Regarding C–C bond formation, the ¹H NMR charts revealed the formation of γ-adduct (*E*)-**8ba** with characteristic signals at: δ = 6.5 ppm and δ = 6.4 ppm for both alkenyl hydrogen atoms (d, *J_E* = 17.6 Hz); δ = 4.9 ppm for the benzylic hydrogen atom; δ = 2.8 ppm for both allylic hydrogen atoms. Regarding the isomerisation process, internal alkene (*E*)-**6b** displayed characteristic signals at: δ = 6.5 ppm (d, *J_E* = 16.2 Hz) for one of the alkenyl hydrogen atoms; δ = 1.6 ppm (d, *J* = 6.9 Hz) for

the methyl group; these data were in agreement with the literature.^[126] It is noted that the potential formation of the α -adduct or the other geometric isomers (*Z*)-**8ba** or (*Z*)-**6b** were *not* observed in any of these experiments. When K–H was used as the sole Brønsted base, γ -adduct **8ba** (36% conv) was observed together with the isomerisation product, β -methyl styrene (**6b**; 27% conv; entry 1). When Fe or Zn Lewis acids were used together with K–H, similar results were obtained (entries 2–3 and 6); the transition metal salt did not seem to display any significant effect on the reaction outcome. In contrast, the combined use of K–H and Cu(I) or Cu(II) species completely shut down the reaction (entries 4 and 5).

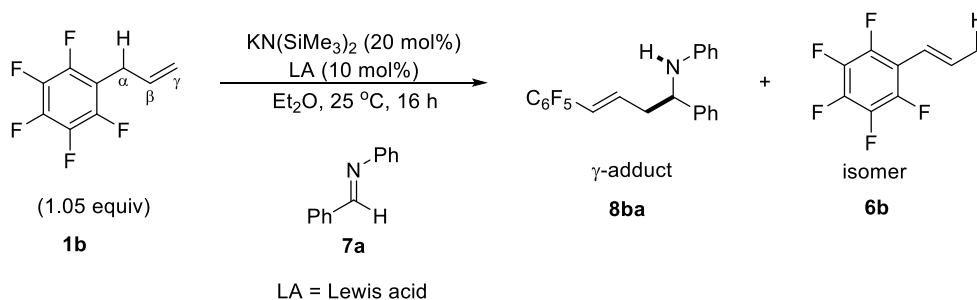


Scheme 3: Proposed Mechanistic Scenario with the Product-Base as Catalytic Key Intermediate.

Regarding a plausible reaction mechanism, the acidic allylic hydrogen of **1b** may be initially taken by the hydride base, thus producing hydrogen gas ($pK_a = >49$ in THF, extrapolated),^[127] which may be considered ‘out of the system’ (\sim inaccessible conjugate acid; Scheme 3).^[128] The *in situ*-generated allyl–metal species may then attack imine **7a** to form the corresponding product-base. If the reaction goes through an initiation pathway, the generated *product-base* would act as a Brønsted base to directly regenerate from **1b** the nucleophilic allyl–metal species, which would lead to a turnover number (TON) of >1 (bold part; Scheme 3). Alternatively, if the reaction went through a catalysis pathway, the formed product-base would have to deprotonate the conjugate acid of KH, hydrogen gas, in order to regenerate the base catalyst; such a turnover would not be possible here thus leading to a TON = 1. According to the obtained result, the TON was around 1~2 (36% conversion with 20 mol% KH); it may not be conclusive enough to rule out any pathway mentioned above. Further experiments were required.

The Combined use of K–N(SiMe₃)₂ and Metal Lewis Acids

Since the conjugate acid of a hydride base would ‘be out of the system’, a milder Brønsted base was selected next to examine the reaction outcome. The use of a metal hexamethyldisilazide, M–N(SiMe₃)₂ ($pK_a = 26$ in THF and 30 in DMSO),^[129] was one option; the initial screening revealed that a turnover could indeed be obtained by using a solution of KN(SiMe₃)₂ (0.5 M in PhMe) as a sole catalyst in ether (65% NMR yield; Table 3, entry 1). In contrast, the combined use of the potassium amide and Fe or Cu salts resulted in the formation of **8ba** in lower NMR yield (entries 2–5); the use of Zn(II) did not seem to have a significant effect on the reaction outcome (entry 6). It was concluded that transition metal salts were *not* required for this C–C bond formation; an alkali metal amide was shown to be sufficient for a TON of >6 .

Table 3: First Catalytic Results Using K–N(SiMe₃)₂ in the Absence or Presence of a Metal Lewis Acid (LA).

entry	LA	yield ^[a] of 8ba (%)	yield ^[a] of 6b (%)
1	–	65	10
2	Fe(OTf) ₂	51	1
3	Fe(OTf) ₃	NR ^[b]	–
4	(CuOTf) ₂ •PhMe	30	4
5	Cu(OTf) ₂	52	10
6	Zn(OTf) ₂	67	3

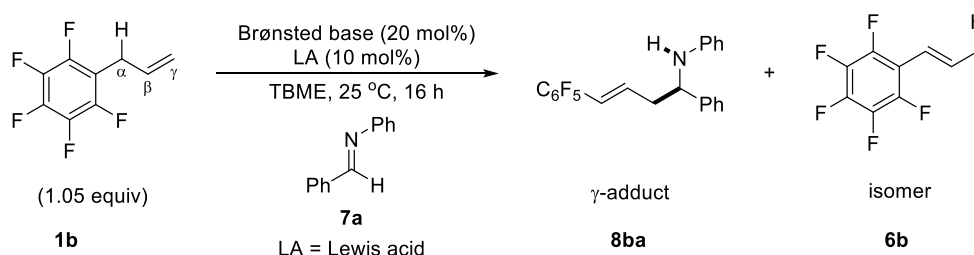
^[a] The yields and geometric selectivities were determined by ¹H NMR spectroscopic analysis of a reaction aliquot; internal standard: dibenzyl ether (25 mol%). ^[b] NR = no reaction; the intended product **8ba** was not detected – only starting materials were recovered (¹H NMR spectroscopic analysis of a reaction aliquot).

These data were to some extent unexpected with respect to the initial plan, where a more Lewis acidic transition metal ion was anticipated to facilitate C–C bond formation through: (1) coordination to the soft C–C double bond to increase the acidity of the allylic hydrogen atom; (2) coordination to the imine to enhance its electrophilicity. The poor reactivity observed for the use of transition metal salts may be ascribed to: (1) the lower polarity of the transition metal amide bond; (2) the lack of reactivity of the *in situ*-generated allyl–transition metal species. The corresponding Pauling electronegativity of Fe ($\chi = 1.8$), Cu ($\chi = 1.9$), and Zn ($\chi = 1.7$) is substantially higher than that of K ($\chi = 0.8$). Thus, if the anion exchange has occurred between KN(SiMe₃)₂ and the corresponding transition metal salt, the formed transition metal amide had to be significantly less reactive (basic) due to the less polarised M–N bond. In addition, the higher formal charges and the decreased ionic radii of Fe(II/III), Cu(II), and Zn (II) used in this scenario would increase the affinity between the nitrogen and the metal, therefore a weaker Brønsted basicity (reactivity) would be expected. The same reasoning may be used to explain the weaker nucleophilicity of the *in situ*-generated allyl–transition metal species.

The Combined Use of Different Alkali Metal–N(SiMe₃)₂ and Fe(II) Lewis Acids

In order to confirm that such type of transition metal has not favoured C–C bond formation, several alkali metal–N(SiMe₃)₂ were tested in the *presence* and *absence* of Fe(OTf)₂ in the reaction between allyl perfluorobenzene (**1b**) and aldimine **7a** (Table 4).

Table 4: Use of Different M–N(SiMe₃)₂ Catalysts in the Presence or Absence of an Iron(II) Lewis acid



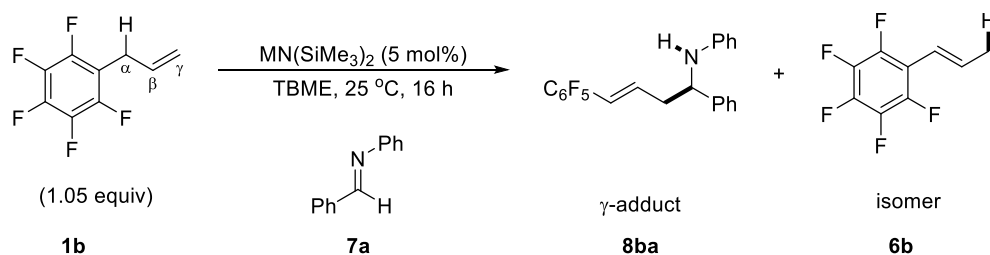
entry	Brønsted base	LA	yield ^[a] of 8ba (%)	yield ^[a] of 6b (%)
1	LiN(SiMe ₃) ₂	–	NR ^[b]	–
2	LiN(SiMe ₃) ₂	Fe(OTf) ₂	NR ^[b]	–
3	NaN(SiMe ₃) ₂	–	39	–
4	NaN(SiMe ₃) ₂	Fe(OTf) ₂	32	0~1
5	KN(SiMe ₃) ₂	–	27	1~2
6	KN(SiMe ₃) ₂	Fe(OTf) ₂	18	1~2

^[a] The yields and geometric selectivities were determined by ¹H NMR spectroscopic analysis of a reaction aliquot; internal standard: dibenzyl ether (25 mol%). ^[b] NR = no reaction; the intended product **8ba** was not detected – only starting materials were recovered (¹H NMR spectroscopic analysis of a reaction aliquot).

The use of LiN(SiMe₃)₂ (1.0 M in THF) alone did not lead to the formation of either the γ -adduct or the isomer (entry 1). When Fe(II) was used as a co-catalyst, the reaction did not proceed either (entry 2). However, the reaction proceeded to form of γ -adduct **8ba** in 39% NMR yield when NaN(SiMe₃)₂ (1.0 M in THF) was used as the catalyst (entry 3). A similar result was observed when Fe(II) was added as a potential co-catalyst (entry 4). The use of KN(SiMe₃)₂ (0.5 M in toluene) led to the formation of **8ba** in 27% NMR yield, together with 1–2% of isomerisation side-product (*E*)-**6b** (entry 5). The additional use of Fe(II) decreased the NMR yield to 18% (entry 6). The formation of (*Z*)-**8ba** or (*Z*)-**6b** was *not* observed. These data revealed that Fe(II) was not a beneficial co-catalyst in this C–C bond formation, at least under these mild reaction conditions. The fact that the use of NaN(SiMe₃)₂ gave both the highest product yield and the best product selectivity may be ascribed to the stronger Lewis acidity (Na vs. K) and the stronger Brønsted basicity (Na vs. Li) of the sodium amide.

The Sole Use of Alkali Metal–N(SiMe₃)₂

At that stage, the following commercially available sources were used: KN(SiMe₃)₂ in PhMe; NaN(SiMe₃)₂ in THF; LiN(SiMe₃)₂ in THF. However, the additional solvent –even in small amounts– may play a role in terms of reactivity and selectivity. For instance, THF may act as a Lewis basic ligand for the metal cation thereby decreasing its Lewis acidity. Thus, at 5 mol% catalyst loading under standard conditions, LiN(SiMe₃)₂, NaN(SiMe₃)₂, and KN(SiMe₃)₂ were used in different ‘states’, i.e., as a solid or in solution in various solvents and at different concentrations (Table 5). Here again, the formation of (*Z*)-**8ba** or (*Z*)-**6b** (C–C bond formation or isomerisation) was *not* observed.

Table 5: Screening of M–N(SiMe₃)₂ in Different ‘States’.

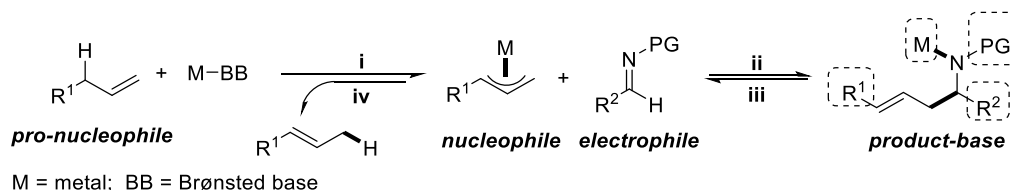
entry	M	State	yield ^[a] of 8ba (%)	yield ^[a] of 6b (%)
1	Li	solid	–	–
2	Li	1 M in THF	–	–
3	Na	solid	42	–
4	Na	1 M in THF	38	–
5	Na	0.6 M in PhMe	32	2
6	K	solid	20	1
7	K	1 M in THF	28	1
8	K	0.5 M in PhMe	15	1

^[a] The yields and geometric selectivities were determined by ¹H NMR spectroscopic analysis of a reaction aliquot; internal standard: dibenzyl ether (25 mol%). ^[b] NR = no reaction; the intended product **8ba** was not detected – only starting materials were recovered (¹H NMR spectroscopic analysis of a reaction aliquot).

The use of LiN(SiMe₃)₂ did not lead at all to the formation of product **8ba** (entries 1 and 2). In contrast, the use of NaN(SiMe₃)₂ as a solid gave **8ba** in 42% yield (TON >8; entry 3). The use of NaN(SiMe₃)₂ solutions gave slightly less good results (entries 4 and 5). Interestingly, the use of KN(SiMe₃)₂, as a solid or in solution, did not give better results either (entries 6–8). In summary, NaN(SiMe₃)₂ –as a solid– was selected as the catalyst of choice for further investigations.

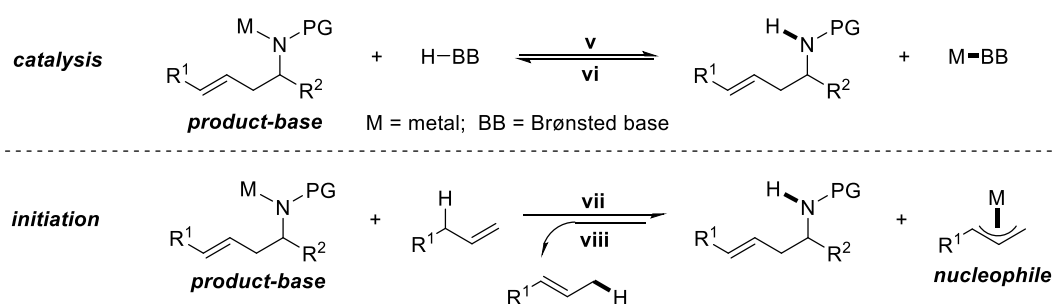
1.2 Alkali Metal Amide-Catalysed Allylic C(sp³)-H Bond Activation

In order to expand the alkali metal amide catalysis to a significant scope, allyl benzene (**1a**) was selected as the pro-nucleophile of choice for a model study. Allylbenzene (**1a**) has a higher pK_a value than allyl perfluorobenzene (**1b**), thus it must be considered a more challenging substrate. According to the proposed reaction flow-chart, the use of **1b**–R¹ (C₆F₅) being more electron-deficient– led to a more stabilised nucleophile (Scheme 4). As a result, step **i** may be favoured over step **iv**, thus the isomerisation (C–H bond formation; *undesired*) would be suppressed. However, the decreased electron density of such an allylic anion could also decrease its intrinsic nucleophilicity, thus leading as well to a lower level of C–C bond formation (step **ii**; *desired*). If allyl benzene (**1a**) was used as a pro-nucleophile, the electron density on R¹ may be increased, which may lead to a more reactive nucleophile; step **ii** may be favoured. However at the same time, the level of isomerisation (step **iv**) may be increased as well. Apart from the influence of the R¹ group, step **i** and **iv** may be also affected by the Lewis acidic metal cation and the Brønsted basic anion. Likewise, step **ii** may be affected by the electrophile, where the *N*-protecting group (PG) and R² may be critical parameters. In terms of step **iii**, it may depend on the metal, the *N*-protecting group, R¹, and R². Generally, electron-rich *N*-protecting groups and/or R¹ / R² substituents may favour steps **iii** and **iv**.



Scheme 4: Reaction Flow-Chart.

Regarding the catalyst regeneration, both pathways (catalysis and initiation) proceeded through a proton transfer step (Scheme 5). It is conceivable that the basicity (reactivity) of the product-base may play a critical role in this context. To be more specific, an electron-rich *N*-protecting group and/or R¹ / R² substituents may lead to a faster catalyst turnover; while electron-poor ones may lead to a slower turnover, or even a termination of the catalytic cycle.

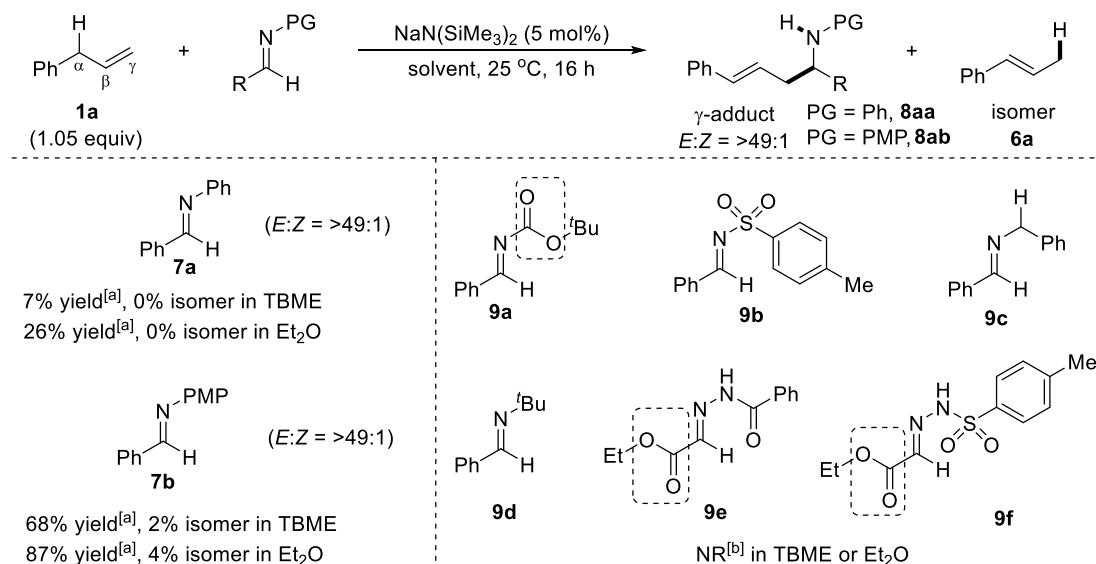


Scheme 5: Catalyst Regeneration.

Thus, the parameters mentioned above (*N*-protecting group, Lewis acidic metal cation, Brønsted basic anion, R¹, R²) and other potential factors were examined in the following sections.

1.2.1 Influence of the *N*-Protecting Group

First, the optimised conditions for the use of allyl perfluorobenzene (**1b**) [NaN(SiMe₃)₂ as catalyst in *tert*-butyl methyl ether (TBME) as solvent] were applied to the reaction between allyl benzene (**1a**) and a variety of benzaldehyde-derived imines bearing different *N*-protecting groups (Scheme 6).



^[a] The yields and geometric selectivities were determined by ¹H NMR spectroscopic analysis of a reaction aliquot; internal standard: dibenzyl ether (25 mol%). ^[b] NR = no reaction; the intended products **8aa** or **8ab** were not detected – only starting materials were recovered (¹H NMR spectroscopic analysis of a reaction aliquot).

Scheme 6: Screening of *N*-Protecting Groups for the Initial Study Using Allyl Benzene as a Pro-Nucleophile.

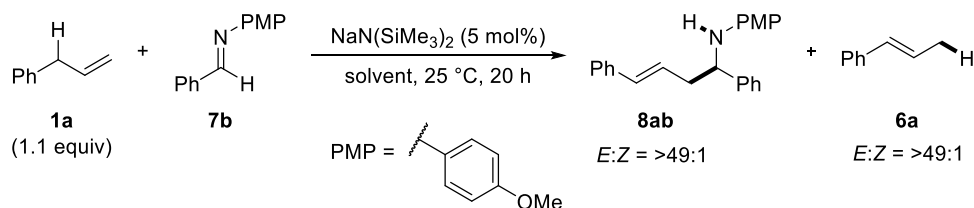
Only the phenyl- and paramethoxyphenyl (PMP)-protected aldimines gave the corresponding γ -adducts **8aa** and **8ab** in 7% and 68% NMR yields, respectively. These results were improved when the solvent was changed to diethyl ether (Et₂O); the use of the PMP-protected imine gave (*E*)-**8ab** in 87% NMR yield, which was considered very promising. In all cases, only 1–2% of the corresponding *Z* isomer were observed, thus providing an *E*:*Z* ratio of >49:1. This result indicated that a polar solvent may increase significantly the reactivity of NaN(SiMe₃)₂ without a decrease in selectivity. In addition, the electron-donating effect of OMe as a substituent on the aromatic ring (*N*-protecting group) may lead to higher rate of turnover, and thus a higher yield of **8ab**. Surprisingly, the use of a more electrophilic *N*-Boc imine, **9a**, did not lead to any product formation, which may point toward an intolerance of the carbamate group regarding the sodium amide catalyst. Alternatively, the reaction may proceed in a reversible manner (favouring the retro-reaction). However, if the reaction was reversible, the isomerization side-product, β -methyl styrene [(*E*)-**6a**], should have been observed instead of allyl benzene (**1a**). The non-reactivity of the benzyl-protected imine **9c** and the two hydrazones **9e** and **9f** may be explained with the presence of acidic hydrogen atoms in these cases; a proton source may indeed decompose the Brønsted base catalyst. On the other hand, the *tert*-butyl-protected imine **9d** may be not sufficiently electrophilic due to the stronger electron-donating effect of a *tert*-butyl group (vs. Bn or Ar).

1.2.2 Solvent Screening

The fact that Et₂O outperformed TBME in the protecting group screening suggested that a more polar solvent may increase the reactivity of NaN(SiMe₃)₂ and potentially of the product-base. However it noted the solubility of the

catalyst and the imine would be important factors to consider as well. Thus, several ether-type solvents were screened in the reaction between allyl benzene (**1a**) and the *N*-PMP-protected imine **7b** (Table 6). Yields were assigned by ¹H NMR spectroscopy, where integration of the alkenyl, benzylic, and allylic hydrogen signals gave reliable data for the yield of the C–C bond formation: δ = 6.5 and 6.1 ppm (*J_E* = 15.8 Hz); δ = 4.4 ppm; δ = 2.7 and 2.6 ppm. Further signals of the PMP (δ = 6.7 and 6.5 ppm) and the N–H (δ = 3.9 ppm) groups could be detected as well. Isomerised product **6a** was quantified by the integration of the ¹H NMR signals in the alkenyl region (δ = 6.2 ppm) if the allylic region (δ = 1.8 ppm) overlapped with solvent signals (e.g. in the case of THF).

Table 6: Solvent Screening for the Use of PMP-Imine as an Electrophile.



entry	solvent (ε)	yield ^[a] of 8ab (%)	yield ^[a] of 6a (%)
1	dioxane (2.3)	99	4
2	TBME (2.6)	68	2
3	Et ₂ O (4.3)	87	4
4	DME (7.2)	14	28
5	THF (7.5)	17	62

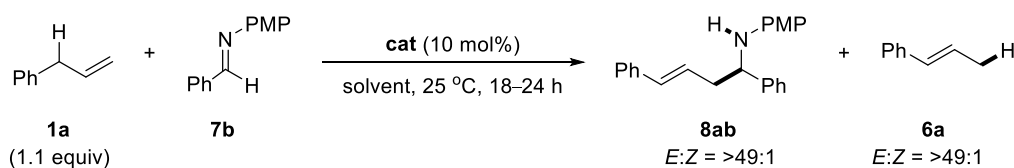
^[a] The yields and geometric selectivities were determined by ¹H NMR spectroscopic analysis of a reaction aliquot of the reaction mixture; internal standard: dibenzyl ether (25 mol%).

The reaction in dioxane gave 99% C–C bond formation alongside 4% isomerisation (entry 1). Good yields and selectivities were also achieved in TBME and Et₂O (entries 2 and 3). A high level of isomerisation was favoured when more polar solvents such as DME (28%) and THF (62%) were used (entries 4 and 5). Thus, dioxane has shown a significant advantage over ethereal solvents.

Dioxane has the lowest polarity among these ethereal solvents, which was in contrast to our initial assumption. It is noted that dioxane did show a better solubility of both the metal amide and the imine, which might be a key for the high product yield obtained. The advantage of ethereal solvents may be ascribed to their Lewis basic nature, thus leading to an enhanced amide Brønsted basicity. However, the increase of the Lewis basicity of the solvent may also decrease significantly the Lewis acidity of the metal cation, which could have a detrimental effect on the reaction outcome.

1.2.3 Screening of Metal–Brønsted Bases

In order to examine the importance of the nature of the metal ion in the amide catalyst, i.e., to demonstrate or not the unique character of sodium (Na) vs. other metals, a screening of metal–Brønsted bases was carried out at 10 mol% catalyst loading (Table 7).

Table 7: Screening of Various Metal–Amides.

entry	M–BB	yield ^[a] of 8ab / 6a (%)	
		in dioxane	in THF
1	LiN ⁱ Pr ₂	NR ^[b]	56 / 13
2	LiTMP	NR ^[b]	32 / 2
3	LiN(SiMe ₃) ₂	NR ^[b]	42 / 4
4	NaN(SiMe ₃) ₂	98 / 5	40 / 0
5	KN(SiMe ₃) ₂	23 / 44	0 / 37
6	M[N(SiMe ₃) ₂] ₂	NR ^[b]	NR ^[b]
	M = Mg, Ca ^[c] , Sr ^[c] , Sn ^[c]		
7	MN(SiMe ₃) ₂	NR ^[b]	–
	M = Cu ^[c] , Ag ^[c]		
8 ^[c]	M[N(SiMe ₃) ₂] ₂	NR ^[b]	–
	M = Zn		
9 ^[c]	M[N(SiMe ₃) ₂] ₃	NR ^[b]	–
	M = Ce, Eu, Gd		
10	LiMe	14 / 2	62 / 22
11	LiBu	10 / 0	74 / 18
12	MgBu ₂	NR ^[b]	NR ^[b]

^[a] The yields and geometric selectivities were determined by ¹H NMR spectroscopic analysis of a reaction aliquot; internal standard: dibenzyl ether (25 mol%). ^[b] NR = no reaction; the intended product **8ab** was not detected – only starting materials were recovered (¹H NMR spectroscopic analysis of a reaction aliquot). ^[c] These experiments were carried out by *Hanno Kossen*.

In dioxane, the lithium amide catalysts showed no reactivity at room temperature (entry 1–3). However, excellent results were obtained using NaN(SiMe₃)₂, which showed a good balance between activity and selectivity for γ -adduct **8ab** (entry 4). The stronger base KN(SiMe₃)₂ was shown to be less effective as a much higher level of isomerisation product **6a** was observed (entry 5). Alkaline earth metal amides^[130] showed no reactivity in dioxane (entry 6). The reaction did not proceed either when using transition metal amides based on Cu(I), Ag(I), and Zn(II) (entries 7 and 8). Likewise, the use of f-block metal amides proved inefficient (entry 9). Regarding alkyl bases, the use of LiMe and LiBu led to the formation of **8ab** in low NMR yields (entries 10 and 11). Finally, the use of MgBu₂ did not afford any product (entry 12). It is noted that the results in THF were to some extent better for lithium amides and alkyl lithium reagents. *However, overall NaN(SiMe₃)₂ proved to be by far the most effective catalyst for this challenging transformation.*

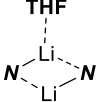
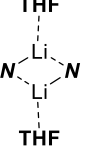
These results of the NaN(SiMe₃)₂ Brønsted base or dual catalysis in C–C bond formation may be considered remarkable when compared to literature precedence. For instance, LiN(SiMe₃)₂ was used stoichiometrically to generate *in situ* from allyl benzene (**1a**) an allyl–Li species that underwent Li-to-Pd transmetalation for subsequent C–C cross-coupling reactions;^[131] however, the observed regioselectivity in C–C bond formation was

opposite compared to our work (branched vs. linear). As shown, the catalytic use of $\text{LiN}(\text{SiMe}_3)_2$ in our reaction proved to be inefficient. The only example of using $\text{NaN}(\text{SiMe}_3)_2$ as a sole catalyst in C–C bond formation was the Lewis base-catalysed Staudinger reaction (Scheme 42, page 32).^[120] In the same line, $\text{KN}(\text{SiMe}_3)_2$ was used as a Brønsted base in α -C–H deprotonation of amides and esters for subsequent asymmetric conjugate addition (Scheme 39; page 30).^[114] As shown, the catalytic use of $\text{KN}(\text{SiMe}_3)_2$ in our reaction proved to be inefficient for C–C bond formation. Likewise, the catalytic use of *various other metal* amides proved to be ineffective in our challenging reaction system under mild conditions, although some of these compounds were reported to function as a catalyst in a variety of contexts: (1) $\text{Ca}[\text{N}(\text{SiMe}_3)_2]_2$ was reported to activate the N–H bond of amines for hydroamination;^[132] (2) $\text{Sr}[\text{N}(\text{SiMe}_3)_2]_2$ was reported to activate the α -C–H bond of malonates for conjugate addition;^[133] (3) group 11-metal amides [Cu(I), Ag] were reported to activate the C–H bond of terminal alkynes for cycloaddition;^[134] (4) $\text{AgN}(\text{SiMe}_3)_2$ was reported to trigger a direct [3+2] cycloaddition between olefins and α -aminophosphonates;^[108] (5) f-block metal amides (Y, La, Nd, Sm, Gd, Yb) were reported to activate the C2–H bond of pyridines for a Mannich-type addition.^[135] Thus, the successful catalytic use of a sodium amide *exclusively* in our reaction system is fairly remarkable.

In addition, our work is also clearly distinct from reported imino-ene chemistry (Scheme 25, page 23): (1) the imino-ene reaction was shown to be catalysed by a Lewis acid, whereas our reaction system relies on Brønsted base or acid–base dual catalysis; (2) a highly electrophilic glyoxylate-derived imine was shown to be critical in the imino-ene reaction (bidentate coordination to Cu^+), which contrasts sharply our results; (3) the connectivity of the terminal olefin used in the imino-ene reaction is different from allyl benzene used in our study; (4) the imino-ene reaction proceeds *via* a cyclic closed transition state without the involvement of a nucleophilic C–M species.

The lack of reactivity of $\text{LiN}(\text{SiMe}_3)_2$ compared with $\text{NaN}(\text{SiMe}_3)_2$ may be explained by the metal cation effect: the ionic radius of lithium (~ 70 pm) is smaller than that of sodium (~ 100 pm), leading to a stronger Li–N bond (2.01 Å) compared to the Na–N bond (2.40 – 2.45 Å).^[136] As a result, the reactivity of a sodium amide base would be expected higher than that of a lithium amide base. In terms of Brønsted acidity, the $\text{p}K_{\text{a}}$ value of HN^iPr_2 is around 36 in THF; the $\text{p}K_{\text{a}}$ value of HTMP is around 39 in DMSO; the $\text{p}K_{\text{a}}$ value of $\text{HN}(\text{SiMe}_3)_2$ is around 26 in THF and 30 in DMSO.^[129] Thus, $\text{M–N}^i\text{Pr}_2$ and M–TMP are expected stronger bases than $\text{M–N}(\text{SiMe}_3)_2$. However, it was also reported that the strength of the M–N bond depends on the nature of the metal, regardless of the amide. The reactivity of LiN^iPr_2 and LiTMP remained low in dioxane regardless of their strongly Brønsted basic amides. However in THF, the higher polarity and stronger coordinating ability of the solvent may lower the dissociation energy of the amide anion, thus increasing the reactivity of the Li–amides. The solvent effect may lead to a ‘break down’ of the Li–N aggregation, and even the liberation of the ‘free’ amide anion, thus the Brønsted basic activity increased. In this context, the structural properties of the three different lithium amides were recently compared by Mulvey and Robertson (Table 8).^[137]

Table 8: Structure of Lithium and Sodium Amides in Different Solvents.

solvent	$\text{LiN}(\text{SiMe}_3)_2$	LiN^iPr_2	LiTMP
toluene / hexane	dimer	trimer/oligomer	oligomer
THF (<1.0 equiv)	disolvated dimer	mono & disolvated dimer	monomer and dimer
THF (>1.0 equiv)	monomer (di-, tri-, or tetramer)	disolvated dimer	monomer and dimer
<div style="display: flex; justify-content: space-around; align-items: center;"> <div style="text-align: center;">  <p>monosolvated dimer</p> </div> <div style="text-align: center;">  <p>disolvated dimer</p> </div> <div> $\text{N} = \text{NR}_2$ </div> </div>			

$\text{LiN}(\text{SiMe}_3)_2$ was observed as dimer in apolar solvents such as toluene and hexane, while LiN^iPr_2 and LiTMP were aggregated as oligomeric species. THF could solvate the aggregations of these Li-amides even in a sub-stoichiometric amount. Monomeric species were observed for $\text{LiN}(\text{SiMe}_3)_2$ and LiTMP in THF; dimeric species were observed for LiN^iPr_2 . These data may give some hint to explain why the used sodium amide demonstrated the highest yield of intended product **8ab** (C–C bond formation) and a very low yield of side-product **6a** (isomerisation).

1.2.4 Screening of Metal-Free Organic Brønsted Bases

Finally, metal-free conditions were investigated in order to confirm, the necessity of a metal cation for a successful C–C bond formation. Indeed, it may be possible that the postulated allylic anion intermediate (π Lewis base) and/or the imine electrophile (σ Lewis base) may require the presence of a coordinating metal cation (Lewis acid) to favour C–C bond formation. In this context, there has been a literature precedent for the use of organobases in the isomerisation of allyl benzene derivatives.^[138] In turn, organic superbases such as Schwesinger's *N*-centered bases and Verkade's *P*-centered bases were tested in the model reaction under 'standard' conditions (Table 9).

Table 9: Use of Organic Superbases in the Model Reaction.

Reaction scheme: **1a** (1.05 equiv) + **7b** $\xrightarrow[\text{solvent, 25 } ^\circ\text{C, 16 h}]{\text{organobase (10 mol\%)}}$ **8ab** (γ -adduct, $E:Z = >49:1$) + **6a** (isomer)

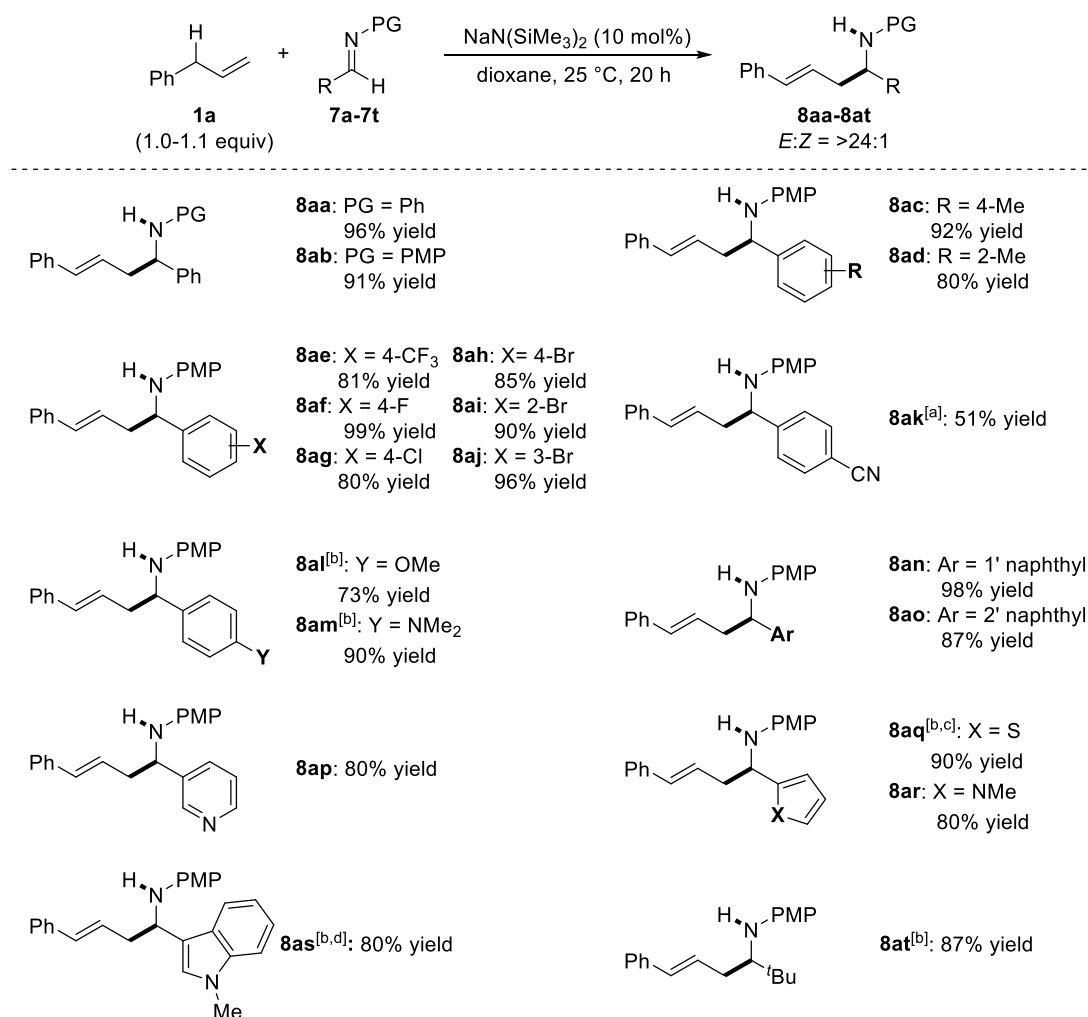
entry	organobase	R	yield ^[a] of 8ab (%)	yield ^[a] of 6a (%)
1		Me	NR ^[b]	
2	P₁	–(CH ₂) ₄ –	NR ^[b]	
3		Et	0	69
4		<i>t</i> Bu	NR ^[b]	–
	P₂			
5		–	0	64 ^[c]
	P₄			
6 ^[d]		Me	NR ^[b]	–
7 ^[d]		<i>i</i> Pr	NR ^[b]	–
8 ^[d]		<i>t</i> Bu	NR ^[b]	–

^[a] The yields and geometric selectivities were determined by ¹H NMR spectroscopic analysis of a reaction aliquot; internal standard: dibenzyl ether (25 mol%). ^[b] NR = no reaction; the intended product **8ab** was not detected – only starting materials were recovered (¹H NMR spectroscopic analysis of a reaction aliquot). ^[c] Decomposition of imine **7b** was detected. ^[d] These experiments were carried out by *Hanno Kossen*.

No intended product **8ab** was observed at all (entries 1–8). Isomer **6a** was obtained in 69% NMR yield when Schwesinger's *P*₂-Et base was used (entry 3). Likewise, the use Schwesinger's *P*₄-*t*Bu base gave **6a** in 64% NMR yield, alongside with decomposition of imine **7b** (entry 5). The use of other Schwesinger or Verkade bases displayed no reactivity at all (entries 1–2, 4, and 6–8). These data showed that a metal cation may be required not only for the stabilisation of the allylic anion, but also for the activation of the imine.

1.2.5 Substrate Scope for Imines

To test the utility of the reaction, the optimised conditions using **1a** were applied to the use of various imine electrophiles (Scheme 7).



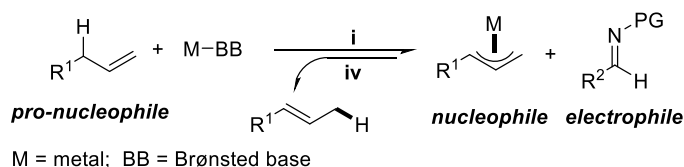
The yields refer to the isolated yields after PTLC purification; *E:Z* ratios were determined after isolation based on ^1H NMR spectroscopic analysis of the purified products. ^[a] 3.0 equiv of allylbenzene **1a** was used. ^[b] Allylbenzene (**1a**, 1.2–2.0 equiv) was added progressively in three portions over 20 h. ^[c] The reaction was carried out at 60 °C for 72 h. ^[d] This reaction was done by *Hanno Kossen*.

Scheme 7: Aldimine Scope.

N-Ph-protected aldimine **7a** and *N*-PMP-protected aldimine **7b** both reacted smoothly to afford intended products **8aa** and **8ab** in 96% and 91% yield, respectively. 4-Me-substituted aldimine **7c** gave a better yield of **8ac** than the 2-Me-substituted aldimine **7d**. The lower yield was likely ascribed to the increased steric hindrance in **7d**.

Electron-withdrawing substituents generally performed very well: 4- CF_3 , 4-F, 4-Cl, 4-Br, 3-Br, and 2-Br gave the intended products (**8ae–8aj**) in excellent yields (80–99%). Even the very challenging 4-CN-substituted aldimine **7k** was converted to **8ak** in 51% yield. The lower yield is likely due to the sensitivity of the CN group under basic conditions, thus the catalyst $\text{NaN}(\text{SiMe}_3)_2$ may have been deactivated partially. However, the nitrile functional group is extremely versatile, and this result must be considered as promising considering the complexity of this transformation.

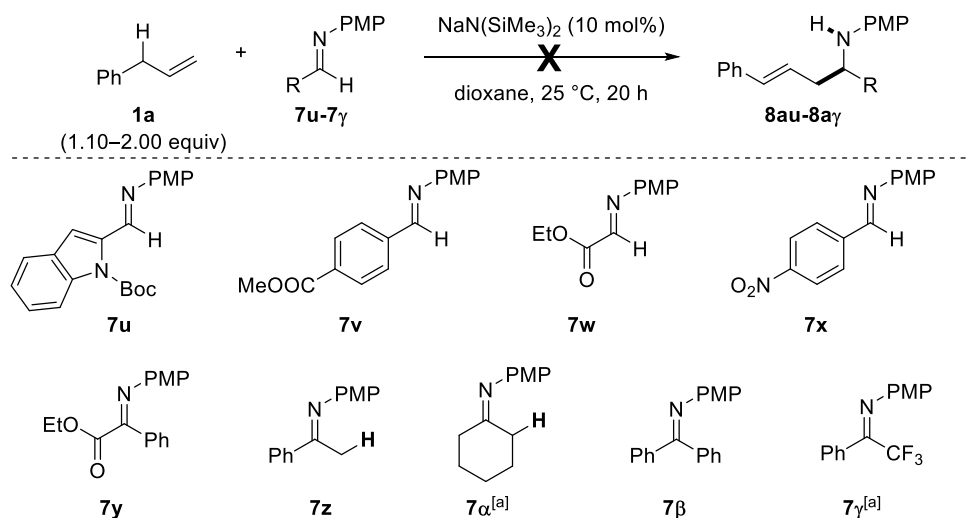
Aldimines with electron-donating substituents display a lower electrophilicity. Thus, the ability of trapping the nucleophilic allyl-M species would be compromised (Scheme 8). The relatively high concentration of the nucleophile might push the reaction backwards, in which case step **iv** would be favoured. As a result, a high level of isomerisation may be observed. In order to address this issue, a higher concentration of the pro-nucleophile might be required to push the reaction to the right side (step **i**).



Scheme 8: Reaction Flow-Chart.

Indeed, aldimines with OMe and NMe₂ substituents at the *para*-position did not react effectively when the pro-nucleophile was present in equimolar quantities. Instead, the use of up to 2.0 equiv of allyl benzene (**1a**) led to the formation of **8al** and **8am** in 73% and 90% yields, respectively. For the 1- and 2-naphthyl-substituted products **8an** and **8ao**, 98% and 87% yields were obtained, respectively.

The electron-poor 3-pyridyl aldimine reacted smoothly to afford product **8ap** in 80% yield. Here, it is worth mentioning that 2- and 4-pyridyl-derived aldimines have proved ineffective in this reaction (around 10% conversion). Regarding electron-rich heteroaromatic aldimines, the thienyl aldimine showed a relatively low level of isomerisation (compared with EDG-substituted aldimines), which allowed the reaction to be carried out at 60 °C. As a result, product **8aq** was isolated in 90% yield. Pyrrole product **8ar** was also formed in 80% yield (*E:Z* = 49:1). Indole product **8as** was most efficiently formed by using a successive addition mode of **1a** (80%). Importantly, an *aliphatic* aldimine (*tert*-butyl-substituted) was converted to product **8ap** in 87% yield.



[a] This reaction was done by Hanno Kossen.

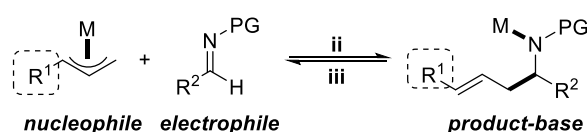
Scheme 9: Unsuccessful Imine Electrophiles.

A few imines have proved unsuccessful under the optimised conditions (Scheme 9). The Boc functionality (**7u**) already displayed an intolerance in the earlier study regarding the *N*-protecting group screening. This is likely due to the sensitivity of the ester-type moiety under basic conditions. Indeed, the ester group was also not tolerated under the reaction conditions (**7v**, **7w**, and **7y**). Nitro-substituted aldimine **7x** also showed no reactivity, which

may be ascribed to the sensitive nitro group. Ketimines **7z** and **7a** bear relatively acidic hydrogen next to the C=N group, therefore the Brønsted basic catalyst was likely deactivated. A high level of isomerisation was observed when ketimines **7β** and **7γ** were used, which may be ascribed to their relatively low electrophilicity.

1.2.6 Other Aromatic Allyl Pro-Nucleophiles

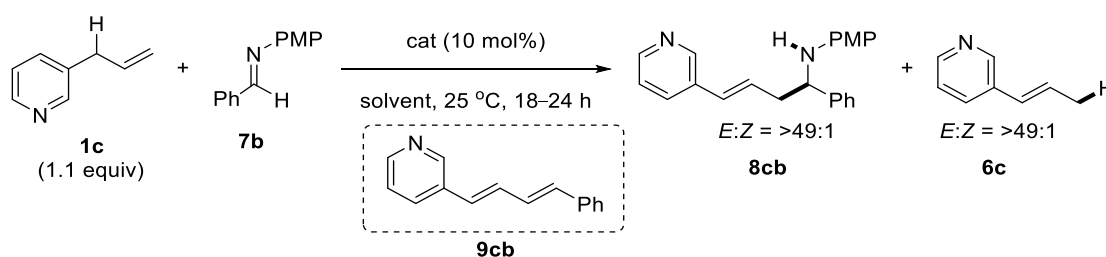
As proposed earlier, the R¹ group of the pro-nucleophile may influence the reactivity and configuration of the nucleophilic allyl–M species, as well as the reactivity of the product-base (Scheme 10). This is to say, configuration-wise, a less hindered R¹ group may lead to a lower geometric selectivity of the final product; reactivity-wise, an electron-poor R¹ group may lead to a lower nucleophilicity of the allyl–M species. In these cases, a modification of the metal–Brønsted base, solvent, and electrophile might be required to maintain high yields and selectivities.



Scheme 10: Reaction Flow-Chart.

First, an electron-poor heteroaromatic pro-nucleophile, 3-allyl pyridine (**1c**), was used instead of allyl benzene (Table 10).

Table 10: Use of 3-Allyl Pyridine as Pro-Nucleophile.



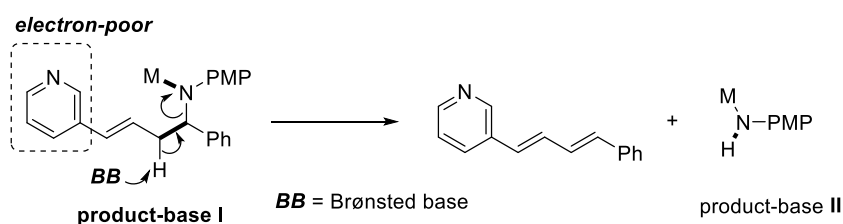
entry	cat	solvent (ε)	yield ^[a] of 8cb (%)	yield ^[a] of 6c (%)	yield ^[a] of 9cb (%)
1	NaN(SiMe ₃) ₂	dioxane (2.3)	NR ^[b]	–	–
2	NaN(SiMe ₃) ₂	TBME (2.6)	77	10	9
3	NaN(SiMe ₃) ₂	Et ₂ O (4.3)	52	16	32
4	NaN(SiMe ₃) ₂	THF (7.5)	0	trace	86
5	LiN(SiMe ₃) ₂	dioxane	88	15	9
6	LiN(SiMe ₃) ₂	THF	18	8	49
7 ^[c]	NaN(SiMe ₃) ₂	dioxane	80	5	3

^[a] The yields and geometric selectivities were determined by ¹H NMR spectroscopic analysis of a reaction aliquot; internal standard: dibenzyl ether (25 mol%). ^[b] NR = no reaction; the intended product **8cb** was not detected – only starting materials were recovered (¹H NMR spectroscopic analysis of a reaction aliquot). ^[c] Ph-protected imine **7a** was used as an electrophile.

Unfortunately, the intended product was not formed when the optimised conditions were used (entry 1). We anticipated that a more polar solvent may be required to enhance the catalyst's Brønsted basicity. When TBME was used, the reaction proceeded to generate the intended product **8cb** in 77% NMR yield, with a small amount

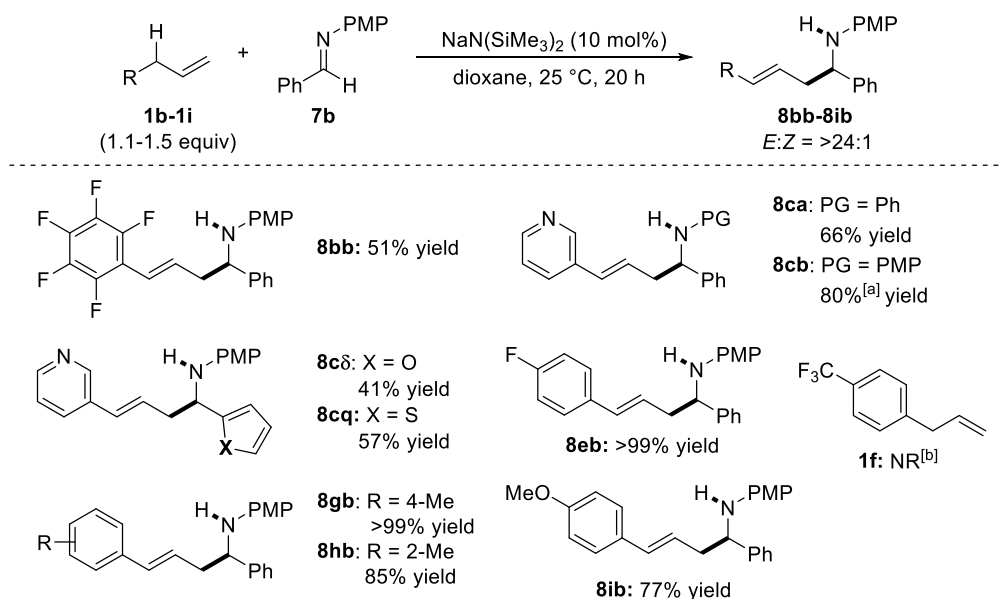
of isomerisation (10%) and dehydroamination (9%; entry 2). By using Et₂O, the yield of **8cb** dropped, with an increased levels of isomerisation (16%) and dehydroamination (32%; entry 3). A further increase of the polarity by using THF lead to an almost exclusive formation of the dehydroamination product **9cb** in 86% NMR yield (entry 4). **9cb** was isolated by PTLC and the ¹H NMR data was in agreement with literature.^[139] When a less reactive base, LiN(SiMe₃)₂, was used in dioxane, the NMR yield of product **8cb** was improved to 88% with good selectivity (entry 5). The use of LiN(SiMe₃)₂ in THF favoured again dehydroamination (entry 6). Also, in contrast to the *N*-PMP-protected imine **7b**, when *N*-Ph-protected imine **7a** was used under the optimized conditions, the reaction proceeded smoothly to form the γ -adduct in 80% NMR yield, alongside isomerisation and dehydroamination (entry 7). These results may suggest a kind of ‘matching effect’ between the pro-nucleophile, the metal–Brønsted base, and the electrophile. This is to say, the electron-poor (pyridyl) pro-nucleophile **1c** may be more suitable to a less reactive metal–Brønsted base; while the electron-poor (pyridyl) allyl–M species may require the more electrophilic imine **7a**.

It is noted that the primary amine H₂N–PMP was also observed in the ¹H NMR spectroscopic analysis of a reaction aliquot. Thus, it is conceivable that the dehydroamination step may occur *after* the formation of the initial product-base **I** (Scheme 11). The acidity of the benzylic hydrogen may be increased due to the electron-poor aromatic ring, thus an elimination reaction may be favoured. The dehydroamination reaction may go through E2 or E1cb mechanisms. The generated product-base **II** (pK_a = 30.5 in DMSO)^[140] may be protonated by pro-nucleophile **1c**, the conjugate acid of the base catalyst [HN(SiMe₃)₂], or the allylic hydrogen of product-base **I** to form the observed aniline by-product.



Scheme 11: Proposed Scenario of Dehydroamination.

Next, the scope of aromatic allyl pro-nucleophiles was investigated (Scheme 12). The perfluorinated product **8bb** was only formed in 51% yield. The decreased electron density of the allylic anion may decrease the nucleophilicity thus leading to a lower yield. When the 3-pyridine allyl pro-nucleophile (**1c**) was used to react with aldimines **7a** and **7b**, products **8ca** and **8cb** were formed in 60% and 80% yields, respectively. It is noted that the high-yielding formation of product **8cb** required the use of LiN(SiMe₃)₂ in dioxane or NaN(SiMe₃)₂ in TBME. Furthermore, **1c** was also used to couple with aldimine **7q** (thiophene) and **7d** (furan), thus affording products **8cq** and **8cd** in 57% and 41% yields, respectively. Complex amines bearing a C=C double bond and two *N*-heterocycles were formed in a single step. Furthermore, the presence of another heteroatom in the substrate and/or product may lead to additional catalyst coordination, which may be critical in view of asymmetric catalysis.



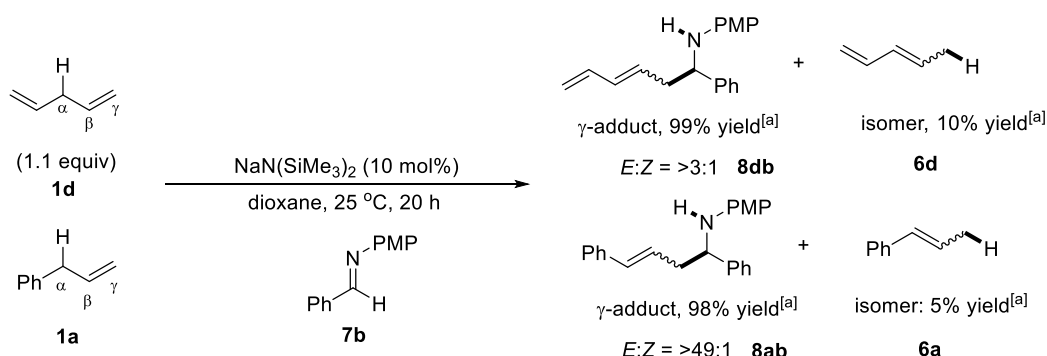
The yields refer to the isolated yields after PTLC purification; $E:Z$ ratios were determined after isolation based on ^1H NMR spectroscopic analysis of the purified products. ^[a] $\text{LiN}(\text{SiMe}_3)_2$ was used as the catalyst in the reaction. ^[b] NR = no reaction; the intended product was not detected – only starting materials were recovered (^1H NMR spectroscopic analysis of a reaction aliquot).

Scheme 12: Scope of Pro-Nucleophiles.

Next, EWG-substituted allyl benzene pro-nucleophiles were tested. While the 4-F-substituted pro-nucleophile resulted in the formation of product **8eb** in quantitative yield, its 4- CF_3 -substituted analogue (**1f**) proved unreactive. The Me-substituted products **8gb** and **8hb** were formed in quantitative yield and 85% yield, respectively. Finally, the use of EDG-substituted pro-nucleophile **1i** afforded product **8ib** in 77% yield.

1.2.7 Use of a Skipped Diene as Pro-Nucleophile

Next, 1,4-pentadiene (**1d**; $\text{p}K_{\text{a}} \sim 34$ in DMSO)^[99] was used as a pro-nucleophile in the model reaction (Scheme 13). This compound has a similar $\text{p}K_{\text{a}}$ value as allyl benzene. The acidity of the allylic hydrogen is the result of two conjugates allyl units. Using 10 mol% of $\text{NaN}(\text{SiMe}_3)_2$, the reaction between pentadiene **1d** and aldimine **7b** proceeded in quantitative yield.



^[a] The yields and geometric selectivities were determined by ^1H NMR spectroscopic analysis of a reaction aliquot; internal standard: dibenzyl ether (25 mol%).

Scheme 13: Use of 1,4-pentadiene as a pro-nucleophile.

The observed chemoselectivity for the use of 1,4-pentadiene was similar to the case of allyl benzene. However, the *E:Z* selectivity (for 1,4-pentadiene) was significantly decreased to >3:1 (compared to >49:1 for allyl benzene). This loss of geometric product selectivity may be ascribed to: (1) the sterically less demanding substituent (*vinyl* vs. *phenyl*) in the allyl–Na intermediate; (2) the possible existence of the generated allyl–Na species as a η^5 complex (vs. η^3 and η^1). In both cases, a higher level of *Z* isomer may be generated subsequently, thus decreasing the *E:Z* selectivity (Figure 2).

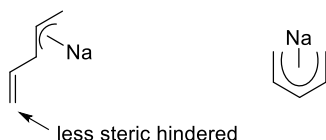
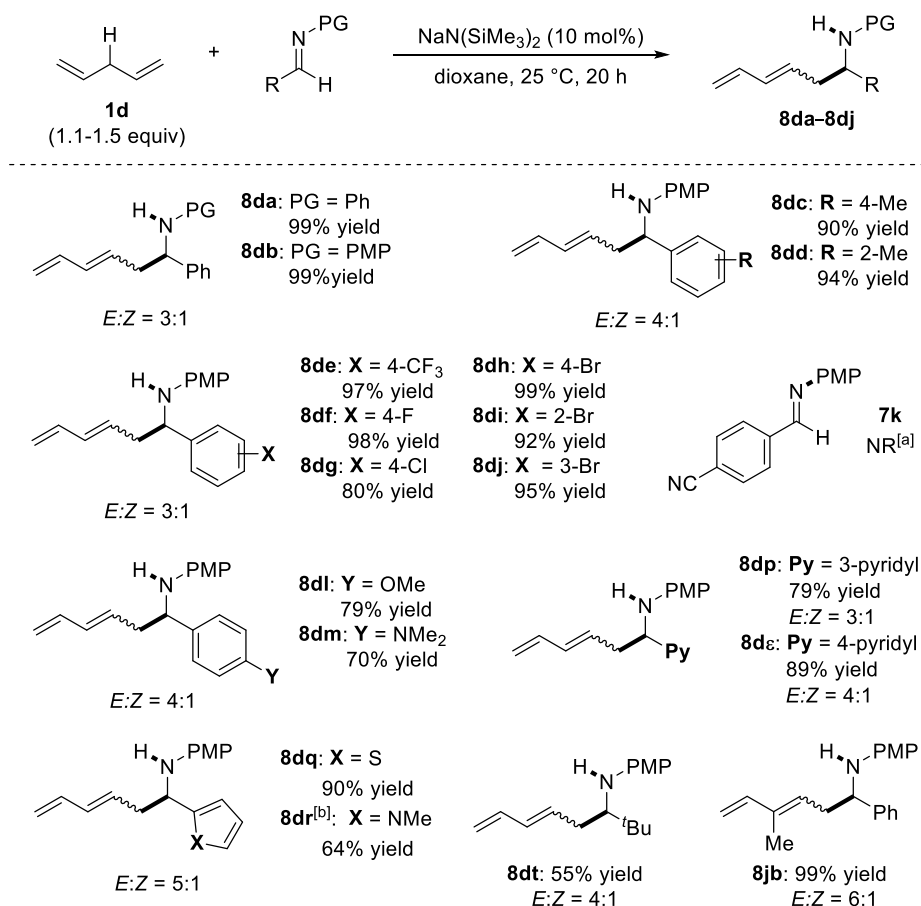


Figure 2: Possible Structures for an Allyl–Na Species Derived from 1,4-Pentadiene.

The scope for the use of 1,4-pentadiene (**1d**) as pro-nucleophile was investigated as well (Scheme 14). The earlier study revealed a much lower *E:Z* selectivity for product **8cb** when **1d** was used. A geometric selectivity of up to 5:1 was observed by reacting **1d** with various aldimines.



The yields refer to the isolated yields after PTLC purification; *E:Z* ratios were determined after isolation based on ¹H NMR spectroscopic analysis of the purified products. ^[a] NR = no reaction; the intended product was not detected – only starting materials were recovered (¹H NMR spectroscopic analysis of a reaction aliquot). ^[b] This reaction and isolation were carried out by *Hanno Kossen*.

Scheme 14: Scope for the Use of 1,4-Pentadienes as Pro-Nucleophiles.

The reaction between **1d** and aldimine **7a** proceeded to give **8da** in 99% yield, with a *E:Z* ratio of 3:1. Me-Substituted products **8dc** and **8dd** were also formed in excellent yields. EWG-Substituted aldimines reacted

smoothly with **1d**, affording products **8de–8dj** in 80–99% yields. CN-substituted aldimine **7k** proved to be unreactive. In terms of electron-donating substituents, a relatively high level of isomerisation was observed when using OMe- and NMe₂-substituted aldimines **7l** and **7m**. As a result, lower yields were obtained for products **8dl** and **8dm**. The electron-poor 3- and 4-pyridyl aldimines **7p** and **7ε** reacted effectively with **1d**, leading to the formation of **8dp** and **8dε** in 79% and 89% yields, respectively. When using electron-rich pyrrol aldimine **7r**, only 64% yield of **8dr** was obtained, which may be ascribed to the high level of isomerisation. Pivaldehyde-derived aldimine **7t** coupled with **1d** to form product **8dt** in 55% yield; this relatively low yield may be due to the decreased electrophilicity of **7t**. However, an increased selectivity of 6:1 was noted for the methyl-substituted product **8jb**. This slightly increased geometric selectivity may be explained by the enhanced steric hindrance of the Me group (Figure 3).

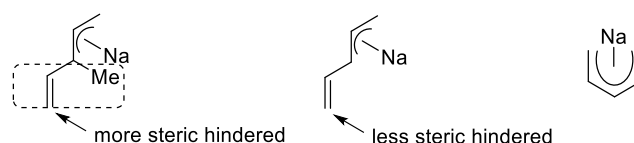


Figure 3: Proposed Steric Effect.

The geometric selectivity turned out to be the major concern regarding the use of pentadiene pro-nucleophiles **1d** and **1j**. To address this issue, the use of a ligand may affect the configuration of the allyl–metal intermediate, which may subsequently increase the geometric selectivity of the final product. Such investigation will be subject of future studies.

1.2.8 Unsuccessful Pro-Nucleophiles

Internal alkene **6a** contains a double bond in conjugation with the benzene ring thus providing a higher thermodynamic stability compared with allyl benzene (*terminal* alkene). However, the allyl–Na intermediate *in situ*-generated through deprotonation of allyl benzene (**1a**) was assumed to be identical to the Na species generated from β-methyl styrene (**6a**). Therefore, reactions with β-methyl styrene (**6a**) were conducted using imine **7b** as the electrophile (Table 11).

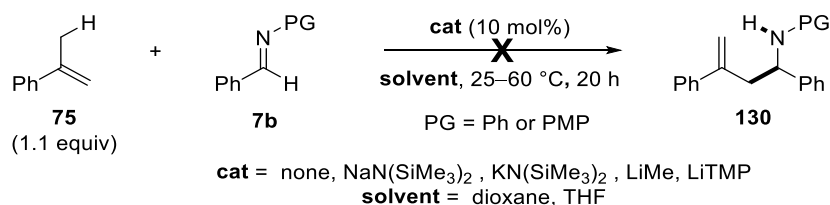
Table 11: Use of β-Methyl Styrene as a Pro-Nucleophile.

	6a (1.1 equiv)	7b			8ab <i>E:Z</i> = >49:1
entry	cat	ligand	solvent	T (°C)	yield ^[a] of 8ab (%)
1	NaN(SiMe ₃) ₂	-	dioxane	25–60	NR ^[b]
2	NaN(SiMe ₃) ₂ (100 mol%)	-	dioxane	25–60	22–38
3	KN(SiMe ₃) ₂	-	dioxane	25–40	NR ^[b]
4	KN(SiMe ₃) ₂	[18]c-6	dioxane	25	NR ^[b]
5	KN(SiMe ₃) ₂	[18]c-6	THF	25	NR ^[b]

^[a] The yields and geometric selectivities were determined by ¹H NMR spectroscopic analysis of a reaction aliquot; internal standard: dibenzyl ether (25 mol%). ^[b] NR = no reaction; the intended product **8ab** was not detected – only starting materials were recovered (¹H NMR spectroscopic analysis of a reaction aliquot).

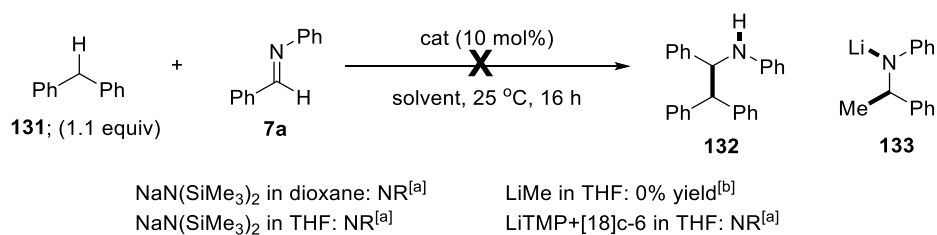
As expected, the reaction did not proceed under optimised conditions even after heating to 60 °C (entry 1). The use of a stoichiometric amount of $\text{NaN}(\text{SiMe}_3)_2$ led to the formation of the intended product in 22% NMR yield at 25 °C, and in 38% NMR yield at 60 °C (entry 2). The $\text{KN}(\text{SiMe}_3)_2$ -catalysed reaction at up to 40 °C in dioxane did not result in the formation of any products; only starting materials were observed in ^1H NMR spectroscopy (entry 3). The addition of a crown ether ligand also did not show the intended product formation in either dioxane or THF (entries 4 and 5). These results showed that the activation of styrene was possible, but required harsher reaction conditions or coordinating solvents. Furthermore, no branched product was observed in this reaction, suggesting that the reaction took place by deprotonation followed by the formation of the same allyl–M intermediate that was generated from allyl benzene.

In addition, the use of α -methyl styrene (**75**) was also tested as a pro-nucleophile (Scheme 15). This substrate was considered to be more challenging regarding a deprotonative allylic $\text{C}(\text{sp}^3)\text{--H}$ bond activation. The generated allylic anion would not be in conjugation to the benzene ring, and thus be substantially less stable. Such a styrene substrate has been previously activated in imino-ene reactions with highly activated imines (enophile) in the presence of a suitable copper(I) Lewis acid, or under heating conditions. However, in our hands, the C–C bond formation did not proceed in the absence of a catalyst by simply heating to 60 °C. The use of $\text{NaN}(\text{SiMe}_3)_2$, $\text{KN}(\text{SiMe}_3)_2$, LiMe, or LiTMP in either THF or dioxane did not result in any product formation, even after heating up to 60 °C. This failure may suggest that the imino-ene reaction using imine **7b** may require a too high activation energy to proceed.



Scheme 15: Use of α -Methyl Styrene as the Pro-Nucleophile.

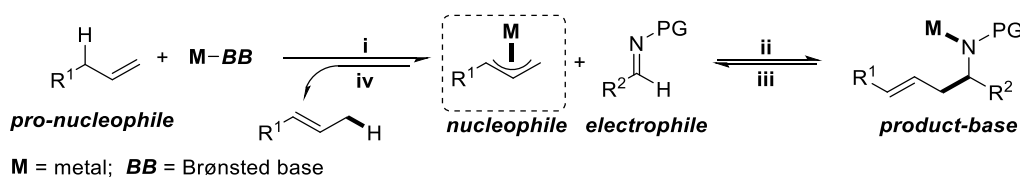
Diphenyl methane (**131**; $\text{p}K_a = 33$ in cyclohexylamine)^[141] has a similar acidity compared with allyl benzene (**1a**); and the corresponding carbonation can be stabilised by two phenyl rings. However, the C–C bond formation did *not* occur when diphenyl methane was used as pro-nucleophile under standard conditions [$\text{NaN}(\text{SiMe}_3)_2$ in dioxane; Scheme 16]. Product **132** was *not* observed when using $\text{NaN}(\text{SiMe}_3)_2$ in THF either. The use of 10 mol% of MeLi led to the methylation of the imine, resulting in the potential formation of **133** in 9% NMR yield; this lack of reactivity may be ascribed to a steric effect.



Scheme 16: Use of Diphenylmethane as a Pro-Nucleophile.

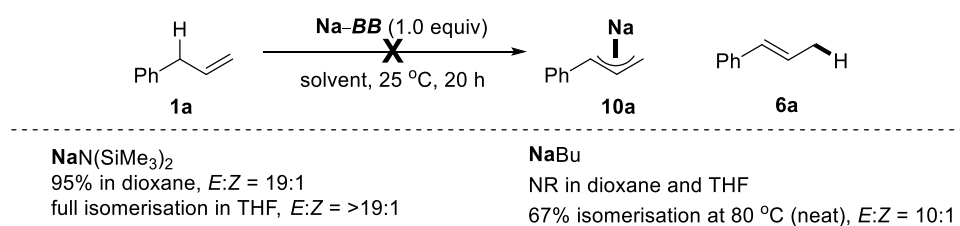
1.2.9 Investigations into the Reaction Mechanism

As discussed earlier, a key intermediate involved in the C–C bond formation should be the *in situ*-generated allyl–metal species (Scheme 17). The structure of such an intermediate may determine: (1) its intrinsic chemical reactivity (nucleophilicity); (2) its chemoselectivity towards an electrophile (reaction as *nucleophile*) or a proton source (reaction as *Brønsted base*); (3) the ‘allyl’ regioselectivity (α or γ) of the C–C(X) bond formation; (4) the geometric configuration (*E* or *Z*) of the ‘allylated’ product. In this context, two features may be considered critical regarding the precise structure of the *in situ* generated allyl–metal species: a) the structure of the pro-nucleophile (R^1 and/or additional substitution patterns); b) the nature of the metal *M*.



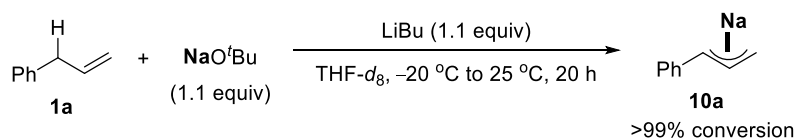
Scheme 17: Proposed Stepwise Procedure for C–C Bond Formation.

As $\text{NaN}(\text{SiMe}_3)_2$ has proved to be the most effective catalyst, the anticipated *in situ*-formed nucleophile should be an allyl–sodium species. In order to understand the structure of this compound, the synthesis of (Ph)allyl–Na (**10a**) was attempted (Scheme 18). However, using a stoichiometric amount of $\text{NaN}(\text{SiMe}_3)_2$ for the direct reaction with allyl benzene (**1a**) –in the absence of an electrophile– in dioxane at 25 °C for 20 h afforded exclusively the corresponding isomerization product **6a**, β -methyl styrene (~ full conversion). When $\text{BuNa}^{[142]}$ was used –instead of the sodium amide– in dioxane or THF, a reaction of **1a** was not observed at all; BuNa is likely too strong a Brønsted base and has presumably deprotonated (and/or ring-opened) these two cyclic ether solvents. When BuNa reacted with **1a** at 80 °C under solvent-free conditions, the starting terminal alkene was converted to internal alkene **6a** with 67% conversion; the observed *E:Z* ratio of the geometric isomers of **6a** was determined as ~ 10:1.



Scheme 18: Unsuccessful Synthesis of Allyl–Na by Using Sodium Amide or Alkyl Sodium Bases.

In our laboratory, NaBu has been prepared by *Jonathan Richards* through anion metathesis between LiBu and NaO'Bu in hexane.^[142] The driving force for this exchange reaction relies on the stronger affinity between *Li* and *O* (hard–hard interaction) as well as *Na* and *C* (soft–soft interaction).^[143] It is noted that (Ph)allyl–Li was synthesised according to a literature procedure by treating allyl benzene (**1a**) with BuLi in hexane.^[144] The good solubility of BuLi in hexane allowed for a smooth deprotonation. Thus, an alternative synthetic pathway was envisaged: the *in situ*-generated (Ph)allyl–Li species may react with NaO'Bu to undergo an anion exchange (–LiO'Bu) resulting in the formation of (Ph)allyl–Na (**10a**; Scheme 19). Indeed, when treating **1a** with NaO'Bu in a Young's NMR tube, followed by addition of BuLi at –20°C under an inert atmosphere, (Ph)allyl–Na (**10a**) was observed in NMR spectroscopy.



Scheme 19: Preparation of (Ph)Allyl–Na *via* an Anion Metathesis Procedure.

The obtained spectra (^1H NMR and ^{13}C NMR) displayed similar chemical shift and coupling constants compared to the reported (*E*)- η^3 -(Ph)allyl–Li species (**10b**), which was prepared independently.^[144] Thus, an η^3 coordination and *E* configuration was confirmed for (Ph)allyl–Na (**10a**) as well. In addition, ^{23}Na NMR spectroscopy was recorded for both the NaO^tBu (starting material) and **10a** (product), showing two distinct signals in the NMR charts: allyl–Na nucleophile **10a** displays a sharp signal at –5.3 ppm, which corresponds to a Na–C species. The signal at +15.3 ppm (Na–O species) for the used sodium reagent, NaO^tBu, entirely disappeared in this synthetic procedure (together with the full consumption of **1a** in ^1H NMR and ^{13}C NMR spectroscopy) suggesting a full conversion of NaO^tBu to allyl–Na nucleophile **10a** (Chart 1).

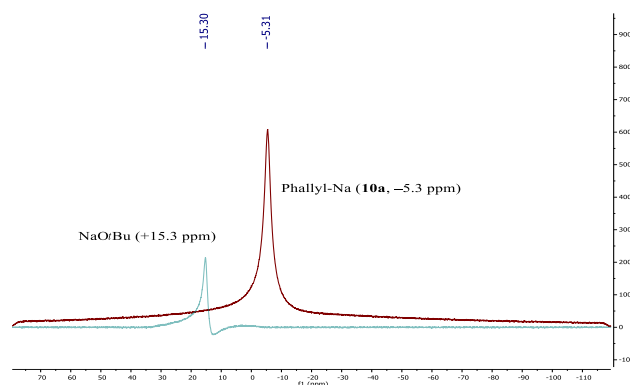
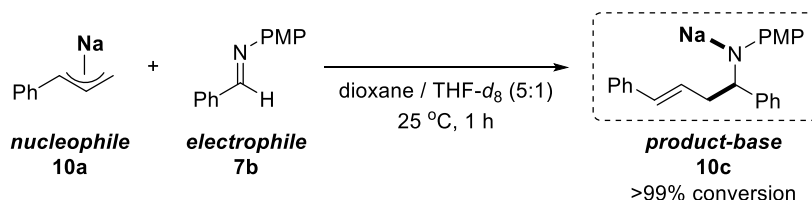


Chart 1: ^{23}Na NMR Spectroscopy of NaO^tBu (blue) and Species **10a** (red).

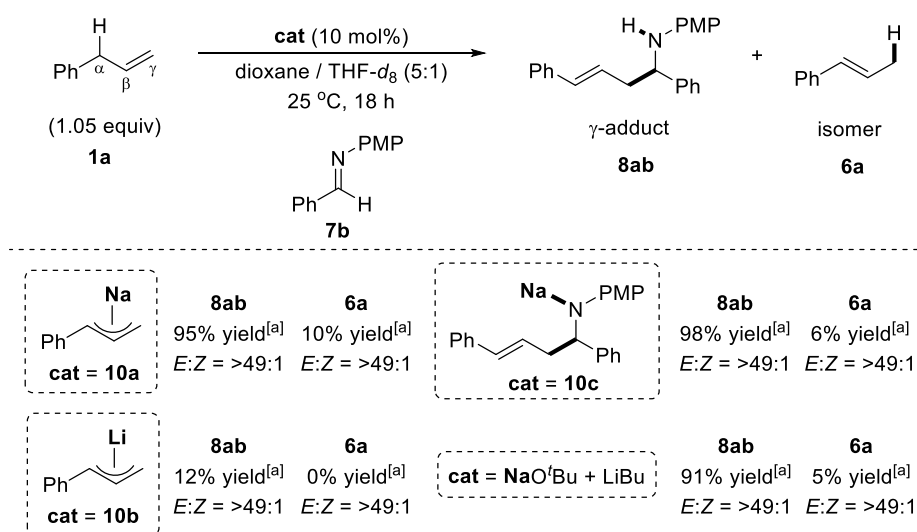
Next, following the reaction flow-chart, the addition of the imine electrophile **7b** may lead to the formation of another potential key intermediate, the product-base (Scheme 20). Thus, (Ph)allyl–Na species **10a** was treated with **7b** in dioxane. The reaction was performed in a Young’s NMR tube and monitored to confirm the full consumption of **10a** based on ^1H NMR and ^{23}Na NMR spectroscopy in only one hour. ^{23}Na NMR spectroscopy displayed the appearance of a broad signal at +4.9 ppm, referring to a Na–N species [reference: δ = +5.3 ppm for $\text{NaN}(\text{SiMe}_3)_2$]. Thus, product-base **10c** was formed smoothly under the mild standard reaction conditions.



Scheme 20: Formation of the Product-Base *via* Reaction with the Imine.

In order to determine the exact role of species **10a** and **10c** in typical catalysis, **10a** and **10c** were used independently in the catalytic model reaction between allyl benzene (**1a**) and imine **7b** in dioxane [in the absence of $\text{NaN}(\text{SiMe}_3)_2$; Scheme 21]. Because **10a** and **10c** were kept in a THF- d_8 solution, the reaction was actually conducted in a mixture solvent of dioxane and THF- d_8 (5:1). When using allyl–Na species **10a** as a catalyst (10 mol%), the reaction proceeded to form intended product **8ab** in 95% NMR yield, alongside isomerisation product

6a in 10% NMR yield; this result proved to be very similar to the data obtained in the $\text{NaN}(\text{SiMe}_3)_2$ catalysis. When product-base **10c** was used as a catalyst (10 mol%), intended product **8ab** was formed in 98% NMR yield, and isomer **6a** was generated in 6% NMR yield; here again, this result proved to be very similar to the data obtained in the $\text{NaN}(\text{SiMe}_3)_2$ catalysis. In contrast, the catalytic use of (Ph)allyl-Li (**10b**) (10 mol%) allowed for the formation of intended product **8ab** in only 12% NMR yield; this result stressed again the substantial difference between Na and Li bases and underlines the importance of the metal Lewis acid in this reaction system (dual catalysis). Finally, the combined use of NaO^tBu and LiBu (each 10 mol%) afforded intended product **8ab** in 91% NMR yield, together with isomer **6a** (5% NMR yield); here again, this result proved to be very similar to the data obtained in the $\text{NaN}(\text{SiMe}_3)_2$ catalysis.



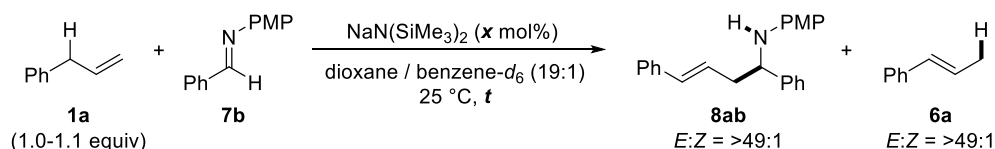
^[a] The yields and geometric selectivities were determined by ¹H NMR spectroscopic analysis of a reaction aliquot; internal standard: dibenzyl ether (25 mol%).

Scheme 21: Control Experiments for the Catalysis Using Different Catalysts.

These results clearly demonstrated that both (Ph)allyl-Na species **10a** and product-base **10c** must be critically important intermediates in the $\text{NaN}(\text{SiMe}_3)_2$ catalysis. Together with the successful result using a catalytic amount of NaO^tBu and LiBu, an initiation mechanism might be involved in this transformation. However, a ‘true’ catalysis pathway cannot be ruled out either at this stage.

1.2.10 Preliminary Kinetic Study

The preliminary kinetic study was performed with the $\text{NaN}(\text{SiMe}_3)_2$ -catalysed model reaction between alkene **1a** and imine **7b**, through monitoring the conversion of **7b** to **8ab** with ^1H NMR spectroscopy (500 MHz; Scheme 22). The detailed process is described in the experimental section.



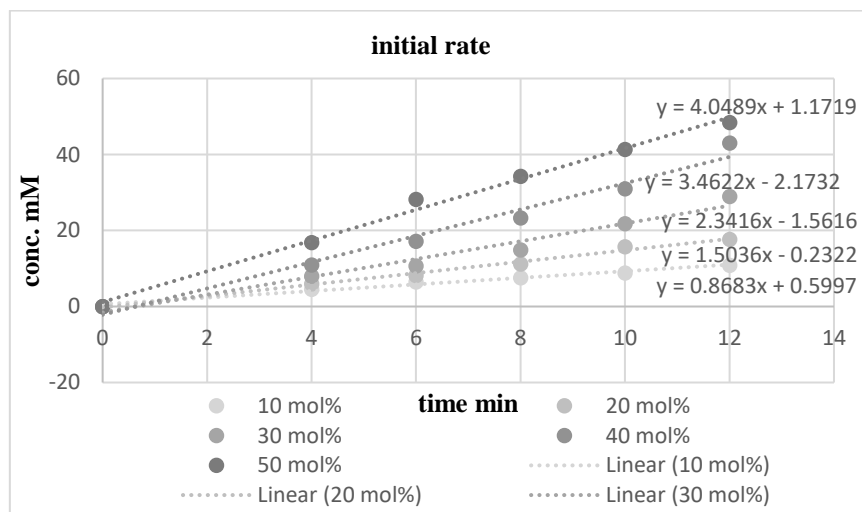
Scheme 22: Conditions for the Preliminary Kinetic Study.

Allyl benzene (**1a**) was added to the reaction mixture in the NMR tube right before introducing this NMR tube into the spectrometer, where it was kept throughout the whole reaction time; since the reaction mixture proved to be homogeneous, magnetic stirring was not required. The first ^1H NMR spectrum was recorded 4 min after the addition of **1a**; further spectra were then recorded every 2 min. Variations of the conditions for the model reaction were concerned with the catalyst loading [10–50 mol% of $\text{NaN}(\text{SiMe}_3)_2$]. The amount of product **8ab** generated was initially calculated in area units relative to the recovered imine **7b**, before converting these units into the concentration of product **8ab**.

Rate Calculation (12 min)

The profiles for the model reaction using 10 mol%, 20 mol%, 30 mol%, 40 mol%, and 50 mol% of $\text{NaN}(\text{SiMe}_3)_2$ are displayed in Figure 4, showing the corresponding concentration of generated product **8ab** vs. the reaction time for a specific catalyst loading.

Figure 4: Product Concentration vs. Reaction Time [10–50 mol% loading in $\text{NaN}(\text{SiMe}_3)_2$].



Calculation of Reaction Order n

The accurate experimental data for these reactions, calculated by the indicated generally used formula for both reaction rate (r) and reaction order (n), are displayed in Table 12. These data are visualized with a plot for the determination of the reaction order (n) in catalyst $[\text{NaN}(\text{SiMe}_3)_2]$ (Figure 5). Accordingly, the reaction order (n) in catalyst $[\text{NaN}(\text{SiMe}_3)_2]$ for this reaction system was determined to be 0.9853 [curve fitting (R^2) = 0.99; ideal =

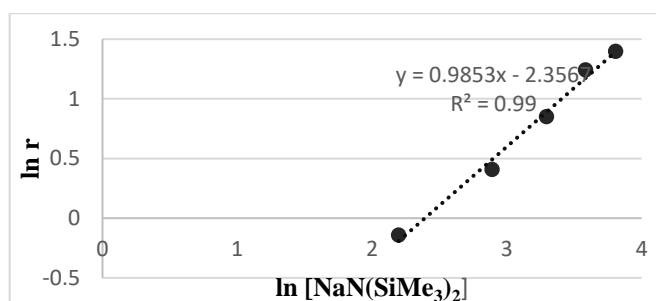
1.0]. Further kinetic experiments to clarify certain aspects of the proposed mechanism will be part of future studies.

Table 12: Calculations for the Determination of the Reaction Order (n) in NaN(SiMe₃)₂.

initial rate $r = k \cdot [\text{NaN}(\text{SiMe}_3)_2]^n$ $\ln r = n \cdot \ln [\text{NaN}(\text{SiMe}_3)_2] + \ln k$ with $n = \text{reaction order}$ and $k = \text{constant}$

NaN(SiMe ₃) ₂ (mg)	NaN(SiMe ₃) ₂ (mol%)	initial rate r	ln [NaN(SiMe ₃) ₂]	ln r
9	10	0.8683	2.197224577	-0.141218002
18	20	1.5036	2.890371758	0.407862233
27	30	2.3416	3.295836866	0.850834456
36	40	3.4622	3.583518938	1.241904225
45	50	4.0489	3.806662490	1.398445239

Figure 5: Product Concentration vs. Reaction Time [10–50 mol% loading in NaN(SiMe₃)₂].



1.2.11 Toward an Asymmetric C–C Bond Formation

Use of Chiral Crown Ethers

$\text{NaN}(\text{SiMe}_3)_2$ has proved to be an excellent catalyst in racemic C–C bond formations to give the corresponding homoallylic amines in high yields. Since a stereogenic centre was formed in these reactions, further investigations focused on an asymmetric version by screening enantiopure ligands. Crown ethers are among the most widely studied ligands for selective complexation of alkali metal ions. For example, [18]c-6 is normally chosen as a host and the potassium ion as a guest in view of the perfect fit between the hole size (2.60–3.20 Å) of the host, and the ionic diameter (2.66 Å) of the guest (Figure 6).^[145]

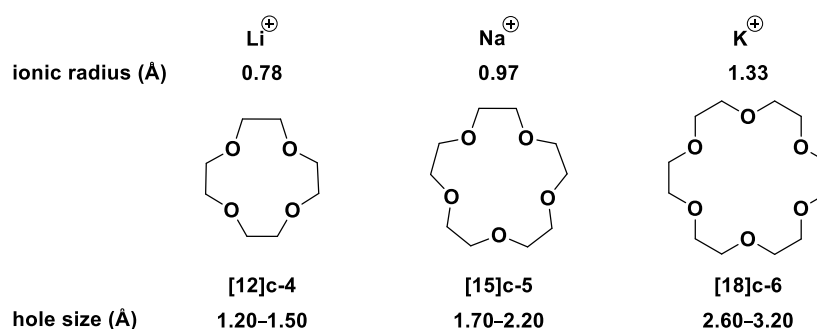


Figure 6: Depiction of Alkali Metal Ions and Relative Ionic Radii as well as Crown Ethers and Sizes.

In turn, commercially available enantiopure crown ethers (*S*)-14[c]-4 (**134**), (*R*)-17[c]-5 (**135**), and (*R*)-20[c]-6 (**136**) were tested in combination with several alkali metal amides (Table 13). In order to facilitate the complexation, apolar solvents such as toluene and heptane were chosen. Using 10 mol% of $\text{LiN}(\text{SiMe}_3)_2$ and 20 mol% of **134** in toluene, the reaction between allyl benzene (**1a**) and aldimine **7e** proceeded with 10% conversion, resulting in the formation of **8ae*** with 4% *ee* (entry 1). When changing the ligand to **135** {[17]c-5}, a product was not obtained (entry 2). When **136** {[20]c-6} was used, 20% of C–C bond formation was observed, albeit without asymmetric induction (entry 3). Next, $\text{NaN}(\text{SiMe}_3)_2$ was used in toluene and heptane (entries 4–9). The best results were obtained in toluene; the screening of all three chiral crown ethers resulted in low conversions (up to 19%) with only a slightly improved asymmetric induction by using **136** {[20]c-6} in toluene (up to 16% *ee*; entry 8). Finally, the metal–base catalyst was changed to $\text{KN}(\text{SiMe}_3)_2$ (entries 10–15). Higher conversions were achieved due to the enhanced reactivity of $\text{KN}(\text{SiMe}_3)_2$ compared to $\text{LiN}(\text{SiMe}_3)_2$ and $\text{NaN}(\text{SiMe}_3)_2$. On the other hand, K^+ is a softer Lewis acid due to its larger ionic radius. Thus, the affinity between K^+ and the nitrogen atom in aldimine **7e** was expected to be weaker in comparison to that in the Na^+ case. Unsurprisingly, the highest *ee* was only 9%, which was obtained by using **136** {[20]c-6} in heptane (entry 15).

The overall low asymmetric induction may be ascribed to the decreased Lewis acidity of the alkali metal centre after complexation by the chiral crown ether ligand, which may also explain the poor conversions in this scenario. As was mentioned earlier, metal-free organic superbases were shown to be ineffective in catalysing C–C bond formations in the present reaction system; the Lewis acidic metal ion seems to be essential in enhancing the electrophilicity of aldimine **7e**, but also in increasing the asymmetric induction through complexation with both chiral crown ether ligand and imine substrate.

Table 13: Effect of Chiral Crown Ethers.

1a (1.1 equiv) + 7e $\xrightarrow[\text{solvent, 25 } ^\circ\text{C, 18 h}]{\text{M-BB (10 mol\%), crown ether (20 mol\%)}}$ 8ae* (E:Z = >24:1)

(S)-[14]crown-4

(R)-[17]crown-5

(R)-[20]crown-6

entry	crown ether	M-BB	solvent	conv ^[a] of 8ae* [%]	ee ^[c] [%]
1	134	LiN(SiMe ₃) ₂	PhMe	10	4
2	135	LiN(SiMe ₃) ₂	PhMe	NR ^[b]	-
3	136	LiN(SiMe ₃) ₂	PhMe	20	0
4	134	NaN(SiMe ₃) ₂	PhMe	19	9
5	134	NaN(SiMe ₃) ₂	heptane	7	3
6	135	NaN(SiMe ₃) ₂	PhMe	14	12
7	135	NaN(SiMe ₃) ₂	heptane	3	2
8	136	NaN(SiMe ₃) ₂	PhMe	9	16
9	136	NaN(SiMe ₃) ₂	heptane	0	-
10	134	KN(SiMe ₃) ₂	PhMe	20	0
11	134	KN(SiMe ₃) ₂	heptane	16	2
12	135	KN(SiMe ₃) ₂	PhMe	11	0
13	135	KN(SiMe ₃) ₂	heptane	50	0
14	136	KN(SiMe ₃) ₂	PhMe	32	4
15	136	KN(SiMe ₃) ₂	heptane	19	9

^[a] The conversions were determined by ¹H NMR spectroscopic analysis of a reaction aliquot. ^[b] NR = no reaction; the intended product **8ae*** was not detected – only starting materials were recovered (¹H NMR spectroscopic analysis of a reaction aliquot). ^[c] The ee was determined by chiral HPLC analysis of an isolated TLC trace sample.

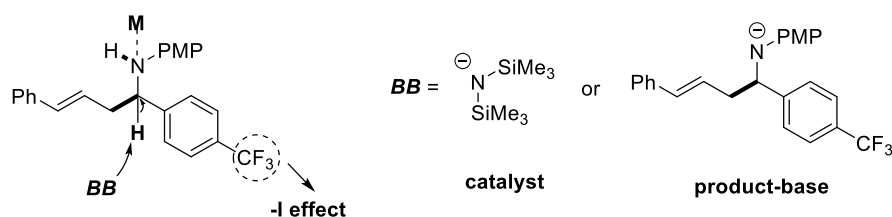


Figure 7: Structure of Product **8ae*** and Implications for Asymmetric Catalysis.

However, it is also notable that the formed product **8ae*** featured a rather acidic hydrogen at the stereogenic centre ($pK_a \sim 30$ in DMSO; Figure 7). Thus, it is also conceivable that the amide Brønsted base (either from the catalyst or the product-base) may deprotonate **8ae***, therefore leading to a potential partial racemisation and thus a lower asymmetric induction.

Use of Chiral BOX Ligands

In order to induce a better level of enantioselection, chiral bisoxazoline (BOX) ligands^[146] were selected as next candidates. Unlike crown ethers, BOX ligands have less coordinating sites. Thus, these bidentate ligands may bind to the metal center, also leaving a vacant Lewis acid site suitable for the activation of the used reagents (Figure 8).

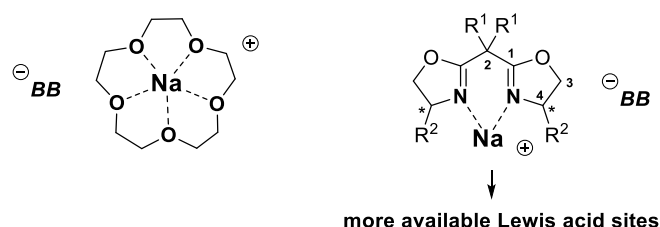
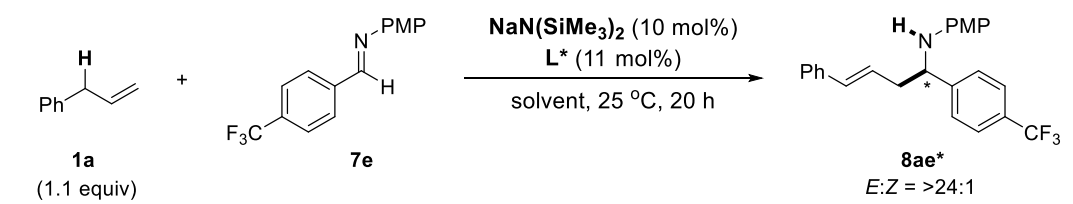


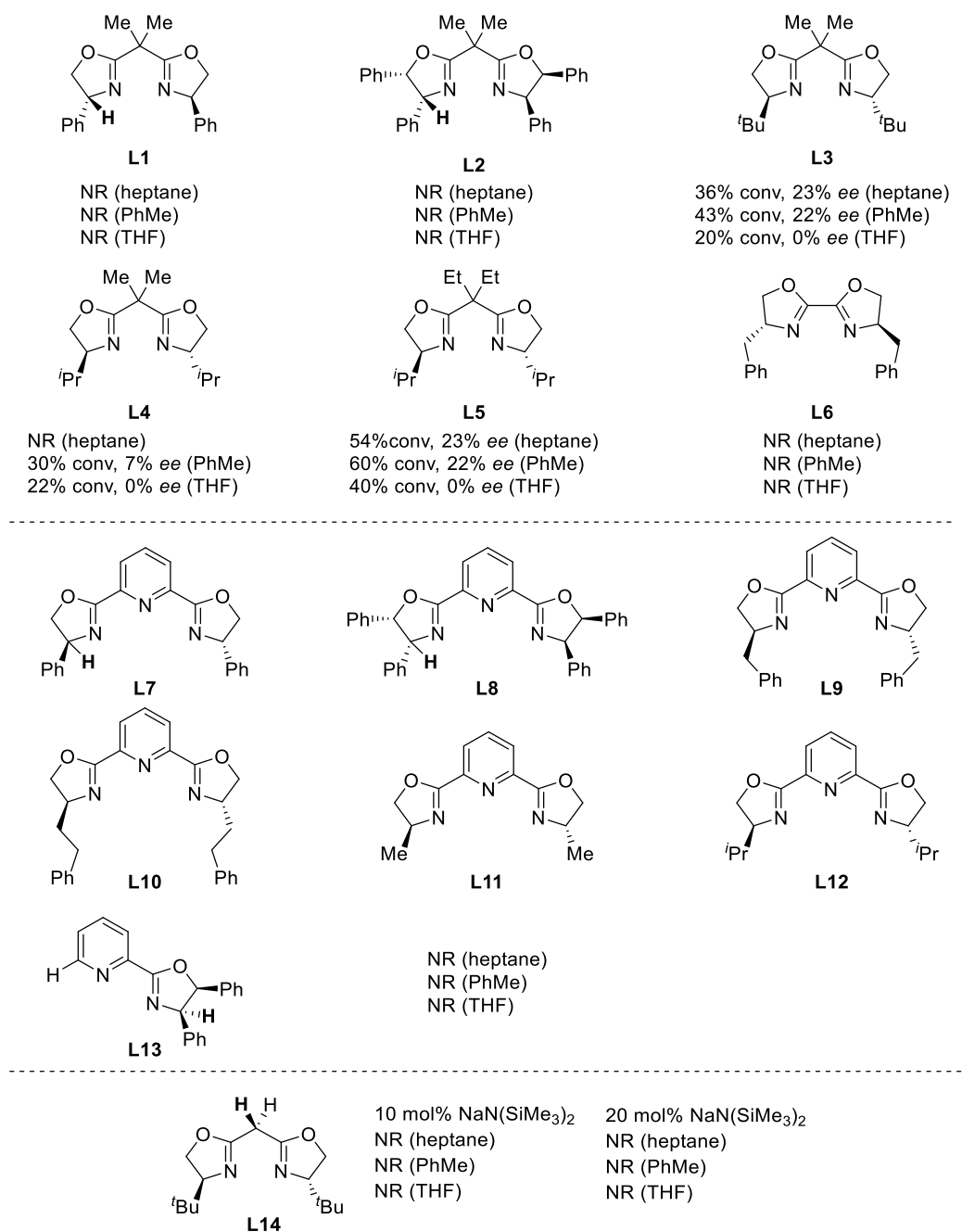
Figure 8: Crown Ether vs. BOX Ligands.

With the previous results in hand, $\text{NaN}(\text{SiMe}_3)_2$ was chosen as the metal–base catalyst in the reaction between allyl benzene (**1a**) and aldimine **7e** in heptane, toluene, or THF (Scheme 23). First, a series of BOX ligands (**L1**–**L6**) with a geminal dimethyl substitution at C2 were screened. When using ligands **L1** and **L2**, the intended reaction did not proceed in all three solvents. These results may be ascribed to the acidic hydrogen ($\text{p}K_{\text{a}} \sim 30$ in DMSO)^[113] at C4 of these BOX ligands (aromatic substituents at C4). Here, the amide base may deprotonate the C4 hydrogen instead of the allylic hydrogen of pro-nucleophile **1a** ($\text{p}K_{\text{a}} \sim 35$ in DMSO).^[123] In order to address this issue, the substituents at C4 were changed to alkyl groups. Fortunately, when using ligand **L3** bearing a *t*Bu group at C4, the reaction in heptane proceeded with 36% conversion to product **8ae***, and a slightly promising 23% *ee* was obtained. When changing the C4 substituent to a smaller group (*i*Pr), the *ee* decreased (ligands **L3** vs. **L4**). When increasing the size of the substituents at C2, the *ee* increased (ligands **L4** vs. **L5**). It is conceivable that the more hindered the substituents at C2 and C4, the higher the asymmetric induction. Finally, the use of **L6**, which does not have a spacer carbon between the two oxazoline rings, did not result in any product formation.

Next, Py-BOX ligands **L7**–**L13** were tested; in all cases, a product was *not* observed. It is notable that ligands **L7**, **L8**, and **L13** have the same issue as ligands **L1** and **L2**, in which the acidic hydrogen at C4 may prevent a reaction. However, using ligands **L9**–**L12** did not give any product either. Thus, it is likely that the pyridine spacer between the two oxazoline rings ‘poisoned’ the metal Lewis acid Na^+ , which is required for the activation of aldimine **7e**.

Finally, **L14** was used; here again, a product was *not* formed when 10 mol% of $\text{NaN}(\text{SiMe}_3)_2$ were used. We anticipated that the acidic hydrogen at C2 might be deprotonated by the amide base, thereby deactivating the catalyst. On the other hand, when increasing the catalyst loading to 20 mol%, the reaction still did not proceed.





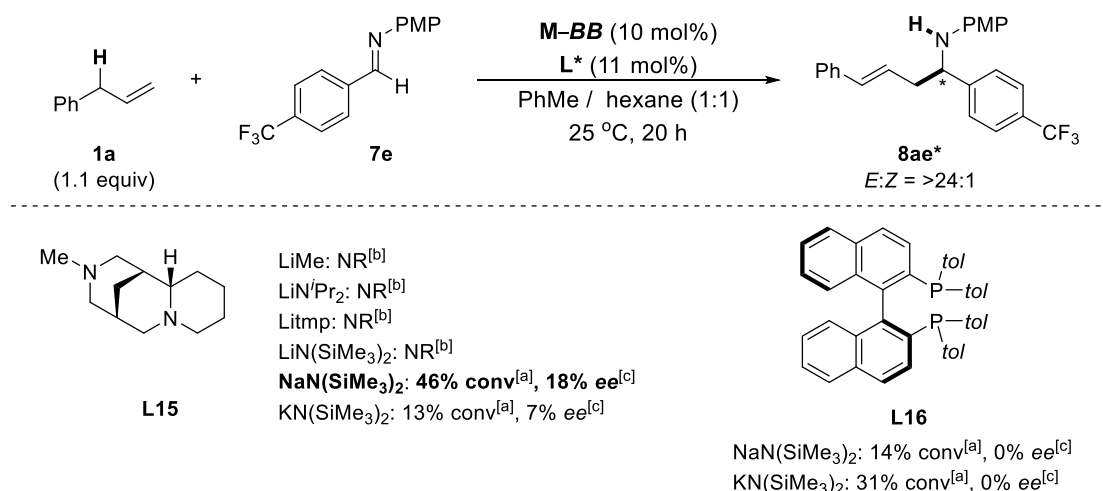
^[a] The conversions were determined by ¹H NMR spectroscopic analysis of a reaction aliquot. ^[b] NR = no reaction; the intended product **8ae*** was not detected – only starting materials were recovered (¹H NMR spectroscopic analysis of a reaction aliquot). ^[c] The *ee* was determined by chiral HPLC analysis of an isolated TLC trace sample.

Scheme 23: Screening of Chiral BOX Ligands.

Use of Miscellaneous Chiral Ligands

So far, 23% *ee* has been achieved by using a commercially available BOX ligand, **L3**. The next step was to examine other ligands. Sparteine^[147] surrogate **L15** was used as an enantiopure ligand in the reaction between allyl benzene (**1a**) and aldimine **7e** (Scheme 24). First, several lithium bases were tested. Unfortunately, the intended reaction did not proceed when LiMe, LiN^{*i*}Pr₂, LiTMP, or LiN(SiMe₃)₂ were used. The reactivity of the lithium base could be enhanced through coordination to ligand **L15**, but the reactivity proved to be insufficient in apolar solvents. When using NaN(SiMe₃)₂, 46% conversion to product **8ae*** were observed (18% *ee*). The use

of $\text{KN}(\text{SiMe}_3)_2$ gave both low conversions and low asymmetric induction. Meanwhile, when using axially chiral diphosphine ligand **L16** with $\text{NaN}(\text{SiMe}_3)_2$ and $\text{KN}(\text{SiMe}_3)_2$, low to moderate conversions were observed, but without any asymmetric induction.

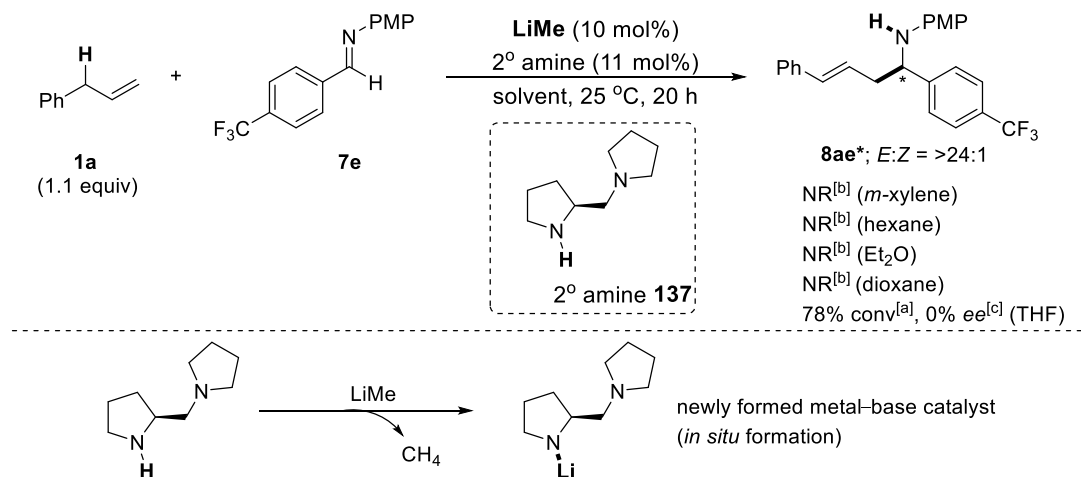


^[a] The conversions were determined by ^1H NMR spectroscopic analysis of a reaction aliquot. ^[b] NR = no reaction; the intended product **8ae*** was not detected – only starting materials were recovered (^1H NMR spectroscopic analysis of a reaction aliquot). ^[c] The *ee* was determined by chiral HPLC analysis of an isolated TLC trace sample.

Scheme 24: Screening of Other Non-Covalent Chiral Ligands.

Use of Chiral Lithium Amides

Another option to achieve asymmetric induction was to use an enantiopure Brønsted base. In the reaction between allyl benzene (**1a**) and aldimine **7e**, MeLi (10 mol%) was used as the metal–base catalyst in the presence of enantiopure secondary amine **137** (11 mol%) in various solvents (Scheme 25).



^[a] The conversions were determined by ^1H NMR spectroscopic analysis of a reaction aliquot. ^[b] NR = no reaction; the intended product **8ae*** was not detected – only starting materials were recovered (^1H NMR spectroscopic analysis of a reaction aliquot). ^[c] The *ee* was determined by chiral HPLC analysis of an isolated TLC trace sample.

Scheme 25: Chiral Brønsted Base-Induced Asymmetry?

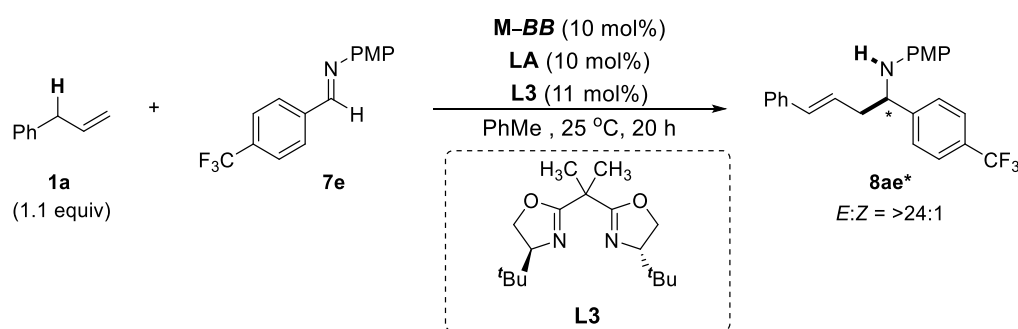
We anticipated that MeLi may deprotonate the secondary amine to form a chiral lithium amide base, which would deprotonate the allyl benzene (**1a**). The resulting conjugate acid **137** (secondary amine) may potentially form a hydrogen bond with aldimine **7e**. Thus, the chiral information may be transferred to product **8ae***. However, the

intended reaction did not proceed in *m*-xylene, hexane, Et₂O, or dioxane. These results are likely ascribed to the poor reactivity of a lithium amide base in the less polar solvents. Indeed, when THF was used, 78% conversion was obtained, albeit without any asymmetric induction. It is conceivable that electrophile **7e** was activated by the Lewis acidic metal ion Li⁺, rather than through hydrogen bonding with secondary amine **137**.

Addition of External Transition Metal Lewis Acids

Now that it was shown that Lewis acidic metals were critical in C–C bond formation as well as for asymmetric induction, the next strategy was to add an external Lewis acid to promote enantioselectivity. In the presence of an alkali metal–base catalyst and BOX ligand **L3**, several transition metal salts were used as additives in the reaction between allyl benzene (**1a**) and aldimine **7e** (Table 14).

Table 14: Screening of External Lewis Acids in View of Asymmetric Catalysis.



entry	LA	M–BB	conv ^[a] of 8ae*	ee ^[c] [%]
1	-	NaN(SiMe ₃) ₂	43	22
2	Fe(OTf) ₂	NaN(SiMe ₃) ₂	NR ^[b]	-
3	Fe(OTf) ₃	NaN(SiMe ₃) ₂	NR ^[b]	-
4	2CuOTf•PhMe	NaN(SiMe ₃) ₂	NR ^[b]	-
5	Cu(OTf) ₂	NaN(SiMe ₃) ₂	2	20
6	Zn(OTf) ₂	NaN(SiMe ₃) ₂	18	25
7	ZnCl ₂	NaN(SiMe ₃) ₂	NR ^[b]	-
8	Sc(OTf) ₃	NaN(SiMe ₃) ₂	NR ^[b]	-
9	La(OTf) ₃	NaN(SiMe ₃) ₂	NR ^[b]	-
10	Zn(OTf) ₂	KN(SiMe ₃) ₂	41	13
11	ZnCl ₂	KN(SiMe ₃) ₂	14	2

^[a] The conversions were determined by ¹H NMR spectroscopic analysis of a reaction aliquot. ^[b] NR = no reaction; the intended product **8ae*** was not detected – only starting materials were recovered (¹H NMR spectroscopic analysis of a reaction aliquot).

^[c] The *ee* was determined by chiral HPLC analysis of an isolated TLC trace sample.

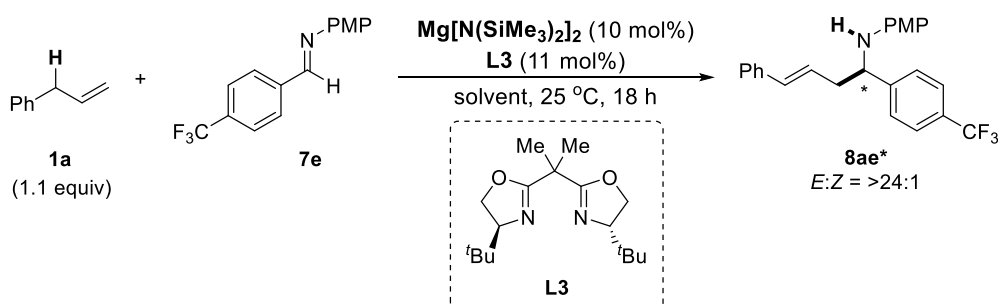
We anticipated that an alkali metal–base may act as a Brønsted base to activate pro-nucleophile **1a**, while a transition metal salt may be coordinated by BOX ligand **L3**; the chiral Lewis acid thus formed may be complexed by aldimine **7e** to introduce asymmetry in C–C bond formation. Alternatively, an alkali metal–base may undergo an anion metathesis with the transition metal salt, in which case the newly formed transition metal–base may become a chiral Lewis acid–Brønsted base dual catalyst. First, NaN(SiMe₃)₂ was fixed as the alkali metal–base catalyst in toluene; in the absence of a transition metal salt, product **8ae*** was formed with 43% conversion and 22% *ee* (reference). When using Fe(OTf)₂, Fe(OTf)₃, or CuOTf as an external Lewis acid, the intended reaction

did not proceed in toluene (entries 2–4). The use of Cu(OTf)₂ resulted in 2% conversion to **8ae*** with 20% *ee* (entry 5). When Zn(OTf)₂ was used, **8ae*** was formed with 18% conversion and 25% *ee* (entry 6). In contrast, the use of ZnCl₂, Sc(OTf)₃, or La(OTf)₃ shut down the reaction (entries 7–9). Finally, KN(SiMe₃)₂ was tried as the alkali metal–base; using two different Zn additives the conversions were increased but the asymmetric induction dropped (entries 10 and 11).

Use of a Magnesium Amide

In order to improve the asymmetric induction, *magnesium* bases were tested because the level of asymmetric induction may rely on the Lewis acidity of the metal (Table 15).

Table 15: Use of Mg[N(SiMe₃)₂]₂ in View of Asymmetric Catalysis.



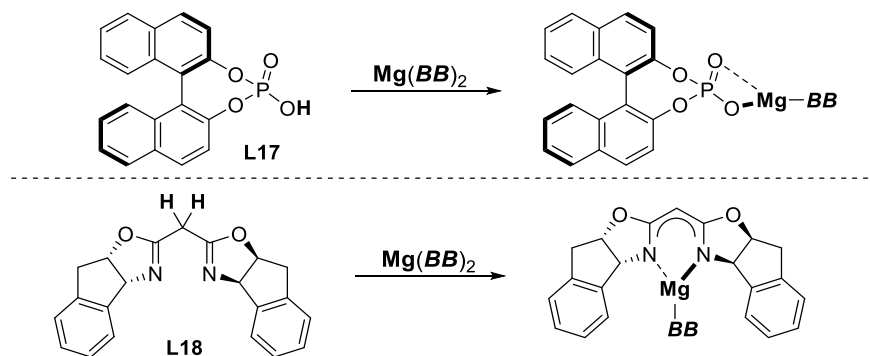
entry	ligand	solvent	conv ^[a] of 8ae * [%]	ee ^[c] [%]
1	-	dioxane	NR ^[b]	-
2	-	THF	NR ^[b]	-
3	-	DMF	90	-
4	L3	dioxane	NR ^[b]	-
5	L3	THF	NR ^[b]	-
6	L3	DMF	92	0

^[a] The conversions were determined by ¹H NMR spectroscopic analysis of a reaction aliquot. ^[b] NR = no reaction; the intended product **8ae*** was not detected – only starting materials were recovered (¹H NMR spectroscopic analysis of a reaction aliquot).

^[c] The *ee* was determined by chiral HPLC analysis of an isolated TLC trace sample.

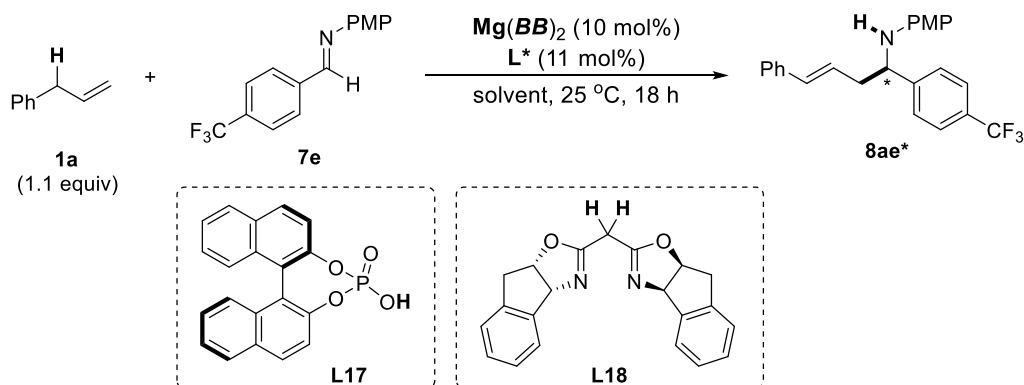
Under standard conditions, using Mg[N(SiMe₃)₂]₂ in dioxane in the absence of a ligand, the racemic ‘background’ reaction did not proceed (entry 1). As neither C–C bond formation nor isomerisation were observed, it was conceivable that the basicity of the amide was decreased by its stronger affinity to Mg(II) compared to Na(I). The use of a more polar and Lewis basic solvent, THF, gave the same result (entry 2). However, when the reaction was carried out in a polar aprotic solvent, DMF, product **8ae** was obtained in 90% NMR yield (entry 3). Next, the use of chiral BOX ligand **L3** was probed to see whether an asymmetric induction could be induced (entries 4–6); indeed, the coordination of such ligand to the Mg center should increase the Brønsted basicity of the amide. However, the combined use of Mg[N(SiMe₃)₂]₂ (10 mol%) and ligand **L3** (11 mol%) did not lead to any product formation in dioxane or THF (entries 4 and 5). On the other hand, when the same reaction was carried out in DMF product **8ae*** was formed in 92% yield, albeit with 0% *ee* (entry 6). This result may indicate that the reaction might go through an acyclic transition state and/or the racemic background reaction was too fast, and the ligand acceleration was insufficient (see entry 3). One reason may be that the Lewis acidity of Mg(II) substantially decreased due to ligand coordination thereby disfavoring the chiral pathway.

Another option was to use different types of enantiopure ligands/counteranions, such as chiral phosphoric acid **L17** and BOX ligand **L18**, which would potentially form –through deprotonation– a covalent bond to the Mg center, thus generating the corresponding enantiopure Mg complex (Scheme 26). It was anticipated that one amide substituent at Mg might deprotonate the acidic hydrogen of the chiral species (to transfer a chiral anion to Mg), while the other amide substituent at Mg may deprotonate pro-nucleophile **1a**.



Scheme 26: Chiral Species with Acidic Hydrogens for the Formation of Chiral Mg Complexes.

Unfortunately, the intended product was not formed in THF when $\text{Mg}[\text{N}(\text{SiMe}_3)_2]_2$ was used alone, or in the presence of chiral BOX ligand **L18** (Table 16; entries 1 and 2). In order to increase the reactivity of the base substituent at Mg, we anticipated that an alkyl base (Bu) might be a better candidate. The sole use of MgBu_2 (10 mol%) in THF did not give any reaction (entry 3). Likewise, a C–C bond formation did not occur when MgBu_2 was used in the presence of **L18** in different solvents (entries 4–6). Similar results were obtained when chiral phosphoric acid **L17** was used (entries 7–9). These disappointing results may be explained as follows: (1) the designated chiral metal–ligand complex was not formed; (2) the complex was formed but the reactivity of the Brønsted basic alkyl substituent was for some reason not apt to activate the pro-nucleophile. It is noted that a minor side-reaction, i.e., nucleophilic butylation of aldimine **7e**, might have occurred when MgBu_2 was used as a catalyst in the presence of BOX ligand **L18** and phosphoric acid **L17**, respectively, which may be ascribed to the enhanced nucleophilicity of the alkyl substituent under these conditions.

Table 16: The Use of Chiral Mg–Brønsted Bases.

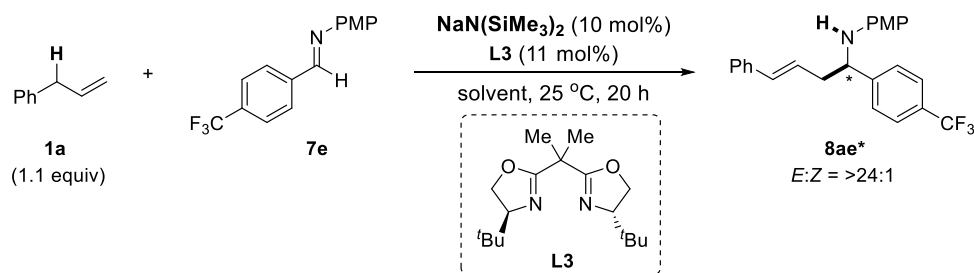
entry	$\text{Mg}(\text{BB})_2$	ligand	solvent	conv ^[a] of 8ae* [%]
1	$\text{Mg}[\text{N}(\text{SiMe}_3)_2]_2$	-	THF	NR ^[b]
2	$\text{Mg}[\text{N}(\text{SiMe}_3)_2]_2$	L18	THF	NR ^[b]
3	MgBu_2	-	THF	NR ^[b]
4	MgBu_2	L18	heptane	NR ^[b]
5	MgBu_2	L18	PhMe	0; poor mass balance
6	MgBu_2	L18	THF	0; poor mass balance
7	MgBu_2	L17	THF	0; poor mass balance
8	MgBu_2	L17	PhMe	0; poor mass balance
9	MgBu_2	L17	heptane	0; poor mass balance

^[a] The conversions were determined by ^1H NMR spectroscopic analysis of a reaction aliquot. ^[b] NR = no reaction; the intended product **8ae*** was not detected – only starting materials were recovered (^1H NMR spectroscopic analysis of a reaction aliquot).

^[c] The *ee* was determined by chiral HPLC analysis of an isolated TLC trace sample.

Solvent Effects

So far, BOX ligand **L3** in combination with $\text{NaN}(\text{SiMe}_3)_2$ has proved to be the best catalyst system for asymmetric induction. The next step was to optimise the reaction conditions to achieve a higher conversion and a higher enantioselection. To this end, the reaction between allyl benzene (**1a**) and aldimine **7e** was carried out in various solvents (Table 17). First, different *apolar* solvents –including aliphatic, aliphatic cyclic, aromatic, etheral, and chlorinated solvents– were examined (entries 1–16). The use of methylpentane, hexane, or octane gave product **8ae*** with decent conversions (26–51%) and asymmetric induction (21–25% *ee*; entries 1–3). Among the aliphatic cyclic solvents, cyclopentane, cyclohexane, or cyclooctane afforded product **8ae*** with 41–60% conversions and 19–21% *ee* (entries 4, 5, and 9). The use of *m*-xylene proved to be the most effective (70% conv, 25% *ee*; entry 11). The use of other aromatic and etheral solvents –with a higher dielectric constant ϵ – were shown to be less effective (entries 10 and 12–16). The use of THF did not induce any asymmetry in **8ae***. This result may be ascribed to the fact that THF is a rather strongly coordinating solvent, which would coordinate to Na^+ , thus preventing effective complexation between Na^+ and **L3**.

Table 17: Solvent Screening in Attempted Asymmetric Sodium Amide Catalysis.

entry	solvent (ϵ)	conv ^[a] of 8ae* [%]	ee ^[c] [%]
1	methylpentane (1.9)	39	23
2	hexane (1.9)	51	21
3	octane (1.9)	26	25
4	cyclopentane (2.0)	41	19
5	cyclohexane (2.0)	50	21
6	methylcyclopentane (2.0)	NR ^[b]	-
7	methylcyclohexane (2.0)	27	18
8	cycloheptane (2.1)	NR ^[b]	-
9	cyclooctane (2.1)	60	20
10	<i>p</i> -xylene (2.2)	NR ^[b]	-
11	<i>m</i>-xylene (2.4)	70	25
12	<i>o</i> -xylene (2.6)	12	15
13	mesitylene (3.4)	43	20
14	THF (7.5)	27	0
15	BTF (9.2)	7	17
16	1,2-dichlorobenzene (9.9)	70	16

^[a] The conversions were determined by ^1H NMR spectroscopic analysis of a reaction aliquot. ^[b] NR = no reaction; the intended product **8ae*** was not detected – only starting materials were recovered (^1H NMR spectroscopic analysis of a reaction aliquot).

^[c] The *ee* was determined by chiral HPLC analysis of an isolated TLC trace sample.

Effect of Substrates

As mentioned earlier, the overall level of asymmetric induction might be limited by: (1) the acidic hydrogen of product **8ae***; (2) the level of isomerisation of the C=N bond (Figure 9). The $\text{p}K_{\text{a}}$ value could be tuned through changing the substituents on the aromatic ring of the aldimine. At the same time, the substituent (nature and position) may affect the asymmetric induction electronically *and* sterically. This is to say, if **X** is more sterically demanding, the aldimine may be more constrained to an *E* configuration, thus the isomerisation of the C=N double bond may be suppressed. A ‘stable’ geometric configuration of C=N double bond normally has a positive effect on the asymmetric induction.^[52]

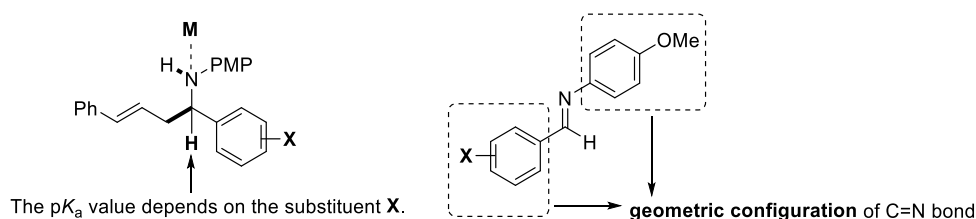
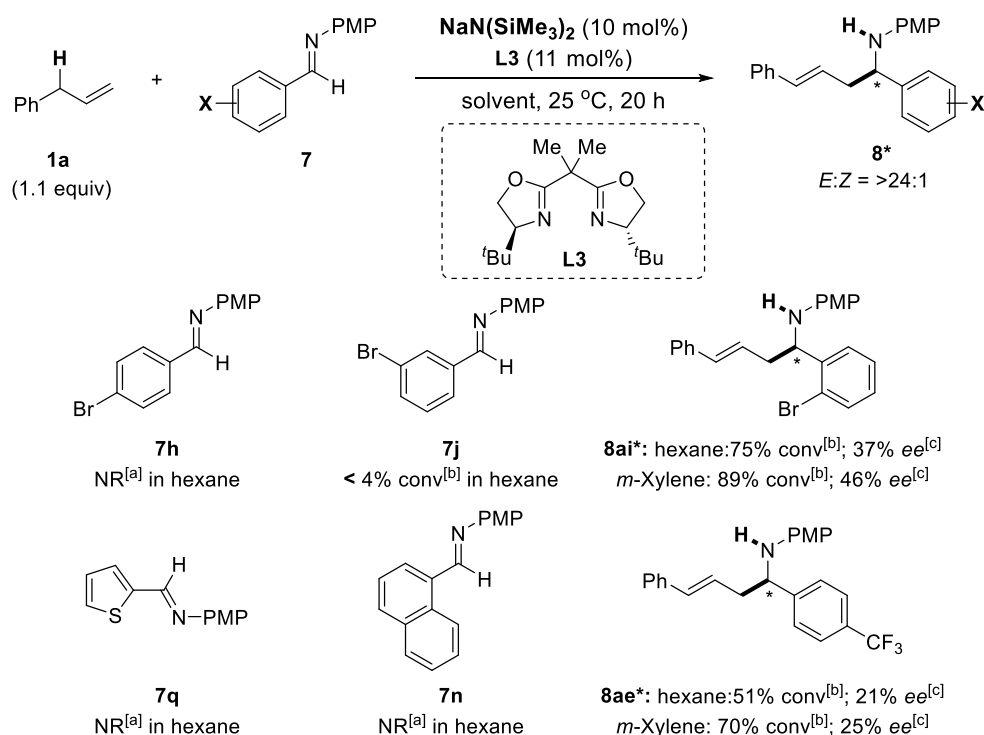


Figure 9: Potential Substrate Effects.

A combination of $\text{NaN}(\text{SiMe}_3)_2$ and BOX ligand **L3** was chosen as the chiral catalytic system for the reaction between allyl benzene (**1a**) and various aldimines **7** in hexane (Scheme 27). The use of *p*-Br- and *m*-Br-substituted aldimines resulted in poor reactivity. Fortunately, when the substituent was changed from *p*-CF₃ to *o*-Br, the corresponding product **8ai*** was obtained with 37% *ee*. When an aromatic solvent, *m*-xylene, the corresponding product **8ai*** was obtained with 46% *ee*. It is conceivable that the *o*-Br substitution may induce a more stable *E* configuration of the imine. In turn, a more stable geometric configuration of the C=N double bond may result in a higher asymmetric induction.



^[a] NR = no reaction; the intended product **8*** was not detected – only starting materials were recovered (¹H NMR spectroscopic analysis of a reaction aliquot). ^[b] The conversions were determined by ¹H NMR spectroscopic analysis of a reaction aliquot. ^[c] The *ee* was determined by chiral HPLC analysis of an isolated TLC trace sample.

Scheme 27: Effects of Various Substituted Aldimine Substrates.

Next, an electron-rich heteroaromatic aldimine, **7q**, was tested; such aldimine features two coordinating sites (the nitrogen and the sulfur atoms; Figure 10). Thus, the resulting product was anticipated to have an improved asymmetric induction (bidentate substrate coordination). However, the reaction did not proceed at all in hexane; likewise, the use of 1-naphthalene aldimine **7n** did not give any product either. These results may be due to poor solubilities of the substrates. However, other solvents (e.g. toluene) were not tested in this context.

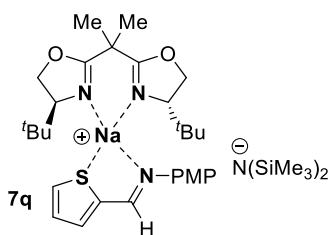
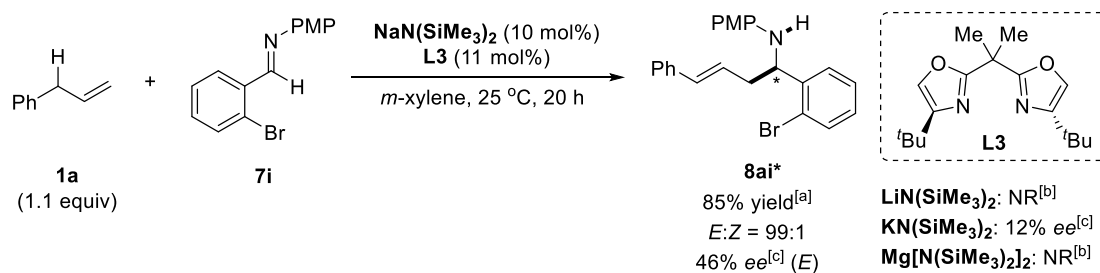


Figure 10: Bidentate Coordination to Na^+ by the Chiral Ligand and the Substrate.

In order to compare directly with the best sodium result (85% yield, 46% *ee*), $\text{LiN}(\text{SiMe}_3)_2$, $\text{KN}(\text{SiMe}_3)_2$, and $\text{Mg}[\text{N}(\text{SiMe}_3)_2]_2$ were used as a catalyst under the optimised conditions using ligand **L3** and substrate **7i** (Scheme 28). However, the reaction did not proceed when $\text{LiN}(\text{SiMe}_3)_2$ or $\text{Mg}[\text{N}(\text{SiMe}_3)_2]_2$ were used, while a poor asymmetric induction was obtained for the use $\text{KN}(\text{SiMe}_3)_2$ (12% *ee*). Here again, sodium has shown a unique advantage over other metals – this time in the context of asymmetric catalysis.



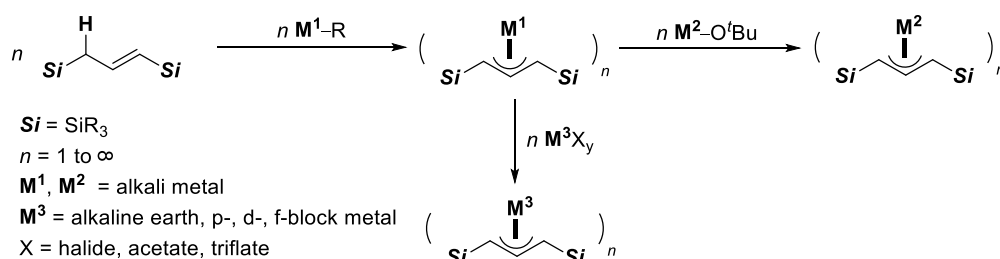
^[a] The yields refer to the isolated yields after PTLC purification; *E:Z* ratios were determined after isolation based on ^1H NMR spectroscopic analysis of the purified product. ^[b] NR = no reaction; the intended product **8ai*** was not detected – only starting materials were recovered (^1H NMR spectroscopic analysis of a reaction aliquot). ^[c] The *ee* was determined by chiral HPLC analysis of a PTLC-purified sample.

Scheme 28: Use of Different Metal Amides in Asymmetric Catalysis.

1.2.12 ‘Functionalised’ C–C Bond Formation

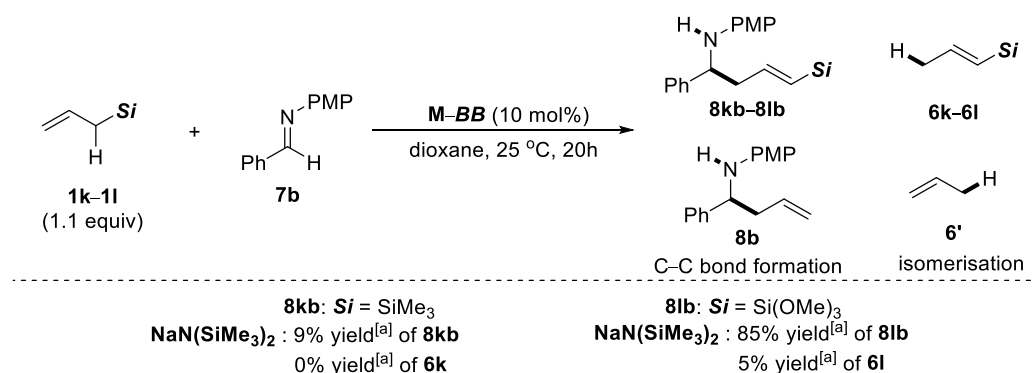
Use of Allyl Silicon Reagents

Silicon has been known to stabilise an α -carbanion through hyperconjugation.^[148, 149] In turn, metallation smoothly occurs at the α -position. (Silyl)allyl–alkali metal species were synthesised by Layfield *et al.* through the reaction between allyl silicon reagents and alkyl–alkali metal Brønsted bases, whereas (silyl)allyl–metal species with *alkaline earth*, *p*-, *d*-, and *f*-block metals were prepared through anion metathesis (Scheme 29).^[150, 151] The exact bonding mode (η^1 , combined η^1/η^3 , η^3 , $\mu:\eta^3-\eta^3$ *etc.*) depends on the nature of metal, ligand, and the substituents at the allyl unit. Polymeric species of such allyl–M compounds were often observed in the solid state or in apolar solvents. In contrast, coordinative solvents such as THF or sterically demanding ligands may break the polymeric aggregation to tetrameric or even monomeric species. These observations led to the anticipation that allyl silicon reagents might be suitable pro-nucleophiles in alkali metal amide-catalysed C–C bond formation.



Scheme 29: Formation of (Silyl)Allyl–Metal Species.

In turn, allyl silane **1k** ($\text{Si} = \text{SiMe}_3$) was treated with model aldimine **7b** under the optimised reaction conditions at 25 °C for 20 h (Scheme 30). ¹H NMR spectroscopic analysis of a reaction aliquot allowed for the identification and quantification of the different products. For instance, isomerised substrate **6k** was identified by comparison with literature data.^[69, 152]



^[a] The yields and geometric selectivities were determined by ¹H NMR spectroscopic analysis of a reaction aliquot without an internal standard (based on ‘relative’ analysis of starting materials and products).

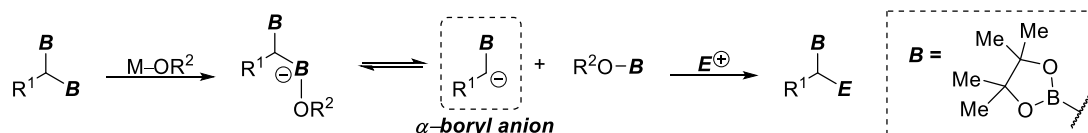
Scheme 30: Attempted Sodium Amide-Catalysed Allylation Using Allyl Silane Reagents.

The use of $\text{NaN}(\text{SiMe}_3)_2$ in dioxane resulted in the generation of product **8kb** in less than 9% NMR yield, without the formation of isomer **6k**. Allyl siloxane **6l** [$\text{Si} = \text{Si}(\text{OMe})_3$] was used as an alternative pro-nucleophile, which was assumed to be more active towards an electrophile. Indeed, the reaction proceeded smoothly under standard C–C bond formation conditions giving product **8lb** in 85% NMR yield, together with isomer **6l** in 5% NMR yield. Product **8lb** was identified by ¹H NMR spectroscopy; characteristic signals include: $\delta = 6.5$ ppm and $\delta = 5.6$ ppm

($J_{\text{trans}} = 18.8$ Hz) for both alkenyl hydrogen atoms; $\delta = 4.3$ ppm for the benzylic hydrogen atom; $\delta = 2.5$ ppm and $\delta = 2.4$ ppm for both allylic hydrogen atoms. In order to avoid overlap with any alkenyl signals, the isomerized side-product **6l** was quantified through integration of the terminal methyl signal ($\delta = 1.6$ ppm, 3H). It is noted that *Lewis* base-induced products **8b** and **6'** were *not* observed, suggesting that under these conditions, $\text{NaN}(\text{SiMe}_3)_2$ exclusively reacted as a *Brønsted* base, which may be explained by: (1) the steric demand of the amide anion; (2) the α -silicon effect. Likewise, the *Z* isomers of **8kb** and **8lb** were *not* observed. Nevertheless, as these results proved to be difficult to get improved further, we turned our attention to other metalloid reagents.

Use of an Allyl Boron Reagent

Allyl pinacolyl boronic ester **1m** was widely used in the nucleophilic allylation of aldehydes, ketones, and imines. However, such a C–C bond formation is triggered through *Lewis* base activation (in a cyclic closed transition state). Thus, the precious Bpin moiety *cannot* be preserved in the allylation product, and results in the generation of a stoichiometric amount of waste. On the other hand, it has been reported that an electron-deficient three-coordinate boron atom was apt to stabilize an α -carbanion, which may be trapped by a suitable electrophile (Scheme 31).^[153]



Scheme 31: Lewis Base-Induced Formation of a Boryl-Stabilised α -Carbanion.

In order to see whether an allyl boronic ester may be activated by a *Brønsted* base, the effect of bases and solvents were investigated, i.e., an amide base screening for the model reaction in different solvents at 25 °C was carried out (Table 19).

Table 19: Use of an Allyl Boron reagent as Pro-Nucleophile.

entry	M	solvent	yield ^[a] of 8mb (%)	yield ^[a] of 8b (%)	yield ^[a] of 6m and 6' (%)	yield ^[a] of 9mb and 9' (%)
1	Na	dioxane	19	0	0	55
2	Na	THF	18	0	0	82
3	K	THF	12	0	0	15
4	Li	THF	12	29	0	0
5	Li	dioxane	11	67	8	0

^[a] The yields and geometric selectivities were determined by ¹H NMR spectroscopic analysis of a reaction aliquot without an internal standard (based on 'relative' analysis of starting materials and products).

^1H NMR spectroscopy showed the formation of intended product **8mb** with the following characteristic signals: $\delta = 6.6$ ppm ($J_E = 17.9$ Hz) and $\delta = 5.6$ ppm ($J_E = 17.9$ Hz) for both alkenyl hydrogen atoms; $\delta = 4.4$ ppm for the benzylic hydrogen atom; $\delta = 2.7$ ppm and $\delta = 2.6$ ppm for both allylic hydrogen atoms. The 1:1 ratio of the *benzylic* hydrogen and the *vinyl*ic hydrogen suggested the formation of **8mb** through the intended *Brønsted* base pathway. However, a substantial amount of other products was observed as well. When $\text{NaN}(\text{SiMe}_3)_2$ was used in dioxane and THF, product **8mb** was only formed in <20% NMR yield; the major products were assigned to be the dehydroamination side-products **9mb** and **9'** (entries 1 and 2). Due to the complexity of the ^1H NMR chart of the reaction mixture, side-products **9mb** and **9'** were hard to be distinguished prior to their isolation; it is noted that isomerization side-products **6m** and **6'** as well as proto-deboration side-product **8b** were not detected at this stage. The use of $\text{KN}(\text{SiMe}_3)_2$ in THF also provided the intended product **8mb** in 12% NMR yield (entry 3); interestingly, the level of dehydroamination decreased to 15%. The use of $\text{LiN}(\text{SiMe}_3)_2$ in dioxane and THF resulted in the predominant formation of the *Lewis* base-triggered side-product **8b** without the detection of dehydroamination products (entries 4 and 5). It is noted that the formation of (*Z*)-**8mb** was *not* observed in any of these cases. The dehydroamination side-product was isolated and confirmed to be *only* compound **9'** (*E*:*Z* = >49:1), after comparison with a literature report.^[139] Most importantly, when the reaction was carried out in a more polar solvent, DMF ($\epsilon = 33$), side-products **8b** and **6'** were *not* observed at all (Table 20).

Table 20: Alkali Metal Amide-Catalyzed Allylation Using Boronic Ester **1m** in DMF.

1m (1.1 equiv) + $\text{M-N}(\text{SiMe}_3)_2$ (10 mol%) in DMF, 25 °C, 20h

Products: **8mb** (C-C bond formation), **6m** (isomerisation), **8b** (not observed), **6'** (not observed)

B =

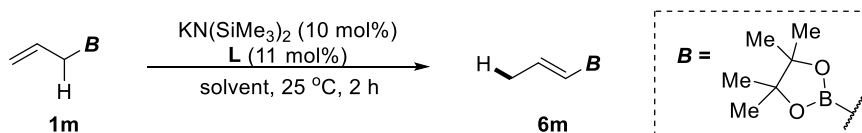
entry	M	yield ^[a] of 8mb (%) ^[a]	yield ^[a] of 6m (%)
1	Li	41	20
2	Na	67	23
3	K	35	34

^[a] The yields and geometric selectivities were determined by ^1H NMR spectroscopic analysis of a reaction aliquot without an internal standard (based on 'relative' analysis of starting materials and products).

This result indicated that the *Lewis* base pathway was significantly suppressed. Furthermore, dehydroamination side-product **9'** was *not* detected in the ^1H NMR chart either. The use of $\text{LiN}(\text{SiMe}_3)_2$ resulted in the formation of product **8mb** in 41% NMR yield, together with isomerisation side-product **6m** in 20% NMR yield (entry 1). The use of $\text{NaN}(\text{SiMe}_3)_2$ gave **8mb** in 67% yield, alongside **6m** in 23% NMR yield (entry 2). The use of $\text{KN}(\text{SiMe}_3)_2$ showed a poor selectivity between C–C bond formation and isomerisation, giving **8mb** and **6m** in 35% and 34% NMR yields, respectively (entry 3). This result was consistent with our earlier study in the context of 'unfunctionalised' C–C bond formation, where $\text{KN}(\text{SiMe}_3)_2$ demonstrated the highest reactivity but lowest selectivity, whereas $\text{NaN}(\text{SiMe}_3)_2$ displayed an excellent balance between reactivity (basicity) and selectivity (*Lewis* acidity).

In order to gain more insight into the reactivity of allyl boronic ester **1m**, the isomerisation of **1m** was investigated in the absence of an electrophile (Table 21). The optimised conditions for alkene isomerisation were previously uncovered in the group using $\text{KN}(\text{SiMe}_3)_2$ and [18]c-6 in THF at 25 °C. Thus, a ligand and solvent screening was carried out in the presence of $\text{KN}(\text{SiMe}_3)_2$ (10 mol%) at 25 °C in various solvents.

Table 21: Isomerisation Study Using Boronic Ester **1m**.



entry	solvent	L	conv ^[a] to 6m (%)	<i>E</i> : <i>Z</i>
1	THF	[18]c-6	72	nd ^[b]
2	dioxane	[18]c-6	43	15:1
3	DMF	-	>99	99:1
4	DMF	[18]c-6	>99	49:1

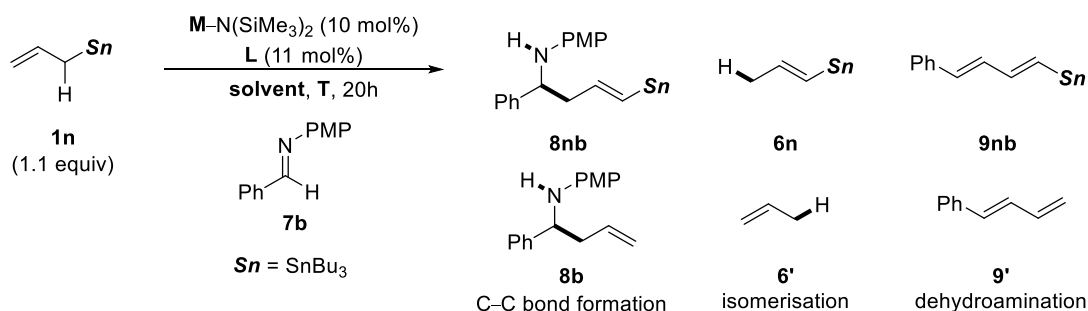
^[a] The conversions and geometric selectivities were determined by ¹H NMR spectroscopic analysis of a reaction aliquot without an internal standard (based on 'relative' analysis of starting material and product). ^[b] nd = not determined.

The use of $\text{KN}(\text{SiMe}_3)_2$ and [18]c-6 (10 mol%) in THF gave product **6m** with 72% conversion (entry 1). When switching to dioxane the conversion dropped to 43% (*E*:*Z* = 15:1; entry 2). Interestingly, the use of DMF—in the absence of any ligand—afforded product **6m** with 99% conversion in an *E*:*Z* ratio of 99:1 (entry 3); when the same experiment was carried out in the presence of [18]c-6, a similar result was obtained (entry 4). Thus, the reactivity of **1m** in terms of isomerisation in DMF was consistent with the results for C–C bond formation in DMF, where the Brønsted base pathway was favoured as well.

Use of an Allyl Tin Reagent

Next, allyl stannane **1n** was used with model imine **7b** in view of a potential ‘functionalised’ C–C bond formation (Table 22). Here, only Lewis base-triggered product **8b** was observed in ¹H NMR spectroscopy.

Table 22: Use of an allyl–SnR₃ reagent.



entry	M	solvent	T	L	yield ^[a] of 8nb (%)	yield ^[a] of 8b' (%)	yield ^[a] of 9' (%)
1	Na	THF	25-60	-	NR ^[b]	-	-
2	Na	dioxane	60	-	NR ^[b]	-	-
3	K	dioxane	25-60	-	NR ^[b]	-	-
4	K	THF	25-60	-	0	15–18	2–5
5	K	THF	25	[18]c-6	0	7	0

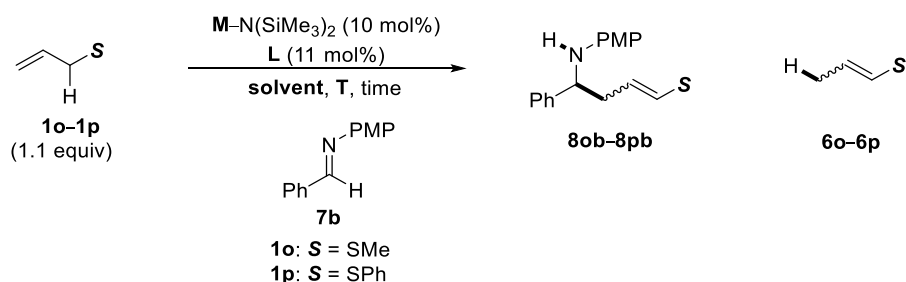
^[a] The yields and geometric selectivities were determined by ¹H NMR spectroscopic analysis of a reaction aliquot without an internal standard (based on ‘relative’ analysis of starting materials and products). ^[b] NR = no reaction; the intended product was not detected – only starting materials were recovered (¹H NMR spectroscopic analysis of a reaction aliquot).

The use of $NaN(SiMe_3)_2$ in dioxane and THF, even under forced conditions, did not result in the formation of any product; only starting materials were recovered (entries 1 and 2). A product was not observed either when $KN(SiMe_3)_2$ was used in dioxane (entry 3). The use of $KN(SiMe_3)_2$ in THF gave only Lewis base-triggered side-products **8b** and **9'** in up to 18% and 5% NMR yields, respectively (entry 4). When the same experiment was carried out in the presence of [18]c-6, a decreased reactivity was noticed; only side-product **8b** was observed (7% yield; entry 5). Interestingly, the use of alkaline earth metal amides did not show the formation of any product either. Next, we turned our attention towards the use of functionalised ‘non-metalloid’ allyl reagents.

Use of Allyl Sulfur Reagents

First, we investigated the reaction between allyl thioethers **6o** ($S = SMe$) or **6p** ($S = SPh$) and model imine **7b** under various conditions (Table 23). Unlike metalloid reagents, allyl thioethers of type **6** cannot undergo a Lewis base activation side-reaction; thus, fewer potential side-reactions were expected. In addition, sulfur has been known to stabilise an α -carbanion through hyperconjugation.^[154] As usual, the reaction monitoring was carried out using ¹H NMR spectroscopy of the corresponding reaction aliquots.

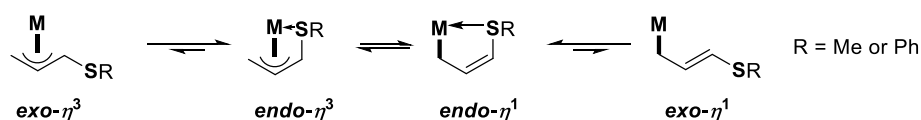
Table 23: Use of Allyl Sulfur Reagents.



entry	pronucleophile	M	solvent	T	L	yield ^[a] of 8ob (%)	<i>E</i> : <i>Z</i>	yield ^[a] of 6o
1	1o	Na	dioxane	25-60	-	52-87	2:1	40-50
2	1o	K	dioxane	25-60	-	19	1.5:1	50-70
3	1o	K	THF	25	[18]c-6	10	1:1	100
4 ^[c]	1p	Li	dioxane	25	-	80 (8pb)	5:1	5 (6p)

^[a] The yields and geometric selectivities were determined by ¹H NMR spectroscopic analysis of a reaction aliquot without an internal standard (based on 'relative' analysis of starting materials and products). ^[b] NR = no reaction; the intended product **8ob** was not detected – only starting materials were recovered (¹H NMR spectroscopic analysis of a reaction aliquot). ^[c] This experiment has been carried out by Hanno Kossen.

With substrate **1o** (*S* = SMe), product signals were recorded for both *E* and *Z* geometric isomers of intended product **8ob** as well as for isomerization side-product **6o**. Characteristic signals for product (*E*)-**8ob** appeared as follows: δ = 6.2 ppm and δ = 5.4 ppm (J_E = 15.0 Hz) for both alkenyl hydrogen atoms; δ = 4.3 ppm for the benzylic hydrogen atom; δ = 2.6 ppm for both allylic hydrogen atoms; δ = 2.2 ppm for the methyl group on the sulfur atom. Characteristic signals for product (*Z*)-**8ob** appeared as follows: δ = 6.1 ppm and δ = 5.6 ppm (J_Z = 9.5 Hz) for both alkenyl hydrogen atoms; δ = 4.4 ppm for the benzylic hydrogen atom; δ = 2.7 ppm and 2.6 ppm for both allylic hydrogen atoms; δ = 2.3 ppm for the methyl group on the sulfur atom. The isomerisation was quantified by integration of the terminal methyl group [(*E*)-**6o**: δ = 1.5 ppm; (*Z*)-**6o**: δ = 1.7 ppm). Typically, the C–C bond formation resulted in the predominant generation of (*E*)-**8ob** although the geometric selectivity was low. The use of NaN(SiMe₃)₂ in dioxane at 25 °C afforded intended product **8ob** in 52% NMR yield, alongside isomerisation side-product **6o** in 40% NMR yield (entry 1); an elevated temperature did not improve this result as the levels of both **8ob** and **6o** increased. The use of KN(SiMe₃)₂ displayed low efficiency (entry 2). The combined use of KN(SiMe₃)₂ and [18]c-6 resulted in the predominant formation of isomerisation side-product **6o** (entry 3). In all cases, the *E*:*Z* ratios were low (1:1 – 2:1). Interestingly, when the aromatic thioether substrate **1p** (*S* = SPh) was used, the predominant formation of (*E*)-**8pb** was greatly enhanced with a LiN(SiMe₃)₂ as the catalyst (80% NMR yield, *E*:*Z* = 5:1; entry 4); the isomerisation side-product **6p** was only obtained in 5% NMR yield. This result was likely due to the steric effect exerted by the Ph group, which may affect the configuration of the *in situ*-generated allyl–metal species (Scheme 32). Because of the electron lone electron pairs on sulfur, the formed allyl–metal species may be expected to favour an *endo*-configuration, thus a decreased geometric selectivity would be observed for the product (*S* = SMe). However, when the substituent on sulfur becomes sterically demanding, the equilibrium may be shifted to the formation of the *exo*-species (*S* = SPh).



Scheme 32: Potential Configuration of the Involved Intermediates.

In order to gain more insight into the geometric selectivity of allyl thioethers, the isomerisation of **1o** was investigated; $\text{KN}(\text{SiMe}_3)_2$ (10 mol%) was used as base in the presence or absence of a variety of ligands in THF at 25 °C (Table 24).

Table 24: Isomerisation of Allyl Sulfur Reagents.

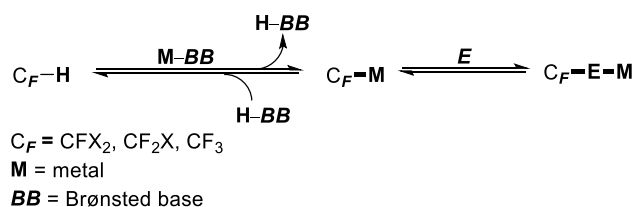
entry	solvent	ligand	conv ^[a] to 6o (%)	<i>E</i> : <i>Z</i>
1	THF	[18]c-6	>99	1:1
2	THF	[15]c-5	25	1:2
3	THF	mes-NHC	>99	1:1
4	THF	dipp-NHC	>99	1:1
5	THF	DB[18]c-6	>99	1:1
6	DME	[18]c-6	>99	1:1
7	DMF	dipp-NHC	>99	1:1
8	<i>m</i> -xylene	-	NR ^[b]	-
9	<i>m</i> -xylene	dipp-NHC	>99	1:19

^[a] The conversions and geometric selectivities were determined by ^1H NMR spectroscopic analysis of a reaction aliquot without an internal standard (based on 'relative' analysis of starting material and product). ^[b] NR = no reaction; the intended product **6o** was not detected – only starting materials were recovered (^1H NMR spectroscopic analysis of a reaction aliquot).

Conversions were monitored using ^1H NMR spectroscopy by comparison of the substrate's internal alkenyl signal ($\delta = 5.9$ ppm, 1H) with the corresponding alkenyl signals of the two geometric products: (*E*)-**6o** ($\delta = 5.8$ ppm and 5.3 ppm, 2H, $J_E = 14.9$ Hz); (*Z*)-**6o** ($\delta = 5.7$ ppm and 5.4 ppm, 2H, $J_Z = 9.4$ Hz).^[155] In almost all cases, a full conversion of substrate **1o** to product **6o** was detected (entries 1, 3–7, and 9). When polar solvents were used, the overall geometric selectivity turned out to be poor ($\sim 1:1$; entries 1 and 3–7). It was interesting to find that the use of [15]c-5 showed a slightly increased geometric selectivity in favour of (*Z*)-**6o** (1:2; entry 2); however, the conversion was rather low in this case (25 %). The rather poor *E*:*Z* ratios may be attributed here again to the coordination of the sulfur atom's lone pair to K^+ (Scheme 32). The use of an apolar solvent, *m*-xylene, did not lead to any conversion of the substrate **1o** (entry 8). However, in the presence of a sterically demanding carbene ligand the reaction proceeded smoothly with >99% conversion to product **6o** with a dramatically increased geometrical selectivity in favour of (*Z*)-**6o** (1:19; entry 9). Thus, the potential interaction between the Lewis basic allyl unit and the Lewis acidic metal centre, complexed by an external ligand or not, seems to be critical for obtaining a high geometric selectivity in the corresponding product (C–C bond formation or isomerisation).

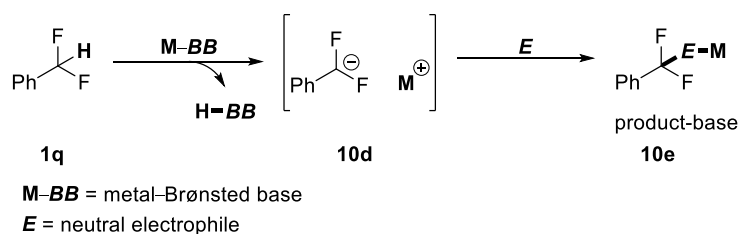
1.2.13 Attempted Brønsted Base Activation of PhCF₂H

Based on the successfully developed alkali metal amide-triggered C(sp³)-H bond activation, we aimed at applying this novel catalytic method to more complex reaction systems. One possibility was to turn fluorinated building blocks through ‘formal’ C^F-H bond activation into nucleophiles that may add to electrophiles. The fluorinated motif may be able to stabilise a carbanion in proximity due to the -I effect of fluorine (Scheme 33).



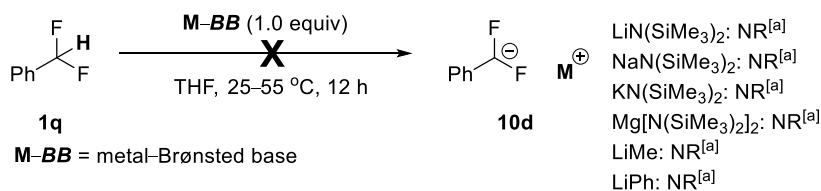
Scheme 33: Proposed Reaction Flow-chart.

Difluoro toluene (**1q**) features a fairly acidic benzylic hydrogen atom due to the strongly electron-withdrawing inductive effect exerted by the two fluorine atoms (Scheme 34). It was anticipated that a fairly ‘easy’ deprotonation may occur in the presence of an alkali metal amide. The resulting PhF₂C-M species (**10d**) may be introduced to a suitable neutral carbon-centered electrophile *E* (C-C bond formation). The newly generated product-base (**10e**) may display a similar basicity (compared with the initial amide catalyst), and may deprotonate another pro-nucleophile (**1q**) in order to regenerate the catalytically active species **10d**; alternatively, the conjugate acid of the amide catalyst (H-BB) may be deprotonated in order to recycle the initial catalyst (M-BB). The interest in aromatic compounds bearing a benzylic difluoromethyl (CF₂) group –which is regarded as a bioisostere of oxygen or sulfur atoms– has grown in the pharmaceutical and agrochemical industries.^[156]



Scheme 34: Proposed Concept for Benzylic C^F-H Bond Activation and Subsequent C-C Bond Formation.

In order to gain insight into the initial activation of the pro-nucleophile, several metal-centered bases were examined in THF at 25 °C to see whether an intermediate of type **10d** was detectable in ¹⁹F NMR spectroscopy (Scheme 35). However, even in the presence of a stoichiometric amount of the potential Brønsted base mediator, new signals were not visible in the charts of the corresponding reaction aliquots.



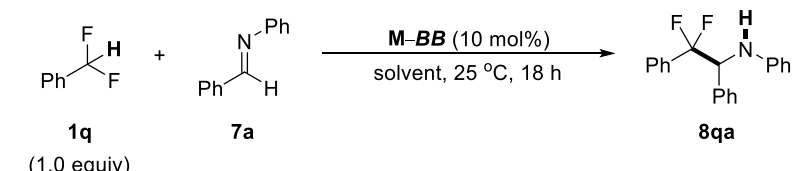
^[a] NR = no reaction; the intended product **10d** was not detected – only starting materials were recovered (¹H and ¹⁹F NMR spectroscopic analysis of a reaction aliquot).

Scheme 35: Base Screening.

Trapping the PhCF_2^- Anion?

We anticipated that when an electrophile of suitable reactivity was used, the potentially formed PhCF_2^- intermediate may be trapped, and thus a potential deprotonation equilibrium may be shifted to the right side. Thus, several metal-centered Brønsted bases were tested as a potential catalyst in the reaction between pro-nucleophile **1q** and model imine **7a** (Table 25). The experiments were monitored by ^1H and ^{19}F NMR spectroscopic analysis of the corresponding reaction aliquots. The starting material displays a signal in ^1H NMR spectroscopy at $\delta = 6.42$ ppm (t, $J = 56.4$ Hz) for the benzylic hydrogen atom, and a signal in ^{19}F NMR spectroscopy at $\delta = -110.8$ ppm (d, $J = 56.4$ Hz) for the two fluorine atoms (homotopic). The large coupling constant results from the *geminal* H–F coupling. Intended product **8qa** displays signals in ^1H NMR spectroscopy at $\delta = 4.91$ ppm (dd, $J = 12.8$, 10.6 Hz) for the benzylic hydrogen atom and at $\delta = 4.50$ (br s) ppm for the N–H hydrogen atom. In addition, **8qa** displays two signals in ^{19}F NMR spectroscopy at $\delta = -103.0$ ppm (dd, $J = 244.1$, 10.5 Hz) and at $\delta = -104.3$ ppm (dd, $J = 244.1$, 12.8 Hz, 1F) for the two fluorine atoms (diastereotopic). Here, the larger coupling constant results from the *geminal* F–F coupling, while the smaller one was assigned to the *vicinal* H–F coupling.

Table 25: Base and Solvent Screening for the Attempted Catalytic C–C Bond Formation.

			
entry	M–BB	solvent	conv ^[a] to 8qa [%]
1	LiN(SiMe ₃) ₂	dioxane	NR ^[b]
2	LiN(SiMe ₃) ₂	THF	NR ^[b]
3	LiTMP	THF	NR ^[b]
4	NaN(SiMe ₃) ₂	dioxane	<1
5	NaN(SiMe ₃) ₂	THF	<1
6	KN(SiMe ₃) ₂	dioxane ($\epsilon = 2$)	<2
7	KN(SiMe ₃) ₂	THF ($\epsilon = 7$)	<5
8	KN(SiMe ₃) ₂	DMF ($\epsilon = 33$)	NR ^[b]
9	KN(SiMe ₃) ₂	PhMe	<1
10	Mg[N(SiMe ₃) ₂] ₂	dioxane	NR ^[b]
11	Mg[N(SiMe ₃) ₂] ₂	THF	NR ^[b]
12	Ca[N(SiMe ₃) ₂] ₂	THF	NR ^[b]
13	Sr[N(SiMe ₃) ₂] ₂	THF	NR ^[b]
14	KN(SiMe ₃) ₂ + (CuOTf) ₂ •PhMe	THF	NR ^[b]

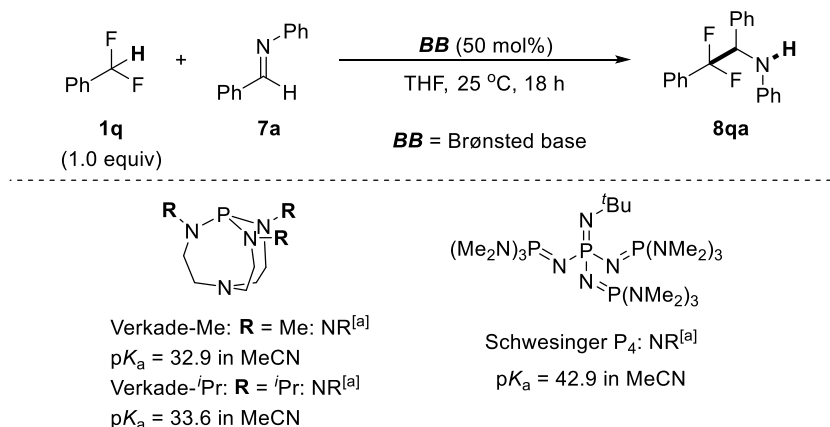
^[a] The conversions were determined by ^{19}F NMR spectroscopic analysis of a reaction aliquot without an internal standard (based on ‘relative’ analysis of both starting materials and product). ^[b] NR = no reaction; the intended product **8qa** was not detected – only starting materials were recovered (^1H and ^{19}F NMR spectroscopic analysis of a reaction aliquot).

The use of lithium amides did not result in any product formation in dioxane and THF (entries 1–3). When NaN(SiMe₃)₂ was used in dioxane and THF, only a trace amount of product **8qa** (<1%) was observed (entries 4 and 5). Likewise, the use of KN(SiMe₃)₂ in dioxane proved to be ineffective (entry 6). However, when KN(SiMe₃)₂ was used in THF, product **8qa** was obtained in 5% NMR yield (entry 7); on the other hand, the

product was not formed in DMF (entry 8). The reaction in toluene resulted only in the formation of a trace amount of product **8qa** (entry 9). The attempted isolation of product **8qa** (entry 7) failed due to the very low conversion, resulting in a mixture containing product and imine in a 1:2 ratio. Next, alkaline earth metal amides were tested (entries 10–13). The formal charge (+II) of these group 2 metals should lead to a more Lewis acidic but less Brønsted basic catalyst; here, a reactivity was not detected. Finally, the combined use of $\text{KN}(\text{SiMe}_3)_2$ (Brønsted base) and $(\text{CuOTf})_2 \cdot \text{PhMe}$ (Lewis acid) did not result in the formation of **8qa** either (entry 14).

Use of Organic Bases

Next, a few commercially available organobases were tested in THF at 50 mol% loading in the reaction between pro-nucleophile **1q** and aldimine **7a** (Scheme 36). These superbases display a strong basicity [$\text{p}K_{\text{a}}$ values of the corresponding conjugate acids (in MeCN): 42.9 for Schwesinger- P_4 ; 32.9 for Verkade-Me; 33.6 for Verkade- $i\text{Pr}$].^[157, 158] However, the reaction did not proceed when these metal-free bases were used; new signals were not detected in ^1H or ^{19}F NMR spectroscopy (reaction aliquots). These results suggested that a Lewis acidic metal cation may be important to enhance the electrophilicity of the imine. Alternatively, here again the reaction may not be detectable due its reversible character.

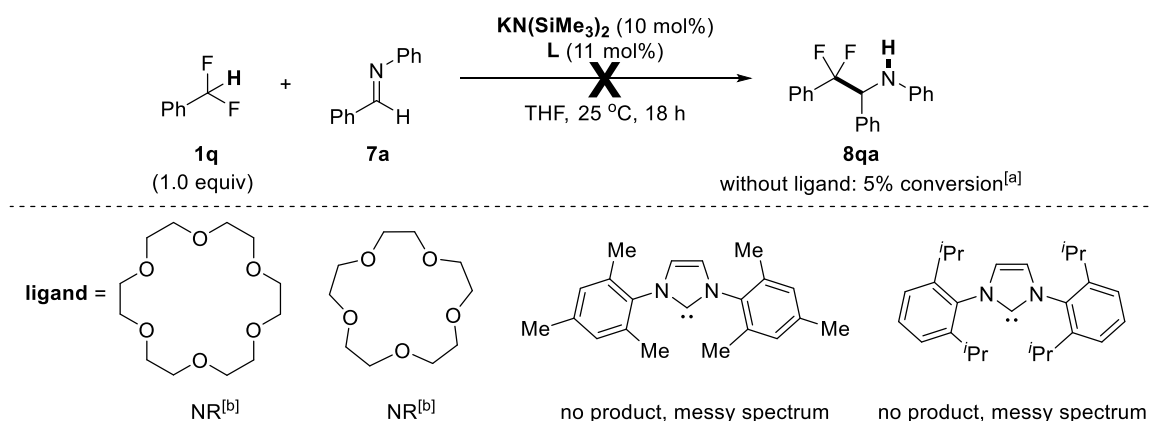


^[a] NR = no reaction; the intended product **8qa** was not detected – only starting materials were recovered (^1H and ^{19}F NMR spectroscopic analysis of a reaction aliquot).

Scheme 36: Experiments Using Strong Organobases at a Sub-Stoichiometric Catalyst Loading.

Combined Use of a Potassium Amide and Ligands

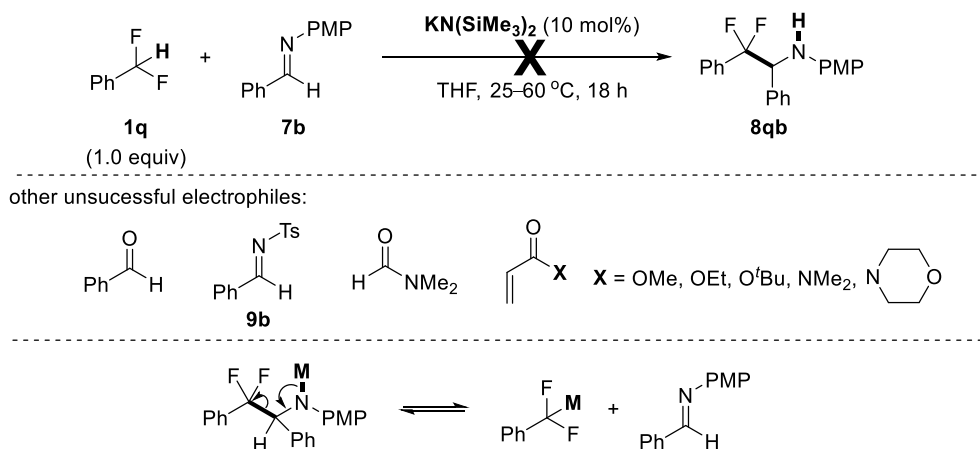
Next, a potassium amide was used in the presence of a variety of ligands in order to see whether the yield of the intended product could be increased (Scheme 37); crown ether and NHC ligands were used. Unfortunately, only the full recovery of both starting materials was observed in the presence of crown ethers, which may be ascribed to the significantly decreased Lewis acidity of K^+ in these cases (no imine activation). Likewise, the use of NHC ligands did not result in product formation either; here, messy ^1H and ^{19}F NMR spectra were obtained indicating a poor mass balance for imine **7a**.



^[a] The conversions were determined by ^{19}F NMR spectroscopic analysis of a reaction aliquot without an internal standard (based on 'relative' analysis of both starting material and product). ^[b] NR = no reaction; the intended product **8qa** was not detected – only starting materials were recovered (^1H and ^{19}F NMR spectroscopic analysis of a reaction aliquot).

Scheme 37: Effect of Ligands.

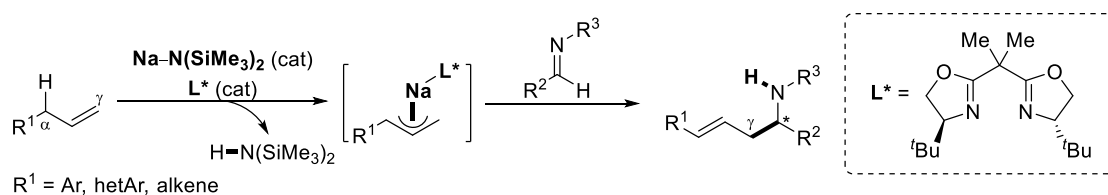
Other electrophiles tested include benzaldehyde, the corresponding *N*-PMP-protected and *N*-Ts-protected imines, DMF, and Michael amides (Scheme 38). However, a product formation was not detected in any of these cases. In this context, it is noted that in our earlier study aldehydes were shown to be not tolerated by the presence of $\text{KN}(\text{SiMe}_3)_2$ (*in situ* formation of the corresponding *N*-TMS-protected imine). Furthermore, it is noted that at least some of these reactions may be *reversible* thus leading to the regeneration of both electrophile and stabilised PhCF_2^- anion.



Scheme 38: Attempted Catalysis Using Other Electrophiles.

Conclusion

We discovered the use of a sodium amide as metal–Brønsted base (M–BB) dual catalyst for the activation of allylic C(sp³)–H bonds of aromatic and heteroaromatic alkenes (Scheme 1). The *in situ*-generated nucleophilic allyl–Na species underwent γ -selective C–C bond formation with imines to afford homoallylic amines in high yields with high geometric selectivities. To the best of our knowledge, this transformation represents the first example of generating a nucleophilic allyl–M species *via* direct C–H bond activation. Moreover, the asymmetric version of this reaction was also achieved through the use of a catalytic amount of a commercially available bisoxazoline (BOX) ligand.



Scheme 1: Sodium Amide-Catalysed C–H Bond Activation for Subsequent C–C Bond Formation.

During the mechanistic investigations, a (Ph)allyl–Na complex and a sodium amide product-base were detected, and their structures characterised by HRMS (EI mode) as well as ¹H, ¹³C, and ²³Na NMR spectroscopy (Figure 1). These two intermediates were shown to be catalytically competent in the model reaction under the mild standard conditions.

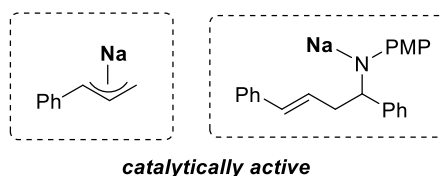
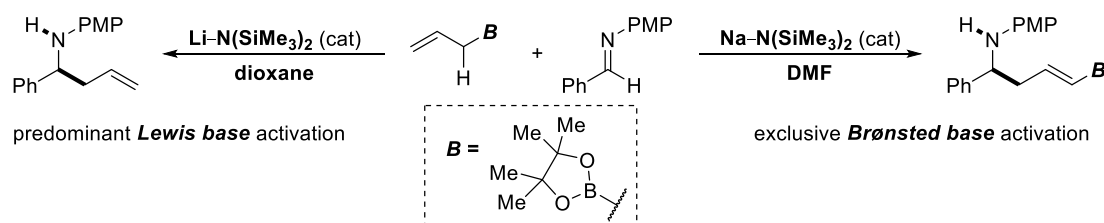


Figure 1: (Ph)Allyl–Na Complex and Sodium Amide Product-Base.

This catalytic method has been further exploited for use of functionalised allyl pro-nucleophiles. Regarding allyl metalloid reagents, e.g. allyl boronic esters, the choice of solvent and base was shown to fully direct the reactivity towards the unprecedented Brønsted base activation pathway (Scheme 2).



Scheme 2: Controlled Reactivity of an Allyl Metalloid, e.g. Allyl Boronic Ester.

2 Catalytic Use of an Alkali Metal–Lewis Base in Catalytic Difluoromethylation

2.1 Introduction

Nucleophilic Difluoromethylation

The ‘CF₂’ group is an isosteric surrogate of the ‘O’ atom. In this context, CF₂-substituted analogues of an EPSP synthase inhibitor and glucose were developed (Figure 1).^[159] In the same context, the difluoromethyl group (CHF₂) has the feature of bearing a slightly acidic C–H bond, allowing it to act as a lipophilic hydrogen bond donor.^[156] Thus, the difluoromethyl group can be recognised as a bioisostere of alcohols and thiols.^[160] Introducing a difluoromethyl group into molecules can therefore increase potential advantages such as modulated bioavailability, metabolic stability, and lipophilicity.^[161]

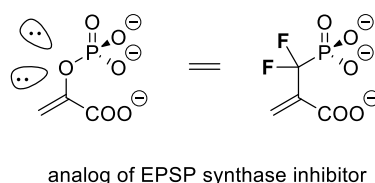
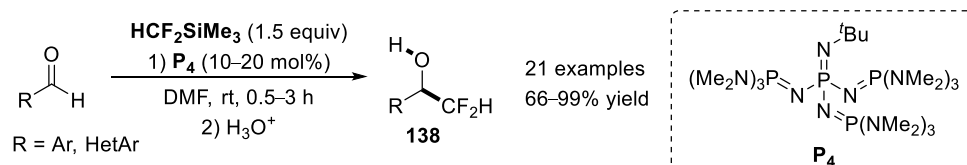


Figure 1: Structure of a CF₂-Phosphonate as Bioisostere of a Phosphate.

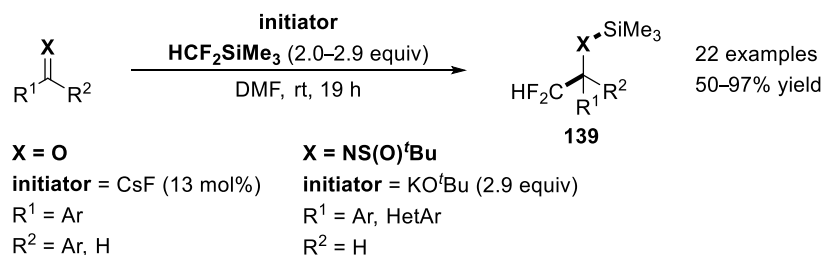
Nucleophilic difluoromethylation reactions require the *in situ* generation of “XCF₂[–]” (X = H or SiMe₃). HCF₂SiMe₃ (**1r**), as an analogue of Me₃SiCF₃, has recently been used as a difluoromethanide anion (HCF₂[–]) source for the nucleophilic introduction of a difluoromethyl group. However, because of the weaker electron-withdrawing ability of the CF₂H group (compared with the CF₃ group), the activation of this reagent typically requires harsher reaction conditions.

In 2015, Hu and co-workers demonstrated an organobase-catalysed difluoromethylation of aldehydes and ketones (Scheme 1).^[162] A catalytic amount of Schwesinger’s superbase **P**₄ was used under mild conditions to activate the C^F–Si bond of HCF₂SiMe₃ (**1r**) and initiate the subsequent difluoromethylation to give difluoromethyl adducts **138** in 66–99% yields. DMF as a polar aprotic solvent was assumed to serve as a ligand in the activation of the silicon atom and/or to stabilise a charged intermediate. However, this method was shown to be not suitable for the use of aliphatic aldehydes and enolisable ketones.



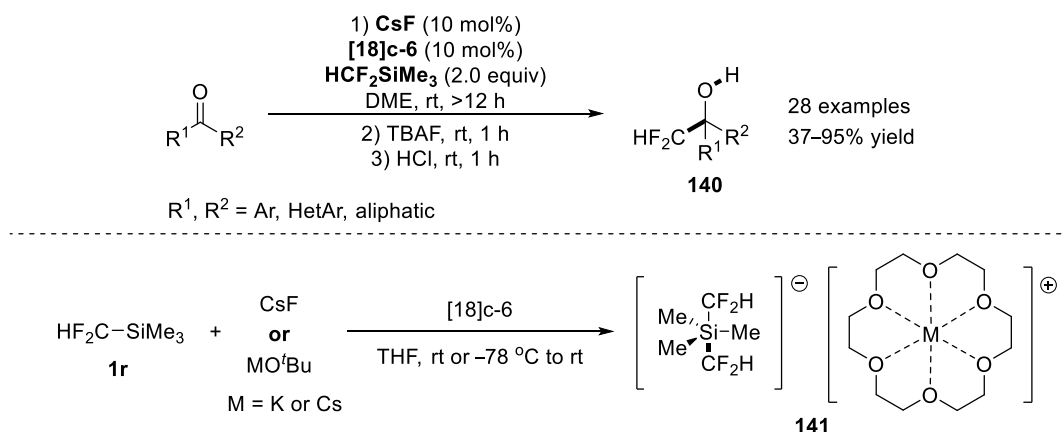
Scheme 1: Organocatalytic Difluoromethylation of Aldehydes and Ketones.

Hu *et al.* have also developed a difluoromethylation of aldehydes, ketones, and imines with **1r** using a metal salt as Lewis base mediator in a suitable solvent to activate the critical C^F–Si bond of **1r** (Scheme 2).^[163] A catalytic amount of CsF was used in DMF for aldehydes and ketones; a super-stoichiometric amount of KO^tBu was used in THF for imines.



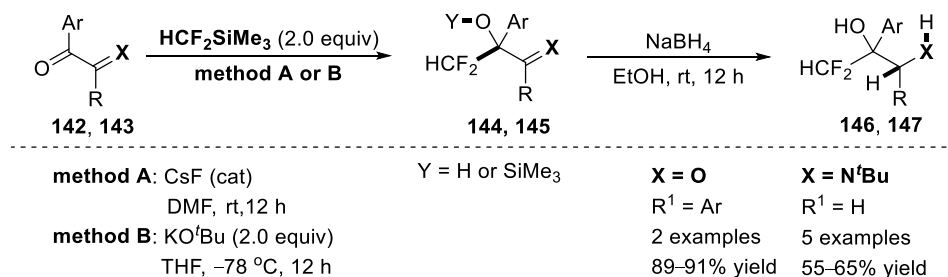
Scheme 2: Metal Salt-Triggered Difluoromethylation of Carbonyl and C=N Compounds.

Regarding enolisable ketones, Hu and co-workers reported the use of a Lewis basic alkali metal fluoride and a crown ether ligand as the catalyst system (Scheme 3).^[164] Here, a pentacoordinate bis(difluoromethyl)silicate anion, $[\text{Me}_3\text{Si}(\text{CF}_2\text{H})_2]^-$ (**141**), was observed for the first time through activation of $\text{HCF}_2\text{SiMe}_3$ (**1r**) by CsF and [18]c-6. Species **141** proved to be the key intermediate in the reaction between **1r** and enolisable ketones, thus giving access –after hydrolysis– to difluoromethylated alcohols **140** in 37–95% yields. This catalytic system was also applied to a single example of an imide electrophile, although resulting in a low product yield (41%).



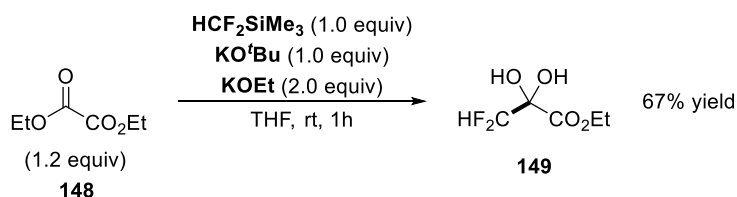
Scheme 3: Catalytic Difluoromethylation of Enolisable Ketones.

Objalska *et al.* reported a chemoselective difluoromethylation of the carbonyl group of aryl glyoxal-derived α -imino ketones **142** and diaryl 1,2-diketones **143**; here, initiators such as KO^tBu or CsF were used (Scheme 4).^[165] When KO^tBu was used a super-stoichiometric amount of this base was required. Subsequent reduction of α -imino alcohols **144** and α -hydroxy ketones **145** with NaBH₄ gave 2-amino 1-difluoromethyl alcohols **146** and difluoromethyl 1,2-diols **147**, respectively.



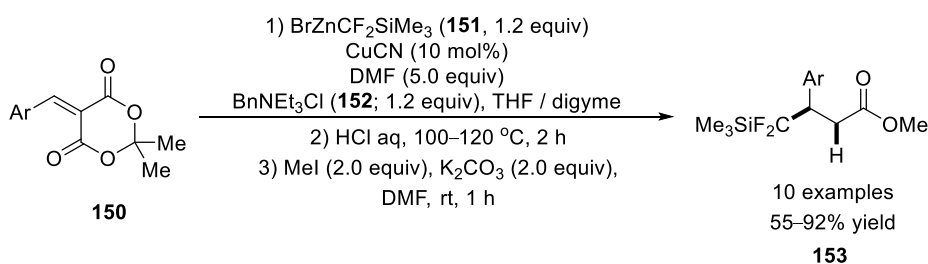
Scheme 4: Metal Salt-Triggered Difluoromethylation of α -Imino Ketones and Diketones.

In addition, diethyl oxalate (**148**) was also reported as an electrophile for stoichiometric difluoromethylation (Scheme 5).^[166] In the presence of super-stoichiometric amounts of KO^tBu and KOEt, the reaction between **148** and CF₂HSiMe₃ (**1r**) gave the hydrated difluoromethyl pyruvate (**149**) in 67% yield.



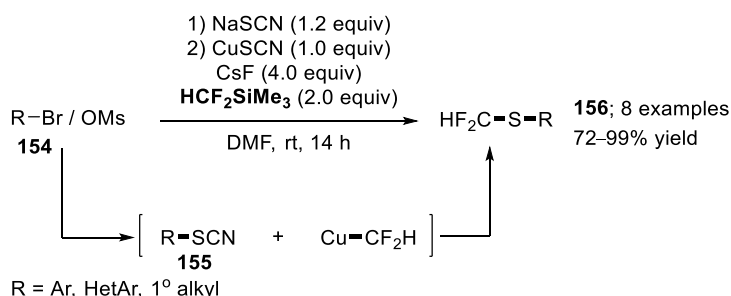
Scheme 5: Stoichiometric Difluoromethylation of an Activated Ester.

An interesting example to introduce the CF₂SiMe₃ group rather than the CF₂H group was reported by Dilman *et al.* who studied a copper-catalysed nucleophilic difluoro(trimethylsilyl)methylation of Meldrum's acid-type arylidenes **150** using BrZn–CF₂SiMe₃ (**151**; Scheme 6).^[167] A conjugate addition was observed to generate products of type **153** in 55–92% yields. The presence of DMF and benzyl triethylammonium chloride (**152**) was required to stabilise the organometallic species and increase the reaction rate. A Zn-to-Cu transmetallation step and coordination of the Lewis acidic Zn to the substrate's C=C double bonds may be involved in the mechanism.



Scheme 6: Cu-Catalysed Conjugate Addition of CF₂SiMe₃.

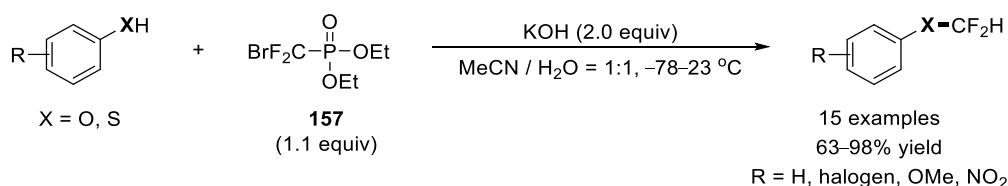
A copper-mediated difluoromethylation of organothiocyanates **155** using HCF₂SiMe₃ (**1r**) was reported to give difluoromethyl thioethers **156** from widely available substrates such as alkyl halides (**154**; Scheme 7).^[168] Organothiocyanates **155** were generated *in situ* by treating alkyl bromides with NaSCN. The second step involved the combined use of HCF₂SiMe₃ (**1r**), CsF, and CuSCN, which generated *in situ* Cu–CF₂H. The latter reacted with **155** to form difluoromethyl thioethers **156** in 72–99% yields. This method has been further applied to the difluoromethylation of arenediazonium salts.^[168]



Scheme 7: Stoichiometric Difluoromethylation *via* Nucleophilic Substitution.

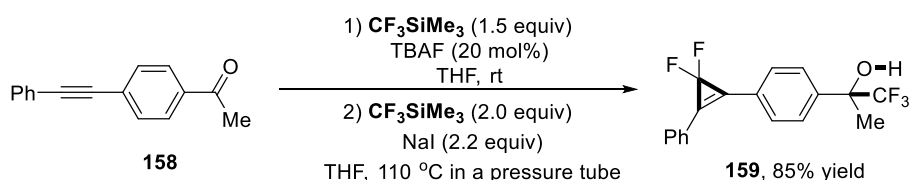
Electrophilic Difluoromethylation

A significant number of electrophilic difluoromethylation methods involve difluorocarbene intermediates. Because there are two fluorine atoms interacting with the carbene centre, difluorocarbene is more stabilised and less reactive than other halocarbenes or dihalocarbenes. The π -donating ability of fluorine imparts the stability of difluorocarbene as well as difluoromethyl radicals compared to their non-fluorinated counterparts and leads to a moderate controlled reactivity.^[169] Difluoromethylation of electron-rich or electron-poor phenols and thiophenols with $\text{BrCF}_2\text{P}(\text{O})(\text{OEt})_2$ (**157**) was described by Zafrani and Segall *et al.*, allowing for the formation of the corresponding products in 63–98% yields (Scheme 8).^[170] The proposed mechanism for the generation of difluorocarbene from **157** consists in the saponification of the diethyl phosphonate unit with release of the BrCF_2^- anion followed by α -elimination of bromide.



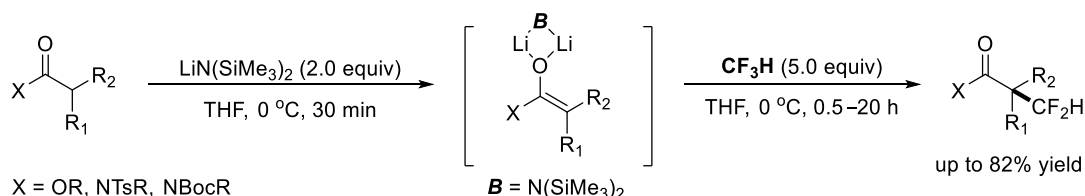
Scheme 8: Difluoromethylation of Phenols and Thiophenols with Ethyl Bromodifluoromethyl Phosphonate.

Due to the lack of commercially available *difluoromethylation* reagents, the electrophilic difluoromethylation was often achieved through the use of nucleophilic *trifluoromethylation* reagents. Under suitable reaction conditions, molecules such as the Ruppert–Prakash reagent (Me_3SiCF_3 ; **1s**) and Fluoroform (HCF_3 ; **1t**) were used as a precursor to an electrophilic CF_2 carbenoid. Olah and co-workers discovered a one-pot sequence of trifluoromethylation and [2+1] cycloaddition of **1s** and substrate **158** containing both an internal alkyne and a ketone (Scheme 9).^[171] This reaction enabled both a fluoride-initiated nucleophilic trifluoromethylation of $\text{C}=\text{O}$ and a NaI-promoted difluoromethylenation of the triple bond to give product **159** in 85% yield.



Scheme 9: One-Pot Sequential Trifluoromethylation and Difluoromethylenation with the Ruppert–Prakash Reagent.

More recently, Mikami's group has reported an $\text{S}_{\text{N}}2$ -type C–C bond formation between the enolised esters/amides and fluoroform (**1t**) in the presence of $\text{LiN}(\text{SiMe}_3)_2$ (2 equiv) in THF (Scheme 10).^[172]



Scheme 10: Difluoromethylation of Lithium Enolates with Fluoroform.

The proposed $\text{S}_{\text{N}}2$ reaction involved a lithium enolate attacking a trifluoromethyl lithium species formed by the deprotonation of HCF_3 (Figure 2). Such scenario may be possible because the interaction of the enolate's lithium with the lithium carbenoid's C–F bond is stronger than with the C–F bond of the neutral HCF_3 . The leaving

fluoride anion from the lithium carbenoid may be the driving force for the S_N2 displacement through coordination to the Lewis acidic lithium cation. This experimental result has been in good agreement with computational data.

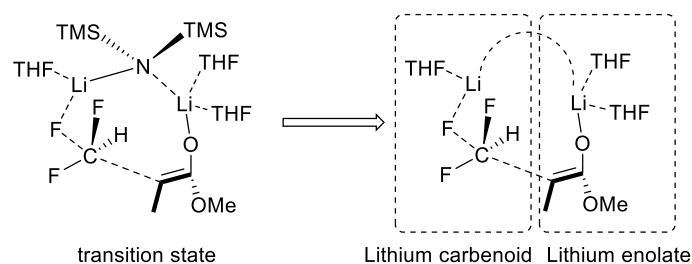
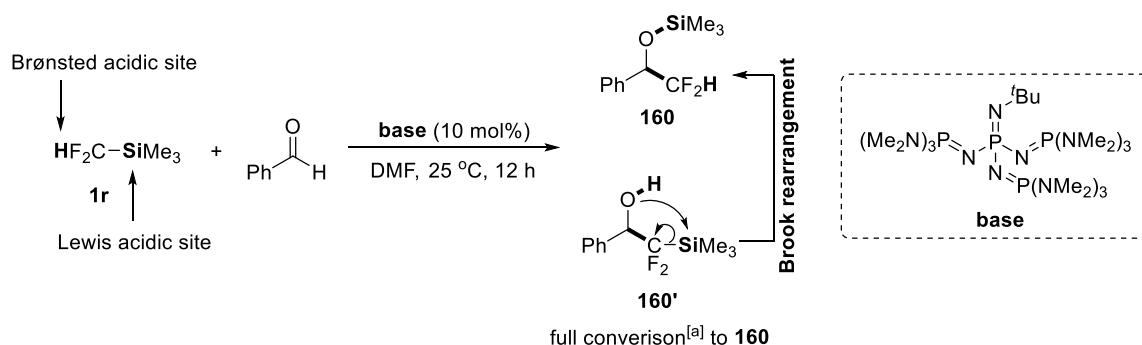


Figure 2: Proposed S_N2 -Type Reaction Mechanism.

2.2 Alkali Metal–Base-Catalysed C^F –Si Bond Activation

Brønsted Base (BB) or Lewis Base (LB) Activation?

Unlike Ruppert's reagent, which has been widely exploited as trifluoromethylation reagent,^[173] the use of $HF_2C-SiMe_3$ (**1r**) has been less common (Scheme 11). In **1r**, a Lewis acidic silicon atom and a Brønsted acidic hydrogen atom are connected through a CF_2 bridge, providing two scenarios for base-induced bond activation and/or catalysis: 1) a Brønsted base may deprotonate **1r** (C^F –H bond activation), generating a difluoromethyl silyl anion, which may subsequently react with a suitable electrophile; 2) a Lewis base may add to the Lewis acidic Si centre of **1r** (C^F –Si bond activation), generating a difluoromethyl anion, which may also react with a suitable electrophile. Here, the formation of a reactive hypervalent silicon species may also be possible.



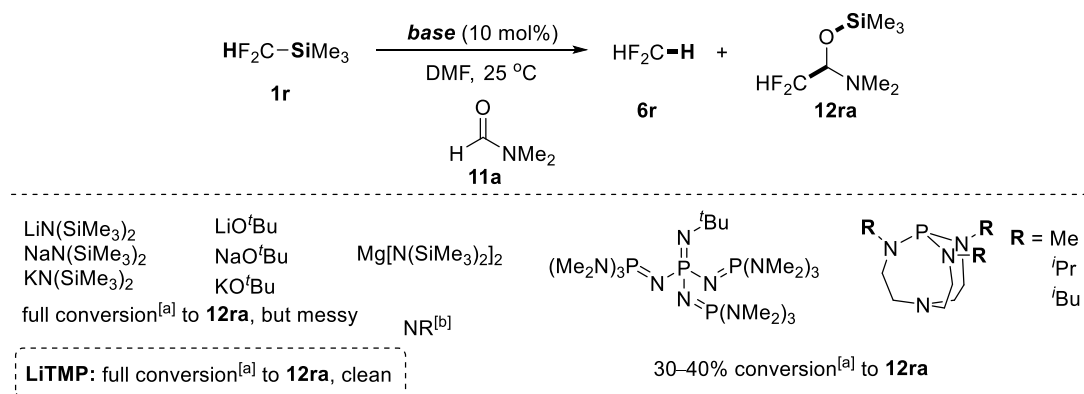
^[a] The conversion was determined by ^{19}F NMR spectroscopic analysis of a reaction aliquot without an internal standard (based on 'relative' analysis of both starting material **1r** and product **160**).

Scheme 11: Initial Experiments with HCF_2-SiMe_3 and Benzaldehyde.

In order to realise the C^F –H bond activation pathway, Schwesinger's P_4 base ($pK_a = 42.7$ in MeCN)^[174] was used in the reaction between HCF_2SiMe_3 (**1r**) and benzaldehyde in DMF at 25 °C (Scheme 11). Due to the strong basicity and the high steric demand of this N -centred base, we anticipated a smooth deprotonation with subsequent C^F –C bond formation to afford alcohol **160'** as a product (with an introduced CF_2SiMe_3 group; Brønsted base activation pathway). However, in the event the corresponding silylether **160** was observed as the exclusive product (with an introduced CF_2H group) suggesting that a C^F –Si bond activation may have occurred instead (Lewis base activation pathway). Product **160** was identified by 1H and ^{19}F NMR spectroscopic analysis of a reaction aliquot, displaying signals: in 1H NMR spectroscopy at $\delta = 5.77$ ppm (dt, $J = 56.0, 4.8$ Hz) for CF_2H and at $\delta = 4.84$ ppm (m) for the benzylic hydrogen atom; in ^{19}F NMR spectroscopy at $\delta = -127.6$ ppm (dd, $J = 283.8,$

56.0 Hz) and at $\delta = -132.1$ ppm (dd, $J = 283.8, 56.0$ Hz) for the two diastereotopic fluorine atoms. Indeed, it is conceivable that the organic base may have reacted as *Lewis* base in this scenario, regardless of its strong *Brønsted* basicity and high steric demand. Alternatively, the initially formed product **160'** may have undergone a Brook rearrangement to form **160**. It is noted that the exclusive formation of **160** has been in agreement with a study published by He *et al.* during the course of our investigations.^[162] Here, Schwesinger's P₄ superbase was used under mild conditions to activate the C^F–Si bond of **1r** for catalytic difluoromethylation of aldehydes and ketones.

In order to investigate a suitable base catalyst for potential C^F–H bond activation, HCF₂SiMe₃ (**1r**) was treated with various metal–base and organobase catalysts in DMF at 25 °C in the *absence* of an electrophile (Scheme 12). We anticipated that the resulting intermediates may be observed and identified by ¹⁹F NMR spectroscopic analysis. However, only the corresponding signals of HF₂C–SiMe₃ (**1r**; substrate), of HF₂C–H (**6r**; hydrolysis product), and *surprisingly* of DMF adduct **12ra** were detected in the ¹⁹F NMR spectra of the reaction aliquots. *To the best of our knowledge, this experiment represents the very first time that a rather unreactive carbonyl electrophile (tertiary formamide) has been activated in such a 'fluorination' context.* This unexpected *O*-silylated *N,O*-hemiaminal product has been synthesized for the first time; it displays signals in ¹H NMR spectroscopy at $\delta = 5.43$ ppm (ddd, $J = 56.3, 55.9, 5.1$ Hz) for the CF₂H fragment, at $\delta = 4.20$ ppm (ddd, $J = 10.1, 5.1, 5.1$ Hz) for the *O*-silylated *N,O*-hemiaminal hydrogen atom, and at $\delta = 2.10$ ppm (s) for the dimethylamino group. Likewise, in ¹⁹F NMR spectroscopy the detected signals at $\delta = -124.6$ ppm (ddd, $J = 284.4, 56.3, 5.1$ Hz) and at $\delta = -129.5$ ppm (ddd, $J = 284.4, 55.9, 10.1$ Hz) confirmed the presence of the CF₂H fragment in the product that bears two diastereotopic fluorine atoms. Overall, the structure of this unusual *O*-silylated difluoromethyl *N,O*-hemiaminal was confirmed after isolation by ¹H, ¹³C, and ¹⁹F NMR spectroscopy.



^[a] The conversions were determined by ¹⁹F NMR spectroscopic analysis of a reaction aliquot without an internal standard (based on 'relative' analysis of both starting material **1r** and product **12ra**). ^[b] NR = no reaction; product **12ra** was not detected – only starting materials were recovered (¹H and ¹⁹F NMR spectroscopic analysis of a reaction aliquot).

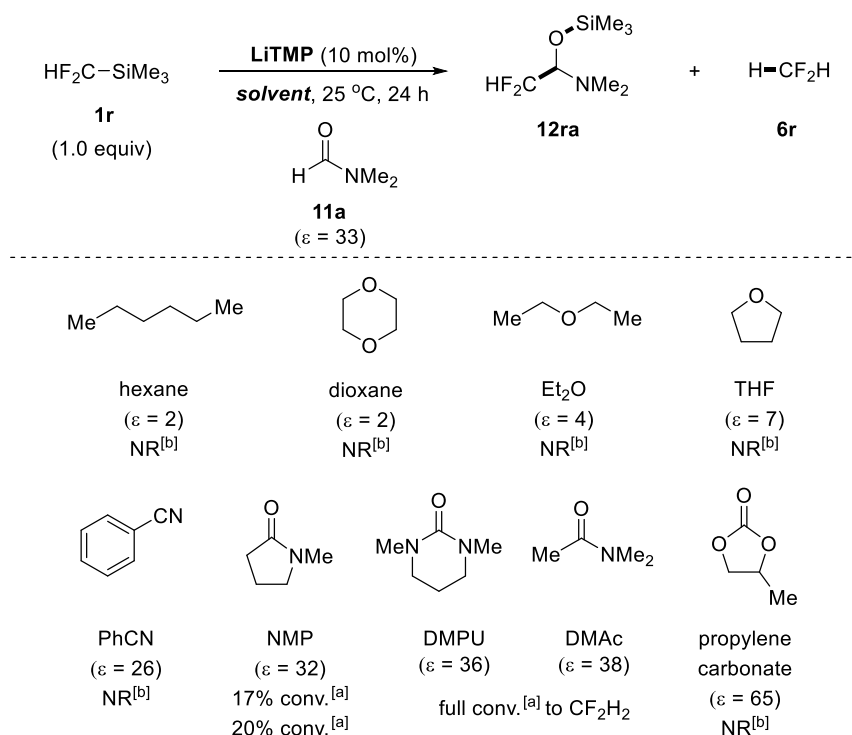
Scheme 12: Base Screening for the Unexpected Reaction between HF₂C–SiMe₃ and DMF.

Two types of metal–base catalysts were used: amides and alkoxides. In almost all cases, a full conversion of **1r** was detected by ¹⁹F NMR spectroscopy; however, the spectra proved to be rather messy. This observation may be due to the fact that these bases display a very high reactivity in DMF (*Brønsted* and *Lewis* basicity); in turn, multiple products were formed under these conditions in most cases. *Only the use of LiTMP provided product 12ra quantitatively in a very clean transformation; other products were not detected.* Based on this observation, LiTMP proved to be superior to the other metal–base catalysts examined. The full recovery of **1r** was observed when Mg[N(SiMe₃)₂]₂ was used, which may be ascribed to its relatively low reactivity. Two *N*- and *P*-centred

superbases were used as well, but product **12ra** was not detected in a significant amount (30–40% conv). It is conceivable that the metal–base catalysts may have an advantage over organobases in the activation of the electrophile, DMF, by the corresponding Lewis acidic metal cation.

Solvent Screening for the Use of DMF as Electrophile

At this point, the obtained unexpected results suggested that (*form*)amides could be good electrophiles for catalytic difluoromethylation in general. However, this process required an excessive amount of DMF, which would be a drawback as it may severely limit the scope (substrate competition). In order to improve the utility of this reaction, and hopefully apply the same catalysis conditions to a broad variety of (form)amide electrophiles, the next step was to select a more suitable solvent for the catalytic difluoromethylation of DMF (Scheme 13).



^[a] The conversions were determined by ^{19}F NMR spectroscopic analysis of a reaction aliquot without an internal standard (based on 'relative' analysis of both starting material **1r** as well as products **12ra** and **6r**). ^[b] NR = no reaction; the intended product **12ra** was not detected – only substrates were recovered (^1H and ^{19}F NMR spectroscopic analysis of a reaction aliquot).

Scheme 13: Solvent Screening for the Catalytic Difluoromethylation of DMF.

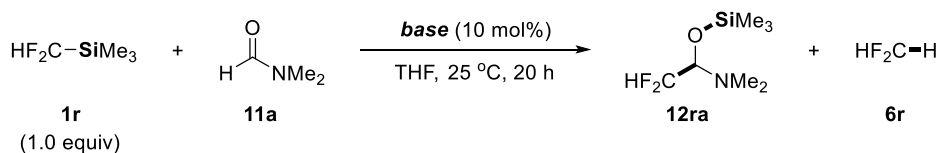
Given that any proton source may result in the formation of the hydrolysis product, CF_2H_2 (**6r**), which would prevent the intended reaction to proceed, the choice was limited to carefully dried *aprotic* solvents. First, several apolar solvents were tested ($\epsilon = 2$ –7; Scheme 13). Unfortunately, none of these led to the formation of product **12ra**. Next, a few polar solvents were tested ($\epsilon = 26$ –65); product **12ra** was not observed in benzonitrile. The use of 1,3-dimethyl-3,4,5,6-tetrahydro-2(1*H*)-pyrimidinone (DMPU) and dimethylacetamide (DMAc) resulted only in full conversion to the hydrolysis product, CF_2H_2 (**6r**). Surprisingly however, when the reaction was conducted in *N*-methyl-2-pyrrolidone (NMP) two sets of product signals – in addition to **1r** (23% conv) and **6r** (40% conv) – were observed in the ^{19}F NMR spectrum (reaction aliquot). One of these sets was assigned to the intended DMF adduct **12ra** (17% conv), the other one to the *unexpected* NMP adduct (20% conv). It is conceivable though that, due to the ring strain in NMP, this γ -lactam may display a similar electrophilicity compared to a formamide (DMF).

However, the formation of a large amount of hydrolysis product **6r** (40% conv) indicated that the α -hydrogen of NMP ($pK_a = 35.2$ in DMSO)^[175] may have acted as a proton source in this reaction (all components were used under strictly anhydrous conditions). In order to address this issue, the solvent polarity had to be decreased in order to render the base catalyst and the formed difluoromethyl anion less basic; alternatively, the nature of the base catalyst had to be adjusted.

Optimisation of Reaction Conditions for the Use of DMF as Electrophile

As demonstrated, a solvent less polar than DMF was required to suppress the deprotonation of the α -hydrogen in lactams. When NMP was used as electrophile, the use of a weaker base, KO^tBu, in THF has shown a substantial advantage in terms of both reactivity and chemoselectivity. In turn, a base screening was carried out in THF at 25 °C to see whether a similar catalyst was applicable to the difluoromethylation of DMF (Table 1). The conversion of **1r** to **12ra** was determined by ¹⁹F NMR spectroscopic analysis of the corresponding reaction aliquot.

Table 1: Base Screening for the Catalytic Difluoromethylation of DMF.



entry	base	conv ^[a] of 12ra [%]	conv ^[a] of 6r [%]
1	LiN ⁱ Pr ₂	NR ^[b]	-
2	LiTMP	NR ^[b]	-
3	LiN(SiMe ₃) ₂	NR ^[b]	-
4	NaN(SiMe ₃) ₂	2	1
5	KN(SiMe ₃) ₂	28	1
6	LiO ^t Bu	NR ^[b]	-
7	NaO ^t Bu	38	2
8	KO ^t Bu	99	1
9	KO ^t Bu / [18]c-6	97 (messy)	3
10	KOMe	98 (messy)	2
11	DBU	NR ^[b]	-
12	proton sponge	NR ^[b]	-
13	P ₁ - ⁱ Bu-tetra	NR ^[b]	-
14	P ₁ - ⁱ Bu	NR ^[b]	-
15	P ₂ -Et	0	1
16	P ₂ - ⁱ Bu	0	<1
17	P ₄ - ⁱ Bu	0	<1
18	V-Me	0	<1
19	V- ⁱ Pr	0	<1
20	V- ⁱ Bu	0	<1
21	KF	NR ^[b]	0
22	CsF	<1	<1
23	CsF / [18]c-6	96	4

^[a] The conversions were determined by ¹⁹F NMR spectroscopic analysis of a reaction aliquot without an internal standard (based on 'relative' analysis of both starting material **1r** as well as products **12ra** and **6r**). ^[b] NR = no reaction; the intended product **12ra** was not detected – only substrates were recovered (¹H and ¹⁹F NMR spectroscopic analysis of a reaction aliquot).

Two types of metal–base catalysts were used in this screening; regarding amide bases (entries 1–5), the use of $\text{KN}(\text{SiMe}_3)_2$ showed a better reactivity than LiN^iPr_2 , LiTMP , and other metal hexamethyldisilazides, but the conversion was low (28%; entry 5). Regarding alkoxide bases (entries 6–10), the use of KO^iBu gave **12ra** with 99% conversion (entry 8), whereas **12ra** was not detected or observed with low conversion when LiO^iBu or NaO^iBu were used, respectively (entries 6 and 7). Although the use of KO^iBu , combined with [18]c-6, or KOMe alone also afforded product **12ra** with 97% and 98% conversion, respectively (entries 9 and 10), the corresponding NMR spectra proved to be messy. Several commercially available organic bases were examined as well; however, product **12ra** was not detected in these cases (entries 11–20). In addition, a few metal fluorides were used (entries 21–23). Interestingly, only the combined use of CsF and [18]c-6 also provided product **12ra** with high conversion (96%; entry 23).

Optimisation of Reaction Conditions for the Use of NMP as Electrophile

As explained, the challenge of using NMP as electrophile lies in the presence of the acidic α -hydrogen ($\text{pK}_a = 35.2$ in DMSO).^[176] In order to favour the C–C bond formation between **1r** and NMP over the hydrolysis of **1r** (C–H bond formation), a base screening was carried out in the presence of an excessive amount of NMP, being both electrophile and solvent (Table 2).

Table 2: Use of NMP as Electrophile and Solvent – Base Screening.

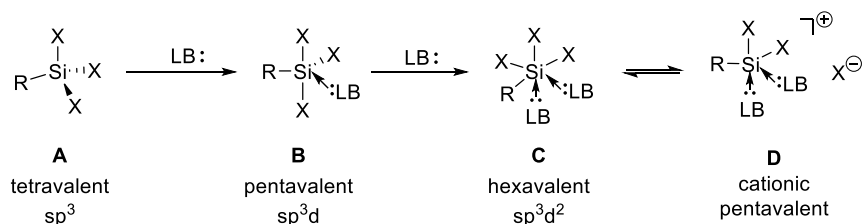
$ \begin{array}{c} \text{HF}_2\text{C}-\text{SiMe}_3 \\ \textbf{1r} \\ (1.0 \text{ equiv}) \end{array} \xrightarrow[\text{NMP, 25 }^\circ\text{C, 24 h}]{\text{Lewis base (10 mol\%)}} \begin{array}{c} \text{HF}_2\text{C}-\text{C}(\text{OSiMe}_3)(\text{NMe}) \\ \textbf{12rb} \end{array} + \text{H}-\text{CF}_2\text{H} \begin{array}{c} \textbf{6r} \end{array} $ <div style="text-align: center; margin-top: 10px;"> <p>11b</p> </div>				
entry	Lewis base	conv ^[a] to 12rb [%]	conv ^[a] to 6r [%]	conv ^[a] [%]
1	LiTMP	38	49	87
2	LiO ⁱ Bu	18	37	55
3	LiOPh	0	0	0
4	LiOH	0	4	4
5	Li ₂ CO ₃	0	0	0
6	NaOH	8	23	31
7	KOH	26	74	>99
8	KOMe	10	90	>99
9	KO ⁱ Bu	50	50	>99
10	KO ⁱ Bu ^[b]	90	5	95
11	KOAc	0	0	0
12	Ba(O ⁱ Pr) ₂	0	0	0
13	Sr(O ⁱ Pr) ₂	0	0	0
14	Fe(OEt) ₃	0	0	0
15	Zn(O ⁱ Bu) ₂	0	0	0
16	DBU	0	1	1
17	P ₄	<1	67	68

^[a] The conversions were determined by ¹⁹F NMR spectroscopic analysis of a reaction aliquot without an internal standard (based on ‘relative’ analysis of both starting material **1r** and product **12rb**). ^[b] This reaction was carried out in THF in the presence of 1 equivalent of NMP.

When LiTMP was used as the base catalyst, the levels of C–C bond formation (product **12rb**) and hydrolysis (product **6r**) were shown to be 38% and 49%, respectively (entry 1; ^{19}F NMR spectroscopic analysis of a reaction aliquot). The use of LiO*t*Bu was also in favour of hydrolysis product **6r** (entry 2). Other lithium bases either resulted in the full recovery of starting materials or the generation of small amounts of hydrolysis product **6r** (entries 3–5). Interestingly, KOH showed a better reactivity than NaOH or LiOH, but **6r** was still the major product (entries 4, 6, and 7). It is conceivable that after the hydroxide anion added to the Si atom, the formed Si–OH group may also act as a decent proton source (α silicon effect). Potassium bases displayed the highest reactivity among all metal-containing bases (entries 8–10); the best result was achieved when KO*t*Bu was used: substrate **1r** was fully converted to afford products **12rb** and **6r** in a 1:1 ratio (entry 9). In contrast, no reactivity was observed when KOAc was used (entry 11). The reaction did not proceed either when alkaline earth metal and transition metal alkoxides were used (entries 12–15). Regarding organobases, Schwesinger's P_4 base gave 68% overall conversion, but almost exclusively hydrolysis product **6r**. Again, it is likely that the metal–base catalysts have an advantage over organobases regarding the activation of the electrophile, NMP, through coordination to the Lewis acidic metal cation. Next, as mentioned earlier, in order to suppress the effect of the α -hydrogen, the solvent polarity had to be decreased (in order to ‘temper’ the basicity); indeed, since NMP is a very polar solvent ($\epsilon = 32$), the thermodynamic proton transfer should be more favoured. Thus, when a less polar solvent (THF; $\epsilon = 7$) was used together with the best base, KO*t*Bu, the fluorinated pro-nucleophile **1r** was fully converted: most significantly, 90% of the intended product **12rb** ($\text{C}^{\text{F}}\text{–C}$ bond formation) and only 5% of the hydrolysis side-product **6r** ($\text{C}^{\text{F}}\text{–H}$ bond formation) were obtained (entry 10). In turn, a highly efficient reaction system has been uncovered for the catalytic difluoromethylation of a γ -lactam: KO*t*Bu as a catalyst in THF.

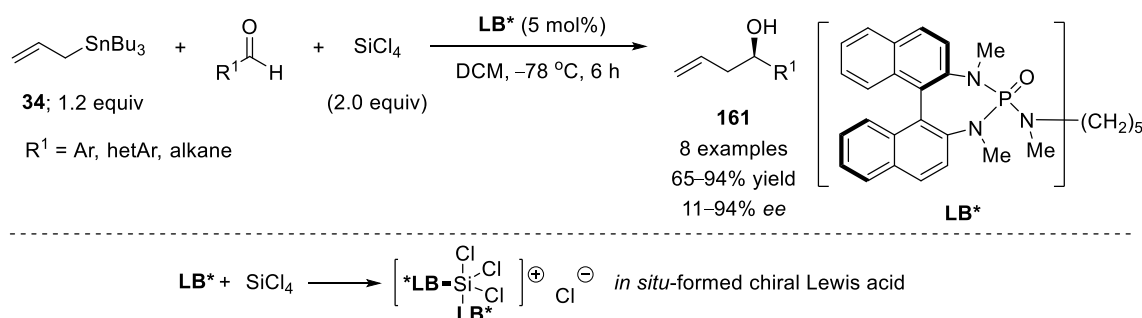
Hypervalent Silicon Species and their Application in Organofluorine Chemistry

Hypervalent silicon species have been extensively used in organic synthesis.^[177–183] For instance, a neutral Lewis basic ligand (LB) may add to the Lewis acidic centre of tetravalent silicon complex A to generate pentavalent silicon complex B; the latter may undergo another Lewis base addition to form hexavalent silicon complex C (Scheme 18).^[184] Species C may be further converted to cationic pentavalent silicon complex D upon dissociation of an anionic ligand X^- . It has been controversial whether the driving force for such “hypervalency” originated from a vacant d orbital at silicon,^[185] or the σ^* orbital of the Si–LB bond.^[186] According to Bent's rule,^[187] when the silicon atom in complex A (sp^3) gets rehybridised to sp^3d in species B, the s character of the silicon atom (δ^+) decreases; as a result the Si–LB bond shall be more polarised, thus leading to the formation of a more Lewis acidic silicon centre. In 1979, Staemmler postulated the so-called “donor–acceptor interaction” theory.^[188] More specifically, Gutmann's fourth rule stated that “upon coordination of a polyatomic donor to a polyatomic acceptor there will be a net *increase* in electron density at the donor atom and a net *decrease* of electron density at the acceptor atom”.^[189] In turn, the use of a stronger (more δ^-) Lewis base (LB) would result in an enhanced Lewis acidity at the silicon centre (more δ^+).



Scheme 18: Hypervalent silicon species.

After initial investigations by Kobayashi^[190] and Nakajima,^[191] the use of neutral Lewis bases in the catalytic activation of tetravalent silicon reagents (Lewis acid) has been extensively investigated by Denmark and co-workers.^[179, 192-196] For instance, Denmark's group reported an asymmetric aldehyde allylation using allyl stannane **34** (Scheme 19).^[192] A catalytic amount of enantiopure phosphoramidate **LB*** was used to activate the weak Lewis acid SiCl_4 . The *in situ*-formed cationic hypervalent silicon species acted as a chiral Lewis acid catalyst to mediate aldehyde allylation using **34**, thus affording homoallylic alcohols **161** in 65–94% yields with up to 94% *ee*.



Scheme 19: Cationic hypervalent silicon species in asymmetric catalysis.

Hypervalent Silicate Anion in Organofluorine Chemistry

The anionic hypervalent silicon complex TASF (**162**) was reported as a powerful nucleophilic *fluoride* source as early as 1985 (Figure 2).^[197] In 1999, Kolomeitsev and co-workers published the corresponding *trifluoromethyl* analogue, compound **163**, which was shown to be stable in the solid state below 0 °C (Figure 2).^[198]

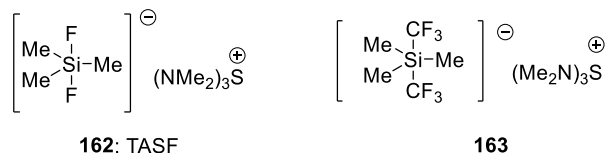
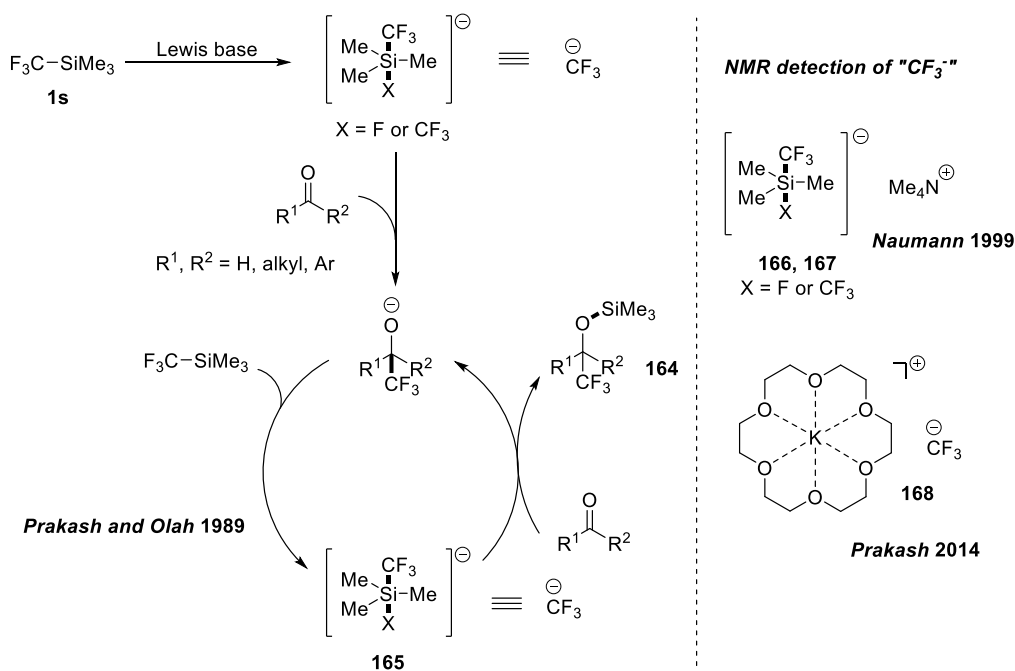


Figure 2: Anionic hypervalent silicon complexes.

In 1989, Prakash and Olah accomplished the nucleophilic *trifluoromethylation* of carbonyl compounds using the Ruppert–Prakash reagent, $\text{F}_3\text{C-SiMe}_3$ (**1s**), as a nucleophilic “ CF_3^- ” precursor (Scheme 20).^[199] In the presence of a catalytic amount of tetrabutylammonium fluoride (TBAF) as an anionic Lewis base the corresponding trifluoromethylated siloxy adducts **164** were formed under mild conditions. The pentavalent anionic silicon complex **165** was postulated as a critical reaction intermediate. In 1999, reactive intermediates **166** and **167** were detected in ^{13}C , ^{19}F , and ^{29}Si NMR spectroscopy in TBAF-initiated trifluoromethylations.^[200] Since then, the detection of the highly reactive “ CF_3^- ” anion seemed to be limited to the observation of the corresponding pentavalent silicate anion. In 2014, however, Prakash and co-workers observed the “long-lived CF_3^- ” anion **168** by treating a sterically demanding reagent, $\text{F}_3\text{C-TIPS}$ (TIPS = triisopropylsilyl; $\text{F}_3\text{C-Si}^i\text{Pr}_3$), with a mixture of KO^tBu and [18]c-6. Here, the bulky TIPS group was shown to inhibit the formation of any undesired pentavalent silicate species.^[173]

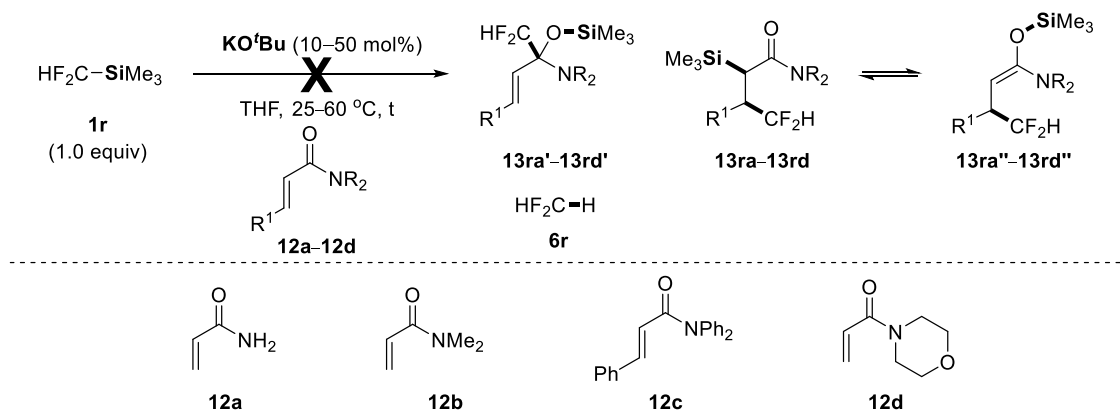


Scheme 20: Anionic hypervalent silicon species as 'CF₃⁻' equivalent in C-C bond formation.

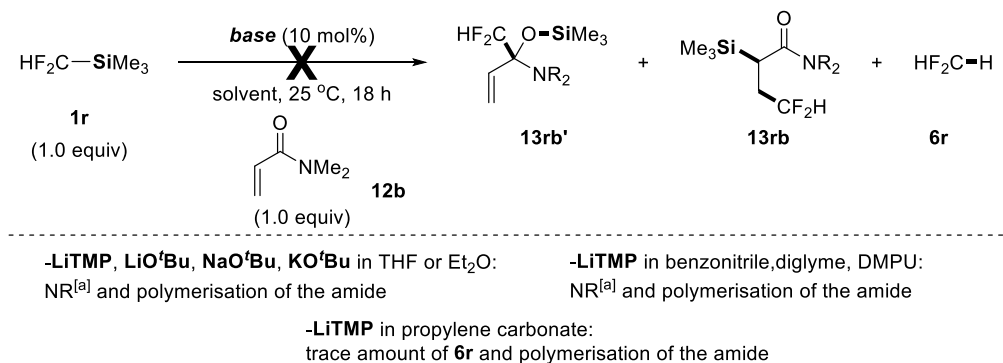
Regarding *difluoromethylation*, Hu and co-workers detected a pentavalent silicate species in ¹⁹F and ²⁹Si NMR spectroscopy (see Scheme 3, page 86).^[164] It is conceivable that the *in situ*-generated pentavalent silicate anion represents a more kinetically labile "CF₂H⁻" nucleophile; in addition, the more Lewis acidic silicon centre may enhance the reactivity of an electrophile. However, in Hu's scenario a crown ether was found to be of critical importance to form the catalytically active pentavalent silicate complex. This stand in sharp contrast to our own study where a crown ether was *not* required in the overall transformation. Thus, it remains unclear in our study whether or not the catalytic difluoromethylation requires a hypervalent silicate intermediate. The mechanism will be clarified in future studies.

α,β-Unsaturated Amides as Potential Electrophiles

In order to apply this catalyst system to further electrophiles, α,β-unsaturated amides were used as potential substrates. The generated CF₂H⁻ anion would be a rather hard nucleophile, thus, we anticipated that the reaction between **1r** and Michael acceptors would undergo a 1,2-addition, rather than a conjugate addition. However, the reaction did not proceed at all even with an increased catalyst loading or at an elevated temperature (Scheme 14).



In order to investigate a suitable catalyst system for Michael acceptors, α,β -unsaturated amide **12b** was chosen as a model substrate (Scheme 15). However, the examination of several metal amides and alkoxides did not lead to any detectable intended C^F–C bond formation; rather, the solidification of the reaction mixtures was observed, i.e., a base-initiated polymerization of monomer **12b** must have occurred. Only a trace amount of hydrolysis product **6r** was detected in the ¹⁹F NMR spectrum when LiTMP was used as a catalyst in propylene carbonate.



^[a] NR = no reaction; products **13rb'**, **13rb**, and **6r** were not detected – only substrates were recovered (¹H and ¹⁹F NMR spectroscopic analysis of a reaction aliquot).

Scheme 15: Screening of Various Reaction Conditions Using Michael Acceptor **12b**.

Next, we examined the reaction using an excess of Michael acceptor **12b**, being both electrophile and solvent. A screening of bases and additives for this model reaction using 30–35 equiv of **12b** at 25 °C was carried out; different inorganic and organic bases were used (Table 3). Interestingly, in most cases the ¹⁹F NMR spectroscopic analysis of the corresponding reaction aliquot revealed the two predicted doublet of doublet (dd) signals for the expected 1,2-adduct **13rb'**, but also a doublet of triplet (dt) signal, which was assigned to the unexpected 1,4-adduct **13rb**.

Table 3: Optimisation of Reaction Conditions.

$$\text{HF}_2\text{C}-\text{SiMe}_3 \xrightarrow[\text{neat, 25 } ^\circ\text{C, 18 h}]{\text{base (x mol\%)}, \text{additive (y mol\%)}} \text{HF}_2\text{C}-\text{O}-\text{SiMe}_3 + \text{Me}_3\text{Si}-\text{CH}(\text{NR}_2)-\text{CH}_2\text{CF}_2\text{H} + \text{HF}_2\text{C}=\text{H}$$

1r (1.0 equiv) + **12b** (30–35 equiv) → **13rb'** (not observed) + **13rb** + **6r**

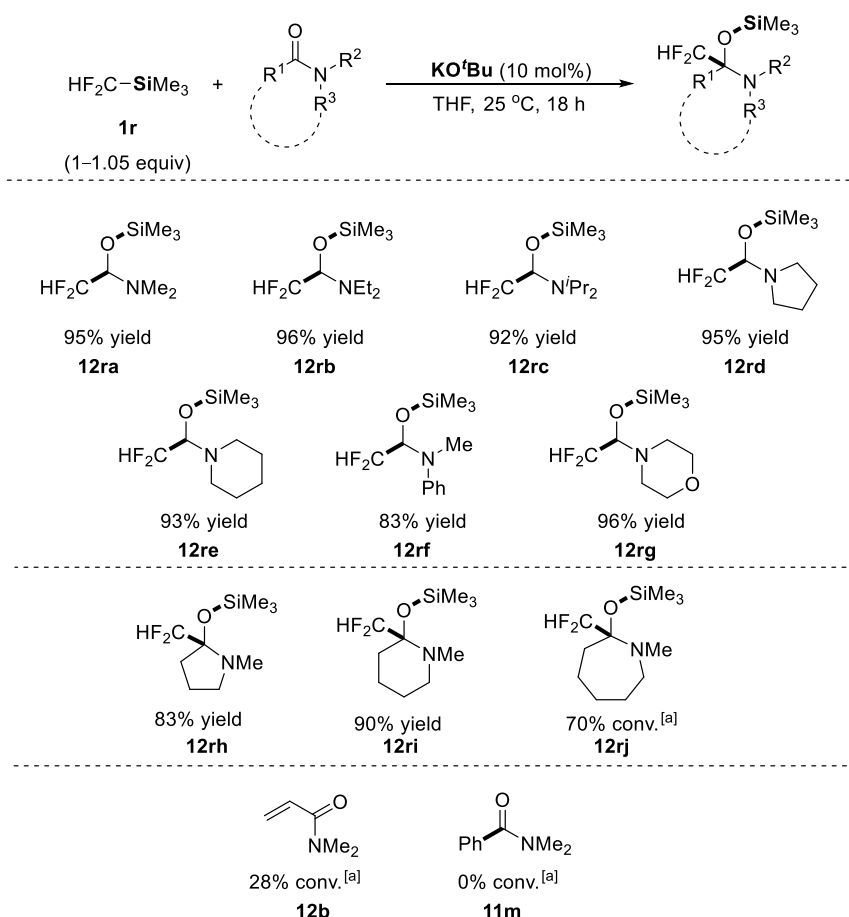
entry	base (x)	additive (y)	ratio ^[a] of 1r [%]	ratio ^[a] of 13rb [%]	ratio ^[a] of 6r [%]
1	LiTMP (10)	-	97	3	0
2	LiTMP (20)	-	78	5	17
3	LiTMP (20)	DMF (20)	69	5	26
4	LiO ^t Bu (20)	-	72	16	12
5	LiO ^t Bu (20)	DMF (20)	72	28	0
6	KO ^t Bu (20)	-	75	9	16
7	KO ^t Bu (20)	DMF (20)	54	24	22
8	LiPh (20)	-	>99	0	0
9	LiOPh (20)	-	>99	0	0
10	DBU (20)	-	93	2	5

^[a] The ratios were determined by ¹⁹F NMR spectroscopic analysis of a reaction aliquot without an internal standard (based on 'relative' analysis of both starting material **1r** as well as products **13rb'**, **13rb**, and **6r**). ^[b] NR = no reaction; the intended product **13rb** was not detected – only substrates were recovered (¹H and ¹⁹F NMR spectroscopic analysis of a reaction aliquot).

When LiTMP was used as catalyst (10 mol%), **13rb** was observed with only 3% conversion together with starting materials (entry 1). When the catalyst loading was increased to 20 mol%, **1r** was converted to **13rb** (5% conv) and hydrolysis product **6r** (17% conv; entry 2). The use of LiTMP with DMF as an additive (20 mol%) increased the amount of undesired **6r** (entry 3). In contrast the use of LiO^tBu alone (entry 4), the combined use of LiO^tBu and DMF afforded intended product **13rb** exclusively (28% conv; entry 5). The use of KO^tBu did not improve this result further (entries 6 and 7). In the same line, the use of LiPh and LiOPh did not afford at all **13rb** (entries 8 and 9). Finally, the use of DBU as a metal-free Lewis base gave both products with a very low conversion (entry 10). The challenge of this intended transformation may be ascribed to the sensitivity of the Michael acceptor under the basic reaction conditions. Interestingly, in none of these experiments the initially expected 1,2-adduct **13rb'** was observed, which may be due to the steric demand of electrophilic carbon centre of the amide group (vs. the more accessible β-position). Since the highest conversion was only 28% after quite some experimentation, this base catalysis approach towards a novel conjugate difluoromethylation was abandoned.

Substrate Scope

Finally, the scope for acyclic and cyclic amide derivatives was investigated using KO^tBu (10 mol%) as a catalyst in THF at 25 °C under strictly anhydrous conditions (Scheme 16). The ratio HF₂CSiMe₃ (**1r**) / electrophile was fixed to 1–1.05:1 unless otherwise mentioned. In a few cases, excessive pro-nucleophile **1r** had to be used to ensure the full consumption of certain electrophiles, which proved to be difficult to be separated from the products during isolation. In the event, DMF underwent full conversion to the desired product **12ra** (¹H NMR spectroscopic analysis of a reaction aliquot). Work-up and isolation of **12ra** proved to be particularly straightforward although conducted in a glove box: THF was evaporated and the resulting mixture was dissolved in hexane. The precipitated catalyst was filtered off through cotton wool, and subsequent evaporation of the obtained solution under high vacuum yielded the difluoromethylated product **12ra** in 95% yield (with >99% purity); no signals of the ^tBu group were detectable in the corresponding ¹H NMR spectrum. It is noted that the NMR analysis was carried out using benzene-*d*₆, as the product decomposed gradually to multiple side-products in chloroform-*d* or other 'acidic' solvents. Furthermore, it is noted that some of the products (particularly **12ra**) proved to be fairly volatile *and* sensitive to water, acid, air and/or heat; with an increasing size of the *N*-substituents the volatility and sensitivity decreased. This simple work-up and isolation method proved to be applicable to the isolation of all products. The Et and ⁱPr analogues of DMF also full converted to the intended products **12rb** and **12rc**, and isolated in 96% and 92% yields, respectively. Product **12rd** was formed with full conversion, and isolated in 95% yield. This product contains a pyrrolidine ring that can be often found in natural products.^[201] The use of the piperidine analogue of DMF resulted in the formation of product **12re** in 93% isolated yield. The use of the *N*-Ph/Me-derived formamide gave the corresponding product **12rf** in 83% isolated yield. Similarly, the use of a morpholine analogue of DMF afforded full conversion to product **12rg**, which was isolated in 96% yield. Importantly, in all these cases the hydrolysis product, CF₂H₂ (**6r**), was *not* formed or only *in trace amounts*, which was 'evaporated out' together with the solvent.

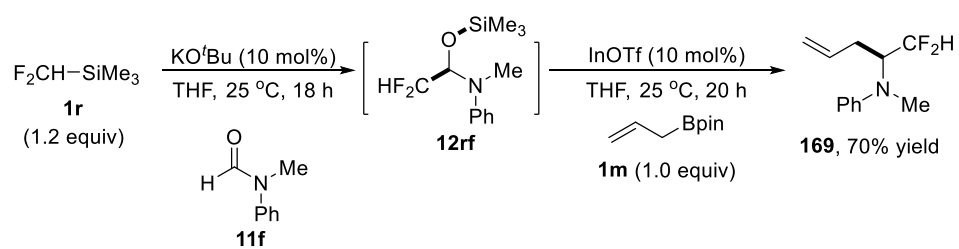


The yields refer to the isolated yields according to the described procedure. ^[a] The conversions were determined by ¹⁹F NMR spectroscopic analysis of a reaction aliquot without an internal standard (based on ‘relative’ analysis of both starting material **1r** and the corresponding products **12**).

Scheme 16: Substrate Scope for Potassium Alkoxide Catalysis.

Next, lactams were tested under the same conditions. For instance, the γ -lactam (NMP) was converted to product **12rh** in 83% isolated yield; here, 1.2 equiv of **1r** were used. The corresponding δ -lactam showed a higher reactivity and gave product **12ri** in 90% isolated yield. In contrast, the ϵ -lactam-derived product **12rj** was not isolated cleanly; a maximum of 70% conversion was detected in ¹⁹F NMR spectroscopy. Further experimentation to improve this result proved to be unsuccessful. As discussed earlier, the conjugate adduct derived from α,β -unsaturated amide **12b** was formed with only 28% conversion using a combination of LiO^tBu (20 mol%) and DMF (20 mol%). Finally, the use of the acyclic benzamide **11m** did result in any product formation.

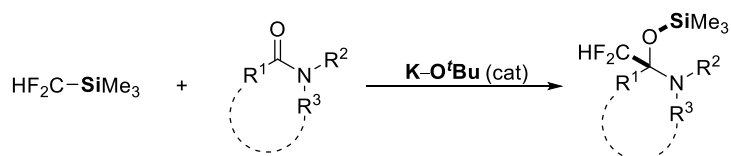
In order to highlight the utility of such transformation, the *in situ*-formed *O*-silylated difluoromethyl *N,O*-hemiaminal **12rf** subsequently underwent smooth ‘one-pot’ Lewis acid-catalysed C–C bond formation –that is the nucleophilic displacement of the OTMS group by an allyl unit– through addition of allyl boronic ester **1m** (1 equiv) in the presence of InOTf^[202] (10 mol%; Scheme 17). In turn, the difluoromethylated homoallylic tertiary amine **169** was formed ‘one-pot’ from the corresponding formamide and isolated in 70% overall yield. It is noted that this chemical transformation of **12rf** did not proceed in the absence of the Lewis acid catalyst.



Scheme 17: Sequence of Catalytic Difluoromethylation/Allylation of a Formamide.

Conclusion

A simple alkali metal–Lewis base (M–LB) catalyst was used for the Lewis base activation of C(sp³)–Si bonds of the commercially available difluoromethylation reagent, HCF₂SiMe₃ (Scheme 3).

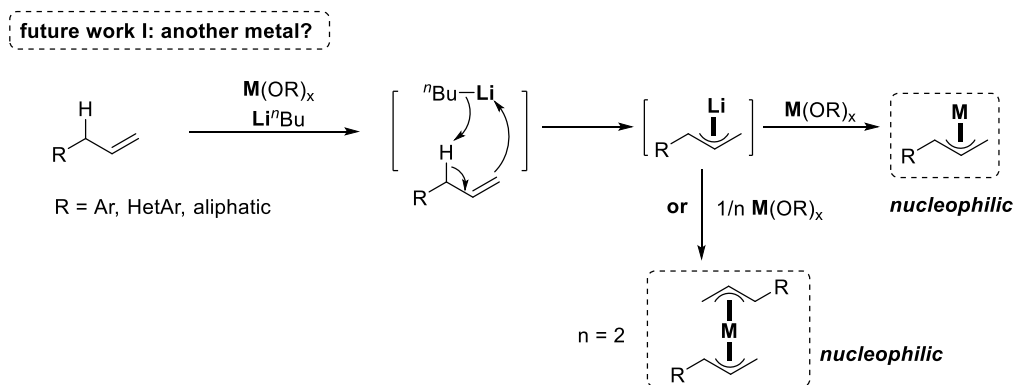


Scheme 3: Difluoromethylation.

Subsequently, the presumed *in situ*-generated catalytic amount of an alkali metal–CF₂H (or a pentacoordinated silicate) complex underwent nucleophilic addition to a series of amides and lactams, thus forming difluorinated silylated *N,O*-hemiaminals in good yields, which has shown potential for further functionalisation. The acidic α hydrogen of the various amide groups was well tolerated.

Future Work

Through the current work a formal C(sp³)–H bond activation was developed by using a commercially available sodium amide. During the mechanistic study, the combined use of a catalytic amount of LiBu/NaO^tBu was shown to be effective to catalyse the model reaction. In this scenario, an *in situ*-formed allyl–Li species underwent Li-to-Na transmetalation to generate a catalytically active allyl–Na nucleophile. The general (step-wise) transmetalation from an allyl–Li/alkali metal species to an allyl–M (M = alkaline earth, p-, d-, f-block metals) has been reported by Layfield.^[150] Thus, it is anticipated that the combined use of LiBu/MO^tBu or MX (X = halide, acetate, triflate) in our model reaction may lead to the *in situ* formation of a catalytically active allyl–M species in view of coupling with a suitable electrophile (Scheme 1). The metal identity may interfere with the regio-, diastereo- and enantioselectivity of the homoallyl product. The selected metal (low electronegativity) is assumed to be in its low-oxidation state in order to ensure the nucleophilicity of the allyl–metal species. Furthermore, with the strong basicity of LiBu, more difficult pro-nucleophiles such as acyclic and cyclic aliphatic alkenes might be activated. However, in this case, a *carbon* electrophile (e.g. CC multiple bonds) may be required in order to achieve catalyst turn-over (product-base principle).

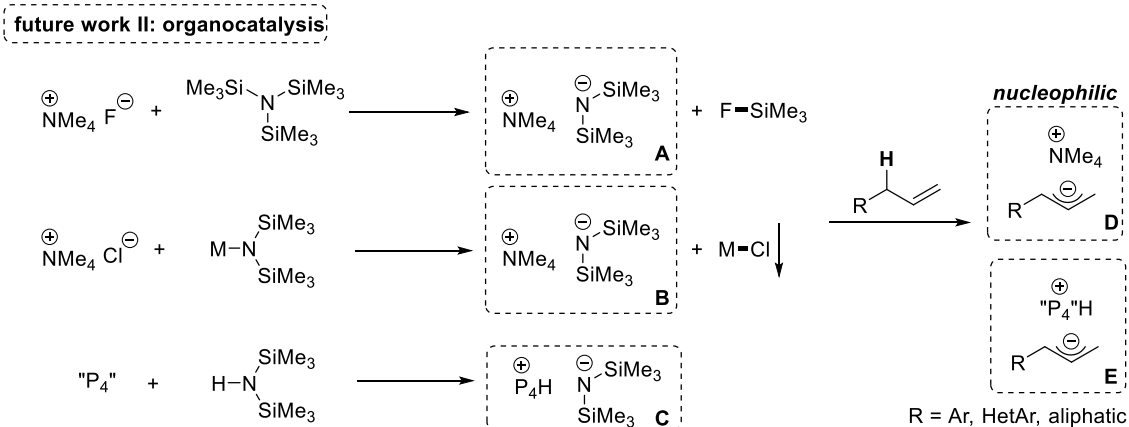


Scheme 1: Investigate the Potential of Other Metals.

Apart from metal–base catalysis, organo-catalysis is also of interest. The NBu₄⁺ paired allyl anion was reported to react with aldimine to generate homoallylic amines in a fluoride initiated Hosomi–Sakurai reaction (normally catalysed by acids). The *in situ* generation of this “organic counter cation paired allyl anion” was achieved *via* Lewis base (NBu₄⁺F[−]) activation of the C(sp³)–Si bond (of allylsilane). However, it is anticipated that the same intermediate (NBu₄⁺ paired allyl anion) may also be prepared through Brønsted base activation pathway. To achieve this goal, several Brønsted base with organic counter cations were proposed below (Scheme 2).

Apart from metal–base catalysis, organocatalysis is also of interest in this context. The NBu₄⁺-paired allyl anion was reported to react with aldimines to generate homoallylic amines in a fluoride-initiated Hosomi–Sakurai reaction (normally catalysed by acids).^[203] The *in situ* generation of this “organic cation-paired allyl anion” was achieved *via* Lewis base (NBu₄⁺F[−]) activation of the C(sp³)–Si bond (of an allyl–silane). However, it is anticipated that the same intermediate (NBu₄⁺-paired allyl anion) may also be prepared through a Brønsted base activation pathway. To achieve this goal, several Brønsted bases with organic counter cations may be proposed (Scheme 2). Brønsted base **A** may be prepared by treating N(SiMe₃)₃ with an organic fluoride source, in which case the strong energy of the Si–F bond would serve as a driving force.^[204] Base **B** may be accessed through precipitation of an inorganic salt (M–Cl), whereas base **C** may be formed by treating a secondary amine with an

organic superbase (e.g. a Schwesinger base). It is anticipated that the formed organic bases **A**, **B**, and **C** shall demonstrate a higher reactivity than the currently used $\text{NaN}(\text{SiMe}_3)_2$, due to a less coordinating cation. Likewise, the generated allyl anion nucleophile (e.g. **D** and **E**) would be expected to display a higher reactivity towards an electrophile.



Scheme 2: Brønsted Base with Organic Counter Cation.

3 Experimental

*The preparation of compounds **8aa-8at**, **8ca**, **8cq**, **8cd**, **8eb-8ib** and **8dr** were conducted in collaboration with Dr Hanno Kossen of the Schneider group. Compounds were prepared in duplicate, with synthesis and work-up labour for these preparations shared between the two PhD candidates. All compounds presented in the thesis have been prepared at least once by the thesis author.

3.1 General Experimental

Nuclear Magnetic Resonance (NMR) spectra were recorded on Bruker AVA 400, Bruker AVA 500 or PRO 500, and Bruker AVA 600 spectrometers, respectively. These spectrometers operate at the following frequencies: 400 MHz, 500 MHz, and 600 MHz (^1H NMR); 100 MHz, 125 MHz, and 150 MHz (^{13}C NMR); 128 MHz (^{19}F NMR); 132 MHz (^{23}Na NMR). Chemical shifts (δ) were quoted in parts per million (ppm) down-field to tetramethyl silane (TMS; $\delta = 0.00$ ppm), unless otherwise stated. Coupling constants (J) are quoted to the nearest 0.1 Hz. Infrared (IR) spectra were recorded on a Shimadzu IR Affinity-1 instrument using the corresponding isolated NMR sample in CDCl_3 (attenuated total reflectance sampling technique). High-resolution mass spectra (HRMS) were recorded on a Thermo MAT 900XP double focus mass spectrometer. Thin-layer chromatography (TLC) was carried out on pre-coated silica gel plates from Merck (DF Alufolien 60F254; 0.2 mm). Chiral high-pressure liquid chromatography (HPLC) analyses were performed on an Agilent 1100 Series G 1311A Quat Pump HPLC machine with an SPD-20A detector (using a 4.6 x 250 mm column of type IA, IB, IC, or IF from DAICEL CHIRALPAK). Preparative thin-layer chromatography (PTLC) was carried out on self-prepared plates using silica gel from Wakogel (B-5F; particle size: 45 μm). Flash column chromatography was carried out using silica gel from Fisher Scientific (60 \AA ; particle size: 40–63 μm). Product spots were visualized by UV light at 254 nm, or with an appropriate stain solution.

Lithium diisopropylamide (LDA; Aldrich, 97%), lithium 2,2,6,6-tetramethylpiperidide (LTMP; Aldrich, 97%), lithium bis(trimethylsilyl)amide (Aldrich, 97%), sodium *tert*-butoxide (Aldrich, 99.9%), sodium bis(trimethylsilyl)amide (Acros, 95+%), potassium bis(trimethylsilyl)amide (Aldrich, 95%), magnesium bis[*N,N*-bis(trimethylsilyl)amide] (Aldrich, 97%), tin(II) bis[*N,N*-bis(trimethylsilyl)amide] (Aldrich), zinc bis[*N,N*-bis(trimethylsilyl)amide] (Aldrich, 97%), cerium(III) tris[*N,N*-bis(trimethylsilyl)amide] (Alfa, 96%), europium(III) tris[*N,N*-bis(trimethylsilyl)amide] (Alfa, 98%), and gadolinium(III) tris[*N,N*-bis(trimethylsilyl)amide] (Alfa, 98%) were stored in a nitrogen glove box.

Calcium and strontium hexamethyldisilazides were synthesised according to a literature procedure by *Hanno Kossen*.^[130] Copper(I)^[205] and silver^[206] hexamethyldisilazides were synthesised according to literature procedures by *Hanno Kossen*. The analytical data have proved to be in full agreement with the reported data. Sodium hydride (Aldrich, 95%) was stored in a nitrogen glovebox; potassium hydride (Aldrich, 30 wt% dispersion in mineral oil) was washed three times with petroleum ether (PE; 40/60), pulverised, dried in high-vacuum, and stored in a nitrogen glove box. Methyl lithium (AcroSeal®, 1.6 M in diethyl ether) and *n*-butyl lithium (AcroSeal®, 1.6 M in hexane) were stored in a refrigerator (2–8 °C) under an inert atmosphere.

Phosphazene base $\text{P}_1\text{-}^t\text{Bu}$ (Aldrich, 97%), phosphazene base $\text{P}_1\text{-}^t\text{Bu}$ -tris(tetramethylene) (Aldrich, 97%), phosphazene base $\text{P}_2\text{-Et}$ (Aldrich, 98%), phosphazene base $\text{P}_2\text{-}^t\text{Bu}$ (Aldrich, 2.0 M in THF), and phosphazene base

$\text{P}_4\text{-}^t\text{Bu}$ (Aldrich, 0.8 M in hexane) were stored in a freezer ($-20\text{ }^\circ\text{C}$) under an inert atmosphere. 2,8,9-Trimethyl-2,5,8,9-tetraaza-1-phosphabicyclo[3.3.3]undecane (Aldrich), 2,8,9-triisopropyl-2,5,8,9-tetraaza-1-phosphabicyclo[3.3.3]undecane (Aldrich), 2,8,9-triisobutyl-2,5,8,9-tetraaza-1-phosphabicyclo[3.3.3]undecane (Aldrich, 97%) were stored in a nitrogen glove box. Allyl benzene (**1a**; Acros, 98%) was distilled over CaH_2 and stored over activated molecular sieves (4 \AA) in a nitrogen glove box. Allyl perfluorobenzene (**1b**; Alfa, 97%), 1,4-pentadiene (**1d**; Aldrich, 99%), 1-allyl-4-fluoro benzene (**1e**; Aldrich, 98%), 4-allyl toluene (**1g**; Aldrich, 97%), 2-allyl toluene (**1h**; Aldrich, 97%), 4-allyl anisole (**1i**; Acros, 98%), 1-allyl-4-trifluoro benzene (**1j**; Aldrich, 97%), allyl trimethyl silane (**1k**; Aldrich, 98%), allyl trimethoxy silane (**1l**; Aldrich, 98%), allyl pinacol boronic ester (**1m**; prepared by *Bo Qin*), allyl tributyl stannane (**1n**; Aldrich, 97%), allyl methyl sulfide (**1o**; Aldrich, 98%), allyl phenyl sulfide (**1p**; Aldrich, 97%), difluoromethyl benzene (**1q**; Aldrich, 97%), difluoromethyl trimethyl silane (**1r**; Fluorochem, 98%) were stored over activated molecular sieves (4 \AA) in a nitrogen glove box. 3-Allyl pyridine^[207] (**1c**) and all imines **7a–7e**, were synthesised according to literature procedures.^[208] Imines **9a–9g** were synthesised by *other group members*. The analytical data have proved to be in full agreement with the reported data. Unless otherwise stated, all reagents purchased from commercial suppliers were used directly without further purification including electrophiles **11a–11m** and **12a–12d**. THF, toluene, and diethyl ether were distilled over sodium–benzophenone and stored over activated molecular sieves (4 \AA) in a nitrogen glove box. All other solvents –including dioxane, TBME, DME, DMF, NMP, DMPU, and $\text{THF-}d_8$ – were used non-distilled, but stored over activated molecular sieves (4 \AA) in a nitrogen glove box. Solvent dryness was confirmed using a Karl–Fischer apparatus. All catalytic reactions were carried out in oven-dried glassware (typically sealed screw-capped vials) under an inert atmosphere. Conventional heating and stirring was performed using a magnetic stirring bar and a hot plate magnetic stirrer (sand bath).

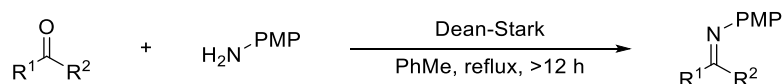
3.2 General Procedures

GP-I^[a]: Preparation of Aldimines^[208]



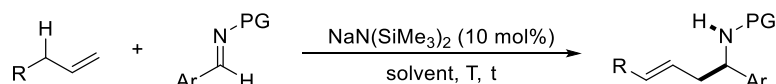
An oven-dried flask with a magnetic stirring bar was charged with the corresponding primary amine (5.00 mmol, 1.0 equiv) and the corresponding aldehyde (6.00 mmol, 1.1 equiv). After addition of DCM (25 mL) and MgSO₄ (4.0 g), the mixture was stirred at room temperature overnight under an inert atmosphere. The reaction mixture was filtered and the solvent was removed *in vacuo* to give the crude imine, which was recrystallized from warm ethanol and filtered to yield the corresponding aldimine with >99% purity. The aldimines were ground and dried in THF over activated molecular sieves (4 Å) in a nitrogen glove box prior to use.

GP-II^[a]: Preparation of Ketimines^[209]



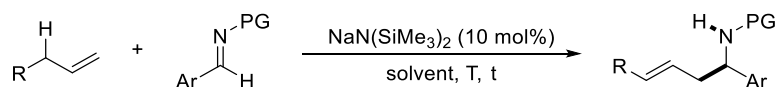
An oven-dried flask with a magnetic stirring bar was charged with 4-methoxyaniline (5.0 mmol, 1.0 equiv) and the corresponding ketone (5.0 mmol, 1.0 equiv). The mixture was stirred overnight in refluxing toluene (30 mL) in a Dean–Stark apparatus. The reaction mixture was cooled to room temperature, and the solvent was removed *in vacuo* to give the crude imine, which was recrystallized from warm ethanol and filtered to yield the corresponding ketimine with >99% purity. The ketimines were ground and dried in THF over activated molecular sieves (4 Å) in a nitrogen glove box prior to use.

GP-III^[a]: Sodium Amide-Catalysed Imine Allylation



In a nitrogen glove box, a dry screw-capped vial with a magnetic stirring bar was charged with sodium hexamethyldisilazide (3.7 mg, 0.02 mmol, 10 mol%), the corresponding imine (0.20 mmol), and dioxane (100 µL). To this mixture were added the corresponding alkene (0.20–0.60 mmol, 1.00–3.00 equiv) and dioxane (200 µL). The reaction mixture was sealed and stirred at 25–60 °C for 18–72 h (*as indicated for the individual product*). The internal standard, dibenzyl ether, was added prior to ¹H NMR spectroscopic analysis using an aliquot of the reaction mixture. The solvent was removed *in vacuo*, and the residue was purified by PTLC on silica gel to give the corresponding product (*as indicated for the individual product*).

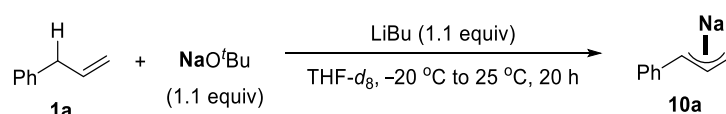
GP-IV^[a]: Imine Allylation – Portionwise Addition



In a nitrogen glove box, a dry screw-capped vial with a magnetic stirring bar was charged with sodium hexamethyldisilazide (3.7 mg, 0.02 mmol, 10 mol%), the corresponding imine (0.20 mmol), and dioxane (100

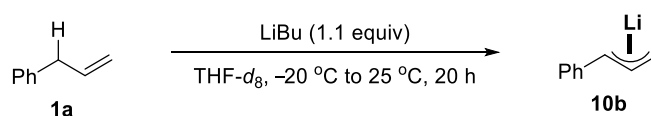
μL). To this mixture were added the corresponding alkene (0.20 mmol, 1.00 equiv) and dioxane (200 μL). The reaction mixture was sealed and stirred at 25 °C for 6 h. To this mixture under an inert atmosphere was re-added the corresponding alkene (0.16–0.20 mmol, 0.80–1.00 equiv), and stirred at 25 °C for 6–12 h. If necessary, to this mixture under an inert atmosphere was re-added the corresponding alkene (0.10 mmol, 0.50 equiv), and stirred at 25 °C for 6 h (*as indicated for the individual product*). The internal standard, dibenzyl ether, was added prior to ^1H NMR spectroscopic analysis using an aliquot of the reaction mixture. The solvent was removed *in vacuo*, and the residue was purified by PTLC on silica gel to give the corresponding product (*as indicated for the individual product*).

GP-V: Preparation of 10a



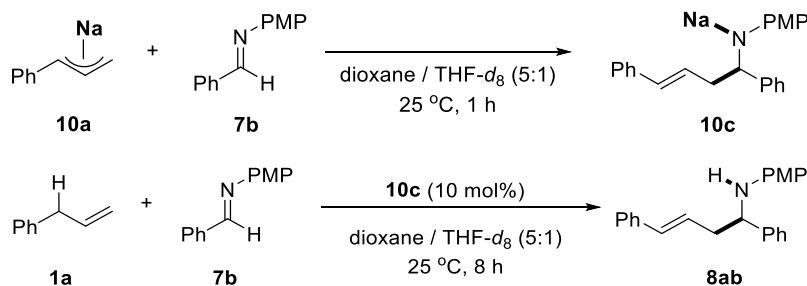
In a nitrogen glove box, a dry Young NMR tube was charged with sodium *tert*-butoxide (10.5 mg, 0.11 mmol, 1.1 equiv), alkene **1a** (11.8 mg, 0.10 mmol), and THF- d_8 (400 μL). The tube was sealed, taken outside of the glove box, cooled to $-20\text{ }^\circ\text{C}$ under a nitrogen atmosphere, and butyl lithium (1.6 M in hexane; 68 μL , 0.11 mmol, 1.1 equiv) was added to the reaction mixture. The reaction mixture was kept at $-20\text{ }^\circ\text{C}$ for 4 h before warming to room temperature during a period of 16 h. The sample was directly subjected to ^1H NMR, ^{13}C NMR, ^{23}Na NMR and HRMS analyses to confirm the formation of η^3 -(*E*)-phenylallyl–Na (**10a**).

GP-VI: Preparation of 10b



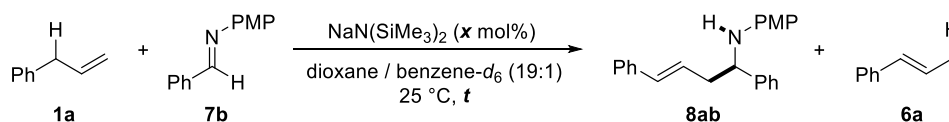
In a nitrogen glove box, a dry Young NMR tube was charged with alkene **1a** (11.8 mg, 0.10 mmol) and THF- d_8 (400 μL). The tube was sealed, taken outside of the glove box, cooled to $-20\text{ }^\circ\text{C}$ under a nitrogen atmosphere, and butyl lithium (1.6 M in hexane; 68 μL , 0.11 mmol, 1.1 equiv) was added to the reaction mixture. The reaction mixture was maintained at $-20\text{ }^\circ\text{C}$ for 4 h before warming to room temperature during a period of 16 h. The sample was directly subjected to ^1H NMR and ^{13}C NMR spectroscopic analyses to confirm the formation of η^3 -(*E*)-phenylallyl–Li (**10b**).^[144, 210]

GP-VII: Preparation of 10c and Imine Allylation Catalysed by 10c



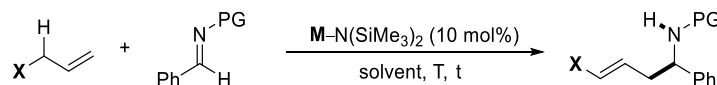
In a nitrogen glove box, a dry Young NMR tube was charged with allyl–Na *nucleophile* **10a** (solution in THF-*d*₈; 80 μ L, 0.02 mmol, 1.0 equiv), imine *electrophile* **7b** (4.2–42.2 mg, 0.02–0.20 mmol, 1–10 equiv), and dioxane (400 μ L). The tube was sealed, and after 1 h it was taken outside of the glove box and directly subjected to ¹H NMR, ¹³C NMR, and ²³Na NMR analyses to confirm the formation of sodium amide *product-base* **10c**. The tube was transferred back to the nitrogen glove box, where alkene **1a** (23.6 mg, 0.20 mmol, 10 equiv) was added to the reaction mixture. The tube was sealed, taken outside of the glove box, and subjected to ¹H NMR spectroscopic analysis (after 1 h and 8 h) to monitor the formation of *product* **8ab**.

GP–VIII: Preliminary Kinetic Study



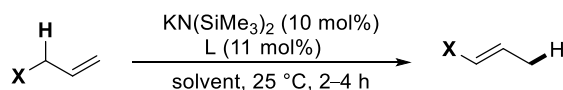
In a nitrogen glove box, a dry Young NMR tube was charged with sodium hexamethyldisilazide (9–45 mg, 0.05–0.25 mmol, 10–50 mol%), imine **7b** (0.50 mmol), dioxane (475 μ L), and C₆D₆ (25 μ L). To this reaction mixture was added allylbenzene (**1a**; 0.52 mmol, 1.05 equiv). The tube was sealed, taken outside of the glove box, and directly subjected to ¹H NMR spectroscopic analysis to monitor the formation of *product* **8ab** (4–30 min). The ¹H NMR spectra were recorded every 2 min applying a dioxane suppression mode.

GP–IX: Imine Alkylation Using Functionalised Allyl Reagents



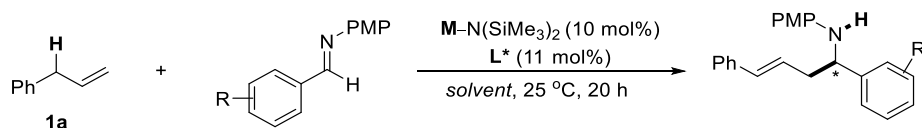
In a nitrogen glove box, a dry screw-capped vial with a magnetic stirring bar was charged with a metal hexamethyldisilazide (0.02 mmol, 10 mol%), the corresponding imine (0.20 mmol), and dioxane (100 μ L). To this mixture were added the corresponding alkene (0.20–0.22 mmol, 1.00–1.10 equiv) and dioxane (200 μ L). The reaction mixture was sealed and stirred at 25–60 °C for 18–72 h (*as indicated for the individual product*). The internal standard, dibenzyl ether, was added prior to ¹H NMR spectroscopic analysis using an aliquot of the reaction mixture. The solvent was removed *in vacuo*, and the residue was purified by PTLC on silica gel to give the corresponding product (*as indicated for the individual product*).

GP–X: Isomerisation of Functionalised Allyl Reagents



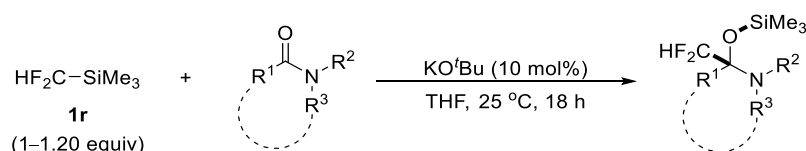
In a nitrogen glove box, a dry screw-capped vial with a magnetic stirring bar was charged with potassium hexamethyldisilazide (4.0 mg, 0.02 mmol, 10 mol%), the ligand L (0.022 mmol, 11 mol%), and the solvent (100 μ L). To this mixture were added the corresponding functionalised allyl reagent (0.20 mmol, 1.00 equiv) and the solvent (100 μ L). The reaction mixture was sealed and stirred at 25 °C for 2–4 h (*as indicated for the individual product*). The internal standard, dibenzyl ether, was added prior to ¹H NMR spectroscopic analysis using an aliquot of the reaction mixture. The solvent was removed *in vacuo*, and the residue was purified –if possible– by PTLC on silica gel to give the corresponding product (*as indicated for the individual product*).

GP–XI: Catalytic Asymmetric Imine Allylation



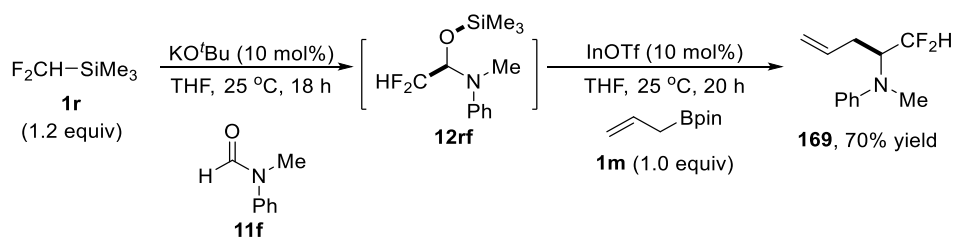
In a nitrogen glove box, a dry screw-capped vial with a magnetic stirring bar was charged with a metal hexamethyldisilazide (0.02 mmol, 10 mol%), the corresponding ligand L* (0.022 mmol, 11 mol%), the corresponding imine (0.20 mmol, 1.0 equiv), and solvent (100 μ L). To this mixture were added alkene **1a** (0.22 mmol, 1.1 equiv) and dioxane (200 μ L). The reaction mixture was sealed and stirred at 25 °C for 20 h. The internal standard, dibenzyl ether, was added prior to ¹H NMR spectroscopic analysis using an aliquot of the reaction mixture. The solvent was removed *in vacuo*, and the residue was purified by PTLC on silica gel to give the corresponding product (*as indicated for the individual product*). The product was subjected to HPLC analysis for the determination of the asymmetric induction.

GP–XII: Catalytic Difluoromethylation of Amides and Lactams



In a nitrogen glove box, a dry screw-capped vial with a magnetic stirring bar was charged with KO^tBu (0.02 mmol, 10 mol%), THF or dioxane (*as indicated for the individual product*; 400 μ L), pro-nucleophile **1r** (0.2 mmol, 1.0 equiv), and the corresponding electrophiles (0.2 mmol, 1.0 equiv). The reaction mixture was sealed and stirred at 25 °C for 18 h. A reaction aliquot was subjected to ¹H NMR and ¹⁹F NMR spectroscopic analyses. If the amides were not fully consumed: to this mixture under an inert atmosphere was re-added the corresponding pro-nucleophile **1r** (2.4–4.8 mg, 0.02–0.04 mmol, 0.1–0.2 equiv, *as indicated for the individual product*), and stirred at 25 °C for 18 h to ensure the full conversion of the amides. The product formation was confirmed by ¹H NMR and ¹⁹F NMR spectroscopic analyses; the conversion to the product was calculated relative to **1r**. THF and the excess amount of **1r** were removed *in vacuo* before adding hexane (500 μ L). The potassium salt was filtered off and the hexane is evaporated *in vacuo* to yield the pure product. The ¹H, ¹³C and ¹⁹F NMR analyses were carried out using benzene-*d*₆ (500 μ L). The use of chloroform-*d* resulted in gradual decomposition of the product within 24 h.

GP–XIII: One-Pot Sequence Difluoromethylation/Allylation



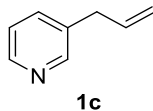
In a nitrogen glove box, a dry screw-capped vial with a magnetic stirring bar was charged with KO^tBu (1.1 mg, 0.01 mmol, 10 mol%), THF (200 μ L), pro-nucleophile **1r** (0.1 mmol, 1.0 equiv), and formamide **11f** (0.2 mmol, 1.0 equiv). The reaction mixture was sealed and stirred at 25 °C for 18 h. The complete product formation was

confirmed by ^1H NMR and ^{19}F NMR spectroscopic analyses. To the reaction mixture with the *in situ*-formed *O*-silylated difluoromethyl *N,O*-hemiaminal **12rf** were added allyl boronic ester **1m** (0.1 mmol, 1.0 equiv) and InOTf (2.6 mg, 0.01 mmol, 10 mol%).^[202] The reaction mixture was stirred at 25 °C for 20 h. The complete product formation was confirmed by ^1H NMR, ^{11}B NMR, and ^{19}F NMR spectroscopic analyses. THF and other volatiles were removed *in vacuo*, and the residue was purified by PTLC on silica gel to give product **169**.

3.3 NMR Data of Prepared Compounds

Preparation of an Alkene

3-Allyl pyridine (**1c**)



Compound **1c** was prepared according to a literature-reported procedure.^[211] An oven-dried 25 mL round-bottom flask was charged with magnesium turnings (109 mg, 4.5 mmol), LiCl (158 mg, 3.8 mmol), dry THF (5 mL) and diisobutylaluminium hydride (DIBALH; 0.1 mmol, 5 mol%, 1.0 M in hexane) under an inert atmosphere. The reaction was stirred at room temperature for 10 min before adding 3-pyridyl bromide (192 μ L, 3.0 mmol). The mixture was stirred at room temperature for 2 h before adding a solution of Fe(acac)₃ (35.3 mg, 0.1 mmol, 5 mol%) in dry THF (2 mL). Allyl acetate (2.0 mmol) was added dropwise, and the mixture was stirred at 40 °C for 1 h before quenching with Na₂CO₃ (sat. aq.; 2 mL) and extraction with EtOAc (4 \times 5 mL). The combined organic phases were dried over MgSO₄. After filtration, volatiles were removed *in vacuo*, and the residue was subjected to flash column chromatography on silica gel (eluent: pure EtOAc).

Red liquid; 296 mg (83% yield).

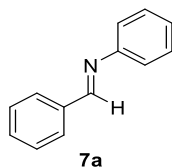
¹H NMR (500 MHz, CDCl₃): δ = 8.47 (s, 2H), 7.50 (d, J = 7.8 Hz, 1H), 7.22 (dd, J = 7.8, 4.8 Hz, 1H), 5.95 (ddt, J = 16.8, 10.1, 6.6 Hz, 1H), 5.14–5.07 (m, 2H), 3.39 (d, J = 6.6 Hz, 2H) ppm.

¹³C NMR (125 MHz, CDCl₃): δ = 150.1, 147.7, 136.2, 136.0, 135.3, 123.4, 116.8, 37.2 ppm.

Preparation of Aldimines

All imines were prepared according to known literature procedures and characterisation data were in full agreement with the reported literature.

N-Phenyl-benzaldimine (**7a**)



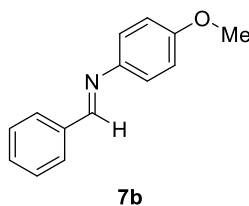
Compound **7a** was prepared according to *GP-I* using benzaldehyde (1.2 g, 1.1 mmol, 1.1 equiv) and aniline (0.93 g, 1.0 mmol, 1.0 equiv). The obtained analytical data were in full agreement with the literature.^[208]

Pale yellow solid; mp: 54–56 °C; 1.6 g (90% yield).

¹H NMR (500 MHz, CDCl₃): δ = 8.47 (s, 1H), 7.94–7.91 (m, 2H), 7.50–7.41 (m, 3H), 7.43–7.39 (m, 2H), 7.27–7.22 (m, 3H) ppm.

¹³C NMR (125 MHz, CDCl₃): δ = 160.4, 152.0, 136.2, 131.4, 129.1 (2C), 128.8 (2C), 128.7 (2C), 125.9, 120.8 (2C) ppm.

N-p-Anisole-benzaldimine (**7b**)



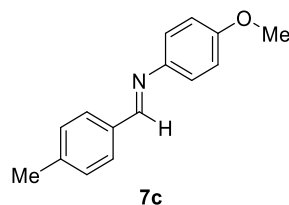
Compound **7b** was prepared according to *GP-I* using benzaldehyde (2.4 g, 2.2 mmol, 1.1 equiv) and *p*-anisidine (2.5 g, 2.0 mmol, 1.0 equiv). The obtained analytical data were in full agreement with the literature.^[212]

Yellow solid; mp: 66–68 °C; 3.8 g (90% yield).

¹H NMR (500 MHz, CDCl₃): δ = 8.47 (s, 1H), 7.92–7.84 (m, 2H), 7.47–7.45 (m, 3H), 7.24 (d, *J* = 8.9 Hz, 2H), 6.94 (d, *J* = 8.9 Hz, 2H), 3.84 (s, 3H) ppm.

¹³C NMR (125 MHz, CDCl₃): δ = 158.7, 158.4, 144.9, 136.5, 131.0, 128.7 (2C), 128.6 (2C), 122.2 (2C), 114.4 (2C), 55.5 ppm.

N-*p*-Anisole-(4-methyl)benzaldimine (**7c**)



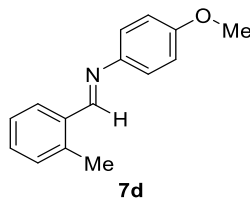
Compound **7c** was prepared according to *GP-I* using 4-methylbenzaldehyde (1.3 g, 1.1 mmol, 1.1 equiv) and *p*-anisidine (1.2 g, 1.0 mmol, 1.0 equiv). The obtained analytical data were in full agreement with the literature.^[208]

Bright yellow solid; mp: 80–82 °C; 1.7 g (76% yield).

¹H NMR (500 MHz, CDCl₃): δ = 8.44 (s, 1H), 7.78 (d, *J* = 8.1 Hz, 2H), 7.28 (d, *J* = 8.1 Hz, 2H), 7.24 (d, *J* = 8.9 Hz, 2H), 6.93 (d, *J* = 8.9 Hz, 2H), 3.83 (s, 3H), 2.41 (s, 3H) ppm.

¹³C NMR (125 MHz, CDCl₃): δ = 158.5, 158.2, 145.0, 141.6, 133.8, 129.5 (2C), 128.7 (2C), 122.2 (2C), 114.4 (2C), 55.5, 21.6 ppm.

N-*p*-Anisole-(2-methyl)benzaldimine (**7d**)



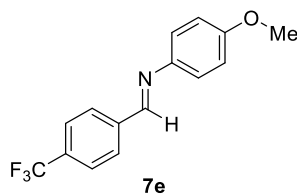
Compound **7d** was prepared according to *GP-I* using 2-methylbenzaldehyde (1.3 g, 1.1 mmol, 1.1 equiv) and *p*-anisidine (1.2 g, 1.0 mmol, 1.0 equiv). The obtained analytical data were in full agreement with the literature.^[213]

Yellow solid; mp: 55–57 °C; 1.9 g (84% yield).

¹H NMR (500 MHz, CDCl₃): δ = 8.77 (s, 1H), 8.06 (dd, *J* = 8.0, 1.5 Hz, 1H), 7.37–7.27 (m, 2H), 7.25–7.19 (m, 3H), 6.94 (d, *J* = 9.0 Hz, 2H), 3.84 (s, 3H), 2.58 (s, 3H) ppm.

¹³C NMR (125 MHz, CDCl₃): δ = 158.2, 157.1, 145.5, 138.3, 134.4, 130.9, 130.7, 127.5, 126.3, 122.1 (2C), 114.3 (2C), 55.5, 19.4 ppm.

N-*p*-Anisole-(4-trifluoromethyl)benzaldimine (**7e**)



Compound **7e** was prepared according to *GP-I* using 4-trifluoromethylbenzaldehyde (1.9 g, 1.1 mmol, 1.1 equiv) and *p*-anisidine (1.2 g, 1.0 mmol, 1.0 equiv). The obtained analytical data were in full agreement with the literature.^[214]

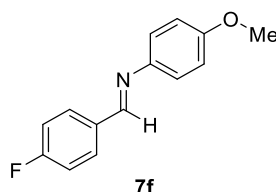
Yellow solid; mp: 124–126 °C; 1.9 g (70% yield).

¹H NMR (500 MHz, CDCl₃): δ = 8.53 (s, 1H), 8.00 (d, *J* = 8.2 Hz, 2H), 7.71 (d, *J* = 8.2 Hz, 2H), 7.27 (d, *J* = 8.9 Hz, 2H), 6.97 (d, *J* = 8.9 Hz, 2H), 3.84 (s, 3H) ppm.

¹³C NMR (125 MHz, CDCl₃): δ = 158.8, 156.2, 144.1, 139.6, 132.5 (q, *J* = 32.5 Hz), 128.7 (2C), 125.6 (q, *J* = 3.2 Hz, 2C), 123.9 (q, *J* = 127.2 Hz), 122.4 (2C), 114.5 (2C), 55.5 ppm.

¹⁹F NMR (471 MHz, CDCl₃): δ = −62.9 (s, 3F) ppm.

N-*p*-Anisole-(4-fluoro)benzaldimine (**7f**)



Compound **7f** was prepared according to *GP-I* using 4-fluorobenzaldehyde (1.4 g, 1.1 mmol, 1.1 equiv) and *p*-anisidine (1.2 g, 1.0 mmol, 1.0 equiv). The obtained analytical data were in full agreement with the literature.^[208]

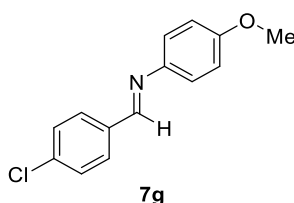
Green solid; mp: 92–94 °C; 2.0 g (90% yield).

¹H NMR (500 MHz, CDCl₃): δ = 8.45 (s, 1H), 7.89 (dd, *J* = 8.7, 5.5 Hz, 2H), 7.24 (d, *J* = 8.9 Hz, 2H), 7.15 (d, *J* = 8.7 Hz, 2H), 6.94 (d, *J* = 8.9 Hz, 2H), 3.84 (s, 3H) ppm.

¹³C NMR (125 MHz, CDCl₃): δ = 164.5 (d, *J* = 250.0 Hz), 158.3, 156.9, 144.7, 132.8, 130.5 (d, *J* = 8.0 Hz, 2C), 122.2 (2C), 115.9 (d, *J* = 22.0 Hz, 2C), 114.4 (2C), 55.5 ppm.

¹⁹F NMR (471 MHz, CDCl₃): δ = −(108.7–108.8, m, 1F) ppm.

N-*p*-Anisole-(4-chloro)benzaldimine (**7g**)



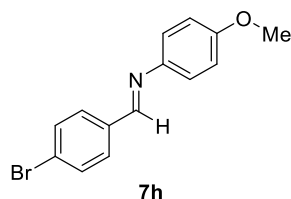
Compound **7g** was prepared according to *GP-I* using 4-chlorobenzaldehyde (1.5 g, 1.1 mmol, 1.1 equiv) and *p*-anisidine (1.2 g, 1.0 mmol, 1.0 equiv). The obtained analytical data were in full agreement with the literature.^[208]

Yellow solid; mp: 120–122 °C; 2.1 g (89% yield).

¹H NMR (500 MHz, CDCl₃): δ = 8.44 (s, 1H), 7.83 (d, *J* = 8.4 Hz, 2H), 7.44 (d, *J* = 8.4 Hz, 2H), 7.26 (d, *J* = 9.0 Hz, 2H), 6.94 (d, *J* = 9.0 Hz, 2H), 3.83 (s, 3H) ppm.

¹³C NMR (125 MHz, CDCl₃): δ = 158.5, 156.7, 144.4, 137.0, 134.9, 129.8 (2C), 129.0 (2C), 122.3 (2C), 114.4 (2C), 55.5 ppm.

***N*-*p*-Anisole-(4-bromo)benzaldimine (**7h**)**



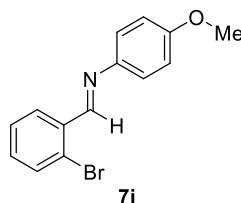
Compound **7h** was prepared according to *GP-I* using 4-bromobenzaldehyde (2.0 g, 1.1 mmol, 1.1 equiv) and *p*-anisidine (1.2 g, 1.0 mmol, 1.0 equiv). The obtained analytical data were in full agreement with the literature.^[215]

Yellow solid; mp: 142–144 °C; 2.6 g (90% yield).

¹H NMR (500 MHz, CDCl₃): δ = 8.42 (s, 1H), 7.75 (d, *J* = 8.5 Hz, 2H), 7.58 (d, *J* = 8.5 Hz, 2H), 7.23 (*J* = 8.8 Hz, 2H), 6.93 (d, *J* = 8.8 Hz, 2H), 3.83 (s, 3H) ppm.

¹³C NMR (125 MHz, CDCl₃): δ = 159.3, 154.8, 149.0, 143.5, 142.0, 129.1 (2C), 124.0 (2C), 122.7 (2C), 114.6 (2C), 55.5 ppm.

***N*-*p*-Anisole-(2-bromo)benzaldimine (**7i**)**



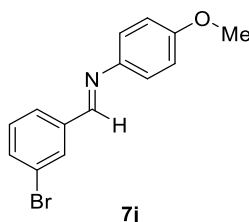
Compound **7i** was prepared according to *GP-I* using 2-bromobenzaldehyde (2.0 g, 1.1 mmol, 1.1 equiv) and *p*-anisidine (1.2 g, 1.0 mmol, 1.0 equiv). The obtained analytical data were in full agreement with the literature.^[216]

Yellow solid; mp: 72–74 °C; 2.3 g (80% yield).

¹H NMR (500 MHz, CDCl₃): δ = 8.87 (s, 1H), 8.22 (dd, *J* = 7.8, 1.8 Hz, 1H), 7.61 (dd, *J* = 7.8, 0.9 Hz, 1H), 7.41–7.37 (m, 1H), 7.31–7.27 (m, 3H), 6.98–6.91 (m, 2H), 3.84 (s, 3H) ppm.

¹³C NMR (125 MHz, CDCl₃): δ = 158.7, 157.1, 144.6, 134.9, 133.2, 132.0, 128.8, 127.7, 125.8, 122.5 (2C), 114.5 (2C), 55.5 ppm.

***N*-*p*-Anisole-(3-bromo)benzaldimine (**7j**)^[217]**



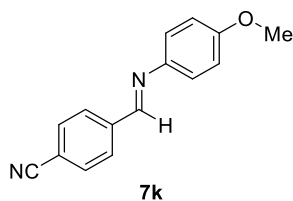
Compound **7j** was prepared according to *GP-I* using 3-bromobenzaldehyde (2.0 g, 1.1 mmol, 1.1 equiv) and *p*-anisidine (1.2 g, 1.0 mmol, 1.0 equiv). The obtained analytical data were in full agreement with the literature.^[217]

Yellow solid; mp: 88–90 °C; 2.6 g (90% yield).

¹H NMR (500 MHz, CDCl₃): δ = 8.42 (s, 1H), 8.08 (dd, *J* = 1.8, 1.0 Hz, 1H), 7.77 (ddd, *J* = 7.6, 1.8, 1.8 Hz, 1H), 7.58 (ddd, *J* = 7.8, 1.8, 1.0 Hz, 1H), 7.33 (dd, *J* = 7.8, 7.6 Hz, 1H), 7.27 (d, *J* = 8.9 Hz, 2H), 6.94 (d, *J* = 8.9 Hz, 2H), 3.84 (s, 3H) ppm.

¹³C NMR (125 MHz, CDCl₃): δ = 158.6, 156.3, 144.2, 138.5, 133.8, 131.1, 130.2, 127.3, 123.0, 122.3 (2C), 114.4 (2C), 55.5 ppm.

***N*-*p*-Anisole-(4-cyano)benzaldimine (**7k**)**



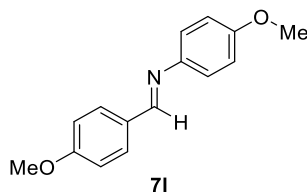
Compound **7k** was prepared according to *GP-I* using 4-cyanobenzaldehyde (1.4 g, 1.1 mmol, 1.1 equiv) and *p*-anisidine (1.2 g, 1.0 mmol, 1.0 equiv). The obtained analytical data were in full agreement with the literature.^[218]

Yellow solid; mp: 109–110 °C; 2.0 g (85% yield).

¹H NMR (500 MHz, CDCl₃): δ = 8.52 (s, 1H), 7.99 (d, *J* = 8.2 Hz, 1H), 7.74 (d, *J* = 8.2 Hz, 1H), 7.28 (d, *J* = 9.0 Hz, 2H), 6.95 (d, *J* = 9.0 Hz, 2H), 3.84 (s, 3H) ppm.

¹³C NMR (125 MHz, CDCl₃): δ = 159.1, 155.4, 143.7, 140.3, 132.5 (2C), 128.9 (2C), 122.6 (2C), 118.6, 114.5 (2C), 113.9, 55.5 ppm.

***N*-*p*-Anisole-(4-methoxy)benzaldimine (**7l**)**



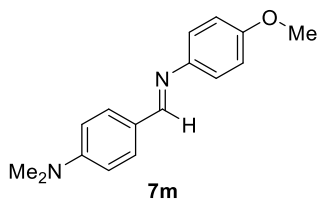
Compound **7l** was prepared according to *GP-I* using 4-methoxybenzaldehyde (1.5 g, 1.1 mmol, 1.1 equiv) and *p*-anisidine (1.2 g, 1.0 mmol, 1.0 equiv). The obtained analytical data were in full agreement with the literature.^[208]

Pale yellow solid; mp: 140–142 °C; 2.1 g (89% yield).

¹H NMR (500 MHz, CDCl₃): δ = 8.41 (s, 1H), 7.86 (d, *J* = 8.0 Hz, 2H), 7.25–7.22 (m, 2H), 6.98 (d, *J* = 8.9 Hz, 2H), 6.93 (d, *J* = 8.9 Hz, 2H), 3.87 (s, 3H), 3.83 (s, 3H) ppm.

¹³C NMR (125 MHz, CDCl₃): δ = 162.0, 158.0, 157.9, 145.3, 130.4 (2C), 129.6, 122.1 (2C), 114.4 (2C), 114.1 (2C), 55.5, 55.4 ppm.

***N*-*p*-Anisole-(4-dimethylamino)benzaldimine (**7m**)**



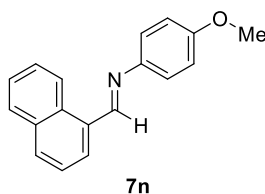
Compound **7m** was prepared according to *GP-I* using 4-*N,N*-dimethylaminobenzaldehyde (1.6 g, 1.1 mmol, 1.1 equiv) and *p*-anisidine (1.2 g, 1.0 mmol, 1.0 equiv). The obtained analytical data were in full agreement with the literature.^[219]

Bright yellow solid; mp: 143–145 °C; 1.8 g (70% yield).

¹H NMR (500 MHz, CDCl₃): δ = 8.34 (s, 1H), 7.75 (d, *J* = 8.9 Hz, 2H), 7.18 (d, *J* = 8.9 Hz, 2H), 6.91 (d, *J* = 8.9 Hz, 2H), 6.73 (d, *J* = 8.9 Hz, 2H), 3.82 (s, 3H), 3.05 (s, 6H) ppm.

¹³C NMR (125 MHz, CDCl₃): δ = 158.6, 157.5, 152.3, 146.0, 130.2 (2C), 124.8, 122.0 (2C), 114.3 (2C), 111.6 (2C), 55.5, 40.2 (2C) ppm.

***N*-p-Anisole-(1-naphthyl)-aldimine (7n)**



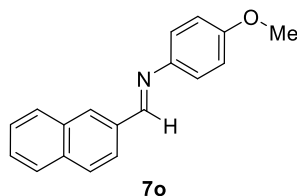
Compound **7n** was prepared according to *GP-I* using 1-naphthylbenzaldehyde (1.7 g, 1.1 mmol, 1.1 equiv) and *p*-anisidine (1.2 g, 1.0 mmol, 1.0 equiv). The obtained analytical data were in full agreement with the literature.^[220]

Yellow solid; mp: 73–75 °C; 1.8 g (70% yield).

¹H NMR (500 MHz, CDCl₃): δ = 9.14 (s, 1H), 9.03 (d, *J* = 9.2 Hz, 1H), 8.10 (dd, *J* = 7.2, 1.3 Hz, 1H), 7.96 (d, *J* = 8.2 Hz, 1H), 7.92 (dd, *J* = 8.2, 1.3 Hz, 1H), 7.62 (ddd, *J* = 8.5, 6.8, 1.3 Hz, 1H), 7.59–7.53 (m, 2H), 7.32 (d, *J* = 8.9 Hz, 2H), 6.98 (d, *J* = 8.9 Hz, 2H), 3.86 (s, 3H) ppm.

¹³C NMR (125 MHz, CDCl₃): δ = 158.4, 158.0, 145.7, 134.0, 131.8, 131.6, 131.5, 129.3, 128.8, 127.3, 126.2, 125.3, 124.2, 122.2 (2C), 114.5 (2C), 55.6 ppm.

***N*-p-Anisole-(2-naphthyl)-aldimine (7o)**



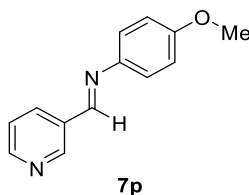
Compound **7o** was prepared according to *GP-I* using 2-naphthylbenzaldehyde (1.7 g, 1.1 mmol, 1.1 equiv) and *p*-anisidine (1.2 g, 1.0 mmol, 1.0 equiv). The obtained analytical data were in full agreement with the literature.^[221]

Yellow solid; mp: 116–118 °C; 2.1 g (80% yield).

¹H NMR (500 MHz, CDCl₃): δ = 8.64 (s, 1H), 8.18 (s, 1H), 8.16 (dd, *J* = 8.5, 1.7 Hz, 1H), 7.95–7.85 (m, 3H), 7.56–7.50 (m, 2H), 7.29 (d, *J* = 8.9 Hz, 2H), 6.96 (d, *J* = 8.9 Hz, 2H), 3.85 (s, 3H) ppm.

¹³C NMR (125 MHz, CDCl₃): δ = 158.4, 158.3, 145.0, 134.9, 134.2, 133.2, 130.8, 128.7, 128.6, 127.9, 127.3, 126.6, 124.0, 122.3 (2C), 114.4 (2C), 55.5 ppm.

***N*-p-Anisole-(3-pyridyl)-aldimine (7p)**



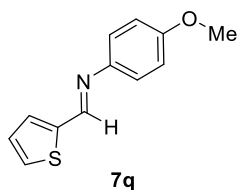
Compound **7p** was prepared according to *GP-I* using 3-pyridinecarboxaldehyde (1.2 g, 1.1 mmol, 1.1 equiv) and *p*-anisidine (1.2 g, 1.0 mmol, 1.0 equiv). The obtained analytical data were in full agreement with the literature.^[222]

Brown solid; mp: 61–63 °C; 1.8 g (88% yield).

¹H NMR (500 MHz, CDCl₃): δ = 9.00 (d, *J* = 1.8 Hz, 1H), 8.68 (dd, *J* = 4.8, 1.8 Hz, 1H), 8.52 (s, 1H), 8.27 (dt, *J* = 7.9, 1.8 Hz, 1H), 7.39 (dd, *J* = 7.9, 4.8 Hz, 1H), 7.27 (d, *J* = 8.9 Hz, 2H), 6.95 (d, *J* = 8.9 Hz, 2H), 3.84 (s, 3H) ppm.

¹³C NMR (125 MHz, CDCl₃): δ = 158.8, 154.9, 151.7, 150.8, 144.2, 134.6, 132.1, 123.8, 122.3 (2C), 114.5 (2C), 55.5 ppm.

***N*-*p*-Anisole-(2-thienyl)-aldimine (**7q**)**



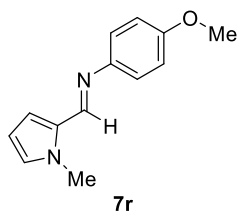
Compound **7q** was prepared according to *GP-I* using 2-thiophenecarboxaldehyde (1.2 g, 1.1 mmol, 1.1 equiv) and *p*-anisidine (1.2 g, 1.0 mmol, 1.0 equiv). The obtained analytical data were in full agreement with the literature.^[223]

Yellow solid; mp: 91–93 °C; 1.9 g (90% yield).

¹H NMR (500 MHz, CDCl₃): δ = 8.58 (s, 1H), 7.50 (d, *J* = 5.0 Hz, 1H), 7.47 (d, *J* = 3.6 Hz, 1H), 7.25 (d, *J* = 8.7 Hz, 2H), 7.15 (dd, *J* = 5.0, 3.6 Hz, 1H), 6.94 (d, *J* = 8.7 Hz, 2H), 3.78 (s, 3H) ppm.

¹³C NMR (125 MHz, CDCl₃): δ = 158.3, 151.1, 144.4, 143.2, 132.0, 130.1, 127.8, 122.5 (2C), 114.2 (2C), 55.5 ppm.

***N*-*p*-Anisole-(*N*-methyl-2-pyrrole)-aldimine (**7r**)**



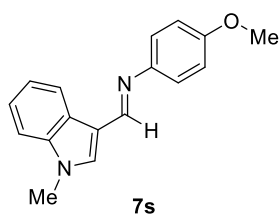
Compound **7r** was prepared previously by *another group member*. The obtained analytical data were in full agreement with the literature.^[224]

Brown solid; mp: 56–58 °C.

¹H NMR (500 MHz, CDCl₃): δ = 8.30 (s, 1H), 7.13 (d, *J* = 8.8 Hz, 2H), 6.90 (d, *J* = 8.8 Hz, 2H), 6.77 (d, *J* = 2.0 Hz, 1H), 6.64 (dd, *J* = 3.8, 2.0 Hz, 1H), 6.19 (dd, *J* = 3.8, 2.6 Hz, 1H), 4.05 (s, 3H), 3.82 (s, 3H) ppm.

¹³C NMR (125 MHz, CDCl₃): δ = 157.6, 151.3, 146.5, 130.2, 128.7, 121.7 (2C), 118.7, 114.4 (2C), 108.7, 55.6, 36.7 ppm.

***N*-*p*-Anisole-(*N*-methyl-3-indole)-aldimine (**7s**)**



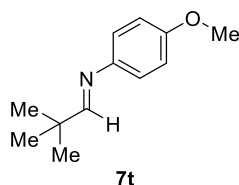
Compound **7s** was prepared previously by *another group member*. The obtained analytical data were in full agreement with the literature.^[225]

Yellow solid; mp: 112–114 °C.

¹H NMR (500 MHz, CDCl₃): δ = 8.64 (s, 1H), 8.46 (d, *J* = 7.8 Hz, 1H), 7.51 (s, 1H), 7.37–7.32 (m, 2H), 7.32–7.26 (m, 1H), 7.22 (d, *J* = 8.9 Hz, 2H), 6.93 (d, *J* = 8.9 Hz, 2H), 3.85 (s, 3H), 3.83 (s, 3H) ppm.

¹³C NMR (125 MHz, CDCl₃): δ = 157.2, 152.5, 146.5, 137.7, 133.5, 125.9, 123.1, 122.0, 121.7 (2C), 121.3, 115.0, 114.2 (2C), 109.3, 55.4, 33.1 ppm.

***N*-*p*-Anisole-*tert*-butylaldimine (**7t**)**



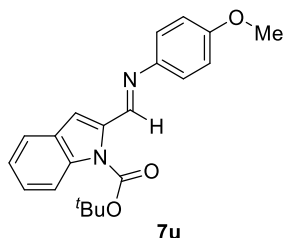
Compound **7t** was prepared according to *GP-I* using pivalaldehyde (1.0 g, 1.1 mmol, 1.1 equiv) and *p*-anisidine (1.2 g, 1.0 mmol, 1.0 equiv). The obtained analytical data were in full agreement with the literature.^[216]

While solid; mp: 49–51 °C; 1.1 g (60% yield).

¹H NMR (500 MHz, CDCl₃): δ = 7.70 (s, 1H), 7.30 (d, *J* = 8.9 Hz, 2H), 6.86 (d, *J* = 8.9 Hz, 2H), 3.80 (s, 3H), 1.17 (s, 9H) ppm.

¹³C NMR (125 MHz, CDCl₃): δ = 171.6, 157.6, 145.6, 121.6 (2C), 114.1 (2C), 55.4, 36.6, 26.8 (3C) ppm.

***N*-*p*-Anisole-(*N*-*tert*-butoxycarbonyl-3-indole)aldimine (**7u**)**



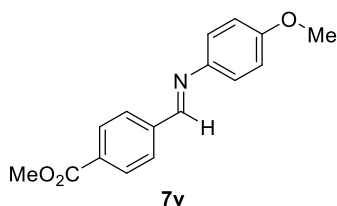
Compound **7u** was prepared previously by *another group member*. The obtained analytical data were in full agreement with the literature.^[226]

White solid; mp: 123–124 °C.

¹H NMR (500 MHz, CDCl₃): δ = 8.65 (s, 1H), 8.55 (d, *J* = 8.0 Hz, 1H), 8.17 (d, *J* = 8.0 Hz, 1H), 7.99 (s, 1H), 7.41–7.34 (m, 2H), 7.25 (d, *J* = 8.9 Hz, 2H), 6.94 (d, *J* = 8.9 Hz, 2H), 3.83 (s, 3H), 1.70 (s, 9H) ppm.

¹³C NMR (100 MHz, CDCl₃): δ = 158.0, 151.9, 149.3, 145.7, 136.2, 130.6, 127.6, 125.5, 123.8, 122.7, 122.0 (2C), 119.7, 115.0, 114.4 (2C), 84.6, 55.5, 28.2 (3C) ppm.

***N*-*p*-Anisole-(4-methoxycarbonyl)benzaldimine (**7v**)**



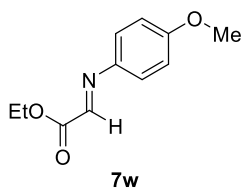
Compound **7v** was prepared previously by *another group member*. The obtained analytical data were in full agreement with the literature.^[215]

Colorless solid; mp: 175–177 °C.

¹H NMR (500 MHz, CDCl₃): δ = 8.53 (s, 1H), 8.12 (d, *J* = 8.2 Hz, 2H), 7.95 (d, *J* = 8.2 Hz, 2H), 7.27 (d, *J* = 8.9 Hz, 2H), 6.95 (d, *J* = 8.9 Hz, 2H), 3.95 (s, 3H), 3.84 (s, 3H) ppm.

¹³C NMR (125 MHz, CDCl₃): δ = 166.7, 158.8, 156.8, 144.3, 140.4, 132.0, 130.0 (2C), 128.4 (2C), 122.4 (2C), 114.5 (2C), 55.5, 52.3 ppm.

***N*-*p*-Anisole-ethyl glyoximine (**7w**)**



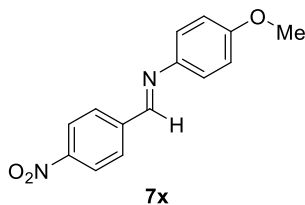
Compound **7w** was prepared according to *GP-I* using ethyl glyoxylate (1.1 mmol, 1.1 equiv) and *p*-anisidine (1.2 g, 1.0 mmol, 1.0 equiv). The obtained analytical data were in full agreement with the literature.^[227]

Colorless oil; 1.4 g (70% yield).

¹H NMR (500 MHz, CDCl₃): δ = 7.93 (s, 1H), 7.38 (d, *J* = 8.9 Hz, 2H), 6.90 (d, *J* = 8.9 Hz, 2H), 4.41 (q, *J* = 7.1 Hz, 2H), 3.84 (s, 3H), 1.41 (t, *J* = 7.1 Hz, 3H) ppm.

¹³C NMR (125 MHz, CDCl₃): δ = 163.6, 160.5, 148.0, 141.4, 123.6 (2C), 114.5 (2C), 61.9, 55.5, 14.2 ppm.

***N*-*p*-Anisole-(4-nitro)benzalimine (**7x**)**



Compound **7x** was prepared previously by *another group member*. The obtained analytical data were in full agreement with the literature.^[215]

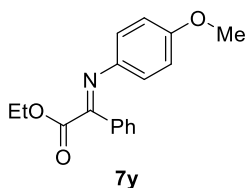
Orange solid; mp: 122–124 °C.

¹H NMR (500 MHz, CDCl₃): δ = 8.57 (s, 1H), 8.30 (d, *J* = 8.8 Hz, 2H), 8.05 (d, *J* = 8.8 Hz, 2H), 7.31 (d, *J* = 9.0 Hz, 2H), 6.96 (d, *J* = 9.0 Hz, 2H), 3.85 (s, 3H) ppm.

¹³C NMR (125 MHz, CDCl₃): δ = 159.3, 154.8, 149.0, 143.6, 142.0, 129.1 (2C), 124.0 (2C), 122.6 (2C), 114.6 (2C), 55.5 ppm.

Preparation of Ketimines

N-*p*-Anisole-phenyl-ethyl glyoxlate-ketimine (**7y**)



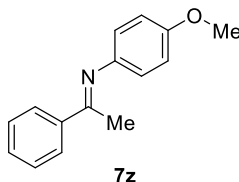
Compound **7y** was prepared according to *GP-II* using ethyl phenylglyoxylate (1.9 g, 1.1 mmol, 1.1 equiv) and *p*-anisidine (1.2 g, 1.0 mmol, 1.0 equiv). The obtained analytical data were in full agreement with the literature.^[228]

Yellow solid; mp: 42–44 °C; 1.9 g (70% yield).

¹H NMR (500 MHz, CDCl₃): δ = 7.88–7.84 (m, 2H), 7.48–7.42 (m, 3H), 6.95 (d, *J* = 9.0 Hz, 2H), 6.85 (d, *J* = 9.0 Hz, 2H), 4.16 (q, *J* = 7.1 Hz, 2H), 3.76 (s, 3H), 1.07 (t, *J* = 7.1 Hz, 3H) ppm.

¹³C NMR (125 MHz, CDCl₃): δ = 166.2, 160.2, 157.9, 144.0, 134.8, 132.2, 129.2 (2C), 128.4 (2C), 121.9 (2C), 114.4 (2C), 62.7, 55.7, 14.2 ppm.

N-*p*-Anisole-acetophenone-ketimine (**7z**)



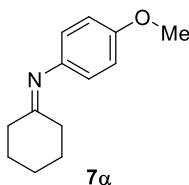
Compound **7z** was prepared according to *GP-II* using acetophenone (1.3 g, 1.1 mmol, 1.1 equiv) and *p*-anisidine (1.2 g, 1.0 mmol, 1.0 equiv). The obtained analytical data were in full agreement with the literature.^[229]

Bright yellow solid; mp: 85–87 °C; 2.0 g (90% yield).

¹H NMR (500 MHz, CDCl₃): δ = 7.98–7.94 (m, 2H), 7.47–7.40 (m, 3H), 6.91 (d, *J* = 8.8 Hz, 2H), 6.75 (d, *J* = 8.8 Hz, 2H), 3.81 (s, 3H), 2.25 (s, 3H) ppm.

¹³C NMR (125 MHz, CDCl₃): δ = 165.7, 156.0, 144.8, 139.8, 130.3, 128.3 (2C), 127.1 (2C), 120.7 (2C), 114.3 (2C), 55.5, 17.3 ppm.

N-*p*-Anisole-cyclohexanone-ketimine (**7a**)



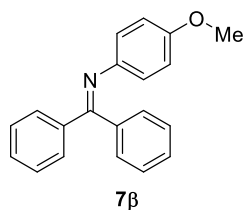
Compound **7a** was prepared according to *GP-II* using cyclohexanone (1.1 g, 1.1 mmol, 1.1 equiv) and *p*-anisidine (1.2 g, 1.0 mmol, 1.0 equiv). The obtained analytical data were in full agreement with the literature.^[230]

Colorless solid; mp: 75–77 °C; 1.6 g (80% yield).

¹H NMR (500 MHz, CDCl₃): δ = 6.84 (d, *J* = 8.9 Hz, 2H), 6.63 (d, *J* = 8.9 Hz, 2H), 3.74 (s, 3H), 2.40 (t, *J* = 6.0 Hz, 2H), 2.22 (t, *J* = 6.0 Hz, 2H), 1.91–1.83 (m, 2H), 1.67–1.61 (m, 4H) ppm.

¹³C NMR (125 MHz, CDCl₃): δ = 175.3, 155.6, 144.0, 120.9 (2C), 114.0 (2C), 55.4, 39.5, 31.1, 27.8, 27.6, 25.8 ppm.

***N*-*p*-Anisole-benzoquinone-ketimine (**7β**)**



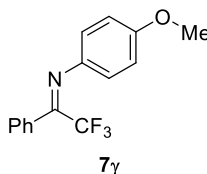
Compound **7β** was prepared according to *GP-II* using benzoquinone (2.0 g, 1.1 mmol, 1.1 equiv) and *p*-anisidine (1.2 g, 1.0 mmol, 1.0 equiv). The obtained analytical data were in full agreement with the literature.^[231]

Bright yellow solid; mp: 69–71 °C; 2.2 g (78% yield).

¹H NMR (500 MHz, CDCl₃): δ = 7.74–7.71 (m, 2H), 7.44–7.41 (m, 1H), 7.40–7.36 (m, 2H), 7.29–7.24 (m, 3H), 7.14–7.10 (m, 2H), 6.71–6.65 (m, 4H), 3.71 (s, 3H) ppm.

¹³C NMR (125 MHz, CDCl₃): δ = 167.7, 155.9, 144.4, 140.1, 136.6, 130.5, 129.6 (2C), 129.2 (2C), 128.5, 128.1 (2C), 128.0 (2C), 122.6 (2C), 113.8 (2C), 55.3 ppm.

***N*-*p*-Anisole-trifluoroacetophenone-ketimine (**7γ**)**



Compound **7γ** was prepared previously by *another group member*. The obtained analytical data were in full agreement with the literature.^[232]

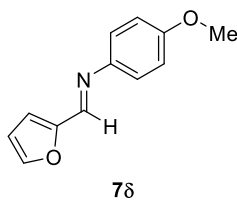
Yellow oil.

¹H NMR (500 MHz, CDCl₃): δ = 7.42–7.31 (m, 3H), 7.28–7.21 (m, 2H), 6.79–6.68 (m, 4H), 3.70 (s, 3H) ppm.

¹³C NMR (125 MHz, CDCl₃): δ = 157.8, 155.3 (q, *J* = 33.5 Hz), 139.6, 130.5, 130.2 (2C), 128.7 (2C), 128.4, 123.2 (2C), 120.1 (q, *J* = 278.7 Hz), 114.1 (2C), 55.2 ppm.

¹⁹F NMR (376 MHz, CDCl₃): δ = –92.1 (s, 3F) ppm.

***N*-*p*-Anisole-2-furyl-aldimine (**7δ**)**



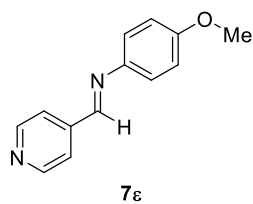
Compound **7δ** was prepared according to *GP-I* using 2-furylaldehyde (1.0 g, 1.1 mmol, 1.1 equiv) and *p*-anisidine (1.2 g, 1.0 mmol, 1.0 equiv). The obtained analytical data were in full agreement with the literature.^[233]

Red solid; mp: 68–72 °C; 1.4 g (70% yield).

¹H NMR (500 MHz, CDCl₃): δ = 8.30 (s, 1H), 7.59 (d, *J* = 1.7 Hz, 1H), 7.26 (d, *J* = 9.0 Hz, 2H), 6.92 (d, *J* = 9.0 Hz, 2H), 6.91 (d, *J* = 3.3 Hz, 1H), 6.54 (dd, *J* = 3.3, 1.7, 1H), 3.82 (s, 3H) ppm.

¹³C NMR (125 MHz, CDCl₃): δ = 158.5, 152.3, 145.7, 145.3, 144.3, 122.3 (2C), 115.5, 114.4 (2C), 112.1, 55.5 ppm.

***N*-*p*-Anisole-4-pyridyl-aldimine (**7ε**)**



Compound **7ε** was prepared according to *GP-I* using 4-pyridinecarboxaldehyde (1.2 g, 1.1 mmol, 1.1 equiv) and *p*-anisidine (1.2 g, 1.0 mmol, 1.0 equiv). The obtained analytical data were in full agreement with the literature.^[234]

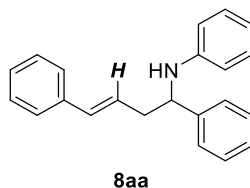
Yellow solid; mp: 57–59 °C; 1.7 g (80% yield).

¹H NMR (500 MHz, CDCl₃): δ = 8.73 (d, *J* = 4.2 Hz, 2H), 8.45 (s, 1H), 7.72 (d, *J* = 4.2 Hz, 2H), 7.28 (d, *J* = 6.8 Hz, 2H), 6.94 (d, *J* = 6.8 Hz, 2H), 3.83 (s, 3H) ppm.

¹³C NMR (125 MHz, CDCl₃): δ = 159.2, 155.3, 150.5 (2C), 143.6, 143.1, 122.6 (2C), 122.1 (2C), 114.5 (2C), 55.5 ppm.

Preparation of Homoallylic Amines^[a]

(*E*)-*N*-(1,4-Diphenylbut-3-enyl)aniline (**8aa**)^[235]



Compound **8aa** was prepared according to *GP-III* from allyl benzene (**1a**; 29.2 μ L, 0.22 mmol, 1.10 equiv) and imine **7a** (36.2 mg, 0.20 mmol), using $\text{NaN}(\text{SiMe}_3)_2$ (3.7 mg, 0.02 mmol, 10 mol%) as the catalyst, in dioxane (300 μ L) at 25 $^\circ\text{C}$ for 18 h. **8aa** was purified by PTLC on silica gel ($\text{Et}_2\text{O}/\text{PE} = 1:9$; *eluted once*).

Yellow liquid.

Yield: 57.5 mg (96%; *E*:*Z* = 49:1).

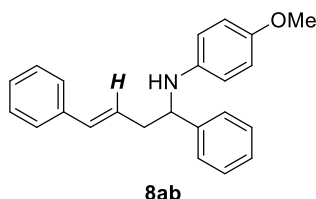
^1H NMR (500 MHz, CDCl_3): $\delta = 7.50\text{--}7.48$ (m, 2H), 7.44–7.38 (m, 6H), 7.35–7.29 (m, 2H), 7.28–7.15 (m, 2H), 6.74 (dd, $J = 7.3, 7.3$ Hz, 1H), 6.63–6.59 (m, 3H), 6.24 (ddd, $J = 15.9, 7.4, 7.0$ Hz, 1H, *E*-CH=CH), 5.79 (ddd, $J = 11.9, 7.0, 6.1$ Hz, 1H, *Z*-CH=CH), 4.56 (dd, $J = 6.3, 6.3$ Hz, 1H), 4.30 (br s, 1H), 2.93–2.83 (m, 1H), 2.78–2.72 (m, 1H) ppm.

^{13}C NMR (125 MHz, CDCl_3): $\delta = 147.2, 143.5, 137.0, 133.3$ (2C), 129.1 (2C), 128.6 (2C), 128.6 (2C), 127.4, 127.0, 126.3 (2C), 126.2 (2C), 126.0, 117.4, 113.5, 57.4, 42.4 ppm.

IR (neat): $\nu = 3412, 3024, 2922, 1601, 1503, 1265, 734, 691$ cm^{-1} .

HRMS (EI): calculated for $\text{C}_{22}\text{H}_{21}\text{N}^+ = [\text{M}^+]$: $m/z = 299.1669$, found: $m/z = 299.1668$.

(*E*)-*N*-(1,4-Diphenylbut-3-enyl)-4-methoxyaniline (**8ab**)



Compound **8ab** was prepared according to *GP-III* from allyl benzene (**1a**; 26.5 μ L, 0.20 mmol, 1.00 equiv) and imine **7b** (42.2 mg, 0.20 mmol), using $\text{NaN}(\text{SiMe}_3)_2$ (3.7 mg, 0.02 mmol, 10 mol%) as the catalyst, in dioxane (300 μ L) at 25 $^\circ\text{C}$ for 18 h. **8ab** was purified by PTLC on silica gel ($\text{Et}_2\text{O}/\text{PE} = 1:9$; *eluted once*).

Yellow liquid.

Yield: 60.0 mg (91%; *E*:*Z* = 99:1).

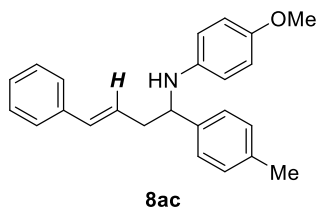
^1H NMR (600 MHz, CDCl_3): $\delta = 7.38\text{--}7.37$ (m, 2H), 7.33–7.27 (m, 6H), 7.24–7.19 (m, 2H), 6.67–6.65 (m, 2H), 6.49 (d, $J = 15.8$ Hz, 1H), 6.46–6.43 (m, 2H), 6.16–6.11 (m, 1H, *E*-CH=CH), 5.69 (ddd, $J = 10.8, 7.1, 7.1$ Hz, 1H, *Z*-CH=CH), 4.42–4.36 (m, 1H), 3.95 (br s, 1H), 3.65 (s, 3H), 2.74–2.70 (m, 1H), 2.65–2.60 (m, 1H) ppm.

^{13}C NMR (150 MHz, CDCl_3): $\delta = 152.1, 143.8, 141.5, 137.1, 133.2, 128.6$ (2C), 128.6 (2C), 127.4, 127.0, 126.4 (2C), 126.2 (2C), 114.8 (3C), 114.8 (2C), 58.4, 55.7, 42.5 ppm.

IR (neat): $\nu = 3389, 3024, 2930, 2830, 1508, 1234, 818, 741, 692$ cm^{-1} .

HRMS (EI): calculated for $\text{C}_{23}\text{H}_{23}\text{NO}^+ = [\text{M}^+]$: $m/z = 329.1774$, found: $m/z = 329.1772$.

(*E*)-*N*-[1-(4-Methylphenyl)-4-phenylbut-3-enyl]-4-methoxyaniline (8ac**)**



Compound **8ac** was prepared according to *GP-III* from allyl benzene (**1a**; 29.2 μ L, 0.22 mmol, 1.10 equiv) and imine **7c** (45.1 mg, 0.20 mmol), using $\text{NaN}(\text{SiMe}_3)_2$ (3.7 mg, 0.02 mmol, 10 mol%) as the catalyst, in dioxane (300 μ L) at 25 $^\circ\text{C}$ for 18 h. **8ac** was purified by PTLC on silica gel ($\text{Et}_2\text{O}/\text{PE} = 1:9$; *eluted once*).

Yellow liquid.

Yield: 63.2 mg (92%; *E*:*Z* = 32:1).

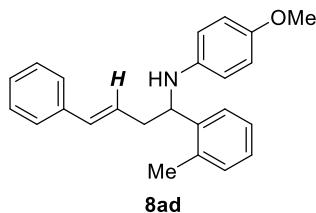
^1H NMR (500 MHz, CDCl_3): δ = 7.37 (d, J = 7.6 Hz, 2H), 7.35–7.29 (m, 2H), 7.28–7.18 (m, 3H), 7.10 (d, J = 7.6 Hz, 2H), 6.65 (dd, J = 8.9, 1.5 Hz, 2H), 6.48–6.39 (m, 3H), 6.08 (ddd, J = 14.5, 7.2, 7.2 Hz, 1H, *E*-CH=CH), 5.64 (ddd, J = 12.1, 7.1, 7.1 Hz, 1H, *Z*-CH=CH), 4.42–4.31 (m, 1H), 3.96 (br s, 1H), 3.66 (s, 3H), 2.77–2.67 (m, 1H), 2.67–2.54 (m, 1H), 2.32 (s, 3H) ppm.

^{13}C NMR (125 MHz, CDCl_3): δ = 152.0, 143.8, 141.6, 137.2, 134.3, 133.1, 129.2 (2C), 128.6 (2C), 127.0, 126.4 (2C), 126.1 (2C), 125.1, 114.7 (2C), 114.7 (2C), 58.4, 55.7, 42.6, 21.2 ppm.

IR (neat): ν = 3401, 3024, 2920, 2832, 1508, 1236, 816, 735, 692 cm^{-1} .

HRMS (EI): calculated for $\text{C}_{24}\text{H}_{25}\text{NO}^+ = [\text{M}^+]$: m/z = 343.1931, found: m/z = 343.1938.

(*E*)-*N*-[1-(2-Methylphenyl)-4-phenylbut-3-enyl]-4-methoxyaniline (8ad**)**



Compound **8ad** was prepared according to *GP-III* from allyl benzene (**1a**; 29.2 μ L, 0.22 mmol, 1.10 equiv) and imine **7d** (45.1 mg, 0.20 mmol), using $\text{NaN}(\text{SiMe}_3)_2$ (3.7 mg, 0.02 mmol, 10 mol%) as the catalyst, in dioxane (300 μ L) at 25 $^\circ\text{C}$ for 18 h. **8ad** was purified by PTLC on silica gel ($\text{Et}_2\text{O}/\text{PE} = 1:9$; *eluted once*).

Yellow liquid.

Yield: 55.0 mg (80%; *E*:*Z* = 99:1).

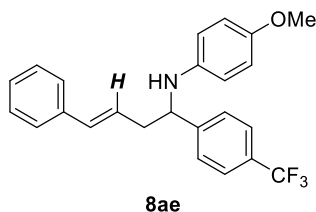
^1H NMR (500 MHz, CDCl_3): δ = 7.42–7.37 (m, 1H), 7.32–7.22 (m, 4H), 7.21–7.08 (m, 4H), 6.62 (d, J = 8.9 Hz, 2H), 6.49 (d, J = 15.8 Hz, 1H), 6.34 (d, J = 8.9 Hz, 2H), 6.14 (ddd, J = 15.8, 7.2, 7.2 Hz, 1H, *E*-CH=CH), 5.68 (ddd, J = 11.9, 7.0, 7.0 Hz, 1H, *Z*-CH=CH), 4.57 (dd, J = 8.1, 4.8 Hz, 1H), 3.91 (br s, 1H), 3.63 (s, 3H), 2.71–2.63 (m, 1H), 2.58–2.47 (m, 1H), 2.43 (s, 3H) ppm.

^{13}C NMR (125 MHz, CDCl_3): δ = 152.0, 141.6, 141.4, 137.1, 134.6, 133.2, 130.7, 128.6 (2C), 127.4, 126.8, 126.5, 126.4, 126.2 (2C), 125.5, 114.8 (2C), 114.5 (2C), 55.8, 54.6, 40.7, 19.2 ppm.

IR (neat): ν = 3395, 3025, 2928, 2832, 1508, 1234, 818, 735, 692 cm^{-1} .

HRMS (EI): calculated for $\text{C}_{24}\text{H}_{25}\text{NO}^+ = [\text{M}^+]$: m/z = 343.1931, found: m/z = 343.1930.

(*E*)-*N*-[1-(4-Trifluoromethylphenyl)-4-phenylbut-3-enyl]-4-methoxyaniline (8ae**)**



Compound **8ae** was prepared according to *GP-III* from allyl benzene (**1a**; 29.2 μ L, 0.22 mmol, 1.10 equiv) and imine **7e** (55.9 mg, 0.20 mmol), using $\text{NaN}(\text{SiMe}_3)_2$ (3.7 mg, 0.02 mmol, 10 mol%) as the catalyst, in dioxane (300 μ L) at 25 $^\circ\text{C}$ for 18 h. **8ae** was purified by PTLC on silica gel ($\text{Et}_2\text{O}/\text{PE} = 1:9$; *eluted twice*).

Yellow liquid.

Yield: 64.4 mg (81%; *E*:*Z* = 99:1).

^1H NMR (500 MHz, CDCl_3): δ = 7.65 (d, J = 7.9 Hz, 2H), 7.57 (d, J = 7.9 Hz, 2H), 7.40–7.35 (m, 4H), 7.31–7.28 (m, 1H), 6.74 (d, J = 8.8 Hz, 2H), 6.58 (d, J = 15.8 Hz, 1H), 6.48 (d, J = 8.8 Hz, 2H), 6.18 (ddd, J = 15.8, 6.8, 5.9 Hz, 1H, *E*-CH=CH), 5.73 (ddd, J = 12.3, 7.1, 7.1 Hz, 1H, *Z*-CH=CH), 4.51 (dd, J = 7.1, 6.1 Hz, 1H), 4.09 (br s, 1H), 3.74 (s, 3H), 2.83–2.78 (m, 1H), 2.71–2.65 (m, 1H) ppm.

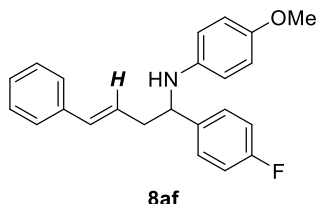
^{13}C NMR (125 MHz, CDCl_3): δ = 152.3, 148.0, 141.0, 136.8, 133.8, 129.3 (q, J = 32.3 Hz), 128.6 (2C), 127.6, 126.7 (2C), 126.2 (2C), 125.6 (q, J = 3.7 Hz, 2C), 125.3, 123.9 (q, J = 272.6 Hz), 114.8 (4C), 58.1, 55.7, 42.4 ppm.

^{19}F NMR (470 MHz, CDCl_3): δ = –62.3 (s, 3F) ppm.

IR (neat): ν = 3391, 3026, 2932, 2833, 1510, 1323, 1236, 1109, 1065, 818, 737, 692 cm^{-1} .

HRMS (EI): calculated for $\text{C}_{24}\text{H}_{22}\text{F}_3\text{NO}^+ = [\text{M}^+]$; m/z = 397.1648, found: m/z = 397.1646.

(*E*)-*N*-[1-(4-Fluorophenyl)-4-phenylbut-3-enyl]-4-methoxyaniline (8af**)**



Compound **8af** was prepared according to *GP-III* from allyl benzene (**1a**; 29.2 μ L, 0.22 mmol, 1.10 equiv) and imine **7f** (45.9 mg, 0.20 mmol), using $\text{NaN}(\text{SiMe}_3)_2$ (3.7 mg, 0.02 mmol, 10 mol%) as the catalyst, in dioxane (300 μ L) at 40 $^\circ\text{C}$ for 18 h. **8af** was purified by PTLC on silica gel ($\text{Et}_2\text{O}/\text{PE} = 1:9$; *eluted once*).

Yellow liquid.

Yield: 68.8 mg (99%; *E*:*Z* = 49:1).

^1H NMR (400 MHz, CDCl_3): δ = 7.41–7.24 (m, 6H), 7.24–7.16 (m, 1H), 7.00 (dd, J = 8.7, 8.7 Hz, 2H), 6.67 (d, J = 8.9 Hz, 2H), 6.49 (d, J = 15.8 Hz, 1H), 6.43 (d, J = 8.9 Hz, 2H), 6.11 (ddd, J = 15.8, 7.2, 7.2 Hz, 1H, *E*-CH=CH), 5.66 (ddd, J = 11.7, 7.0, 7.0 Hz, 1H, *Z*-CH=CH), 4.37 (dd, J = 7.6, 5.3 Hz, 1H), 3.94 (br s, 1H), 3.67 (s, 3H), 2.75–2.65 (m, 1H), 2.65–2.54 (m, 1H) ppm.

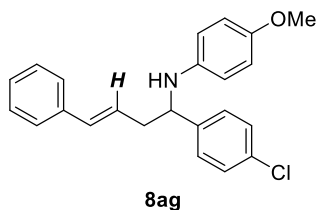
^{13}C NMR (125 MHz, CDCl_3): δ = 161.8 (d, J = 244.7 Hz), 152.1, 141.3, 139.4 (d, J = 2.9 Hz), 137.0, 133.5, 128.6 (2C), 127.8 (d, J = 7.9 Hz, 2C), 127.5, 126.2 (2C), 125.8, 115.4 (d, J = 21.3 Hz, 2C), 114.8 (2C), 114.7 (2C), 57.8, 55.7, 42.6 ppm.

^{19}F NMR (376 MHz, CDCl_3): δ = –115.9 (s, 1F) ppm.

IR (neat): ν = 3385, 3026, 2930, 2832, 1506, 1234, 1219, 818, 735, 692 cm^{-1} .

HRMS (EI): calculated for $\text{C}_{23}\text{H}_{22}\text{FNO}^+ = [\text{M}^+]$; m/z = 347.1680, found: m/z = 347.1683.

(E)-N-[1-(4-Chlorophenyl)-4-phenylbut-3-enyl]-4-methoxyaniline (8ag**)**



Compound **8ag** was prepared according to *GP-III* from allyl benzene (**1a**; 29.2 μ L, 0.22 mmol, 1.10 equiv) and imine **7g** (49.1 mg, 0.20 mmol), using $\text{NaN}(\text{SiMe}_3)_2$ (3.7 mg, 0.02 mmol, 10 mol%) as the catalyst, in dioxane (300 μ L) at 25 $^\circ\text{C}$ for 18 h. **8ag** was purified by PTLC on silica gel ($\text{Et}_2\text{O}/\text{PE} = 1:9$, *eluted once*).

Yellow liquid.

Yield: 58.2 mg (80%; *E:Z* = 49:1).

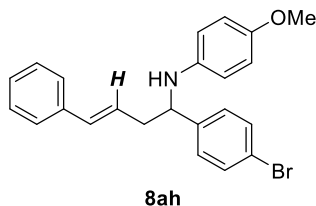
^1H NMR (500 MHz, CDCl_3): δ = 7.38–7.26 (m, 8H), 7.25–7.15 (m, 1H), 6.67 (d, J = 8.9 Hz, 2H), 6.50 (d, J = 15.8 Hz, 1H), 6.41 (d, J = 8.9 Hz, 2H), 6.10 (ddd, 15.8, 7.8, 7.3 Hz, 1H, *E*-CH=CH), 5.65 (ddd, J = 11.8, 7.0, 7.0 Hz, 1H, *Z*-CH=CH), 4.36 (dd, J = 5.7, 5.7 Hz, 1H), 3.93 (br s, 1H), 3.67 (s, 3H), 2.76–2.65 (m, 1H), 2.65–2.52 (m, 1H).

^{13}C NMR (125 MHz, CDCl_3): δ = 152.2, 142.4, 141.2, 137.0, 133.6, 132.6, 128.8 (2C), 128.7 (2C), 127.8 (2C), 127.6, 126.3 (2C), 125.7, 114.8 (2C), 114.8 (2C), 57.9, 55.8, 42.5 ppm.

IR (neat): ν = 3402, 3024, 2930, 2832, 1510, 1238, 818, 744, 694 cm^{-1} .

HRMS (EI): calculated for $\text{C}_{23}\text{H}_{22}^{35}\text{ClNO}^+ = [\text{M}^+]$: m/z = 363.1384, found: m/z = 363.1391.

(E)-N-[1-(4-Bromophenyl)-4-phenylbut-3-enyl]-4-methoxyaniline (8ah**)**



Compound **8ah** was prepared according to *GP-III* from allyl benzene (**1a**; 29.2 μ L, 0.22 mmol, 1.10 equiv) and imine **7h** (58.0 mg, 0.20 mmol), using $\text{NaN}(\text{SiMe}_3)_2$ (3.7 mg, 0.02 mmol, 10 mol%) as the catalyst, in dioxane (300 μ L) at 25 $^\circ\text{C}$ for 18 h. **8ah** was purified by PTLC on silica gel ($\text{Et}_2\text{O}/\text{PE} = 1:9$; *eluted once*).

Yellow liquid.

Yield: 69.4 mg (85%; *E:Z* = 99:1).

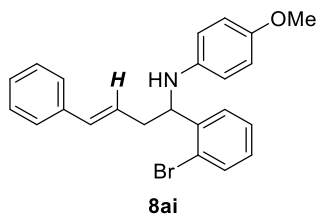
^1H NMR (500 MHz, CDCl_3): δ = 7.44 (d, J = 8.4 Hz, 2H), 7.34–7.18 (m, 7H), 6.66 (d, J = 8.9 Hz, 2H), 6.49 (d, J = 15.8 Hz, 1H), 6.41 (d, J = 8.9 Hz, 2H), 6.09 (ddd, J = 15.8, 7.2, 7.2 Hz, 1H, *E*-CH=CH), 5.64 (ddd, J = 11.8, 7.1, 7.1 Hz, 1H, *Z*-CH=CH), 4.34 (ddd, J = 8.7, 4.8, 4.1 Hz, 1H), 3.93 (d, J = 4.1 Hz, 1H), 3.66 (s, 3H), 2.75–2.64 (m, 1H), 2.63–2.51 (m, 1H) ppm.

^{13}C NMR (125 MHz, CDCl_3): δ = 152.2, 142.9, 141.1, 136.9, 133.6, 131.7 (2C), 128.6 (2C), 128.2 (2C), 127.5, 126.2 (2C), 125.6, 120.7, 114.8 (2C), 114.7 (2C), 57.8, 55.7, 42.4 ppm.

IR (neat): ν = 3401, 3026, 2926, 2832, 1510, 1236, 818, 741, 694 cm^{-1} .

HRMS (EI): calculated for $\text{C}_{23}\text{H}_{22}^{79}\text{BrNO}^+ = [\text{M}^+]$: m/z = 407.0879, found: m/z = 407.0884.

(E)-N-[1-(2-Bromophenyl)-4-phenylbut-3-enyl]-4-methoxyaniline (8ai**)**



Compound **8ai** was prepared according to *GP-III* from allyl benzene (**1a**; 29.2 μ L, 0.22 mmol, 1.10 equiv) and imine **7i** (58.0 mg, 0.20 mmol), using $\text{NaN}(\text{SiMe}_3)_2$ (3.7 mg, 0.02 mmol, 10 mol%) as the catalyst, in dioxane (300 μ L) at 25 $^\circ\text{C}$ for 18 h. **8ai** was purified by PTLC on silica gel (EtOAc/PE = 1:9; *eluted once*).

Yellow liquid.

Yield: 73.5 mg (90%; *E:Z* = 49:1).

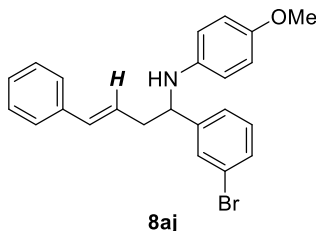
^1H NMR (500 MHz, CDCl_3): δ = 7.58 (dd, J = 7.8, 1.1 Hz, 1H), 7.45 (dd, J = 7.8, 1.7 Hz, 1H), 7.35 (dd, J = 7.8, 1.1 Hz, 2H), 7.30 (dd, J = 7.6, 7.6 Hz, 2H), 7.24 (dd, J = 7.6, 7.6 Hz, 2H), 7.10 (ddd, J = 7.6, 7.6, 1.7 Hz, 1H), 6.67 (d, J = 9.0 Hz, 2H), 6.54 (d, J = 15.8 Hz, 1H), 6.38 (d, J = 9.0 Hz, 2H), 6.19 (ddd, J = 15.8, 7.8, 6.7 Hz, 1H, *E*-CH=CH), 5.74 (ddd, J = 11.8, 8.1, 5.9 Hz, 1H, *Z*-CH=CH), 4.81 (dd, J = 8.3, 4.2 Hz, 1H), 4.05 (br s, 1H), 3.67 (s, 3H), 2.85–2.80 (m, 1H), 2.57–2.50 (m, 1H) ppm.

^{13}C NMR (125 MHz, CDCl_3): δ = 152.1, 141.9, 141.0, 137.0, 133.5, 133.1, 128.6 (2C), 128.6, 127.9, 127.9, 127.5, 126.3 (2C), 125.9, 123.0, 114.8 (2C), 114.6 (2C), 57.0, 55.7, 40.2 ppm.

IR (neat): ν = 3402, 3024, 2930, 2830, 1508, 1236, 1020, 818, 743, 692 cm^{-1} .

HRMS (EI): calculated for $\text{C}_{23}\text{H}_{22}^{79}\text{BrNO}^+ = [\text{M}^+]$: m/z = 407.0879, found: m/z = 407.0880.

(E)-N-[1-(3-Bromophenyl)-4-phenylbut-3-enyl]-4-methoxyaniline (8aj**)**



Compound **8aj** was prepared according to *GP-III* from allyl benzene (**1a**; 30.5 μ L, 0.23 mmol, 1.15 equiv) and imine **7j** (58.0 mg, 0.20 mmol), using $\text{NaN}(\text{SiMe}_3)_2$ (3.7 mg, 0.02 mmol, 10 mol%) as the catalyst, in dioxane (300 μ L) at 25 $^\circ\text{C}$ for 18 h. **8aj** was purified by PTLC on silica gel (EtOAc/PE = 1:9; *eluted twice*).

Yellow liquid.

Yield: 78.4 mg (96%; *E:Z* = 49:1).

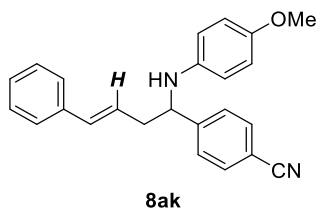
^1H NMR (400 MHz, CDCl_3): δ = 7.55 (dd, J = 1.8, 1.8 Hz, 1H), 7.39–7.26 (m, 6H), 7.24–7.13 (m, 2H), 6.69 (d, J = 9.0 Hz, 2H), 6.50 (d, J = 15.8 Hz, 1H), 6.43 (d, J = 9.0 Hz, 2H), 6.10 (ddd, J = 15.8, 7.8, 6.6 Hz, 1H, *E*-CH=CH), 5.65 (ddd, J = 11.7, 7.1, 7.1 Hz, 1H, *Z*-CH=CH), 4.34 (dd, J = 8.0, 5.0, 1H), 4.00 (br s, 1H), 3.67 (s, 3H), 2.76–2.66 (m, 1H), 2.65–2.53 (m, 1H) ppm.

^{13}C NMR (125 MHz, CDCl_3): δ = 152.3, 146.4, 141.1, 136.9, 133.7, 130.2, 130.2, 129.5, 128.6 (2C), 127.5, 126.2 (2C), 125.6, 125.1, 122.9, 114.8 (2C), 114.8 (2C), 58.1, 55.7, 42.5 ppm.

IR (neat): ν = 3395, 3024, 2930, 2830, 1508, 1234, 818, 739, 692 cm^{-1} .

HRMS (EI): calculated for $\text{C}_{23}\text{H}_{22}^{79}\text{BrNO}^+ = [\text{M}^+]$: m/z = 407.0879, found: m/z = 407.0879.

(E)-N-[1-(4-Cyanophenyl)-4-phenylbut-3-enyl]-4-methoxyaniline (8ak**)**



Compound **8ak** was prepared according to *GP-III* from allyl benzene (**1a**; 79.5 μ L, 0.60 mmol, 3.00 equiv) and imine **7k** (47.3 mg, 0.20 mmol), using $\text{NaN}(\text{SiMe}_3)_2$ (3.7 mg, 0.02 mmol, 10 mol%) as the catalyst, in dioxane (300 μ L) at 25 $^\circ\text{C}$ for 20 h. **8ak** was purified by PTLC on silica gel (EtOAc/PE = 1:9; *eluted twice*).

Yellow liquid.

Yield: 35.4 mg (50%; *E:Z* = >99:1).

^1H NMR (500 MHz, CDCl_3): δ = 7.66 (d, J = 8.3 Hz, 2H), 7.54 (d, J = 8.3 Hz, 2H), 7.37–7.31 (m, 4H), 7.28–7.25 (m, 1H), 6.70 (d, J = 9.0 Hz, 2H), 6.54 (d, J = 15.8 Hz, 1H), 6.41 (d, J = 9.0 Hz, 2H), 6.11 (ddd, J = 15.8, 7.8, 6.7 Hz, 1H), 4.47 (dd, J = 7.9, 5.1 Hz, 1H), 4.01 (br s, 1H), 3.71 (s, 3H), 2.80–2.73 (m, 1H), 2.68–2.61 (m, 1H) ppm.

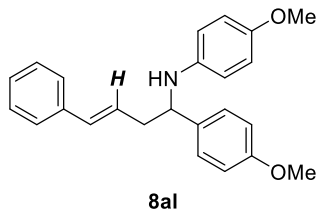
^{13}C NMR (125 MHz, CDCl_3): δ = 152.5, 149.6, 140.7, 136.7, 134.1, 132.6 (2C), 128.7 (2C), 127.7, 127.2 (2C), 126.2 (2C), 124.9, 118.9, 114.8 (4C), 111.0, 58.2, 55.7, 42.2 ppm.

The Z-isomer could not be detected.

IR (neat): ν = 3390, 3026, 2926, 2225, 1510, 1238, 1035, 820, 748, 694 cm^{-1} .

HRMS (EI): calculated for $\text{C}_{24}\text{H}_{22}\text{N}_2\text{O}^+$ = $[\text{M}^+]$; m/z = 354.1727, found: m/z = 354.1716.

(E)-N-[1-(4-Methoxyphenyl)-4-phenylbut-3-enyl]-4-methoxyaniline (8al**)**



Compound **8al** was prepared according to *GP-IV* from allyl benzene (**1a**; 47.7 μ L, 0.36 mmol, 1.80 equiv) and imine **7l** (48.3 mg, 0.20 mmol), using $\text{NaN}(\text{SiMe}_3)_2$ (3.7 mg, 0.02 mmol, 10 mol%) as the catalyst, in dioxane (300 μ L) at 25 $^\circ\text{C}$ for 18 h. **8al** was purified by PTLC on silica gel (EtOAc/PE = 1:9; *eluted twice*).

Yellow liquid.

Yield: 52.5 mg (73%; *E:Z* = 99:1).

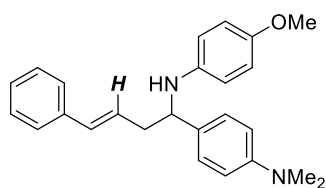
^1H NMR (600 MHz, CDCl_3): δ = 7.33–7.28 (m, 6H), 7.24–7.20 (m, 1H), 6.87 (d, J = 8.9 Hz, 2H), 6.67 (d, J = 8.9 Hz, 2H), 6.50 (d, J = 15.8 Hz, 1H), 6.46 (d, J = 8.9 Hz, 2H), 6.14 (ddd, J = 15.8, 7.6, 6.9 Hz, 1H, *E*-CH=CH), 5.68 (ddd, J = 11.8, 7.7, 6.3 Hz, 1H, *Z*-CH=CH), 4.35 (dd, J = 7.4, 5.6 Hz, 1H), 3.92 (br s, 1H), 3.79 (s, 3H), 3.68 (s, 3H), 2.74–2.69 (m, 1H), 2.66–2.61 (m, 1H) ppm.

^{13}C NMR (125 MHz, CDCl_3): δ = 158.6, 152.0, 141.6, 137.1, 135.7, 133.1, 128.6 (2C), 127.4 (2C), 127.4, 126.3, 126.2 (2C), 114.8 (2C), 114.7 (2C), 114.0 (2C), 57.8, 55.7, 55.3, 42.7 ppm.

IR (neat): ν = 3399, 3024, 2932, 2832, 1508, 1238, 1034, 820, 742, 694 cm^{-1} .

HRMS (EI): calculated for $\text{C}_{24}\text{H}_{25}\text{NO}_2^+$ = $[\text{M}^+]$; m/z = 359.1880, found: m/z = 359.1884.

(*E*)-*N*-[1-(4-*N,N*-Dimethylaminophenyl)-4-phenylbut-3-enyl]-4-methoxyaniline (8am**)**



8am

Compound **8am** was prepared according to *GP-IV* from allyl benzene (**1a**; 66.4 μ L, 0.50 mmol, 2.50 equiv) and imine **7m** (50.9 mg, 0.20 mmol), using $\text{NaN}(\text{SiMe}_3)_2$ (3.7 mg, 0.02 mmol, 10 mol%) as the catalyst, in dioxane (300 μ L) at 25 $^\circ\text{C}$ for 18 h. **8am** was purified by PTLT on silica gel (EtOAc/PE = 1:9; *eluted twice*).

Yellow liquid.

Yield: 67.1 mg (90%; *E*:*Z* = 49:1).

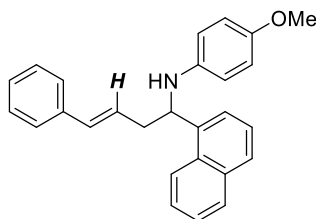
^1H NMR (601 MHz, CDCl_3): δ = 7.34–7.32 (m, 2H), 7.28 (dd, J = 7.7, 7.3 Hz, 2H), 7.24 (d, J = 8.7 Hz, 2H), 7.20 (dd, J = 7.3, 7.3 Hz, 1H), 6.72 (d, J = 8.7 Hz, 2H), 6.67 (d, J = 8.9 Hz, 2H), 6.50 (d, J = 15.5 Hz, 1H), 6.47 (d, J = 8.9 Hz, 2H), 6.16 (ddd, J = 15.5, 7.6, 6.8 Hz, 1H, *E*-CH=CH), 5.69 (ddd, J = 11.8, 7.7, 6.3 Hz, 1H, *Z*-CH=CH), 4.32 (dd, J = 7.5, 5.5 Hz, 1H), 4.02 (br s, 1H), 3.68 (s, 3H), 2.93 (s, 6H), 2.73–2.69 (m, 1H), 2.66–2.61 (m, 1H) ppm.

^{13}C NMR (125 MHz, CDCl_3): δ = 151.9, 149.7, 141.9, 137.3, 132.8, 131.5, 128.5 (2C), 127.3, 127.1 (2C), 126.8, 126.2 (2C), 114.8 (2C), 114.7 (2C), 112.8 (2C), 57.8, 55.8, 42.6, 40.7 (2C) ppm.

IR (neat): ν = 3395, 3024, 2916, 2830, 1508, 1234, 1036, 818, 733, 692 cm^{-1} .

HRMS (EI): calculated for $\text{C}_{25}\text{H}_{28}\text{N}_2\text{O}^+ = [\text{M}^+]$; m/z = 372.2196, found: m/z = 372.2188.

(*E*)-*N*-[1-(1-Naphthyl)-4-phenylbut-3-enyl]-4-methoxyaniline (8an**)**



8an

Compound **8an** was prepared according to *GP-III* from allyl benzene (**1a**; 29.2 μ L, 0.22 mmol, 1.10 equiv) and imine **7n** (52.3 mg, 0.20 mmol), using $\text{NaN}(\text{SiMe}_3)_2$ (3.7 mg, 0.02 mmol, 10 mol%) as the catalyst, in dioxane (300 μ L) at 25 $^\circ\text{C}$ for 20 h. **8an** was purified by PTLT on silica gel (Et₂O/PE = 1:9; *eluted once*).

Yellow liquid.

Yield: 74.4 mg (98%; *E*:*Z* = 24:1).

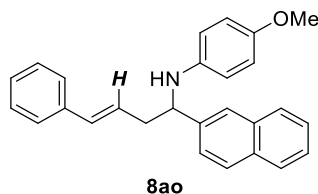
^1H NMR (500 MHz, CDCl_3): δ = 8.21 (d, J = 8.5 Hz, 1H), 7.91 (d, J = 8.2 Hz, 1H), 7.75 (d, J = 8.2 Hz, 1H), 7.66 (d, J = 7.2, 1H), 7.56 (dd, J = 7.6, 7.4 Hz, 1H), 7.51 (dd, J = 7.6, 7.4 Hz, 1H), 7.41 (dd, J = 7.7, 7.7 Hz, 1H), 7.33–7.26 (m, 4H), 7.22–7.19 (m, 1H), 6.61 (d, J = 8.9 Hz, 2H), 6.55 (d, J = 15.8 Hz, 1H), 6.40 (d, J = 8.9 Hz, 2H), 6.22 (ddd, J = 15.4, 7.1, 7.1 Hz, 1H, *E*-CH=CH), 5.80 (ddd, J = 11.7, 7.2, 7.2 Hz, 1H, *Z*-CH=CH), 5.23 (dd, J = 7.7, 3.9 Hz, 1H), 4.17 (br s, 1H), 3.62 (s, 3H), 2.98–2.93 (m, 1H), 2.72–2.66 (m, 1H) ppm.

^{13}C NMR (125 MHz, CDCl_3): δ = 151.9, 141.4, 138.3, 137.0, 134.2, 133.2, 130.7, 129.2, 128.6 (2C), 127.5, 127.4, 126.4, 126.2 (2C), 126.1, 125.82, 125.4, 123.3, 122.4, 114.7 (2C), 114.5 (2C), 55.7, 54.0, 41.0 ppm.

IR (neat): ν = 3404, 3026, 2932, 2830, 1508, 1236, 1036, 818, 779, 734, 692 cm^{-1} .

HRMS (EI): calculated for $\text{C}_{27}\text{H}_{25}\text{NO}^+ = [\text{M}^+]$; m/z = 379.1931, found: m/z = 379.1922.

(E)-N-[1-(2-Naphthyl)-4-phenylbut-3-enyl]-4-methoxyaniline (8ao**)**



Compound **8ao** was prepared according to *GP-III* from allyl benzene (**1a**; 29.2 μ L, 0.22 mmol, 1.10 equiv) and imine **7o** (52.3 mg, 0.20 mmol), using $\text{NaN}(\text{SiMe}_3)_2$ (3.7 mg, 0.02 mmol, 10 mol%) as the catalyst, in dioxane (300 μ L) at 25 $^\circ\text{C}$ for 20 h. **8ao** was purified by PTLC on silica gel ($\text{Et}_2\text{O}/\text{PE} = 1:9$; *eluted once*).

Yellow liquid.

Yield: 66.0 mg (87%; *E:Z* = 24:1).

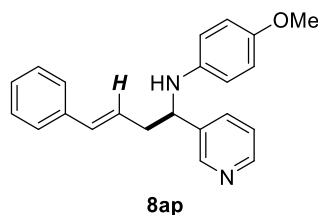
^1H NMR (500 MHz, CDCl_3): δ = 7.83–7.78 (m, 4H), 7.51 (d, J = 8.6 Hz, 1H), 7.46–4.40 (m, 2H), 7.32–7.25 (m, 4H), 7.22–7.18 (m, 1H), 6.64 (d, J = 7.9 Hz, 2H), 6.52 (d, J = 15.9 Hz, 1H, *E*-CH=CH), 6.48 (d, J = 7.9 Hz, 2H), 6.15 (ddd, J = 15.9, 8.1, 6.7 Hz, 1H), 5.71 (ddd, J = 12.7, 7.2, 7.2 Hz, 1H, *Z*-CH=CH), 4.54 (dd, J = 7.9, 5.1 Hz, 1H), 4.04 (br s, 1H), 3.63 (s, 3H), 2.83–2.78 (m, 1H), 2.72–2.66 (m, 1H) ppm.

^{13}C NMR (125 MHz, CDCl_3): δ = 152.1, 141.5, 141.3, 137.0, 133.6, 133.3, 132.8, 128.6 (2C), 128.4, 127.9, 127.7, 127.4, 126.2 (2C), 126.1, 126.0, 125.5, 125.0, 124.7, 114.8 (2C), 114.7 (2C), 58.6, 55.7, 42.5 ppm.

IR (neat): ν = 3402, 3024, 2930, 2830, 1508, 1236, 1036, 818, 746, 692 cm^{-1} .

HRMS (EI): calculated for $\text{C}_{27}\text{H}_{25}\text{NO}^+ = [\text{M}^+]$: m/z = 379.1931, found: m/z = 379.1929.

(E)-N-[1-(Pyridin-3-yl)-4-phenylbut-3-enyl]-4-methoxyaniline (8ap**)**



Compound **8ap** was prepared according to *GP-III* from allyl benzene (**1a**; 29.2 μ L, 0.22 mmol, 1.10 equiv) and imine **7p** (42.4 mg, 0.20 mmol), using $\text{NaN}(\text{SiMe}_3)_2$ (3.7 mg, 0.02 mmol, 10 mol%) as the catalyst, in dioxane (300 μ L) at 25 $^\circ\text{C}$ for 20 h. **8ap** was purified by PTLC on silica gel (EtOAc ; *eluted once*).

Yellow liquid.

Yield: 52.8 mg (80%; *E:Z* = 99:1).

^1H NMR (500 MHz, CDCl_3): δ = 8.70 (d, J = 2.0 Hz, 1H), 8.54 (dd, J = 4.8, 1.6 Hz, 1H), 7.73 (dt, J = 7.8, 2.0 Hz, 1H), 7.40–7.31 (m, 3H), 7.30–7.24 (m, 3H), 6.71 (d, J = 9.0 Hz, 2H), 6.55 (d, J = 15.8 Hz, 1H), 6.47 (d, J = 9.0 Hz, 2H), 6.15 (ddd, J = 15.8, 7.9, 6.8 Hz, 1H), 4.49 (dd, J = 7.8, 5.2 Hz, 1H), 3.98 (s, 1H), 3.71 (s, 3H), 2.79 (dddd, J = 14.4, 6.8, 5.2, 1.6 Hz, 1H), 2.69 (dddd, J = 14.4, 7.9, 7.8, 1.3 Hz, 1H) ppm.

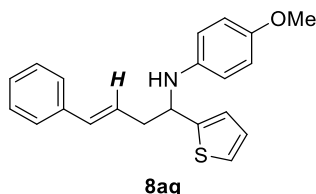
^{13}C NMR (125 MHz, CDCl_3): δ = 152.4, 148.7, 148.6, 140.8, 139.0, 136.8, 134.0, 133.9, 128.6 (2C), 127.5, 126.2, 125.1 (2C), 123.6, 114.9 (2C), 114.8 (2C), 56.2, 55.7, 42.3 ppm.

The Z-isomer could not be detected.

IR (neat): ν = 3365, 3026, 2929, 2831, 1502, 1234, 1026, 1002, 819, 746, 692 cm^{-1} .

HRMS (EI): calculated for $\text{C}_{21}\text{H}_{20}\text{N}_2^+ = [\text{M}^+]$: m/z = 330.17267, found: m/z = 330.17216.

(E)-N-[1-(Thiophen-2-yl)-4-phenylbut-3-enyl]-4-methoxyaniline (8aq**)**



Compound **8aq** was prepared according to *GP-III* from allyl benzene (**1a**; 39.8 μ L, 0.30 mmol, 1.50 equiv) and imine **7q** (43.5 mg, 0.20 mmol), using $\text{NaN}(\text{SiMe}_3)_2$ (3.7 mg, 0.02 mmol, 10 mol%) as the catalyst, in dioxane (300 μ L) at 60 $^\circ\text{C}$ for 72 h. **8aq** was purified by PTLC on silica gel ($\text{Et}_2\text{O}/\text{PE} = 1:9$; *eluted once*).

Yellow liquid.

Yield: 60.4 mg (90%; *E:Z* = 99:1).

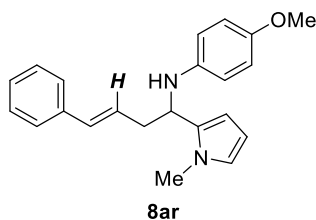
^1H NMR (500 MHz, CDCl_3): δ = 7.33–7.28 (m, 4H), 7.24–7.17 (m, 2H), 6.99 (d, J = 3.4 Hz, 1H), 6.95 (dd, J = 4.9, 3.4 Hz, 1H), 6.72 (d, J = 8.9 Hz, 2H), 6.57 (d, J = 8.9 Hz, 2H), 6.52 (d, J = 15.8 Hz, 1H), 6.19 (ddd, J = 15.8, 7.3, 7.3 Hz, 1H, *E*-CH=CH), 5.72 (ddd, J = 11.8, 6.9, 6.9 Hz, 1H, *Z*-CH=CH), 4.72 (dd, J = 6.3, 6.3 Hz, 1H), 3.94 (br s, 1H), 3.71 (s, 3H), 2.83–2.79 (m, 2H) ppm.

^{13}C NMR (125 MHz, CDCl_3): δ = 152.5, 149.0, 141.1, 137.1, 133.6, 128.6 (2C), 127.5, 126.8, 126.2 (2C), 125.6, 123.8, 123.5, 115.2 (2C), 114.8 (2C), 55.7, 54.8, 42.4 ppm.

IR (neat): ν = 3387, 3026, 2928, 2832, 1508, 1234, 818, 735, 692 cm^{-1} .

HRMS (EI): calculated for $\text{C}_{21}\text{H}_{21}\text{NO}^{32}\text{S}^+ = [\text{M}^+]$: m/z = 335.1338, found: m/z = 335.1342.

(E)-N-[1-(1-Methyl-1H-pyrrol-2-yl)-4-phenylbut-3-enyl]-4-methoxyaniline (8ar**)**



Compound **8ar** was prepared according to *GP-IV* from allyl benzene (**1a**; 29.2 μ L, 0.22 mmol, 1.10 equiv) and imine **7r** (42.9 mg, 0.20 mmol), using $\text{NaN}(\text{SiMe}_3)_2$ (3.7 mg, 0.02 mmol, 10 mol%) as the catalyst, in dioxane (300 μ L) at 25 $^\circ\text{C}$ for 18 h. **8ar** was purified by PTLC on silica gel ($\text{EtOAc}/\text{PE} = 1:9$; *eluted twice*).

Yellow liquid.

Yield: 53.2 mg (80%; *E:Z* = >99:1).

^1H NMR (500 MHz, CDCl_3): δ = 7.31–7.24 (m, 4H), 7.21–7.18 (m, 1H), 6.76 (d, J = 8.9 Hz, 2H), 6.62–6.52 (m, 3H), 6.48 (d, J = 15.9 Hz, 1H), 6.22 (ddd, J = 15.9, 7.3, 7.3 Hz, 1H), 6.18 (dd, J = 3.4, 1.5 Hz, 1H), 6.08 (dd, J = 3.4, 2.8 Hz, 1H), 4.47 (dd, J = 7.3, 5.8 Hz, 1H), 3.73 (s, 3H), 3.57 (s, 3H), 3.56 (br s, 1H), 2.89–2.84 (m, 1H), 2.82–2.76 (m, 1H) ppm.

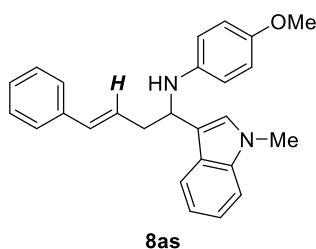
^{13}C NMR (125 MHz, CDCl_3): δ = 152.2, 141.3, 137.3, 133.4, 132.6, 128.5 (2C), 127.2, 126.8, 126.1 (2C), 122.5, 115.0 (2C), 114.8 (2C), 106.7, 106.5, 55.8, 51.5, 38.3, 34.0 ppm.

The Z-isomer could not be detected.

IR (neat): ν = 3379, 3024, 2916, 2832, 1508, 1236, 1034, 818, 735, 712, 692 cm^{-1} .

HRMS (EI): calculated for $\text{C}_{22}\text{H}_{24}\text{N}_2\text{O}^+ = [\text{M}^+]$: m/z = 332.1883, found: m/z = 332.1887.

(E)-N-[1-(1-Methyl-1H-indol-3-yl)-4-phenylbut-3-enyl]-4-methoxyaniline (8as**)**



Compound **8as** was prepared according to *GP-IV* from allyl benzene (**1a**; 53.0 μ L, 0.40 mmol, 2.00 equiv) and imine **7s** (52.9 mg, 0.20 mmol), using $\text{NaN}(\text{SiMe}_3)_2$ (3.7 mg, 0.02 mmol, 10 mol%) as the catalyst, in dioxane (300 μ L) at 25 $^\circ\text{C}$ for 20 h. **8as** was purified by PTLC on silica gel ($\text{Et}_2\text{O}/\text{PE} = 1:9$; *eluted three times*). This experiment was carried out by *Hanno Kossen*.

Yellow liquid.

Yield: 61.2 mg (80%; *E:Z* = 99:1).

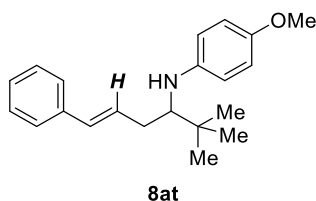
^1H NMR (500 MHz, CDCl_3): δ = 7.71 (d, J = 7.9 Hz, 1H), 7.33–7.26 (m, 5H), 7.25–7.22 (m, 1H), 7.22–7.18 (m, 1H), 7.13 (ddd, J = 7.9, 7.0, 1.0 Hz, 1H), 6.97 (s, 1H), 6.70 (d, J = 9.0 Hz, 2H), 6.57 (d, J = 9.0 Hz, 2H), 6.53 (d, J = 15.8 Hz, 1H), 6.24 (ddd, J = 15.8, 7.2, 7.2 Hz, 1H, *E*-CH=CH), 5.78 (ddd, J = 11.6, 7.1, 7.1 Hz, 1H, *Z*-CH=CH), 4.78 (dd, J = 6.2, 6.2 Hz, 1H), 3.91 (br s, 1H), 3.73 (s, 3H), 3.70 (s, 3H), 2.97–2.91 (m, 1H), 2.86–2.81 (m, 1H) ppm.

^{13}C NMR (125 MHz, CDCl_3): δ = 151.9, 142.0, 137.5, 137.3, 132.7, 128.5 (2C), 127.2, 127.0, 126.6, 126.3, 126.1 (2C), 121.6, 119.3, 118.9, 116.7, 114.8 (2C), 114.7 (2C), 109.4, 55.7, 51.7, 40.5, 32.7 ppm.

IR (neat): ν = 3435, 3358, 3022, 3022, 2831, 1510, 1238, 824, 738, 692 cm^{-1} .

HRMS (ESI): calculated for $\text{C}_{26}\text{H}_{27}\text{N}_2\text{O}^+ = [\text{M}+\text{H}]^+$: m/z = 383.2118, found: m/z = 383.2140.

(E)-N-(2,2-Dimethyl-6-phenylhex-5-en-3-yl)-4-methoxyaniline (8at**)**



Compound **8at** was prepared according to *GP-IV* from allyl benzene (**1a**; 53.0 μ L, 0.40 mmol, 2.00 equiv) and imine **7t** (38.3 mg, 0.20 mmol), using $\text{NaN}(\text{SiMe}_3)_2$ (3.7 mg, 0.02 mmol, 10 mol%) as the catalyst, in dioxane (300 μ L) at 25 $^\circ\text{C}$ for 18 h. **8at** was purified by PTLC on silica gel ($\text{Et}_2\text{O}/\text{PE} = 1:9$; *eluted once*).

Yellow liquid.

Yield: 53.8 mg (87%; *E:Z* = 49:1).

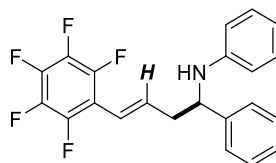
^1H NMR (600 MHz, CDCl_3): δ = 7.21–7.18 (m, 2H), 7.15–7.10 (m, 3H), 6.72 (d, J = 8.5 Hz, 2H), 6.55 (d, J = 8.5 Hz, 2H), 6.38 (d, J = 15.8 Hz, 1H), 6.16 (ddd, J = 15.8, 8.1, 8.1 Hz, 1H, *E*-CH=CH), 5.69 (ddd, J = 11.5, 6.9, 6.9 Hz, 1H, *Z*-CH=CH), 3.72 (s, 3H), 3.24 (br s, 1H), 3.12 (dd, J = 9.4, 3.5 Hz, 1H), 2.61–2.57 (m, 1H), 2.22–2.17 (m, 1H), 1.00 (s, 9H) ppm.

^{13}C NMR (150 MHz, CDCl_3): δ = 151.4, 143.9, 137.7, 131.2, 129.3, 128.4 (2C), 126.8, 126.0 (2C), 115.0 (2C), 114.4 (2C), 63.9, 55.9, 35.9, 35.9, 27.1 (3C) ppm.

IR (neat): ν = 3404, 3024, 2951, 2832, 1508, 1232, 816, 739, 692 cm^{-1} .

HRMS (EI): calculated for $\text{C}_{21}\text{H}_{27}\text{NO}^+ = [\text{M}]^+$: m/z = 309.2087, found: m/z = 309.2091.

(E)-N-[4-Pentafluorophenyl-1-phenylbut-3-enyl]-aniline (8ba**)**



8ba

Compound **8ba** was prepared according to *GP-III* from allylpentafluorobenzene (**1b**; 46 mg, 0.22 mmol, 1.10 equiv) and imine **7a** (36.2 mg, 0.20 mmol), using $\text{KN}(\text{SiMe}_3)_2$ (3.7 mg, 0.02 mmol, 10 mol%) as the catalyst, in Et_2O (300 μL) at 25 °C for 18 h. **8ba** was purified by PTLC on silica gel (EtOAc/PE = 1:9; *eluted once*).

Yellow liquid.

Yield: 46.7 mg (60%; *E:Z* = >99:1).

^1H NMR (500 MHz, CDCl_3): δ = 7.43–7.35 (m, 4H), 7.31–7.27 (m, 1H), 7.15–7.09 (m, 2H), 6.69 (t, J = 7.3 Hz, 1H), 6.56 (d, J = 7.6 Hz, 2H), 6.53–6.47 (m, 1H), 6.40 (d, J = 16.3 Hz, 1H), 4.56 (dd, J = 7.3, 5.8 Hz, 1H), 4.16 (br s, 1H), 2.92–2.67 (m, 2H) ppm.

^{13}C NMR (150 MHz, CDCl_3): δ = 147.0, 144.6 (d, J = 242.3 Hz, 2C), 142.8, 140.8, 139.7 (d, J = 256.6 Hz), 137.7 (d, J = 255.7 Hz, 2C), 136.4 (td, J = 7.3, 2.2 Hz), 129.1 (2C), 128.7 (2C), 127.3, 126.3 (2C), 117.7, 117.2, 113.6 (2C), 57.4, 43.4 ppm.

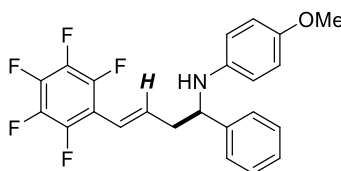
^{19}F NMR (138 MHz, CDCl_3): δ = –143.3 (dd, J = 22.0, 8.5 Hz, 2F), –156.7 (t, J = 22.0 Hz, 1F), –163.0 (td, J = 22.0, 8.5 Hz, 2F) ppm.

The Z-isomer could not be detected.

IR (neat): ν = 3028, 2362, 1519, 1495, 1315, 1111, 993, 750, 699 cm^{-1} .

HRMS (EI): calculated for $\text{C}_{22}\text{H}_{16}\text{F}_5\text{N}^+$ = $[\text{M}^+]$: m/z = 389.1303, found: m/z = 389.1327.

(E)-N-[4-Pentafluorophenyl-1-phenylbut-3-enyl]-4-methoxyaniline (8bb**)**



8bb

Compound **8bb** was prepared according to *GP-III* from allylpentafluorobenzene (**1b**; 46 mg, 0.22 mmol, 1.10 equiv) and imine **7b** (42.2 mg, 0.20 mmol), using $\text{NaN}(\text{SiMe}_3)_2$ (3.7 mg, 0.02 mmol, 10 mol%) as the catalyst, in dioxane (300 μL) at 25 °C for 18 h. **8bb** was purified by PTLC on silica gel (EtOAc/PE = 1:9; *eluted once*).

Yellow liquid.

Yield: 42.7 mg (51%; *E:Z* = >99:1).

^1H NMR (500 MHz, CDCl_3): δ = 7.42–7.33 (m, 3H), 7.30–7.25 (m, 2H), 6.71 (d, J = 9.0 Hz, 2H), 6.50 (d, J = 9.0 Hz, 2H), 6.49 (dt, J = 16.3, 7.4 Hz, 1H), 6.38 (d, J = 16.3 Hz, 1H), 4.47 (dd, J = 7.3, 5.8 Hz, 1H), 3.90 (br s, 1H), 3.71 (s, 3H), 2.85–2.71 (m, 2H) ppm.

^{13}C NMR (125 MHz, CDCl_3): δ = 152.2, 144.6 (d, J = 246.1 Hz, 2C), 143.0, 141.2, 139.6 (d, J = 240.9 Hz, 2C), 137.6 (d, J = 242.3 Hz), 136.5 (td, J = 7.4, 2.2 Hz), 128.7 (2C), 127.2, 126.3 (2C), 117.1, 114.9 (2C), 114.7 (2C), 111.9 (dt, J = 14.2, 6.9 Hz), 58.2, 55.7, 43.5 ppm.

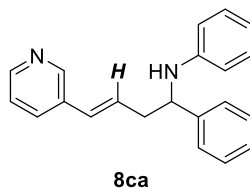
^{19}F NMR (138 MHz, CDCl_3): δ = –141.2 – –145.7 (m, 2F), –156.3 – –158.7 (m, 1F), –161.15 – –165.24 (m, 2F) ppm.

The Z-isomer could not be detected.

IR (neat): ν = 3398, 3026, 2904, 2831, 1510, 1502, 1236, 1026, 970, 817, 752, 700 cm^{-1} .

HRMS (EI): calculated for $\text{C}_{23}\text{H}_{18}\text{F}_5\text{NO}^+$ = $[\text{M}^+]$: m/z = 419.1303, found: m/z = 419.1327.

(E)-N-[4-(Pyridin-3-yl)-1-phenylbut-3-enyl]-aniline (8ca**)**



Compound **8ca** was prepared according to *GP-III* from 3-allyl pyridine (**1c**; 35.8 mg, 0.30 mmol, 1.50 equiv) and imine **7a** (36.2 mg, 0.20 mmol), using $\text{NaN}(\text{SiMe}_3)_2$ (3.7 mg, 0.02 mmol, 10 mol%) as the catalyst, in dioxane (300 μL) at 25 °C for 20 h. **8ca** was purified by PTLC on silica gel (EtOAc; *eluted twice*).

Yellow liquid.

Yield: 39.7 mg (66%; *E:Z* = 99:1).

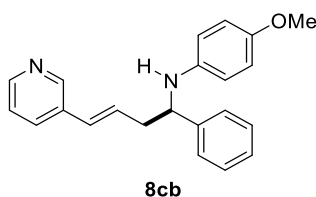
¹H NMR (500 MHz, CDCl_3): δ = 8.54 (d, *J* = 1.9 Hz, 1H), 8.44 (dd, *J* = 4.8, 1.4 Hz, 1H), 7.61 (ddd, *J* = 7.9, 1.9, 1.9 Hz, 1H), 7.39–7.32 (m, 4H), 7.26–7.23 (m, 1H), 7.20 (dd, *J* = 7.9, 4.8 Hz, 1H), 7.09–7.06 (m, 2H), 6.64 (dd, *J* = 7.3, 7.3 Hz, 1H), 6.51 (d, *J* = 8.4 Hz, 2H), 6.47 (d, *J* = 15.9 Hz, 1H), 6.21 (ddd, *J* = 15.9, 7.2, 7.2 Hz, 1H, *E*-CH=CH), 5.84 (ddd, *J* = 11.7, 7.2, 7.2 Hz, 1H, *Z*-CH=CH), 4.51–4.49 (m, 1H), 4.19 (br s, 1H), 2.80–2.74 (m, 1H), 2.73–2.67 (m, 1H) ppm.

¹³C NMR (125 MHz, CDCl_3): δ = 148.5, 148.2, 147.1, 143.2, 132.6, 132.6, 129.6, 129.1 (2C), 128.7 (2C), 128.7, 127.2, 126.3 (2C), 123.4, 117.6, 113.5 (2C), 57.5, 42.4 ppm

IR (neat): ν = 3406, 3287, 3026, 2922, 2851, 1601, 1501, 1317, 964, 748, 692 cm^{-1} .

HRMS (EI): calculated for $\text{C}_{21}\text{H}_{20}\text{N}_2^+$ = $[\text{M}^+]$: m/z = 300.1621, found: m/z = 300.1621.

(E)-N-[4-(Pyridin-3-yl)-1-phenylbut-3-enyl]-aniline (8cb**)**



Compound **8cb** was prepared according to *GP-III* from 3-allyl pyridine (**1c**; 35.8 mg, 0.30 mmol, 1.50 equiv) and imine **7b** (42.2 mg, 0.20 mmol), using $\text{LiN}(\text{SiMe}_3)_2$ (3.4 mg, 0.02 mmol, 10 mol%) as the catalyst, in dioxane (300 μL) at 25 °C for 20 h. **8cb** was purified by PTLC on silica gel (EtOAc; *eluted twice*).

Yellow liquid.

Yield: 52.8 mg (80%; *E:Z* = 49:1).

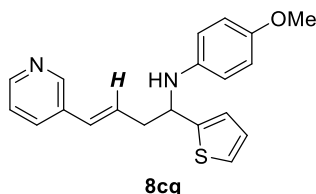
¹H NMR (500 MHz, CDCl_3): δ = 8.57 (d, *J* = 2.0 Hz, 1H), 8.48 (dd, *J* = 4.8, 1.6 Hz, 1H), 7.65 (dt, *J* = 7.9, 2.0 Hz, 1H), 7.42–7.34 (m, 3H), 7.30–7.26 (m, 2H), 7.24 (dd, *J* = 7.9, 4.8 Hz, 1H), 6.71 (d, *J* = 9.0 Hz, 2H), 6.51 (d, *J* = 15.9 Hz, 1H), 6.50 (d, *J* = 9.0 Hz, 2H), 6.25 (ddd, *J* = 15.9, 7.2, 7.2 Hz, 1H, *E*-CH=CH), 5.88 (ddd, *J* = 11.7, 7.2, 7.2 Hz, 1H, *Z*-CH=CH), 4.46 (dd, *J* = 7.6, 5.5 Hz, 1H), 3.96 (br s, 1H), 3.71 (s, 3H), 2.83–2.67 (m, 2H) ppm.

¹³C NMR (125 MHz, CDCl_3): δ = 152.1, 148.5, 148.2, 143.4, 141.3, 132.6, 132.5, 129.6, 128.8, 128.7 (2C), 127.2, 126.4 (2C), 123.4, 114.8 (4C), 58.4, 55.7, 42.5 ppm.

IR (neat): ν = 3400, 3026, 2904, 1502, 1236, 1037, 1002, 819, 702 cm^{-1} .

HRMS (EI): calculated for $\text{C}_{22}\text{H}_{22}\text{N}_2\text{O}^+$ = $[\text{M}^+]$: m/z = 330.1727, found: m/z = 330.1731.

(E)-N-[4-(Pyridin-3-yl)-1-(thiophen-2-yl)phenylbut-3-enyl]-4-methoxyaniline (8cq**)**



Compound **8cq** was prepared according to *GP-III* from allyl pyridine (**1c**; 35.8 mg, 0.30 mmol, 1.50 equiv) and aldimine **7q** (43.5 mg, 0.20 mmol), using $\text{NaN}(\text{SiMe}_3)_2$ (3.7 mg, 0.02 mmol, 10 mol%) as the catalyst, in dioxane (300 μL) at 25 °C for 20 h. **8cq** was purified by PTLC (EtOAc, *eluted twice*).

Yellow liquid.

Yield: 38.4 mg (57%, *E:Z* = 32:1).

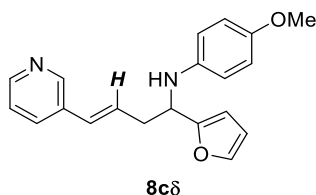
¹H NMR (500 MHz, CDCl_3): δ = 8.55 (d, *J* = 1.8 Hz, 1H), 8.45 (dd, *J* = 4.6, 1.2 Hz, 1H), 7.63 (ddd, *J* = 7.9, 1.8, 1.8 Hz, 1H), 7.23–7.18 (m, 2H), 6.99–6.95 (m, 2H), 6.73 (d, *J* = 8.9 Hz, 2H), 6.58 (d, *J* = 8.9 Hz, 2H), 6.49 (d, *J* = 16.0 Hz, 1H), 6.27 (ddd, *J* = 16.0, 7.2, 7.2 Hz, 1H, *E*-CH=CH), 5.87 (ddd, *J* = 11.6, 7.2, 7.2 Hz, 1H, *Z*-CH=CH), 4.74 (dd, *J* = 6.4, 6.4 Hz, 1H), 3.90 (br s, 1H), 3.71 (s, 3H), 2.85–2.82 (m, 2H) ppm.

¹³C NMR (125 MHz, CDCl_3): δ = 152.6, 148.6, 148.5, 148.2, 141.0, 132.6, 132.6, 129.9, 128.2, 126.9, 124.0, 123.6, 123.4, 115.2 (2C), 114.8 (2C), 55.7, 54.7, 42.3 ppm.

IR (neat): ν = 3379, 3287, 3028, 2926, 2832, 1508, 1234, 1036, 818, 702 cm^{-1} .

HRMS (EI): calculated for $\text{C}_{20}\text{H}_{20}\text{N}_2\text{OS}^+ = [\text{M}^+]$: m/z = 336.1291, found: m/z = 336.1300.

(E)-N-[4-(Pyridin-3-yl)-1-(furan-2-yl)phenylbut-3-enyl]-4-methoxyaniline (8cd**)**



Compound **8cd** was prepared according to *GP-III* from allyl pyridine (**1c**; 35.8 mg, 0.30 mmol, 1.50 equiv) and aldimine **7d** (40.2 mg, 0.20 mmol), using $\text{NaN}(\text{SiMe}_3)_2$ (3.7 mg, 0.02 mmol, 10 mol%) as the catalyst, in dioxane (300 μL) at 25 °C for 20 h. **8cd** was purified by PTLC (EtOAc, *eluted twice*).

Yellow liquid.

Yield: 26.3 mg (41%, *E:Z* = 32:1).

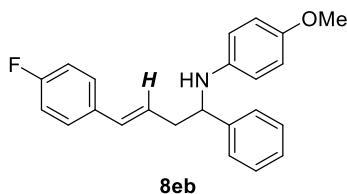
¹H NMR (500 MHz, CDCl_3): δ = 8.53 (d, *J* = 2.0 Hz, 1H), 8.44 (dd, *J* = 4.8, 1.6 Hz, 1H), 7.61 (ddd, *J* = 8.0, 2.0, 2.0 Hz, 1H), 7.36 (s, 1H), 7.20 (dd, *J* = 8.0, 4.8 Hz, 1H), 6.74 (d, *J* = 8.9 Hz, 2H), 6.59 (d, *J* = 8.9 Hz, 2H), 6.45 (d, *J* = 15.8 Hz, 1H), 6.29 (dd, *J* = 3.3, 1.9 Hz, 1H), 6.22 (ddd, *J* = 15.8, 7.2, 7.2 Hz, 1H, *E*-CH=CH), 6.17 (d, *J* = 7.2 Hz, 1H), 5.85 (ddd, *J* = 12.3, 7.4, 7.4 Hz, 1H, *Z*-CH=CH), 4.57 (dd, *J* = 6.4, 6.4 Hz, 1H), 3.78 (br s, 1H), 3.72 (s, 3H), 2.84–2.82 (m, 2H) ppm.

¹³C NMR (125 MHz, CDCl_3): δ = 155.6, 152.6, 148.4, 148.2, 141.6, 140.9, 132.7, 132.6, 129.6, 128.3, 123.4, 115.3 (2C), 114.8 (2C), 110.2, 106.3, 55.7, 52.7, 38.6 ppm

IR (neat): ν = 3366, 3275, 3028, 2932, 2832, 1508, 1234, 1034, 818, 733, 706 cm^{-1} .

HRMS (EI): calculated for $\text{C}_{20}\text{H}_{20}\text{N}_2\text{O}_2^+ = [\text{M}^+]$: m/z = 320.1519, found: m/z = 320.1510.

(E)-N-[4-(4-Fluorophenyl)-1-phenylbut-3-enyl]-4-methoxyaniline (8eb**)**



Compound **8eb** was prepared according to *GP-III* from the 4-allyl fluorobenzene **1e** (29.7 μ L, 0.22 mmol, 1.10 equiv) and imine **7b** (42.2 mg, 0.20 mmol), using $\text{NaN}(\text{SiMe}_3)_2$ (3.7 mg, 0.02 mmol, 10 mol%) as the catalyst, in dioxane (300 μ L) at 25 $^\circ\text{C}$ for 20 h. **8eb** was purified by PTLC on silica gel (EtOAc/PE = 1:9; *eluted once*).

Yellow liquid.

Yield: 68.8 mg (99%; *E:Z* = 49:1).

^1H NMR (500 MHz, CDCl_3): δ = 7.37 (d, J = 7.3 Hz, 2H), 7.32 (dd, J = 7.6, 7.6 Hz, 2H), 7.29–7.21 (m, 3H), 6.96 (dd, J = 8.7, 8.7 Hz, 2H), 6.66 (d, J = 9.0 Hz, 2H), 6.49–6.40 (m, 3H), 6.04 (ddd, J = 15.8, 7.2, 7.2 Hz, 1H, *E*-CH=CH), 5.67 (ddd, J = 11.7, 7.2, 7.2 Hz, 1H, *Z*-CH=CH), 4.38 (dd, J = 7.8, 5.3 Hz, 1H), 3.94 (br s, 1H), 3.65 (s, 3H), 2.74–2.66 (m, 1H), 2.65–2.56 (m, 1H) ppm.

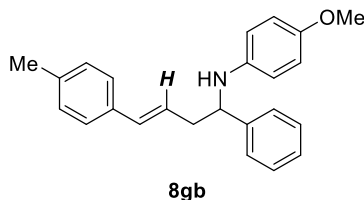
^{13}C NMR (125 MHz, CDCl_3): δ = 162.2 (d, J = 246.6 Hz), 152.1, 143.7, 141.5, 133.2 (d, J = 3.3 Hz), 132.0, 128.6 (2C), 127.6 (d, J = 7.9, 2C), 127.0, 126.4, 126.0 (d, J = 2.1, 2C), 115.5, 115.3, 114.7 (2C), 114.6 (2C), 58.4, 55.7, 42.4 ppm.

^{19}F NMR (376 MHz, CDCl_3): δ = -114.6 (ddd, J = 13.2, 6.7, 3.9 Hz) ppm.

IR (neat): ν = 3402, 3026, 2931, 2832, 1506, 1229, 818, 737, 700 cm^{-1} .

HRMS (EI): calculated for $\text{C}_{23}\text{H}_{22}\text{FNO}^+ = [\text{M}^+]$; m/z = 347.1680, found: m/z = 347.1687.

(E)-N-[4-(4-Methylphenyl)-1-phenylbut-3-enyl]-4-methoxyaniline (8gb**)**



Compound **8gb** was prepared according to *GP-III* from the 4-allyl toluene **1g** (33.7 μ L, 0.22 mmol, 1.10 equiv) and imine **7b** (42.2 mg, 0.20 mmol), using $\text{NaN}(\text{SiMe}_3)_2$ (3.7 mg, 0.02 mmol, 10 mol%) as the catalyst, in dioxane (300 μ L) at 25 $^\circ\text{C}$ for 20 h. **8gb** was purified by PTLC on silica gel (EtOAc/PE = 1:9; *eluted once*).

Yellow liquid.

Yield: 68.0 mg (99%; *E:Z* = 99:1).

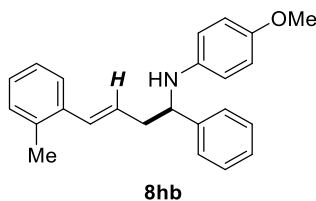
^1H NMR (500 MHz, CDCl_3): δ = 7.38 (d, J = 7.2 Hz, 2H), 7.36–7.30 (m, 3H), 7.26–7.21 (m, 1H), 7.13 (d, J = 3.1 Hz, 3H), 6.76–6.64 (m, 3H), 6.46 (d, J = 9.0 Hz, 2H), 6.01 (ddd, J = 15.6, 7.8, 6.7 Hz, 1H, *E*-CH=CH), 5.73 (ddd, J = 11.4, 7.3, 7.3 Hz, 1H, *Z*-CH=CH), 4.40 (ddd, J = 7.6, 5.0, 4.4 Hz, 1H), 3.98 (d, J = 4.4 Hz, 1H), 3.67 (s, 3H), 2.79–2.72 (m, 1H), 2.70–2.63 (m, 1H), 2.31 (s, 3H) ppm.

^{13}C NMR (125 MHz, CDCl_3): δ = 152.0, 143.8, 141.6, 137.2, 134.3, 133.1, 129.2 (2C), 128.6 (2C), 127.0, 126.4 (2C), 126.1 (2C), 125.1, 114.7 (2C), 114.7 (2C), 58.4, 55.7, 42.6, 21.2 ppm.

IR (neat): ν = 3397, 3024, 2930, 2830, 1510, 1236, 818, 746, 700 cm^{-1} .

HRMS (EI): calculated for $\text{C}_{24}\text{H}_{25}\text{NO}^+ = [\text{M}^+]$; m/z = 343.1931, found: m/z = 343.1945.

(E)-N-[4-(2-Methylphenyl)-1-phenylbut-3-enyl]-4-methoxyaniline (8hb**)**



Compound **8hb** was prepared according to *GP-III* from the 2-allyl toluene **1h** (33.7 μ L, 0.22 mmol, 1.10 equiv) and imine **7b** (42.2 mg, 0.20 mmol), using $\text{NaN}(\text{SiMe}_3)_2$ (3.7 mg, 0.02 mmol, 10 mol%) as the catalyst, in dioxane (300 μ L) at 25 $^\circ\text{C}$ for 20 h. **8hb** was purified by PTLC on silica gel (EtOAc/PE = 1:9; *eluted once*).

Yellow liquid.

Yield: 58.4 mg (85%; *E:Z* = 49:1).

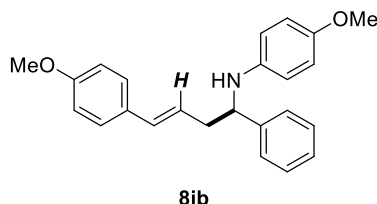
^1H NMR (500 MHz, CDCl_3): δ = 7.37 (d, J = 7.3 Hz, 2H), 7.31 (dd, J = 7.5, 7.3 Hz, 2H), 7.24–7.21 (m, 3H), 7.09 (d, J = 7.5 Hz, 2H), 6.65 (d, J = 8.9 Hz, 2H), 6.48–6.43 (m, 3H), 6.08 (ddd, J = 14.7, 7.2, 7.2 Hz, 1H, *E*-CH=CH), 5.64 (ddd, J = 11.5, 7.2, 6.4 Hz, 1H, *Z*-CH=CH), 4.37 (dd, J = 6.4, 6.4 Hz, 1H), 3.95 (br s, 1H), 3.65 (s, 3H), 2.73–2.69 (m, 1H), 2.63–6.57 (m, 1H), 2.31 (s, 3H) ppm.

^{13}C NMR (125 MHz, CDCl_3): δ = 152.1, 143.8, 141.6, 136.3, 135.1, 131.3, 130.3, 128.6 (2C), 127.6, 127.4, 127.0, 126.5 (2C), 126.1, 125.7, 114.8 (2C), 114.8 (2C), 58.4, 55.8, 42.8, 19.9 ppm.

IR (neat): ν = 3399, 3024, 2924, 2830, 1508, 1234, 816, 750, 700 cm^{-1} .

HRMS (EI): calculated for $\text{C}_{24}\text{H}_{25}\text{NO}^+ = [\text{M}^+]$: m/z = 343.1931, found: m/z = 343.1922.

(E)-N-[4-(4-Methoxyphenyl)-1-phenylbut-3-enyl]-4-methoxyaniline (8ib**)**



Compound **8ib** was prepared according to *GP-IV* from the 4-allyl anisole **1i** (33.8 μ L, 0.22 mmol, 1.10 equiv) and imine **7b** (42.2 mg, 0.20 mmol), using $\text{NaN}(\text{SiMe}_3)_2$ (3.7 mg, 0.02 mmol, 10 mol%) as the catalyst, in dioxane (300 μ L) at 40 $^\circ\text{C}$ for 20 h. **8ib** was purified by PTLC on silica gel (EtOAc/PE = 1:9; *eluted twice*).

Yellow liquid.

Yield: 55.4 mg (77%; *E:Z* = 24:1).

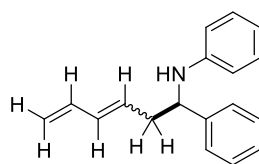
^1H NMR (500 MHz, CDCl_3): δ = 7.38–7.37 (m, 2H), 7.32–7.30 (m, 2H), 7.26–7.21 (m, 3H), 6.83 (d, J = 8.7 Hz, 2H), 6.66 (d, J = 8.7 Hz, 2H), 6.46–6.43 (m, 3H), 5.99 (ddd, J = 15.6, 7.2, 7.2 Hz, 1H, *E*-CH=CH), 5.59 (ddd, J = 12.0, 7.0, 7.0 Hz, 1H, *Z*-CH=CH), 4.37 (dd, J = 5.7, 5.7 Hz, 1H), 3.97 (br s, 1H), 3.78 (s, 3H), 3.66 (s, 3H), 2.73–2.68 (m, 1H), 2.62–2.56 (m, 1H) ppm.

^{13}C NMR (125 MHz, CDCl_3): δ = 159.1, 152.0, 143.9, 141.6, 132.6, 129.0, 128.6 (2C), 127.3 (2C), 126.9, 126.4 (2C), 123.9, 114.7 (4C), 114.0 (2C), 58.4, 55.7, 55.3, 42.6 ppm

IR (neat): ν = 3397, 3026, 2932, 2832, 1508, 1236, 1032, 818, 752, 700 cm^{-1} .

HRMS (EI): calculated for $\text{C}_{24}\text{H}_{25}\text{NO}_2^+ = [\text{M}^+]$: m/z = 359.1880, found: m/z = 359.1878.

(*E/Z*)-*N*-(1-Phenylhexa-3,5-dienyl)-aniline (8da**)**



8da

Compound **8da** was prepared according to *GP-III* from 1,4-pentadiene (**1d**; 15.0 mg, 0.22 mmol, 1.10 equiv) and imine **7a** (36.2 mg, 0.20 mmol), using $\text{NaN}(\text{SiMe}_3)_2$ (3.7 mg, 0.02 mmol, 10 mol%) as the catalyst, in dioxane (300 μL) at 25 °C for 20 h. **8da** was purified by PTLC on silica gel (EtOAc/PE = 1:9; *eluted once*).

Yellow liquid.

Yield: 49.7 mg (99%; *E:Z* = 3:1).

(*E*)-8da: ^1H NMR (500 MHz, CDCl_3): δ = 7.42–7.36 (m, 4H), 7.31–7.26 (m, 1H), 7.15–7.10 (m, 2H), 6.69 (t, J = 7.3 Hz, 1H), 6.56–6.51 (m, 2H), 6.35 (dt, J = 16.8, 10.3 Hz, 1H), 6.27–6.20 (m, 1H), 5.68 (dt, J = 14.8, 7.3 Hz, 1H), 5.22 (d, J = 16.8 Hz, 1H), 5.09 (d, J = 10.3 Hz, 1H), 4.45 (dd, J = 7.9, 5.4 Hz, 1H), 4.17 (br s, 1H), 2.69 (ddd, J = 7.3, 5.4, 1.3 Hz, 1H), 2.58 (ddd, J = 7.9, 7.3, 1.3 Hz, 1H) ppm.

(*Z*)-8da: ^1H NMR (500 MHz, CDCl_3): δ = 7.42–7.36 (m, 4H), 7.31–7.26 (m, 1H), 7.15–7.10 (m, 2H), 6.68 (t, J = 7.3 Hz, 1H), 6.66 (dddd, J = 16.8, 11.1, 10.3, 1.2 Hz, 1H), 6.56–6.51 (m, 2H), 6.27–6.20 (m, 1H), 5.48 (dd, J = 11.1, 7.3 Hz, 1H), 5.32 (d, J = 16.8 Hz, 1H), 5.23 (d, J = 10.3 Hz, 1H), 4.46 (dd, J = 7.9, 5.4 Hz, 1H), 4.17 (br s, 1H), 2.75 (ddd, J = 7.3, 5.4, 1.6 Hz, 1H), 2.71–2.65 (m, 1H) ppm.

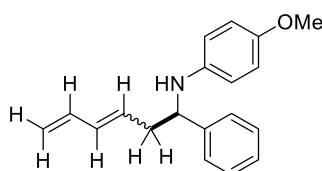
(*E*)-8da: ^{13}C NMR (125 MHz, CDCl_3): δ = 147.3, 143.5, 136.6, 134.3, 130.2, 129.1 (2C), 128.6 (2C), 127.0, 126.3 (2C), 117.4, 116.4, 113.5 (2C), 57.5, 42.1 ppm.

(*Z*)-8da: ^{13}C NMR (125 MHz, CDCl_3): δ = 147.3, 143.4, 132.4, 131.7, 129.1 (2C), 128.6 (2C), 127.6, 127.1, 126.3 (2C), 118.7, 117.4, 113.5 (2C), 57.8, 36.9 ppm.

IR (neat): ν = 3408, 3024, 2904, 1598, 1502, 1313, 1234, 1002, 749, 696 cm^{-1} .

HRMS (EI): calculated for $\text{C}_{18}\text{H}_{19}\text{NO}^+ = [\text{M}^+]$; m/z = 249.1512, found: m/z = 249.1500.

(*E/Z*)-*N*-(1-Phenylhexa-3,5-dienyl)-4-methoxyaniline (8db**)**



8db

Compound **8db** was prepared according to *GP-III* from 1,4-pentadiene (**1d**; 15.0 mg, 0.22 mmol, 1.10 equiv) and imine **7b** (42.2 mg, 0.20 mmol), using $\text{NaN}(\text{SiMe}_3)_2$ (3.7 mg, 0.02 mmol, 10 mol%) as the catalyst, in dioxane (300 μL) at 25 °C for 20 h. **8db** was purified by PTLC on silica gel (EtOAc/PE = 1:9; *eluted once*).

Yellow liquid.

Yield: 55.2 mg (99%; *E:Z* = 3:1).

(*E*)-8db: ^1H NMR (500 MHz, CDCl_3): δ = 7.43–7.34 (m, 4H), 7.30–7.25 (m, 1H), 6.72 (d, J = 9.0 Hz, 2H), 6.50 (d, J = 9.0 Hz, 2H), 6.35 (dt, J = 17.0, 10.4 Hz, 1H), 6.22 (dd, J = 15.0, 10.4 Hz, 1H), 5.68 (ddd, J = 15.0, 7.3, 7.3 Hz, 1H), 5.21 (d, J = 17.0 Hz, 1H), 5.08 (d, J = 10.4 Hz, 1H), 4.37 (dd, J = 8.3, 5.2 Hz, 1H), 3.94 (br s, 1H), 3.73 (s, 3H), 2.67 (dd, J = 7.3, 5.2 Hz, 1H), 2.56 (dd, J = 8.3, 7.3 Hz, 1H) ppm.

(*Z*)-8db: ^1H NMR (500 MHz, CDCl_3): δ = 7.43–7.34 (m, 4H), 7.30–7.25 (m, 1H), 6.72 (d, J = 9.0 Hz, 2H), 6.67 (dddd, J = 16.8, 11.1, 10.1, 0.9 Hz, 1H), 6.50 (d, J = 9.0 Hz, 2H), 6.26–6.20 (m, 1H), 5.48 (dt, J = 11.3, 7.4 Hz, 1H), 5.31 (d, J = 16.8 Hz, 1H), 5.21 (d, J = 10.1 Hz, 1H), 4.37 (dd, J = 8.0, 5.4 Hz, 1H), 3.94 (br s, 1H), 3.73 (s, 3H), 2.73 (dd, J = 7.4, 5.4 Hz, 1H), 2.60–2.52 (m, 1H) ppm.

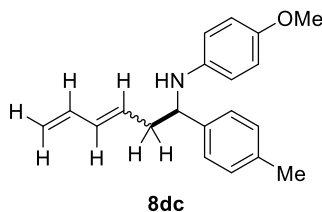
(*E*)-8db: ^{13}C NMR (125 MHz, CDCl_3): δ = 152.0, 143.7, 141.5, 136.7, 134.2, 130.4, 128.6(2C), 127.0, 126.4 (2C), 116.4, 114.8 (4C), 58.4, 55.8, 42.2 ppm.

(Z)-8db: ^{13}C NMR (125 MHz, CDCl_3): δ = 152.0, 143.6, 141.6, 132.3, 131.7, 128.6 (2C), 127.8, 127.0, 126.4 (2C), 118.6, 114.8 (4C), 58.6, 55.8, 37.0 ppm.

IR (neat): ν = 3390, 3082, 2999, 2829, 1502, 1234, 1035, 1002, 902, 817, 752, 700 cm^{-1} .

HRMS (EI): calculated for $\text{C}_{19}\text{H}_{21}\text{NO}^+ = [\text{M}^+]$; m/z = 279.1618, found: m/z = 279.1610.

(E/Z)-N-[1-(4-Methyl)phenylhexa-3,5-dienyl]-4-methoxyaniline (8dc)



Compound **8dc** was prepared according to *GP-III* from 1,4-pentadiene (**1d**; 15.0 mg, 0.22 mmol, 1.10 equiv) and imine **7c** (45.1 mg, 0.20 mmol), using $\text{NaN}(\text{SiMe}_3)_2$ (3.7 mg, 0.02 mmol, 10 mol%) as the catalyst, in dioxane (300 μL) at 25 $^\circ\text{C}$ for 20 h. **8dc** was purified by PTLC on silica gel (EtOAc/PE = 1:9; *eluted once*).

Yellow liquid.

Yield: 52.7 mg (90%; $E:Z$ = 4:1).

(E)-8dc: ^1H NMR (500 MHz, CDCl_3): δ = 7.24 (d, J = 7.9 Hz, 2H), 7.13 (d, J = 7.9 Hz, 2H), 6.68 (d, J = 9.0 Hz, 2H), 6.46 (d, J = 9.0 Hz, 2H), 6.30 (dt, J = 16.8, 10.1 Hz, 1H), 6.18 (dd, J = 15.1, 10.5 Hz, 1H), 5.64 (dt, J = 15.1, 7.3 Hz, 1H), 5.16 (d, J = 16.8 Hz, 1H), 5.03 (d, J = 10.1 Hz, 1H), 4.29 (dd, J = 7.9, 5.3 Hz, 1H), 3.86 (br s, 1H), 3.69 (s, 3H), 2.70–2.45 (m, 2H), 2.33 (s, 3H) ppm.

(Z)-8dc: ^1H NMR (500 MHz, CDCl_3): δ = 7.24 (d, J = 7.9 Hz, 2H), 7.13 (d, J = 7.9 Hz, 2H), 6.68 (d, J = 9.0 Hz, 2H), 6.66–6.59 (m, 1H), 6.46 (d, J = 9.0 Hz, 2H), 6.15 (dd, J = 10.1, 10.1 Hz, 1H), 5.47–5.41 (m, 1H), 5.26 (d, J = 16.8 Hz, 1H), 5.17 (d, J = 10.1 Hz, 1H), 4.29 (dd, J = 7.9, 5.3 Hz, 1H), 3.86 (br s, 1H), 3.69 (s, 3H), 2.70–2.45 (m, 2H), 2.33 (s, 3H) ppm.

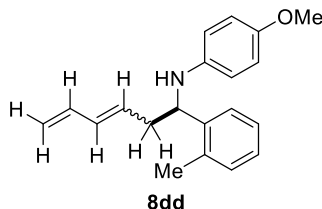
(E)-8dc: ^{13}C NMR (125 MHz, CDCl_3): δ = 152.0, 141.6, 140.7, 136.7, 136.5, 134.1, 130.6, 129.3 (2C), 126.2 (2C), 116.2, 114.7 (4C), 58.0, 55.8, 42.2, 21.8 ppm.

(Z)-8dc: ^{13}C NMR (125 MHz, CDCl_3): δ = 152.0, 141.7, 140.6, 136.7, 136.5, 132.2, 131.8, 128.0 (2C), 126.2 (2C), 118.5, 114.7 (4C), 58.3, 37.0, 32.9, 21.8 ppm.

IR (neat): ν = 3381, 2931, 2831, 1501, 1234, 1035, 1002, 902, 817, 698 cm^{-1} .

HRMS (EI): calculated for $\text{C}_{20}\text{H}_{23}\text{NO}^+ = [\text{M}^+]$; m/z = 293.1774, found: m/z = 293.1786.

(E/Z)-N-[1-(2-Methyl)phenylhexa-3,5-dienyl]-4-methoxyaniline (8dd)



Compound **8dd** was prepared according to *GP-III* from 1,4-pentadiene (**1d**; 15.0 mg, 0.22 mmol, 1.10 equiv) and imine **7d** (45.1 mg, 0.20 mmol), using $\text{NaN}(\text{SiMe}_3)_2$ (3.7 mg, 0.02 mmol, 10 mol%) as the catalyst, in dioxane (300 μL) at 25 $^\circ\text{C}$ for 20 h. **8dd** was purified by PTLC on silica gel (EtOAc/PE = 1:9; *eluted once*).

Yellow liquid.

Yield: 55.1 mg (94%; $E:Z$ = 4:1).

(E)-8dd: ^1H NMR (500 MHz, CDCl_3): δ = 7.48–7.44 (m, 1H), 7.23–7.17 (m, 3H), 6.72 (d, J = 9.0 Hz, 2H), 6.43 (d, J = 9.0 Hz, 2H), 6.36 (dt, J = 16.8, 10.3 Hz, 1H), 6.25 (dd, J = 14.9, 10.3 Hz, 1H), 5.72 (dt, J = 14.9, 7.3 Hz,

1H), 5.22 (d, $J = 16.8$ Hz, 1H), 5.09 (d, $J = 10.3$ Hz, 1H), 4.57 (dd, $J = 8.2, 4.7$ Hz, 1H), 3.92 (br s, 1H), 3.72 (s, 3H), 2.66–2.60 (m, 1H), 2.50–2.46 (m, 1H), 2.48 (s, 3H) ppm.

(Z)-8dd: $^1\text{H NMR}$ (500 MHz, CDCl_3): $\delta = 7.48\text{--}7.44$ (m, 1H), 7.23–7.17 (m, 3H), 6.72 (d, $J = 9.0$ Hz, 2H), 6.71–6.66 (m, 1H), 6.43 (d, $J = 9.0$ Hz, 2H), 6.25 (dd, $J = 10.3, 10.2$ Hz, 1H), 5.51 (dt, $J = 10.2, 7.3$ Hz, 1H), 5.32 (d, $J = 16.8$ Hz, 1H), 5.22 (d, $J = 10.2$ Hz, 1H), 4.57 (dd, $J = 8.2, 4.7$ Hz, 1H), 3.92 (br s, 1H), 3.72 (s, 3H), 2.67–2.64 (m, 1H), 2.63–2.60 (m, 1H), 2.47 (s, 3H) ppm.

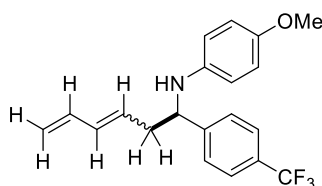
(E)-8dd: $^{13}\text{C NMR}$ (125 MHz, CDCl_3): $\delta = 152.0, 141.6, 141.3, 136.7, 134.6, 134.1, 130.7, 130.6, 126.7, 126.5, 125.5, 116.4, 114.8$ (2C), 114.5 (2C), 55.8, 54.6, 40.2, 19.2 ppm.

(Z)-8dd: $^{13}\text{C NMR}$ (125 MHz, CDCl_3): $\delta = 152.0, 141.6, 141.2, 134.7, 132.3, 131.7, 130.7, 130.6, 128.0, 126.8, 125.5, 118.6, 114.8$ (2C), 114.5 (2C), 55.8, 54.8, 35.2, 19.2 ppm.

IR (neat): $\nu = 3398, 2929, 2831, 1504, 1234, 1035, 1002, 815, 752, 725$ cm^{-1} .

HRMS (EI): calculated for $\text{C}_{20}\text{H}_{23}\text{NO}^+ = [\text{M}^+]$: $m/z = 293.1774$, found: $m/z = 293.1762$.

(E/Z)-N-[1-(4-Trifluoromethyl)phenylhexa-3,5-dienyl]-4-methoxyaniline (8de**)**



8de

Compound **8de** was prepared according to *GP-III* from 1,4-pentadiene (**1d**; 15.0 mg, 0.22 mmol, 1.10 equiv) and imine **7e** (55.9 mg, 0.20 mmol), using $\text{NaN}(\text{SiMe}_3)_2$ (3.7 mg, 0.02 mmol, 10 mol%) as the catalyst, in dioxane (300 μL) at 25 $^\circ\text{C}$ for 20 h. **8de** was purified by PTLC on silica gel (EtOAc/PE = 1:9; *eluted once*).

Yellow liquid.

Yield: 67.3 mg (97%; $E:Z = 3:1$).

(E)-8de: $^1\text{H NMR}$ (500 MHz, CDCl_3): $\delta = 7.62$ (d, $J = 8.1$ Hz, 2H), 7.52 (d, $J = 8.1$ Hz, 2H), 6.72 (d, $J = 9.0$ Hz, 2H), 6.45 (d, $J = 9.0$ Hz, 2H), 6.34 (ddd, $J = 16.8, 10.3, 9.8$ Hz, 1H), 6.22 (dd, $J = 15.8, 9.8$ Hz, 1H), 5.64 (dt, $J = 15.8, 7.3$ Hz, 1H), 5.22 (d, $J = 16.8$ Hz, 1H), 5.10 (d, $J = 10.3$ Hz, 1H), 4.41 (dd, $J = 7.8, 5.8$ Hz, 1H), 3.93 (br s, 1H), 3.72 (s, 3H), 2.66 (ddd, $J = 15.6, 7.3, 5.8$ Hz, 1H), 2.53 (ddd, $J = 15.6, 7.8, 7.3$ Hz, 1H) ppm.

(Z)-8de: $^1\text{H NMR}$ (500 MHz, CDCl_3): $\delta = 7.62$ (d, $J = 8.1$ Hz, 2H), 7.52 (d, $J = 8.1$ Hz, 2H), 6.72 (d, $J = 9.0$ Hz, 2H), 6.62 (dddd, $J = 16.8, 11.1, 10.2, 1.1$ Hz, 1H), 6.45 (d, $J = 9.0$ Hz, 2H), 6.22 (dd, $J = 11.2, 11.1$ Hz, 1H), 5.44 (dt, $J = 11.2, 7.3$ Hz, 1H), 5.32 (d, $J = 16.8$ Hz, 1H), 5.22 (d, $J = 10.2$ Hz, 1H), 4.41 (dd, $J = 7.8, 5.1$ Hz, 1H), 3.93 (br s, 1H), 3.72 (s, 3H), 2.73–2.69 (m, 2H) ppm.

(E)-8de: $^{13}\text{C NMR}$ (125 MHz, CDCl_3): $\delta = 152.3, 148.0, 141.0, 136.4, 134.8, 129.5, 129.4$ (q, $J = 32.5$ Hz, 2C), 126.8, 125.6 (q, $J = 3.7$ Hz, 2C), 124.2 (q, $J = 271.9$ Hz), 116.8, 114.8 (2C), 114.7 (2C), 58.0, 55.7, 42.0 ppm.

(Z)-8de: $^{13}\text{C NMR}$ (125 MHz, CDCl_3): $\delta = 152.3, 147.9, 141.1, 132.9, 131.4, 129.5$ (q, $J = 32.5$ Hz, 2C), 126.8, 126.7, 125.6 (q, $J = 3.7$ Hz, 2C), 124.2 (q, $J = 271.9$ Hz), 119.1, 114.8 (2C), 114.7 (2C), 58.3, 53.4, 36.8 ppm.

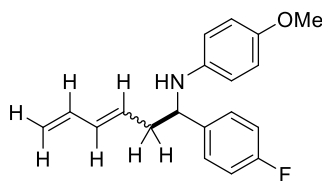
(E)-8de: $^{19}\text{F NMR}$ (471 MHz, CDCl_3): $\delta = -62.3$ (s, 3F) ppm.

(Z)-8de: $^{19}\text{F NMR}$ (471 MHz, CDCl_3): $\delta = -62.4$ (s, 3F) ppm.

IR (neat): $\nu = 3388, 3082, 2904, 2360, 1616, 1502, 1330, 1236, 1004, 817, 754, 607$ cm^{-1} .

HRMS (EI): calculated for $\text{C}_{20}\text{H}_{20}\text{F}_3\text{NO}^+ = [\text{M}^+]$: $m/z = 347.1492$, found: $m/z = 347.1498$.

(*E/Z*)-*N*-[1-(4-Fluoro)phenyl]hexa-3,5-dienyl]-4-methoxyaniline (8df**)**



8df

Compound **8df** was prepared according to *GP-III* from 1,4-pentadiene (**1d**; 15.0 mg, 0.22 mmol, 1.10 equiv) and imine **7f** (45.9 mg, 0.20 mmol), using $\text{NaN}(\text{SiMe}_3)_2$ (3.7 mg, 0.02 mmol, 10 mol%) as the catalyst, in dioxane (300 μL) at 25 °C for 20 h. **8df** was purified by PTLC on silica gel (EtOAc/PE = 1:9; *eluted once*).

Yellow liquid.

Yield: 58.3 mg (98%; *E:Z* = 3:1).

(*E*)-8df: ^1H NMR (500 MHz, CDCl_3): δ = 7.39–7.31 (m, 2H), 7.04 (d, J = 8.7 Hz, 2H), 6.72 (d, J = 9.0 Hz, 2H), 6.47 (d, J = 9.0 Hz, 2H), 6.34 (dt, J = 16.9, 10.3 Hz, 1H), 6.20 (dd, J = 15.1, 10.3 Hz, 1H), 5.65 (dt, J = 15.1, 7.3 Hz, 1H), 5.20 (d, J = 16.9 Hz, 1H), 5.08 (d, J = 10.3 Hz, 1H), 4.34 (dd, J = 8.0, 5.4 Hz, 1H), 3.92 (br s, 1H), 3.72 (s, 3H), 2.62 (ddd, J = 14.4, 7.3, 5.4 Hz, 1H), 2.52 (dddd, J = 14.4, 8.0, 7.3, 1.3 Hz, 1H) ppm.

(*Z*)-8df: ^1H NMR (500 MHz, CDCl_3): δ = 7.39–7.31 (m, 2H), 7.04 (d, J = 8.7 Hz, 2H), 6.72 (d, J = 9.0 Hz, 2H), 6.64 (dddd, J = 16.8, 11.2, 10.2, 1.1 Hz, 1H), 6.47 (d, J = 9.0 Hz, 2H), 6.20 (dd, J = 11.2, 10.6 Hz, 1H), 5.45 (dt, J = 10.6, 8.1 Hz, 1H), 5.28 (d, J = 16.8 Hz, 1H), 5.21 (d, J = 10.2 Hz, 1H), 4.34 (dd, J = 8.0, 5.4 Hz, 1H), 3.92 (br s, 1H), 3.72 (s, 3H), 2.71–2.65 (m, 2H) ppm.

(*E*)-8df: ^{13}C NMR (125 MHz, CDCl_3): δ = 161.8 (d, J = 244.7 Hz), 152.2, 141.3, 139.4 (d, J = 3.0 Hz), 136.6, 134.4, 130.0, 127.8 (d, J = 7.9 Hz, 2C), 116.5, 115.4 (d, J = 21.4 Hz, 2C), 114.8 (2C), 114.8 (2C), 57.7, 55.7, 42.2 ppm.

(*Z*)-8df: ^{13}C NMR (125 MHz, CDCl_3): δ = 161.9 (d, J = 244.7 Hz), 152.2, 141.3, 139.3 (d, J = 3.0 Hz), 132.5, 131.6, 127.9 (d, J = 7.9 Hz, 2C), 127.4, 118.8, 115.4 (d, J = 21.4 Hz, 2C), 114.8 (2C), 114.8 (2C), 58.0, 55.7, 37.1 ppm.

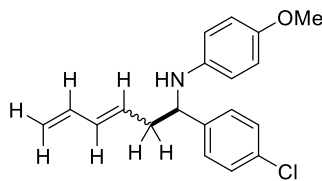
(*E*)-8df: ^{19}F NMR (471 MHz, CDCl_3): δ = -116.1 – -116.2 (m, 1F) ppm.

(*Z*)-8df: ^{19}F NMR (471 MHz, CDCl_3): δ = -115.9 – -116.1 (m, 1F) ppm.

IR (neat): ν = 3400, 3082, 2904, 2831, 1602, 1502, 1236, 1037, 1004, 902, 817, 754 cm^{-1} .

HRMS (EI): calculated for $\text{C}_{19}\text{H}_{20}\text{FNO}^+ = [\text{M}^+]$: m/z = 297.1523, found: m/z = 297.1509.

(*E/Z*)-*N*-[1-(4-Chloro)phenyl]hexa-3,5-dienyl]-4-methoxyaniline (8dg**)**



8dg

Compound **8dg** was prepared according to *GP-III* from 1,4-pentadiene (**1d**; 15.0 mg, 0.22 mmol, 1.10 equiv) and imine **7g** (49.1 mg, 0.20 mmol), using $\text{NaN}(\text{SiMe}_3)_2$ (3.7 mg, 0.02 mmol, 10 mol%) as the catalyst, in dioxane (300 μL) at 25 °C for 20 h. **8dg** was purified by PTLC on silica gel (EtOAc/PE = 1:9; *eluted once*).

Yellow liquid.

Yield: 50.2 mg (80%; *E:Z* = 3:1).

(*E*)-8dg: ^1H NMR (500 MHz, CDCl_3): δ = 7.35–7.30 (m, 4H), 6.71 (d, J = 9.0 Hz, 2H), 6.45 (d, J = 9.0 Hz, 2H), 6.33 (dt, J = 16.8, 10.3 Hz, 1H), 6.20 (dd, J = 15.2, 10.3 Hz, 1H), 5.63 (dt, J = 15.2, 7.3 Hz, 1H), 5.20 (d, J = 16.8 Hz, 1H), 5.08 (d, J = 10.3 Hz, 1H), 4.32 (dd, J = 8.0, 5.2 Hz, 1H), 3.89 (br s, 1H), 3.72 (s, 3H), 2.61 (ddd, J = 15.5, 7.3, 5.2 Hz, 1H), 2.50 (ddd, J = 15.5, 8.0, 7.3 Hz, 1H) ppm.

(Z)-8dg: ^1H NMR (500 MHz, CDCl_3): δ = 7.35–7.30 (m, 4H), 6.71 (d, J = 9.0 Hz, 2H), 6.63 (dddd, J = 16.8, 11.2, 10.2, 1.1 Hz, 1H), 6.45 (d, J = 9.0 Hz, 2H), 6.20 (dd, J = 11.2, 10.7 Hz, 1H), 5.43 (dt, J = 10.7, 7.6 Hz, 1H), 5.30 (d, J = 16.8 Hz, 1H), 5.21 (d, J = 10.2 Hz, 1H), 4.32 (dd, J = 8.0, 5.2 Hz, 1H), 3.89 (br s, 1H), 3.72 (s, 3H), 2.70–2.65 (m, 1H), 2.63–2.59 (m, 1H) ppm.

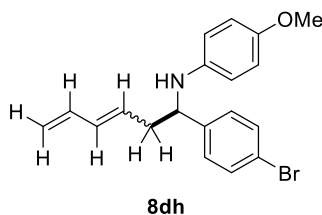
(E)-8dg: ^{13}C NMR (125 MHz, CDCl_3): δ = 152.2, 142.3, 141.2, 136.5, 134.5, 132.6, 129.8, 128.7 (2C), 127.7 (2C), 116.6, 114.8 (4C), 57.8, 55.7, 42.1 ppm.

(Z)-8dg: ^{13}C NMR (125 MHz, CDCl_3): δ = 152.2, 142.2, 141.2, 132.6, 131.5, 128.7 (2C), 127.8, 127.7 (2C), 127.2, 118.9, 114.7 (4C), 58.1, 55.7, 36.9 ppm.

IR (neat): ν = 3394, 3082, 2881, 1502, 1236, 1037, 1004, 817, 756 cm^{-1} .

HRMS (EI): calculated for $\text{C}_{19}\text{H}_{20}\text{ClNO}^+ = [\text{M}^+]$: m/z = 313.1228, found: m/z = 313.1231.

(E/Z)-N-[1-(4-Bromo)phenylhexa-3,5-dienyl]-4-methoxyaniline (8dh)



Compound **8dh** was prepared according to *GP-III* from 1,4-pentadiene (**1d**; 15.0 mg, 0.22 mmol, 1.10 equiv) and imine **7h** (58.0 mg, 0.20 mmol), using $\text{NaN}(\text{SiMe}_3)_2$ (3.7 mg, 0.02 mmol, 10 mol%) as the catalyst, in dioxane (300 μL) at 25 $^\circ\text{C}$ for 20 h. **8dh** was purified by PTLC on silica gel (EtOAc/PE = 1:9; *eluted once*).

Yellow liquid.

Yield: 70.6 mg (99%; $E:Z$ = 3:1).

(E)-8dh: ^1H NMR (500 MHz, CDCl_3): δ = 7.47 (d, J = 8.4 Hz, 2H), 7.27 (d, J = 8.4 Hz, 2H), 6.72 (d, J = 8.9 Hz, 2H), 6.46 (d, J = 8.9 Hz, 2H), 6.34 (dt, J = 16.9, 10.3 Hz, 1H), 6.21 (dd, J = 15.2, 10.3 Hz, 1H), 5.64 (dt, J = 15.2, 7.3 Hz, 1H), 5.21 (d, J = 16.9 Hz, 1H), 5.09 (d, J = 10.3 Hz, 1H), 4.31 (dd, J = 7.9, 5.2 Hz, 1H), 3.87 (brs, 1H), 3.72 (s, 3H), 2.62 (ddd, J = 14.9, 7.3, 5.2 Hz, 1H), 2.51 (ddd, J = 14.9, 7.9, 7.3 Hz, 1H) ppm.

(Z)-8dh: ^1H NMR (500 MHz, CDCl_3): δ = 7.47 (d, J = 8.4 Hz, 2H), 7.27 (d, J = 8.4 Hz, 2H), 6.72 (d, J = 8.9 Hz, 2H), 6.63 (dddd, J = 16.9, 11.2, 10.1, 1.2 Hz, 1H), 6.46 (d, J = 8.9 Hz, 2H), 6.21 (dd, J = 11.2, 10.7 Hz, 1H), 5.44 (dt, J = 10.7, 8.3 Hz, 1H), 5.30 (d, J = 16.8 Hz, 1H), 5.22 (d, J = 10.1 Hz, 1H), 4.31 (dd, J = 7.9, 5.2 Hz, 1H), 3.87 (brs, 1H), 3.72 (s, 3H), 2.71–2.66 (m, 1H), 2.64–2.60 (m, 1H) ppm.

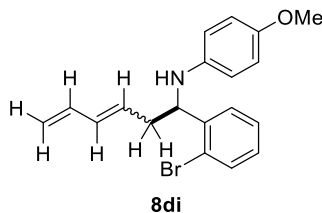
(E)-8dh: ^{13}C NMR (125 MHz, CDCl_3): δ = 152.2, 142.8, 141.1, 136.5, 134.6, 131.7 (2C), 129.8, 128.2 (2C), 120.7, 116.7, 114.8 (4C), 57.8, 55.7, 42.0 ppm.

(Z)-8dh: ^{13}C NMR (125 MHz, CDCl_3): δ = 152.2, 142.7, 141.2, 132.6, 131.7 (2C), 131.5, 128.2 (2C), 127.2, 120.7, 118.9, 114.8 (4C), 58.2, 55.7, 36.9 ppm.

IR (neat): ν = 3388, 3082, 2899, 2360, 1502, 1234, 1029, 1006, 902, 817, 756 cm^{-1} .

HRMS (EI): calculated for $\text{C}_{19}\text{H}_{20}^{79}\text{BrNO}^+ = [\text{M}^+]$: m/z = 357.0723, found: m/z = 357.0727.

(E/Z)-N-[1-(2-Bromo)phenylhexa-3,5-dienyl]-4-methoxyaniline (8di)



Compound **8di** was prepared according to *GP-III* from 1,4-pentadiene (**1d**; 15.0 mg, 0.22 mmol, 1.10 equiv) and imine **7i** (58.0 mg, 0.20 mmol), using $\text{NaN}(\text{SiMe}_3)_2$ (3.7 mg, 0.02 mmol, 10 mol%) as the catalyst, in dioxane (300 μL) at 25 °C for 20 h. **8di** was purified by PTLC on silica gel (EtOAc/PE = 1:9; *eluted once*).

Yellow liquid.

Yield: 65.7 mg (92%; *E:Z* = 3:1).

(E)-8di: ^1H NMR (500 MHz, CDCl_3): δ = 7.60 (dd, J = 7.8, 1.2 Hz, 1H), 7.47 (dd, J = 7.8, 1.7 Hz, 1H), 7.27 (ddd, J = 7.8, 7.8, 1.2 Hz, 1H), 7.13 (ddd, J = 7.8, 7.8, 1.7 Hz, 1H), 6.72 (d, J = 8.9 Hz, 2H), 6.43 (d, J = 8.9 Hz, 2H), 6.37 (ddd, J = 17.9, 10.8, 10.5 Hz, 1H), 6.25 (dd, J = 15.0, 10.5 Hz, 1H), 5.73 (dt, J = 15.0, 7.3 Hz, 1H), 5.22 (d, J = 17.9 Hz, 1H), 5.09 (d, J = 10.8 Hz, 1H), 4.78 (dd, J = 8.6, 4.3 Hz, 1H), 4.02 (br s, 1H), 3.71 (s, 3H), 2.75 (ddd, J = 14.6, 7.3, 4.3 Hz, 1H), 2.43 (ddd, J = 14.6, 8.6, 7.3 Hz, 1H) ppm.

(Z)-8di: ^1H NMR (500 MHz, CDCl_3): δ = 7.60 (dd, J = 7.8, 1.2 Hz, 1H), 7.47 (dd, J = 7.8, 1.7 Hz, 1H), 7.27 (ddd, J = 7.8, 7.8, 1.2 Hz, 1H), 7.13 (ddd, J = 7.8, 7.8, 1.7 Hz, 1H), 6.75–6.65 (m, 1H), 6.72 (d, J = 8.9 Hz, 2H), 6.43 (d, J = 8.9 Hz, 2H), 6.28–6.21 (m, 1H), 5.53 (dt, J = 11.1, 7.6 Hz, 1H), 5.32 (dd, J = 16.8, 1.5 Hz, 1H), 5.22 (d, J = 10.5 Hz, 1H), 4.78 (dd, J = 8.6, 4.3 Hz, 1H), 4.02 (br s, 1H), 3.71 (s, 3H), 2.82 (ddd, J = 7.6, 4.3, 1.5 Hz, 1H), 2.65–2.57 (m, 1H) ppm.

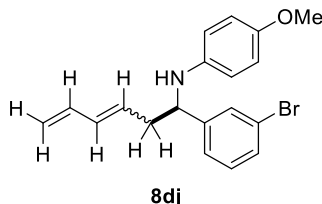
(E)-8di: ^{13}C NMR (125 MHz, CDCl_3): δ = 152.1, 141.9, 141.0, 136.6, 134.4, 133.0, 130.1, 128.5, 127.8 (2C), 123.0, 116.5, 114.8 (2C), 114.5 (2C), 57.0, 55.7, 39.8 ppm.

(Z)-8di: ^{13}C NMR (125 MHz, CDCl_3): δ = 152.1, 141.8, 141.0, 133.0, 132.7, 131.7, 128.6, 127.9 (2C), 127.4, 123.0, 118.8, 114.8 (2C), 114.5 (2C), 57.4, 55.7, 34.7 ppm

IR (neat): ν = 3394, 2930, 2829, 1501, 1236, 1037, 1002, 902, 817, 752 cm^{-1} .

HRMS (EI): calculated for $\text{C}_{19}\text{H}_{20}^{79}\text{BrNO}^+ = [\text{M}^+]$: m/z = 357.0723, found: m/z = 357.0727.

(E/Z)-N-[1-(3-Bromo)phenylhexa-3,5-dienyl]-4-methoxyaniline (8dj**)**



Compound **8dj** was prepared according to *GP-III* from 1,4-pentadiene (**1d**; 15.0 mg, 0.22 mmol, 1.10 equiv) and imine **7j** (58.0 mg, 0.20 mmol), using $\text{NaN}(\text{SiMe}_3)_2$ (3.7 mg, 0.02 mmol, 10 mol%) as the catalyst, in dioxane (300 μL) at 25 °C for 20 h. **8dj** was purified by PTLC on silica gel (EtOAc/PE = 1:9; *eluted once*).

Yellow liquid.

Yield: 67.8 mg (95%; *E:Z* = 3:1).

(E)-8dj: ^1H NMR (500 MHz, CDCl_3): δ = 7.61–7.49 (m, 1H), 7.45–7.39 (m, 1H), 7.35–7.31 (m, 1H), 7.26–7.22 (m, 1H), 6.73 (d, J = 9.0 Hz, 2H), 6.47 (d, J = 9.0 Hz, 2H), 6.35 (dt, J = 16.9, 10.3 Hz, 1H), 6.21 (dd, J = 15.3, 10.3 Hz, 1H), 5.64 (dt, J = 15.3, 7.3 Hz, 1H), 5.21 (d, J = 16.9 Hz, 1H), 5.10 (d, J = 10.3 Hz, 1H), 4.30 (dd, J = 8.1, 5.0 Hz, 1H), 3.90 (br s, 1H), 3.73 (s, 3H), 2.63 (ddd, J = 13.1, 7.3, 5.0 Hz, 1H), 2.51 (ddd, J = 13.1, 8.1, 7.3 Hz, 1H) ppm.

(Z)-8dj: ^1H NMR (500 MHz, CDCl_3): 7.61–7.49 (m, 1H), 7.45–7.39 (m, 1H), 7.35–7.31 (m, 1H), 7.26–7.22 (m, 1H), 6.73 (d, J = 9.0 Hz, 2H), 6.64 (dddd, J = 16.8, 11.2, 10.2, 1.1 Hz, 1H), 6.47 (d, J = 9.0 Hz, 2H), 6.21 (dd, J = 11.2, 10.3 Hz, 1H), 5.46 (dt, J = 10.3, 7.3 Hz, 1H), 5.32 (dd, J = 16.8, 1.7 Hz, 1H), 5.21 (d, J = 10.2 Hz, 1H), 4.30 (dd, J = 8.1, 5.0 Hz, 1H), 3.90 (br s, 1H), 3.73 (s, 3H), 2.70–2.66 (m, 2H) ppm.

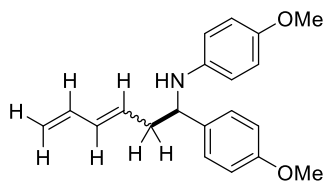
(E)-8dj: ^{13}C NMR (125 MHz, CDCl_3): δ = 152.3, 146.5, 141.2, 136.5, 134.6, 130.2, 130.1, 129.7, 129.4, 125.0, 122.8, 116.7, 114.8 (2C), 114.7 (2C), 58.0, 55.8, 42.1 ppm.

(Z)-8dj: ^{13}C NMR (125 MHz, CDCl_3): δ = 152.3, 146.4, 141.2, 132.7, 131.5, 130.2, 130.2, 129.4, 127.1, 125.1, 122.9, 119.0, 114.8 (2C), 114.7 (2C), 58.3, 55.8, 37.0 ppm.

IR (neat): ν = 3392, 3082, 2899, 2360, 1502, 1234, 1028, 1002, 902, 817, 781, 696 cm^{-1} .

HRMS (EI): calculated for $\text{C}_{19}\text{H}_{20}^{79}\text{BrNO}^+ = [\text{M}^+]$: m/z = 357.0723, found: m/z = 357.0729.

(*E/Z*)-*N*-[1-(4-Methoxy)phenylhexa-3,5-dienyl]-4-methoxyaniline (8dl**)**



8dl

Compound **8dl** was prepared according to *GP-III* from 1,4-pentadiene (**1d**; 15.0 mg, 0.22 mmol, 1.10 equiv) and imine **7l** (48.3 mg, 0.20 mmol), using $\text{NaN}(\text{SiMe}_3)_2$ (3.7 mg, 0.02 mmol, 10 mol%) as the catalyst, in dioxane (300 μL) at 25 °C for 20 h. **8dl** was purified by PTLC on silica gel (EtOAc/PE = 1:9; *eluted once*).

Yellow liquid.

Yield: 48.8 mg (79%; *E:Z* = 4:1).

(*E*)-8dl: ^1H NMR (500 MHz, CDCl_3): δ = 7.29 (d, J = 8.6 Hz, 2H), 6.89 (d, J = 8.6 Hz, 2H), 6.71 (d, J = 8.9 Hz, 2H), 6.49 (d, J = 8.9 Hz, 2H), 6.33 (dt, J = 16.9, 10.3 Hz, 1H), 6.20 (dd, J = 15.2, 10.3 Hz, 1H), 5.66 (ddd, J = 15.2, 7.3, 7.3 Hz, 1H), 5.19 (d, J = 16.9 Hz, 1H), 5.06 (d, J = 10.3 Hz, 1H), 4.30 (dd, J = 7.8, 5.4 Hz, 1H), 3.92 (br s, 1H), 3.82 (s, 3H), 3.72 (s, 3H), 2.62 (ddd, J = 12.3, 7.3, 5.4 Hz, 1H), 2.52 (ddd, J = 12.3, 7.8, 7.3 Hz, 1H) ppm.

(*Z*)-8dl: ^1H NMR (500 MHz, CDCl_3): δ = 7.29 (d, J = 8.6 Hz, 2H), 6.89 (d, J = 8.6 Hz, 2H), 6.71 (d, J = 8.9 Hz, 2H), 6.65 (ddd, J = 16.8, 11.2, 10.2 Hz, 1H), 6.49 (d, J = 8.9 Hz, 2H), 6.20 (dd, J = 11.2, 10.3 Hz, 1H), 5.46 (dt, J = 10.3, 7.3 Hz, 1H), 5.29 (d, J = 16.8 Hz, 1H), 5.19 (d, 10.2 Hz, 1H), 4.30 (dd, J = 7.8, 5.4 Hz, 1H), 3.92 (br s, 1H), 3.82 (s, 3H), 3.72 (s, 3H), 2.75–2.65 (m, 2H) ppm.

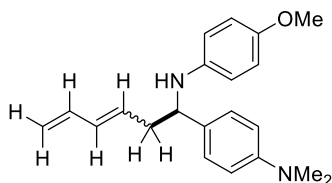
(*E*)-8dl: ^{13}C NMR (125 MHz, CDCl_3): δ = 158.6, 152.0, 141.6, 136.7, 135.7, 134.1, 130.5, 127.4 (2C), 116.2, 114.8 (2C), 114.7 (2C), 114.0 (2C), 57.8, 55.8, 55.2, 42.2 ppm.

(*Z*)-8dl: ^{13}C NMR (125 MHz, CDCl_3): δ = 158.6, 152.0, 141.6, 135.6, 132.2, 131.8, 127.9, 127.4 (2C), 118.5, 114.8 (2C), 114.7 (2C), 114.0 (2C), 58.1, 55.8, 55.2, 37.0 ppm.

IR (neat): ν = 3390, 3082, 2931, 2833, 1610, 1502, 1236, 1029, 817, 750 cm^{-1} .

HRMS (EI): calculated for $\text{C}_{20}\text{H}_{23}\text{NO}_2^+ = [\text{M}^+]$: m/z = 309.1723, found: m/z = 309.1726.

(*E/Z*)-*N*-[1-(4-*N,N*-Dimethylamino)phenylhexa-3,5-dienyl]-4-methoxyaniline (8dm**)**



8dm

Compound **8dm** was prepared according to *GP-III* from 1,4-pentadiene (**1d**; 15.0 mg, 0.22 mmol, 1.10 equiv) and imine **7m** (50.9 mg, 0.20 mmol), using $\text{NaN}(\text{SiMe}_3)_2$ (3.7 mg, 0.02 mmol, 10 mol%) as the catalyst, in dioxane (300 μL) at 25 °C for 20 h. **8dm** was purified by PTLC on silica gel (EtOAc/PE = 1:9; *eluted once*).

Yellow liquid.

Yield: 45.1 mg (70%; *E:Z* = 4:1).

(*E*)-8dm: ^1H NMR (500 MHz, CDCl_3): δ = 7.21 (d, J = 8.7 Hz, 2H), 6.71 (d, J = 8.7 Hz, 2H), 6.68 (d, J = 8.9 Hz, 2H), 6.48 (d, J = 8.9 Hz, 2H), 6.31 (ddd, J = 16.9, 10.3, 10.3 Hz, 1H), 6.18 (dd, J = 15.2, 10.3 Hz, 1H), 5.66 (dt, J = 15.2, 7.3 Hz, 1H), 5.15 (d, J = 16.9 Hz, 1H), 5.02 (d, J = 10.3 Hz, 1H), 4.24 (dd, J = 7.6, 5.6 Hz, 1H), 3.83 (br s, 1H), 3.69 (s, 3H), 2.93 (s, 6H), 2.59 (ddd, J = 12.3, 7.3, 5.6 Hz, 1H), 2.50 (ddd, J = 12.3, 7.6, 7.3 Hz, 1H) ppm.

(*Z*)-8dm: ^1H NMR (500 MHz, CDCl_3): δ = 7.21 (d, J = 8.7 Hz, 2H), 6.71 (d, J = 8.7 Hz, 2H), 6.68 (d, J = 8.9 Hz, 2H), 6.66–6.60 (m, 1H), 6.48 (d, J = 8.9 Hz, 2H), 6.18 (dd, J = 11.2, 10.3 Hz, 1H), 5.46 (dt, J = 10.3, 7.4 Hz, 1H), 5.25 (d, J = 16.8 Hz, 1H), 5.15 (d, J = 10.2 Hz, 1H), 4.24 (dd, J = 7.6, 5.6 Hz, 1H), 3.83 (br s, 1H), 3.69 (s, 3H), 2.93 (s, 6H), 2.72–2.63 (m, 2H) ppm.

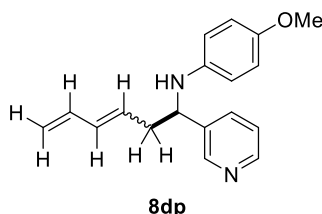
(E)-8dm: ^{13}C NMR (125 MHz, CDCl_3): δ = 151.8, 149.7, 141.9, 136.8, 133.8, 131.4, 131.0, 127.1 (2C), 116.0, 114.7 (4C), 112.8 (2C), 57.7, 55.8, 42.1, 40.7 (2C) ppm.

(Z)-8dm: ^{13}C NMR (125 MHz, CDCl_3): δ = 151.8, 149.7, 141.9, 131.9, 131.8, 131.3, 128.4, 127.1 (2C), 118.2, 114.7 (4C), 112.8 (2C), 58.0, 55.8, 40.7 (2C), 37.0 ppm.

IR (neat): ν = 3390, 3080, 2927, 2829, 1612, 1508, 1234, 815, 758, 648 cm^{-1} .

HRMS (EI): calculated for $\text{C}_{21}\text{H}_{26}\text{N}_2\text{O}^+ = [\text{M}^+]$; m/z = 322.2039, found: m/z = 322.2035.

(E/Z)-N-(1-Pyridin-3-ylhexa-3,5-dienyl)-4-methoxyaniline (8dp)



Compound **8dp** was prepared according to *GP-III* from 1,4-pentadiene (**1d**; 15.0 mg, 0.22 mmol, 1.10 equiv) and imine **7p** (42.4 mg, 0.20 mmol), using $\text{NaN}(\text{SiMe}_3)_2$ (3.7 mg, 0.02 mmol, 10 mol%) as the catalyst, in dioxane (300 μL) at 25 $^\circ\text{C}$ for 20 h. **8dp** was purified by PTLC on silica gel (EtOAc; *eluted twice*).

Yellow liquid.

Yield: 44.2 mg (79%; $E:Z$ = 3:1).

(E)-8dp: ^1H NMR (500 MHz, CDCl_3): δ = 8.65 (d, J = 2.0 Hz, 1H), 8.52 (dd, J = 4.7, 1.3 Hz, 1H), 7.69 (d, J = 7.8 Hz, 1H), 7.28–7.24 (m, 1H), 6.70 (d, J = 8.9 Hz, 2H), 6.46 (d, J = 8.9 Hz, 2H), 6.32 (dt, J = 17.8, 10.6 Hz, 1H), 6.24–6.16 (m, 1H), 5.63 (ddd, J = 14.8, 7.3, 7.3 Hz, 1H), 5.20 (d, J = 17.8 Hz, 1H), 5.08 (d, J = 10.6 Hz, 1H), 4.40 (dd, J = 7.8, 5.2 Hz, 1H), 3.86 (br s, 1H), 3.71 (s, 3H), 2.70–2.50 (m, 2H) ppm.

(Z)-8dp: ^1H NMR (500 MHz, CDCl_3): δ = 8.65 (d, J = 2.0 Hz, 1H), 8.52 (dd, J = 4.7, 1.3 Hz, 1H), 7.69 (d, J = 7.8 Hz, 1H), 7.28–7.24 (m, 1H), 6.70 (d, J = 8.9 Hz, 2H), 6.64–6.55 (m, 1H), 6.46 (d, J = 8.9 Hz, 2H), 6.24–6.16 (m, 1H), 5.47–5.39 (m, 1H), 5.30 (d, J = 17.0 Hz, 1H), 5.21 (d, J = 10.4 Hz, 1H), 4.40 (dd, J = 7.8, 5.2 Hz, 1H), 3.86 (br s, 1H), 3.71 (s, 3H), 2.73–2.58 (m, 2H) ppm.

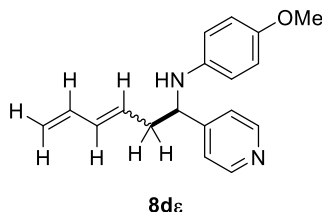
(E)-8dp: ^{13}C NMR (125 MHz, CDCl_3): δ = 152.4, 148.7, 148.6, 140.9, 136.4, 134.9, 134.0, 129.2, 123.6, 116.9, 116.4, 114.9 (2C), 114.8 (2C), 56.2, 55.7, 41.9 ppm.

(Z)-8dp: ^{13}C NMR (125 MHz, CDCl_3): δ = 152.4, 148.7, 148.6, 140.9, 139.0, 136.4, 132.9, 131.3, 128.5, 123.7, 116.7, 114.9 (2C), 114.8 (2C), 56.5, 55.7, 36.7 ppm.

IR (neat): ν = 3368, 3060, 2930, 2895, 1505, 1411, 1234, 904, 819, 759 cm^{-1} .

HRMS (EI): calculated for $\text{C}_{18}\text{H}_{20}\text{N}_2\text{O}^+ = [\text{M}^+]$; m/z = 280.1570, found: m/z = 280.1587.

(E/Z)-N-(1-Pyridin-4-ylhexa-3,5-dienyl)-4-methoxyaniline (8de)



Compound **8de** was prepared according to *GP-III* from 1,4-pentadiene (**1d**; 15.0 mg, 0.22 mmol, 1.10 equiv) and imine **7e** (42.4 mg, 0.20 mmol), using $\text{NaN}(\text{SiMe}_3)_2$ (3.7 mg, 0.02 mmol, 10 mol%) as the catalyst, in dioxane (300 μL) at 25 $^\circ\text{C}$ for 20 h. **8de** was purified by PTLC on silica gel (EtOAc; *eluted twice*).

Yellow liquid.

Yield: 49.8 mg (89%; $E:Z$ = 4:1).

(*E*)-**8dg**: ^1H NMR (500 MHz, CDCl_3): δ = 8.57 (d, J = 5.9 Hz, 2H), 7.31 (d, J = 5.9 Hz, 2H), 6.71 (d, J = 9.0 Hz, 2H), 6.42 (d, J = 9.0 Hz, 2H), 6.32 (dt, J = 16.8, 10.3 Hz, 1H), 6.20 (dd, J = 15.1, 10.3 Hz, 1H), 5.61 (dt, J = 15.1, 7.3 Hz, 1H), 5.21 (d, J = 16.8 Hz, 1H), 5.09 (d, J = 10.3 Hz, 1H), 4.33 (dd, J = 7.9, 5.1 Hz, 1H), 3.92 (br s, 1H), 3.72 (s, 3H), 2.65 (dddd, J = 14.3, 7.3, 5.1, 1.3 Hz, 1H), 2.52 (dddd, J = 14.3, 7.9, 7.3, 1.3 Hz, 1H) ppm.

(*Z*)-**8dg**: ^1H NMR (500 MHz, CDCl_3): δ = 8.57 (d, J = 5.9 Hz, 2H), 7.31 (d, J = 5.9 Hz, 2H), 6.71 (d, J = 9.0 Hz, 2H), 6.61 (dddd, J = 16.8, 11.2, 10.1, 1.1 Hz, 1H), 6.42 (d, J = 9.0 Hz, 2H), 6.21 (dd, J = 11.8, 11.2 Hz, 1H), 5.41 (dt, J = 11.8, 7.3 Hz, 1H), 5.32 (d, J = 16.8 Hz, 1H), 5.22 (d, J = 10.1 Hz, 1H), 4.33 (dd, J = 7.9, 5.1 Hz, 1H), 3.92 (brs, 1H), 3.72 (s, 3H), 2.68 (ddd, J = 14.3, 7.3, 5.1 Hz, 1H), 2.64 (ddd, J = 14.3, 7.9, 7.3 Hz, 1H) ppm.

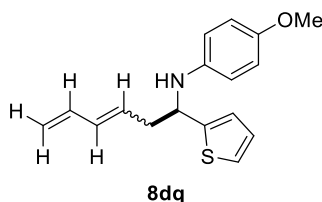
(*E*)-**8dg**: ^{13}C NMR (125 MHz, CDCl_3): δ = 153.0, 152.4, 150.1 (2C), 140.8, 136.3, 135.0, 129.0, 121.6 (2C), 117.0, 114.8 (2C), 114.7 (2C), 57.5, 55.7, 41.4 ppm.

(*Z*)-**8dg**: ^{13}C NMR (125 MHz, CDCl_3): δ = 152.8, 152.4, 150.1 (2C), 140.8, 133.1, 131.3, 126.4, 121.7 (2C), 119.3, 114.8 (2C), 114.7 (2C), 57.8, 55.7, 36.2 ppm.

IR (neat): ν = 3379, 3260, 3028, 2929, 2831, 1597, 1510, 1411, 1234, 904, 815, 756 cm^{-1} .

HRMS (EI): calculated for $\text{C}_{18}\text{H}_{20}\text{N}_2\text{O}^+ = [\text{M}^+]$: m/z = 280.1570, found: m/z = 280.1561.

(*E/Z*)-*N*-(1-Thienyl-3,5-dienyl)-4-methoxyaniline (**8dq**)



Compound **8dq** was prepared according to *GP-III* from 1,4-pentadiene (**1d**; 20.5 mg, 0.30 mmol, 1.50 equiv) and imine **7q** (43.5 mg, 0.20 mmol), using $\text{NaN}(\text{SiMe}_3)_2$ (3.7 mg, 0.02 mmol, 10 mol%) as the catalyst, in dioxane (300 μL) at 25 $^\circ\text{C}$ for 20 h. **8dq** was purified by PTLC on silica gel (EtOAc/PE = 1:9; *eluted once*).

Yellow liquid.

Yield: 51.4 mg (90%; *E:Z* = 5:1).

(*E*)-**8dq**: ^1H NMR (500 MHz, CDCl_3): δ = 7.19 (dd, J = 4.8, 1.4 Hz, 1H), 7.00–6.95 (m, 2H), 6.75 (d, J = 9.0 Hz, 2H), 6.59 (d, J = 9.0 Hz, 2H), 6.33 (ddd, J = 16.8, 10.4, 10.1 Hz, 1H), 6.21 (dd, J = 15.0, 10.4 Hz, 1H), 5.70 (dt, J = 15.0, 7.3 Hz, 1H), 5.19 (d, J = 16.8 Hz, 1H), 5.07 (d, J = 10.1 Hz, 1H), 4.66 (dd, J = 6.4, 6.4 Hz, 1H), 3.87 (br s, 1H), 3.74 (s, 3H), 2.75–2.65 (m, 2H) ppm.

(*Z*)-**8dq**: ^1H NMR (500 MHz, CDCl_3): δ = 7.19 (dd, J = 4.8, 1.4 Hz, 1H), 7.00–6.95 (m, 2H), 6.75 (d, J = 9.0 Hz, 2H), 6.68–6.62 (m, 1H), 6.59 (d, J = 9.0 Hz, 2H), 6.20 (dt, J = 10.8, 7.4 Hz, 1H), 5.55–5.46 (m, 1H), 5.29 (d, J = 16.8 Hz, 1H), 5.20 (d, J = 10.3 Hz, 1H), 4.66 (dd, J = 6.4, 6.4 Hz, 1H), 3.87 (br s, 1H), 3.74 (s, 3H), 2.85–2.79 (m, 2H) ppm.

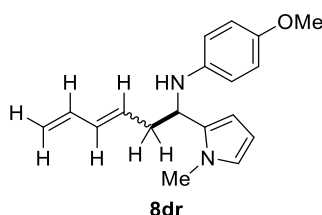
(*E*)-**8dq**: ^{13}C NMR (125 MHz, CDCl_3): δ = 152.5, 148.9, 141.2, 136.6, 134.6, 129.7, 126.8, 123.8, 123.4, 116.5, 115.2 (2C), 114.8 (2C), 55.7, 54.7, 42.0 ppm.

(*Z*)-**8dq**: ^{13}C NMR (125 MHz, CDCl_3): δ = 152.5, 148.8, 141.2, 132.5, 131.7, 129.7, 127.1, 123.8, 123.5, 118.7, 115.1 (2C), 114.8 (2C), 54.9, 36.9, 30.9 ppm.

IR (neat): ν = 3387, 2933, 2585, 1508, 1238, 1033, 819, 700 cm^{-1} .

HRMS (EI): calculated for $\text{C}_{17}\text{H}_{19}\text{NOS}^+ = [\text{M}^+]$: m/z = 285.1182, found: m/z = 285.1174.

(*E/Z*)-*N*-(1-*N*-Methyl-pyrrol-2-ylhexa-3,5-dienyl)-4-methoxyaniline (8dr**)**



Compound **8dr** was prepared according to *GP-III* from 1,4-pentadiene (**1d**; 15.0 mg, 0.22 mmol, 1.10 equiv) and imine **7r** (42.9 mg, 0.20 mmol), using $\text{NaN}(\text{SiMe}_3)_2$ (3.7 mg, 0.02 mmol, 10 mol%) as the catalyst, in dioxane (300 μL) at 25 °C for 20 h. **8dr** was purified by PTLC on aluminium oxide gel (EtOAc/PE = 1:9; *eluted once*).

Yellow liquid.

Yield: 36.1 mg (64%; *E:Z* = 5:1).

(*E*)-8dr: ^1H NMR (500 MHz, CDCl_3): δ = 6.76 (d, J = 8.9 Hz, 2H), 6.55 (d, J = 8.9 Hz, 2H), 6.27 (dt, J = 16.9, 10.4 Hz, 1H), 6.19 (dd, J = 3.8, 2.6 Hz, 1H), 6.15 (dd, J = 15.2, 10.4 Hz, 1H), 6.11–6.09 (m, 1H), 6.07 (dd, J = 3.8, 2.6 Hz, 1H), 5.72 (dt, J = 15.2, 7.2 Hz, 1H), 5.12 (d, J = 16.9 Hz, 1H), 5.00 (d, J = 10.4 Hz, 1H), 4.40 (dd, J = 7.4, 5.9 Hz, 1H), 3.82 (br s, 1H), 3.73 (s, 3H), 3.58 (s, 3H), 2.75–2.70 (m, 1H), 2.63 (ddd, J = 13.6, 7.4, 7.2 Hz, 1H) ppm.

(*Z*)-8dr: ^1H NMR (500 MHz, CDCl_3): δ = 6.76 (d, J = 8.9 Hz, 2H), 6.75–6.71 (m, 1H), 6.55 (d, J = 8.9 Hz, 2H), 6.19 (dd, J = 3.8, 2.6 Hz, 1H), 6.15 (dd, J = 11.2, 10.3 Hz, 1H), 6.11–6.09 (m, 1H), 6.07 (dd, J = 3.8, 2.6 Hz, 1H), 5.48 (dt, J = 10.3, 7.4 Hz, 1H), 5.23 (d, J = 16.8 Hz, 1H), 5.12 (d, J = 10.3 Hz, 1H), 4.40 (dd, J = 7.4, 5.9 Hz, 1H), 3.82 (br s, 1H), 3.73 (s, 3H), 3.58 (s, 3H), 2.87 (dddd, J = 7.4, 7.4, 5.9, 1.5 Hz, 2H) ppm.

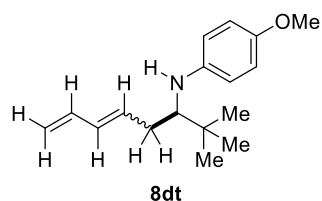
(*E*)-8dr: ^{13}C NMR (125 MHz, CDCl_3): δ = 152.3, 141.2, 137.0, 133.7, 133.4, 131.0, 122.6, 116.0, 115.0 (2C), 114.8 (2C), 106.7, 106.5, 55.8, 51.4, 37.7, 34.0 ppm.

(*Z*)-8dr: ^{13}C NMR (125 MHz, CDCl_3): δ = 152.3, 141.2, 133.3, 132.0, 131.3, 130.6, 122.6, 118.0, 115.0 (2C), 114.8 (2C), 106.7, 106.5, 55.6, 51.4, 32.8, 31.0 ppm.

IR (neat): ν = 3360, 3107, 2927, 2900, 2360, 1510, 1242, 1029, 823, 715, 698 cm^{-1} .

HRMS (EI): calculated for $\text{C}_{18}\text{H}_{22}\text{N}_2\text{O}^+ = [\text{M}^+]$: m/z = 282.1727, found: m/z = 282.1728.

(*E/Z*)-*N*-(1-*Tert*-butylhexa-3,5-dienyl)-4-methoxyaniline (8dt**)**



Compound **8dt** was prepared according to *GP-III* from 1,4-pentadiene (**1d**; 15.0 mg, 0.22 mmol, 1.10 equiv) and imine **7t** (38.3 mg, 0.20 mmol), using $\text{NaN}(\text{SiMe}_3)_2$ (3.7 mg, 0.02 mmol, 10 mol%) as the catalyst, in dioxane (300 μL) at 25 °C for 20 h. **8dt** was purified by PTLC on silica gel (EtOAc/PE = 1:9; *eluted once*).

Yellow liquid.

Yield: 28.5 mg (55%; *E:Z* = 4:1).

(*E*)-8dt: ^1H NMR (500 MHz, CDCl_3): δ = 6.73 (d, J = 8.9 Hz, 2H), 6.53 (d, J = 8.9 Hz, 2H), 6.22 (dt, J = 17.0, 10.2 Hz, 1H), 6.06 (dd, J = 14.9, 10.2 Hz, 1H), 5.68 (dt, J = 14.9, 7.0 Hz, 1H), 5.06 (d, J = 17.0 Hz, 1H), 4.93 (d, J = 10.2 Hz, 1H), 3.74 (s, 3H), 3.18 (br s, 1H), 3.06 (dd, J = 9.6, 3.6 Hz, 1H), 2.50 (dddd, J = 14.5, 7.0, 3.6, 1.3 Hz, 1H), 2.09 (dddd, J = 14.5, 9.6, 7.0, 1.3 Hz, 1H), 0.96 (s, 9H) ppm.

(*Z*)-8dt: ^1H NMR (500 MHz, CDCl_3): δ = 6.73 (d, J = 8.9 Hz, 2H), 6.61 (dddd, J = 16.8, 11.0, 10.1, 1.2 Hz, 1H), 6.53 (d, J = 8.9 Hz, 2H), 5.99 (t, J = 11.0 Hz, 1H), 5.47 (dt, J = 11.0, 7.4 Hz, 1H), 5.19 (d, J = 16.8 Hz, 1H), 5.11 (d, J = 10.1 Hz, 1H), 3.73 (s, 3H), 3.18 (br s, 1H), 3.09 (dd, J = 9.4, 3.6 Hz, 1H), 2.62 (dddd, J = 14.9, 7.4, 3.6, 1.4 Hz, 1H), 2.18 (dddd, J = 14.9, 9.4, 7.4, 1.4 Hz, 1H), 0.98 (s, 9H) ppm.

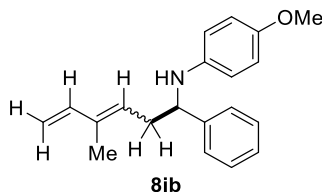
(E)-8dt: ^{13}C NMR (125 MHz, CDCl_3): δ = 151.3, 143.9, 137.2, 133.3, 132.5, 115.0, 114.8 (2C), 114.2 (2C), 63.5, 55.8, 36.0, 35.3, 27.0 (3C) ppm.

(Z)-8dt: ^{13}C NMR (125 MHz, CDCl_3): δ = 151.3, 143.9, 132.1, 130.6, 130.2, 117.4, 114.8 (2C), 113.8 (2C), 63.5, 55.8, 36.1, 30.1, 26.9 (3C) ppm.

IR (neat): ν = 3398, 2953, 2904, 2848, 1508, 1230, 814, 748, 655 cm^{-1} .

HRMS (EI): calculated for $\text{C}_{17}\text{H}_{25}\text{NO}^+ = [\text{M}^+]$; m/z = 259.1931, found: m/z = 259.1932.

(E/Z)-N-(1-Phenylhexa-4-methyl-3,5-dienyl)-4-methoxyaniline (8jb)



Compound **8jb** was prepared according to *GP-III* from 3-methyl-1,4-pentadiene (**1j**; 18.0 mg, 0.22 mmol, 1.10 equiv) and imine **7b** (42.2 mg, 0.20 mmol), using $\text{NaN}(\text{SiMe}_3)_2$ (3.7 mg, 0.02 mmol, 10 mol%) as the catalyst, in dioxane (300 μL) at 25 $^\circ\text{C}$ for 20 h. **8jb** was purified by PTLC on silica gel (EtOAc/PE = 1:9; *eluted once*).

Yellow liquid.

Yield: 58.1 mg (99%; $E:Z$ = 6:1).

(E)-8jb: ^1H NMR (500 MHz, CDCl_3): δ = 7.43–7.40 (m, 2H), 7.38–7.34 (m, 2H), 7.30–7.26 (m, 1H), 6.73 (d, J = 9.0 Hz, 2H), 6.51 (d, J = 9.0 Hz, 2H), 6.41 (dd, J = 17.4, 10.7 Hz, 1H), 5.55 (t, J = 7.0 Hz, 1H), 5.19 (d, J = 17.4 Hz, 1H), 5.03 (d, J = 10.7 Hz, 1H), 4.38 (t, J = 7.0 Hz, 1H), 3.86 (br s, 1H), 3.73 (s, 3H), 2.68 (t, J = 7.0 Hz, 2H), 1.78 (s, 3H) ppm.

(Z)-8jb: ^1H NMR (500 MHz, CDCl_3): δ = 7.43–7.40 (m, 2H), 7.38–7.34 (m, 2H), 7.30–7.26 (m, 1H), 6.81 (dd, J = 17.2, 10.8 Hz, 1H), 6.73 (d, J = 9.0 Hz, 2H), 6.51 (d, J = 9.0 Hz, 2H), 5.45 (t, J = 7.5 Hz, 1H), 5.33 (d, J = 17.2 Hz, 1H), 5.21 (d, J = 10.8 Hz, 1H), 4.35 (dd, J = 7.9, 7.5 Hz, 1H), 3.86 (br s, 1H), 3.73 (s, 3H), 2.68 (dd, J = 7.9, 7.5 Hz, 2H), 1.78 (s, 3H) ppm.

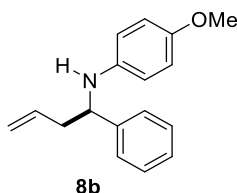
(E)-8jb: ^{13}C NMR (125 MHz, CDCl_3): δ = 152.0, 143.8, 141.6, 141.1, 136.9, 128.6 (2C), 128.3, 127.0, 126.4 (2C), 114.8 (2C), 114.8 (2C), 111.7, 58.9, 55.8, 37.8, 12.0 ppm.

(Z)-8jb: ^{13}C NMR (125 MHz, CDCl_3): δ = 152.0, 143.9, 141.7, 135.5, 133.3, 128.6 (2C), 126.9, 126.4 (2C), 126.4, 114.9, 114.8 (2C), 114.7 (2C), 58.9, 55.8, 36.8, 20.1 ppm.

IR (neat): ν = 3392, 2999, 2900, 2831, 1508, 1236, 1029, 810, 700, 632 cm^{-1} .

HRMS (EI): calculated for $\text{C}_{20}\text{H}_{23}\text{NO}^+ = [\text{M}^+]$; m/z = 293.1774, found: m/z = 293.1764.

N-(1-Phenylbut-3-en-1-yl)-4-methoxy-aniline (8b)



Compound **8b** was prepared according to *GP-IX* from allyl boronic ester **1m** (37.0 mg, 0.22 mmol, 1.10 equiv) and imine **7b** (42.2 mg, 0.20 mmol) using $\text{LiN}(\text{SiMe}_3)_2$ (3.4 mg, 0.02 mmol, 10 mol%) as the catalyst in dioxane (300 μL) at 25 $^\circ\text{C}$ for 20 h. **8b** was purified by PTLC on silica gel (EtOAc/PE = 1:9; *eluted once*). The obtained NMR data was in agreement with the literature reported data.^[236]

Colorless oil.

Yield: 30.1 mg (60% yield).

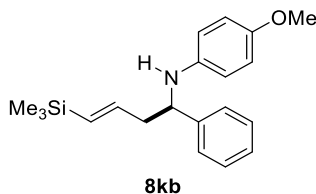
¹H NMR (500 MHz, CDCl₃): δ = 7.35–7.27 (m, 4H), 7.21–7.19 (m, 1H), 6.67 (d, *J* = 8.8 Hz, 2H), 6.45 (d, *J* = 8.8 Hz, 2H), 5.78–5.72 (m, 1H), 5.18–5.11 (m, 2H), 4.31 (dd, *J* = 8.0, 5.2 Hz, 1H), 3.92 (br s, 1H), 3.64 (s, 3H), 2.58 (dt, *J* = 8.0, 5.2 Hz, 1H), 2.48 (dt, *J* = 8.0, 6.3 Hz, 1H) ppm.

¹³C NMR (125 MHz, CDCl₃): δ = 152.0, 143.8, 141.6, 134.8, 128.6 (2C), 126.9, 126.3 (2C), 118.2, 114.7 (2C), 114.6 (2C), 58.0, 55.8, 43.4 ppm.

IR (neat): ν = 2918, 2848, 2357, 1529, 1238, 1037, 918, 817, 700, 667 cm⁻¹.

HRMS (EI): calculated for C₁₇H₁₉NO⁺ = [M⁺]: *m/z* = 253.1461, found: *m/z* = 253.1467.

(*E*)-*N*-(1-Phenyl-4-trimethylsilyl-3-butenyl)-4-methoxyaniline (8kb**)**



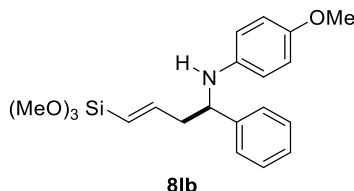
Compound **8kb** was prepared according to *GP-IX* from allyl silane **1k** (25.1 mg, 0.22 mmol, 1.10 equiv) and imine **7b** (42.2 mg, 0.20 mmol) using NaN(SiMe₃)₂ (3.7 mg, 0.02 mmol, 10 mol%) as the catalyst in dioxane (300 μL) at 25 °C for 20 h. *The isolation of (E)-8kb was attempted; however, due to its sensitivity only the proto-desilylated compound 8b was obtained after PTLC on silica gel or neutral alumina (EtOAc/PE = 1:9; eluted once).* <9% NMR yield.

(*E*)-8kb: **¹H NMR** (500 MHz, C₆D₆): δ = 7.43–7.21 (m, 5H), 6.66 (d, *J* = 8.9 Hz, 2H), 6.43 (d, *J* = 8.9 Hz, 2H), 5.95 (ddd, *J* = 18.6, 7.2, 6.0 Hz, 1H), 5.70 (d, *J* = 18.6 Hz, 1H), 4.23 (dt, *J* = 8.1, 5.2 Hz, 1H), 3.71 (d, *J* = 5.2 Hz, 1H), 3.68 (s, 3H), 2.50–2.44 (m, 1H), 2.41–2.34 (m, 1H), 0.05 (s, 9H) ppm.

The Z-isomer was not detected.

HRMS (EI): calculated for C₂₀H₂₇NO²⁸Si⁺ = [M⁺]: *m/z* = 325.1856, found: *m/z* = 325.1835.

(*E*)-*N*-(1-Phenyl-4-trimethoxysilyl-3-butenyl)-4-methoxyaniline (8lb**)**



Compound **8lb** was prepared according to *GP-IX* from allyl silane **8l** (35.6 mg, 0.22 mmol, 1.10 equiv) and imine **7b** (42.2 mg, 0.20 mmol) using NaN(SiMe₃)₂ (3.7 mg, 0.02 mmol, 10 mol%) as the catalyst in dioxane (300 μL) at 25 °C for 20 h. *The isolation of (E)-8lb was attempted; however, due to its sensitivity only the proto-desilylated compound 8b was obtained after PTLC on silica gel or neutral alumina (EtOAc/PE = 1:9; eluted once).*

85% NMR yield.

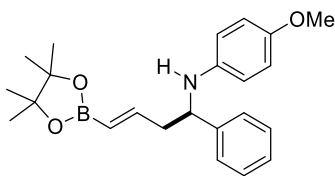
(*E*)-8lb: **¹H NMR** (500 MHz, CDCl₃): δ = 7.30–7.25 (m, 3H), 7.14–7.05 (m, 2H), 6.72 (d, *J* = 8.9 Hz, 2H), 6.52 (ddd, *J* = 18.8, 7.1, 6.2 Hz, 1H), 6.45 (d, *J* = 8.9 Hz, 2H), 5.61 (dt, *J* = 18.8, 1.5 Hz, 1H), 4.30 (dt, *J* = 7.8, 5.3 Hz, 1H), 3.70 (d, *J* = 5.3 Hz, 1H), 3.68 (s, 3H), 3.64 (s, 9H), 2.54–2.49 (m, 1H), 2.46–2.42 (m, 1H) ppm.

The Z-isomer was not detected.

IR (neat): ν = 3375, 2943, 2837, 1510, 1452, 1238, 1068, 817, 700 cm⁻¹.

HRMS (EI): calculated for C₂₀H₂₇NO₄²⁸Si⁺ = [M⁺]: *m/z* = 373.1703, found: *m/z* = 373.1678.

(E)-N-(1-Phenyl-4-pinacolatoborane-3-butenyl)-4-methoxyaniline (8mb**)**



8mb

Compound **8mb** was prepared according to *GP-IX* from allyl boronic ester **1m** (37.0 mg, 0.22 mmol, 1.10 equiv) and imine **7b** (42.2 mg, 0.20 mmol) using $\text{NaN}(\text{SiMe}_3)_2$ (3.7 mg, 0.02 mmol, 10 mol%) as the catalyst in DMF (300 μL) at 25 °C for 20 h. **8mb** was purified by PTLC on silica gel (EtOAc/PE = 1:9; *eluted once*).

Colorless liquid.

Yield: 45.5 mg (60%; *E:Z* = >99:1).

(E)-8mb: ^1H NMR (500 MHz, CDCl_3): δ = 7.40–7.37 (m, 2H), 7.35–7.31 (m, 2H), 7.26–7.22 (m, 1H), 6.69 (d, J = 8.9 Hz, 2H), 6.63 (ddd, J = 17.9, 7.4, 6.1 Hz, 1H), 6.46 (d, J = 8.9 Hz, 2H), 5.61 (d, J = 17.9 Hz, 1H), 4.38 (dd, J = 8.8, 4.6 Hz, 1H), 3.88 (br s, 1H), 3.71 (s, 3H), 2.73–2.69 (m, 1H), 2.60–2.56 (m, 1H), 1.29 (s, 12H) ppm.

(E)-8mb: ^{13}C NMR (125 MHz, CDCl_3): δ = 151.9, 149.8, 143.8, 141.5, 128.6 (2C), 126.9, 126.3 (2C), 116.4, 114.8, 114.7 (2C), 114.6 (2C), 83.3, 57.3, 55.8, 45.6, 24.8 (4C) ppm.

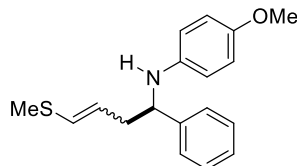
(E)-8mb: ^{11}B NMR (128 MHz, CDCl_3) δ = +29.9 ppm.

The Z-isomer was not detected.

IR (neat): ν = 3388, 2976, 1635, 1502, 1359, 1236, 1141, 1002, 970, 817, 700 cm^{-1} .

HRMS (EI): calculated for $\text{C}_{23}\text{H}_{30}\text{BNO}_3^+$ = $[\text{M}^+]$: m/z = 379.2313, found: m/z = 379.2325.

(E/Z)-N-(1-Phenyl-4-methylsulfide-3-butenyl)-4-methoxyaniline (8ob**)**



8ob

Compound **8ob** was prepared according to *GP-IX* from allyl sulfide **1o** (19.3 mg, 0.22 mmol, 1.10 equiv) and imine **7b** (42.2 mg, 0.20 mmol) using $\text{NaN}(\text{SiMe}_3)_2$ (3.7 mg, 0.02 mmol, 10 mol%) as the catalyst in dioxane (300 μL) at 25–60 °C for 24 h. **8ob** was purified by PTLC on silica gel (EtOAc/PE = 1:9; *eluted once*).

Colourless liquid.

Yield: 51.9 mg (87%; *E:Z* = 2:1).

(E)-8ob: ^1H NMR (500 MHz, CDCl_3): δ = 7.43–7.32 (m, 3H), 7.29–7.21 (m, 2H), 6.70 (d, J = 8.8 Hz, 2H), 6.48 (d, J = 8.8 Hz, 2H), 6.17 (dt, J = 15.0, 1.3 Hz, 1H), 5.35 (dt, J = 15.0, 7.3 Hz, 1H), 4.32 (dd, J = 7.9, 5.1 Hz, 1H), 3.95 (br s, 1H), 3.71 (s, 3H), 2.63 (dddd, J = 14.3, 7.3, 5.1, 1.3 Hz, 1H), 2.58 (dddd, J = 14.3, 7.9, 7.3, 1.3 Hz, 1H), 2.24 (s, 3H) ppm.

(Z)-8ob: ^1H NMR (500 MHz, CDCl_3): δ = 7.43–7.32 (m, 3H), 7.29–7.21 (m, 2H), 6.70 (d, J = 8.8 Hz, 2H), 6.48 (d, J = 8.8 Hz, 2H), 6.08 (dt, J = 9.5, 1.4 Hz, 1H), 5.55 (dt, J = 9.5, 7.2 Hz, 1H), 4.37 (dd, J = 7.7, 5.8 Hz, 1H), 3.95 (br s, 1H), 3.71 (s, 3H), 2.68 (dddd, J = 14.0, 7.2, 5.8, 1.4 Hz, 1H), 2.60 (dddd, J = 14.0, 7.7, 7.2, 1.4 Hz, 1H), 2.33 (s, 3H) ppm.

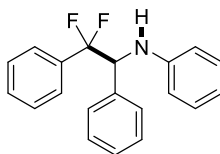
(E)-8ob: ^{13}C NMR (125 MHz, CDCl_3): δ = 151.9, 143.5, 141.4, 130.0, 128.4 (2C), 126.8, 126.2 (2C), 121.8, 114.6 (4C), 58.3, 55.6, 42.4, 14.7 ppm.

(Z)-8ob: ^{13}C NMR (125 MHz, CDCl_3): δ = 151.8, 143.6, 141.6, 128.4 (2C), 127.6, 126.8, 126.3 (2C), 124.1, 114.6 (2C), 114.4 (2C), 58.5, 55.6, 38.2, 17.0 ppm.

IR (neat): ν = 3388, 3024, 2918, 1616, 1502, 1234, 1029, 1002, 817, 750, 700 cm^{-1} .

HRMS (EI): calculated for $\text{C}_{18}\text{H}_{21}\text{NOS}^+$ = $[\text{M}^+]$: m/z = 299.1338, found: m/z = 299.1349.

***N*-(1-Phenyl-2,2-difluoro-2-phenyl-eth-1-yl)-aniline (**8qa**)**



8qa

Compound **8qa** was prepared according to *GP-III* from difluorotoluene **1q** (12.8 mg, 0.10 mmol, 1.10 equiv) and imine **7a** (18.3 mg, 0.10 mmol) using $\text{KN}(\text{SiMe}_3)_2$ (2.0 mg, 0.01 mmol, 10 mol%) as the catalyst in THF (300 μL) at 25–60 °C for 18 h. **8qa** was purified by PTLC on silica gel (EtOAc/PE = 1:9; *eluted twice*).

<5 % NMR yield, isolation resulted in a mixture of **8qa** and **7a** in 1:2 ratio based on ^1H NMR analysis.

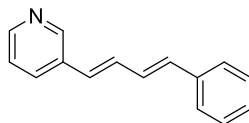
^1H NMR (500 MHz, CDCl_3): δ = 7.26–7.22 (m, 6H), 7.20–7.17 (m, 2H), 7.12–7.08 (m, 2H), 6.81–6.76 (m, 1H), 6.71 (dd, J = 8.6, 1.0 Hz, 2H), 6.59–6.57 (m, 2H), 4.91 (ddd, J = 12.8, 10.5, 7.0 Hz, 1H), 4.51 (d, J = 7.0 Hz, 1H) ppm.

^{19}F NMR (471 MHz, CDCl_3): δ = –103.0 (dd, J = 244.1, 10.5 Hz, 1F), –104.3 (dd, J = 244.1, 12.8 Hz, 1F) ppm.

HRMS (EI): calculated for $\text{C}_{20}\text{H}_{17}\text{F}_2\text{N}^+ = [\text{M}^+]$: m/z = 309.1324, found: m/z = 309.1336.

Preparation of Dehydroaminated Products

3-[(1E,3E)-4-Phenylbuta-1,3-dienyl]-pyridine (**9cb**)



9cb

Compound **9cb** was a *side-product* prepared according to *GP-III* from 3-allyl pyridine (**1c**; 35.8 mg, 0.30 mmol, 1.50 equiv) and imine **7b** (42.2 mg, 0.20 mmol), using $\text{NaN}(\text{SiMe}_3)_2$ (3.7 mg, 0.02 mmol, 10 mol%) as the catalyst, in THF (300 μL) at 25 °C for 20 h. **9cb** was purified by PTLC on silica gel (pure EtOAc; *eluted twice*). The obtained NMR data was in agreement with the literature reported data.^[139]

Pale yellow liquid.

Yield: 28.9 mg (70%).

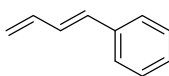
¹H NMR (500 MHz, CDCl_3): δ = 8.63 (d, J = 2.0 Hz, 1 H), 8.44 (dd, J = 4.9, 1.3 Hz, 1H), 7.46 (ddd, J = 7.9, 2.0, 2.0 Hz, 1H), 7.43–7.36 (m, 3H), 7.33 (dd, J = 7.9, 4.9 Hz, 1H), 7.26–7.22 (m, 2H), 7.13 (dd, J = 15.4, 10.4 Hz, 1H), 6.96 (dd, J = 15.4, 10.4 Hz, 1H), 6.78 (d, J = 15.4 Hz, 1H), 6.58 (d, J = 15.4 Hz, 1H) ppm.

¹³C NMR (125 MHz, CDCl_3): δ = 148.5, 148.4, 136.9, 134.2, 133.0, 132.4, 131.2, 128.8 (2C), 128.7, 128.6, 127.9, 126.5 (2C), 123.5 ppm.

IR (neat): ν = 3014, 2358, 2339, 1562, 1490, 1413, 999, 748, 690 cm^{-1} .

HRMS (EI): calculated for $\text{C}_{15}\text{H}_{13}\text{N}^+ = [\text{M}^+]$: m/z = 207.1043, found: m/z = 207.1049.

(*E*)-1-Phenyl-1,3-butadiene (**9'**)



9'

Compound **9'** is a *side-product* prepared according to *GP-III* from allyl boronic ester **1m** (37.0 mg, 0.22 mmol, 1.10 equiv) and imine **7b** (42.2 mg, 0.20 mmol) when using $\text{KN}(\text{SiMe}_3)_2$ (4.0 mg, 0.02 mmol, 10 mol%) as the catalyst in THF (300 μL) at 25 °C for 20 h. **9'** was purified by PTLC on silica gel (PE; *eluted once*). The obtained NMR data was in agreement with literature reported data.^[139]

Colorless liquid.

Yield: 20.8 mg (80%).

¹H NMR (500 MHz, CDCl_3): δ = 7.43–7.41 (m, 2H), 7.35–7.31 (m, 2H), 7.26–7.22 (m, 1H), 6.80 (dd, J = 16.1, 10.1 Hz, 1H), 6.58 (dd, J = 16.1 Hz, 1H), 6.52 (ddd, J = 16.9, 10.1, 10.1 Hz, 1H), 5.35 (d, J = 16.9 Hz, 1H), 5.19 (d, J = 10.1 Hz, 1H) ppm.

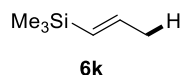
¹³C NMR (125 MHz, CDCl_3): δ = 137.2, 137.1, 132.8, 129.6, 128.6 (2C), 127.6, 126.4 (2C), 117.6 ppm.

IR (neat): ν = 2973, 2859, 1650, 1605 cm^{-1} .

HRMS (EI): calculated for $\text{C}_{10}\text{H}_{10}^+ = [\text{M}^+]$: m/z = 130.0770, found: m/z = 130.0772.

Preparation of Functionalised Internal Alkenes

(E)-1-Trimethylsilyl-1-propene (**6k**)



Compound **6k** was prepared according to *GP-X* from allyl silane **1k** (22.8 mg, 0.20 mmol, 1.00 equiv) using $\text{KN}(\text{SiMe}_3)_2$ (4.0 mg, 0.02 mmol, 10 mol %) as the catalyst, [18]crown-6 as the ligand (5.8 mg, 0.022 mmol, 11 mol %) in THF (200 μL) at 25 °C for 2 h. **6k** was not isolated; the product formation was confirmed by ^1H NMR and ^{13}C NMR spectroscopic analysis of a reaction aliquot: spectral data was in agreement with the literature reported data.^[237, 238]

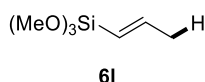
>95% NMR yield, $E:Z = >49:1$.

^1H NMR (500 MHz, CDCl_3): δ = 6.39 (dq, J = 14.0, 6.8 Hz, 1H, $Z\text{-CH=CH}$), 6.00 (dq, J = 18.4, 6.1 Hz, 1H, $E\text{-CH=CH}$), 5.69 (dq, J = 18.4, 1.6 Hz, 1H, $E\text{-CH=CH}$), 5.50 (dq, J = 14.0, 1.5 Hz, 1H, $Z\text{-CH=CH}$), 1.84 (d, J = 6.8, 1.5 Hz, 3H, $Z\text{-CH}_3$), 1.68 (dd, J = 6.1, 1.6 Hz, 3H, $E\text{-CH}_3$), 0.11 (s, 9H) ppm.

^{13}C NMR (125 MHz, $\text{C}_4\text{D}_8\text{O}$): δ = 139.8, 129.2, 19.9, -3.9 (3C) ppm.

HRMS (EI): calculated for $\text{C}_6\text{H}_{15}^{28}\text{Si}^+ = [\text{M}+\text{H}^+]$: m/z = 116.0938, found: m/z = 116.0950.

(E)-1-Trimethoxysilyl-1-propene (**6l**)



Compound **6l** was prepared according to *GP-X* from allyl silane **1l** (32.4 mg, 0.20 mmol, 1.00 equiv) using $\text{KN}(\text{SiMe}_3)_2$ (4.0 mg, 0.02 mmol, 10 mol %) as the catalyst, [18]crown-6 as the ligand (5.8 mg, 0.022 mmol, 11 mol %) in THF (200 μL) at 25 °C for 2 h. **6l** was not isolated; the product formation was confirmed by ^1H NMR and ^{13}C NMR spectroscopic analysis of a reaction aliquot: spectral data was in agreement with the literature reported data.^[239]

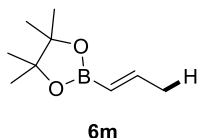
>90% NMR yield; $E:Z = >10:1$.

^1H NMR (500 MHz, CDCl_3): δ = 6.57 (dq, J = 14.2, 6.8 Hz, 1H, $Z\text{-CH=CH}$), 6.47 (dq, J = 18.6, 6.3 Hz, 1H, $E\text{-CH=CH}$), 5.51 (dq, J = 18.6, 1.7 Hz, 1H, $E\text{-CH=CH}$), 5.46 (dq, J = 14.2, 1.5 Hz, 1H, $Z\text{-CH=CH}$), 3.47 (s, 9H), 1.63 (dd, J = 6.8, 1.5 Hz, 3H, $Z\text{-CH}_3$), 1.61 (dd, J = 6.3, 1.7 Hz, 3H, $E\text{-CH}_3$) ppm.

^{13}C NMR (125 MHz, $\text{C}_4\text{D}_8\text{O}$): δ = 148.1, 120.1, 49.4 (3C), 21.6 ppm.

HRMS (EI): calculated for $\text{C}_6\text{H}_{14}\text{O}_3^{28}\text{Si}^+ = [\text{M}^+]$: m/z = 162.0707, found: m/z = 162.0709.

(E)-1-Pinacolatoborane-1-propene (**6m**)



Compound **6m** was prepared according to *GP-X* from allyl boronic ester **1m** (33.6 mg, 0.20 mmol, 1.00 equiv) using $\text{KN}(\text{SiMe}_3)_2$ (2.0 mg, 0.01 mmol, 5 mol %) as the catalyst in DMF (200 μL) at 25 °C for 2 h. **6m** was not isolated; the product formation was confirmed by ^1H and ^{11}B NMR spectroscopic analysis of a reaction aliquot: spectral data was in agreement with the literature reported data.^[240-242]

>99% NMR yield; $E:Z = >99:1$.

^1H NMR (500 MHz, CDCl_3): δ = 6.58 (dq, J = 17.8, 6.4 Hz, 1H), 5.38 (dq, J = 17.8, 1.7 Hz, 1H), 1.77 (dd, J = 6.4, 1.7 Hz, 3H), 1.19 (s, 12H) ppm.

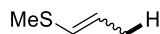
^{11}B NMR (128 MHz, CDCl_3): δ = +29.7 ppm.

^{13}C NMR (125 MHz, $\text{C}_4\text{D}_8\text{O}$): δ = 149.0 (2C), 82.8 (2C), 24.3 (4C), 21.0 ppm.

The *Z*-isomer was not detected.

HRMS (EI): calculated for $C_9H_{17}BO_2^+ = [M^+]$: $m/z = 168.1316$, found: $m/z = 168.1326$.

(*E/Z*)-1-Methylthio-1-propene (6o**)**



6o

Compound **6o** was prepared according to *GP-X* from allyl sulfide **1o** (17.6 mg, 0.20 mmol, 1.00 equiv) $KN(SiMe_3)_2$ (4.0 mg, 0.02 mmol, 10 mol%) as the catalyst, [18]crown-6 as the ligand (5.8 mg, 0.022 mmol, 11 mol%) in THF (200 μ L) at 25 °C for 4 h. **6o** was not isolated; the product formation was confirmed by 1H and ^{13}C NMR spectroscopic analysis of a reaction aliquot: spectral data was in agreement with the literature reported data.^[155]

>99% NMR yield; *E:Z* = 1:1.

***E*-6o**: 1H NMR (500 MHz, $CDCl_3$): δ = 5.81 (dq, J = 14.9, 1.6 Hz, 1H), 5.26 (dq, J = 14.9, 6.6 Hz, 1H), 1.81 (s, 3H), 1.50 (dd, J = 6.6, 1.6 Hz, 3H) ppm.

***Z*-6o**: 1H NMR (500 MHz, $CDCl_3$): δ = 5.72 (dq, J = 9.4, 1.5 Hz, 1H), 5.43 (dq, J = 9.4, 6.8 Hz, 1H), 1.82 (s, 3H), 1.67 (dd, J = 6.8, 1.5 Hz, 3H) ppm.

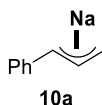
***E*-6o**: ^{13}C NMR (125 MHz, C_4D_8O): δ = 125.1, 121.0, 17.5, 13.9 ppm.

***Z*-6o**: ^{13}C NMR (125 MHz, C_4D_8O): δ = 128.2, 121.7, 15.2, 13.6 ppm.

HRMS (EI): calculated for $C_4H_9^{32}S^+ = [M+H^+]$: $m/z = 89.0419$, found: $m/z = 89.0419$.

Detection of Reaction Intermediates

(*E*)- η^3 -Phenyl-allyl-sodium (**10a**)



Compound **10a** was prepared according to *GP-V* from **1a** (11.8 mg, 0.10 mmol, 1.0 equiv) and NaO^tBu (10.5 mg, 0.11 mmol, 1.1 equiv)/BuLi (1.6 M in hexane; 68 μ L, 0.11 mmol, 1.1 equiv) in THF-*d*₈ (400 μ L) at –20 °C to room temperature for 20 h. The formation of **10a** was confirmed by ¹H NMR, ¹³C NMR, ²³Na NMR, and HRMS analyses. The structure of **10a** was assigned to be an η^3 -(*E*)-phenylallyl–Na species based on ¹H NMR and ¹³C NMR spectroscopy.^[124] The data have been carefully compared with the independently synthesised lithium analogue **10b** (according to *GP-VI*).^[144]

>99% NMR yield; stored in THF-*d*₈.

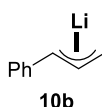
¹H NMR (500 MHz, C₄D₈O): δ = 6.70 (d, *J* = 15.4 Hz, 1H), 6.52 (br s, 2H), 6.32 (br s, 2H), 5.70 (br s, 1H), 4.19 (br s, 1H), 3.33 (d, *J* = 15.4 Hz, 1H), 2.89 (br s, 1H) ppm.

¹³C NMR (125 MHz, C₄D₈O): δ = 148.4, 136.5, 128.8 (2C), 122.5 (2C), 109.0, 66.3 (2C) ppm.

²³Na NMR (132 MHz, C₄D₈O): δ = –5.3 ppm.

HRMS (EI): calculated for C₉H₉[–] = [M–Na⁺][–]: *m/z* = 117.0698, found: *m/z* = 117.0691.

(*E*)- η^3 -Phenyl-allyl-lithium (**10b**)



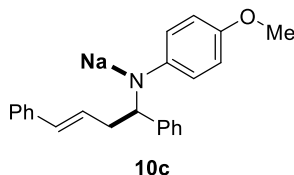
Compound **10b** was prepared according to *GP-VI* from **1a** (11.8 mg, 0.1 mmol, 1.0 equiv) and BuLi (1.6 M in hexane; 68 μ L, 0.11 mmol, 1.1 equiv) in THF-*d*₈ (400 μ L) at –20 °C to room temperature for 20 h. The formation of **10b** was confirmed by ¹H NMR and ¹³C NMR analyses; the data proved to be in full agreement with the literature.^[144]

>99% NMR yield; stored in THF-*d*₈.

¹H NMR (500 MHz, C₄D₈O): δ = 6.67 (ddd, *J* = 15.1, 12.3, 8.3 Hz, 1H), 6.59–6.47 (m, 2H), 6.35 (d, *J* = 7.0 Hz, 2H), 5.77 (d, *J* = 7.6 Hz, 1H), 4.14 (d, *J* = 12.3 Hz, 1H), 3.11 (d, *J* = 15.1 Hz, 1H), 2.74 (d, *J* = 8.3 Hz, 1H) ppm.

¹³C NMR (125 MHz, C₄D₈O): δ = 148.9, 137.5, 128.6 (2C), 117.3 (2C), 110.2, 77.8 (2C) ppm.

Sodium-(*E*)-*N*-(1,4-diphenylbut-3-enyl)-4-methoxyphenyl-amide (**10c**)



Compound **10c** was prepared according to *GP-VII* from allyl–Na nucleophile **10a** (solution in THF-*d*₈; 80 μ L, 0.02 mmol, 1.0 equiv) and imine electrophile **7b** (4.8 mg, 0.02 mmol, 1.0 equiv) in dioxane/THF-*d*₈ [5:1 (v/v); 480 μ L] at 25 °C for 1 h. The formation of **10c** was confirmed by ¹H NMR, ¹³C NMR, and ²³Na NMR spectroscopy.

>99% NMR yield; stored in THF-*d*₈.

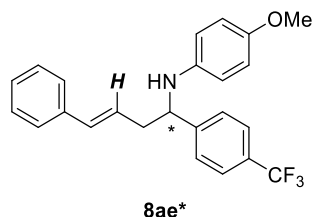
¹H NMR (500 MHz, C₄D₈O): δ = 7.32–7.10 (m, 10H), 6.68–6.33 (m, 4H), 5.97 (br s, 2H), 4.21 (s, 1H), 3.80 (s, 3H), 2.71–2.50 (m, 2H) ppm.

¹³C NMR (125 MHz, C₄D₈O): δ = 157.9, 151.4, 145.6, 138.2, 131.2, 129.0 (2C), 128.8, 128.2 (2C), 127.9 (2C), 126.4 (2C), 122.7 (2C), 116.6 (2C), 114.7 (2C), 66.1, 55.3, 42.0 ppm.

²³Na NMR (132 MHz, C₄D₈O): δ = +4.9 ppm.

Attempted Asymmetric Catalysis

(*E*)-*N*-[1-(4-Trifluoromethyl)-4-phenylbut-3-enyl]-4-methoxyaniline (**8ae***)



Compound **8ae*** was prepared according to GP-XI from allyl benzene (**1a**; 24.8 μ L, 0.21 mmol, 1.05 equiv) and imine **7e** (55.9 mg, 0.20 mmol), using $\text{NaN}(\text{SiMe}_3)_2$ (3.7 mg, 0.02 mmol, 10 mol%) and (*S*)-**L3** (6.4 mg, 0.022 mmol, 11 mol%) in hexane (300 μ L) at 25 $^\circ\text{C}$ for 20 h. **8ae*** was purified by PTLC on silica gel (EtOAc/PE = 1:9; *eluted once*).

Yellow liquid.

Yield: 35.7 mg (45%; *E*:*Z* = >24:1); 21% *ee* (*E*).

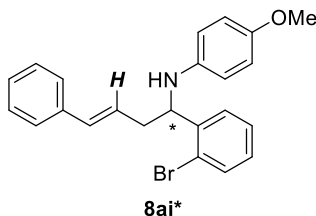
^1H NMR (500 MHz, CDCl_3): δ = 7.65 (d, J = 7.9 Hz, 2H), 7.57 (d, J = 7.9 Hz, 2H), 7.40–7.35 (m, 4H), 7.31–7.28 (m, 1H), 6.74 (d, J = 8.8 Hz, 2H), 6.58 (d, J = 15.8 Hz, 1H), 6.48 (d, J = 8.8 Hz, 2H), 6.18 (ddd, J = 15.8, 6.8, 5.9 Hz, 1H, *E*-CH=CH), 5.73 (ddd, J = 12.3, 7.1, 7.1 Hz, 1H, *Z*-CH=CH), 4.51 (dd, J = 7.1, 6.1 Hz, 1H), 4.09 (br s, 1H), 3.74 (s, 3H), 2.83–2.78 (m, 1H), 2.71–2.65 (m, 1H) ppm.

^{13}C NMR (125 MHz, CDCl_3): δ = 152.3, 148.0, 141.0, 136.8, 133.8, 129.3 (q, J = 32.3 Hz), 128.6 (2C), 127.6, 126.7 (2C), 126.2 (2C), 125.6 (q, J = 3.7 Hz, 2C), 125.3, 123.9 (q, J = 272.6 Hz), 114.8 (4C), 58.1, 55.7, 42.4 ppm.

^{19}F NMR (470 MHz, CDCl_3): δ = –62.3 (s, 3F) ppm.

HPLC (DAICEL CHIRALPAK IC; eluent: hexane/*i*PrOH = 9:1); debit: 1 mL/min, injected volume: 20 μ L, detection: UV 254 nm): t_R = 4.3 min (major), 7.2 min (minor).

(*E*)-*N*-[1-(2-Bromophenyl)-4-phenylbut-3-enyl]-4-methoxyaniline (**8ai***)



Compound **8ai*** was prepared according to GP-XI from allyl benzene (**1a**; 24.8 μ L, 0.21 mmol, 1.05 equiv) and imine **7i** (57.8 mg, 0.20 mmol), using $\text{NaN}(\text{SiMe}_3)_2$ (3.7 mg, 0.02 mmol, 10 mol%) and (*S*)-**L3** (6.4 mg, 0.022 mmol, 11 mol%) in *m*-xylene (300 μ L) at 25 $^\circ\text{C}$ for 20 h. **8ai*** was purified by PTLC on silica gel (EtOAc/PE = 1:9; *eluted once*).

Yellow liquid.

Yield: 69.5 mg (85%; *E*:*Z* = 99:1); 46% *ee* (*E*).

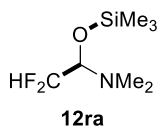
^1H NMR (500 MHz, CDCl_3): δ = 7.58 (dd, J = 7.8, 1.1 Hz, 1H), 7.45 (dd, J = 7.8, 1.7 Hz, 1H), 7.35 (dd, J = 7.8, 1.1 Hz, 2H), 7.30 (dd, J = 7.6, 7.6 Hz, 2H), 7.24 (dd, J = 7.6, 7.6 Hz, 2H), 7.10 (ddd, J = 7.6, 7.6, 1.7 Hz, 1H), 6.67 (d, J = 9.0 Hz, 2H), 6.54 (d, J = 15.8 Hz, 1H), 6.38 (d, J = 9.0 Hz, 2H), 6.19 (ddd, J = 15.8, 7.8, 6.7 Hz, 1H, *E*-CH=CH), 5.74 (ddd, J = 11.8, 8.1, 5.9 Hz, 1H, *Z*-CH=CH), 4.81 (dd, J = 8.3, 4.2 Hz, 1H), 4.05 (br s, 1H), 3.67 (s, 3H), 2.85–2.80 (m, 1H), 2.57–2.50 (m, 1H) ppm.

^{13}C NMR (125 MHz, CDCl_3): δ = 152.1, 141.9, 140.9, 137.0, 133.4, 133.0, 128.6 (2C), 128.5, 127.9, 127.8, 127.4, 126.2 (2C), 125.9, 123.0, 114.8 (2C), 114.5 (2C), 57.0, 55.7, 40.2 ppm.

HPLC (DAICEL CHIRALPAK IA; eluent: hexane/*i*PrOH = 198:1); debit: 1 mL/min, injected volume: 20 μ L, detection: UV 254 nm): t_R = 15.3 min (major), 16.7 min (minor).

Catalytic Difluoromethylation of Amides and Lactams

N,N-Dimethyl-2,2-difluoro-1-trimethylsilyloxy-ethanamine (**12ra**)



Compound **12ra** was prepared and isolated according to *GP-XII* from $\text{HCF}_2\text{SiMe}_3$ (**1r**; 24.0 mg, 0.20 mmol, 1.0 equiv) and dimethyl formamide (**11a**; 14.6 mg, 0.20 mmol, 1.0 equiv) using KO^tBu (2.2 mg, 10 mol%) as the catalyst in THF at 25 °C for 18 h. The solvent and the excess amount of **1r** were removed *in vacuo* before adding hexane (500 μL). The potassium salt was filtered off and the hexane was evaporated *in vacuo* to yield the pure compound.

Colorless liquid.

Yield: 37.4 mg (95%).

¹H NMR (500 MHz, C_6D_6): δ = 5.43 (ddd, J = 56.3, 55.9, 5.1 Hz, 1H), 4.20 (ddd, J = 10.1, 5.1, 5.1 Hz, 1H), 2.10 (s, 6H), 0.09 (s, 9H) ppm.

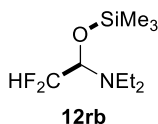
¹³C NMR (125 MHz, C_6D_6): δ = 114.2 (dd, J = 244.3, 244.3 Hz), 87.1 (dd, J = 26.8, 26.8 Hz), 38.9 (2C), 0.3 (3C) ppm.

¹⁹F NMR (471 MHz, C_6D_6): δ = -124.6 (ddd, J = 284.4, 56.3, 5.1 Hz, 1F), -129.5 (ddd, J = 284.4, 55.9, 10.1 Hz, 1F) ppm.

IR (neat): ν = 2990, 2859, 1437, 1420, 1300, 1112, 1034, 736 cm^{-1} .

HRMS (EI): calculated for $\text{C}_7\text{H}_{17}\text{F}_2\text{NO}^{28}\text{Si}^+ = [\text{M}^+]$: m/z = 197.1048, found: m/z = 197.0000.

N,N-Diethyl-2,2-difluoro-1-trimethylsilyloxy-ethanamine (**12rb**)



Compound **12rb** was prepared and isolated according to *GP-XII* from $\text{HCF}_2\text{SiMe}_3$ (**1r**; 24.0 mg, 0.20 mmol, 1.0 equiv) and diethyl formamide (**11b**; 20.2 mg, 0.20 mmol, 1.0 equiv) using KO^tBu (2.2 mg, 10 mol%) as the catalyst in THF at 25 °C for 18 h. The solvent and the excess amount of **1r** were removed *in vacuo* before adding hexane (500 μL). The potassium salt was filtered off and the hexane was evaporated *in vacuo* to yield the pure compound.

Yellow liquid.

Yield: 43.2 mg (96%).

¹H NMR (500 MHz, C_6D_6): δ = 5.44 (ddd, J = 56.5, 56.3, 5.3 Hz, 1H), 4.40 (ddd, J = 9.9, 5.3, 5.3 Hz, 1H), 2.62–2.55 (m, 2H), 2.48–2.33 (m, 2H), 0.92 (t, J = 7.2 Hz, 6H), 0.12 (s, 9H) ppm.

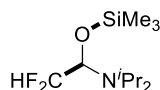
¹³C NMR (125 MHz, C_6D_6): δ = 114.8 (dd, J = 244.3, 244.3 Hz), 85.7 (dd, J = 27.2, 27.2 Hz), 43.6 (2C), 14.6 (2C), 0.4 (3C) ppm.

¹⁹F NMR (471 MHz, C_6D_6): δ = -123.9 (ddd, J = 281.0, 56.5, 5.3 Hz, 1F), -129.3 (ddd, J = 281.0, 56.3, 9.9 Hz, 1F) ppm.

IR (neat): ν = 2984, 2918, 1442, 1317, 1294, 1056, 765 cm^{-1} .

HRMS (EI): calculated for $\text{C}_9\text{H}_{21}\text{F}_2\text{NO}^{28}\text{Si}^+ = [\text{M}^+]$: m/z = 225.1355, found: m/z = 225.1408.

***N,N*-Diisopropyl-2,2-difluoro-1-trimethylsilyloxy-ethanamine (**12rc**)**



12rc

Compound **12rc** was prepared according to *GP-XII* from $\text{HCF}_2\text{SiMe}_3$ (**1r**; 24.0 mg, 0.20 mmol, 1.0 equiv) and diisopropyl formamide (**11c**; 25.8 mg, 0.20 mmol, 1.0 equiv) using KO^tBu (2.2 mg, 10 mol%) as the catalyst in THF at 25 °C for 18 h. The solvent and the excess amount of **1r** were removed *in vacuo* before adding hexane (500 μL). The potassium salt was filtered off and the hexane was evaporated *in vacuo* to yield the pure compound.

Yellow liquid.

Yield: 46.6 mg (92%).

¹H NMR (500 MHz, C_6D_6): δ = 5.35 (ddd, J = 56.8, 56.8, 5.6 Hz, 1H), 4.58 (ddd, J = 9.1, 5.6, 5.6 Hz, 1H), 3.05 (hept, J = 6.7 Hz, 2H), 1.01 (d, J = 6.7 Hz, 6H), 0.93 (d, J = 6.7 Hz, 6H), 0.18 (s, 9H) ppm.

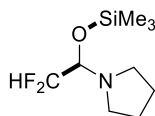
¹³C NMR (125 MHz, C_6D_6): δ = 114.5 (dd, J = 245.3, 243.9 Hz), 81.3 (dd, J = 29.1, 27.6 Hz), 45.2 (2C), 24.0 (2C), 22.4 (2C), 0.9 (3C) ppm.

¹⁹F NMR (471 MHz, C_6D_6): δ = -122.5 (ddd, J = 274.9, 56.8, 5.6 Hz, 1F), -129.6 (ddd, J = 274.9, 56.8, 9.1 Hz, 1F) ppm.

IR (neat): ν = 2974, 2937, 1442, 1307, 1205, 1099, 777, 603 cm^{-1} .

HRMS (EI): calculated for $\text{C}_{11}\text{H}_{25}\text{F}_2\text{NO}^{28}\text{Si}^+ = [\text{M}^+]$: m/z = 253.1603, found: m/z = 253.1635.

***N*-(2,2-Difluoro-1-trimethylsilyloxyeth-1-yl)-pyrrolidine (**12rd**)**



12rd

Compound **12rd** was prepared and isolated according to *GP-XII* from $\text{HCF}_2\text{SiMe}_3$ (**1r**; 24.0 mg, 0.20 mmol, 1.0 equiv) and 1-formyl pyrrolidine (**11d**; 19.8 mg, 0.20 mmol, 1.0 equiv) using KO^tBu (2.2 mg, 10 mol%) as the catalyst in THF at 25 °C for 18 h. The solvent and the excess amount of **1r** were removed *in vacuo* before adding hexane (500 μL). The potassium salt was filtered off and the hexane was evaporated *in vacuo* to yield the pure compound.

Brown liquid.

Yield: 42.4 mg (95%).

¹H NMR (500 MHz, C_6D_6): δ = 5.48 (ddd, J = 56.0, 56.0, 5.0 Hz, 1H), 4.52 (ddd, J = 10.3, 5.0, 5.0 Hz, 1H), 2.82–2.76 (m, 2H), 2.70–2.62 (m, 2H), 1.70–1.46 (m, 4H), 0.11 (s, 9H) ppm.

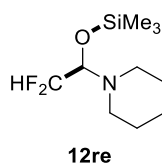
¹³C NMR (125 MHz, C_6D_6): δ = 114.9 (dd, J = 244.5, 244.5 Hz), 83.4 (dd, J = 26.2, 26.2 Hz), 46.8 (2C), 24.4 (2C), 0.2 (3C) ppm.

¹⁹F NMR (471 MHz, C_6D_6): δ = -124.8 (ddd, J = 282.1, 56.0, 5.0 Hz, 1F), -129.6 (ddd, J = 282.1, 56.0, 10.3 Hz, 1F) ppm.

IR (neat): ν = 2970, 2877, 1421, 1384, 1112, 1058, 705, 605 cm^{-1} .

HRMS (EI): calculated for $\text{C}_9\text{H}_{19}\text{F}_2\text{NO}^{28}\text{Si}^+ = [\text{M}^+]$: m/z = 223.1199, found: m/z = 223.1197.

***N*-(2,2-Difluoro-1-trimethylsilyloxyeth-1-yl)-piperidine (**12re**)**



Compound **12re** was prepared and isolated according to *GP-XII* from $\text{HCF}_2\text{SiMe}_3$ (**1r**; 24.0 mg, 0.20 mmol, 1.0 equiv) and 1-formyl piperidine (**11e**; 22.6 mg, 0.20 mmol, 1.0 equiv) using KO^tBu (2.2 mg, 10 mol%) as the catalyst in THF at 25 °C for 18 h. The solvent and the excess amount of **1r** were removed *in vacuo* before adding hexane (500 μL). The potassium salt was filtered off and the hexane was evaporated *in vacuo* to yield the pure compound.

Yellow liquid.

Yield: 44.1 mg (93%).

^1H NMR (500 MHz, C_6D_6): δ = 5.51 (ddd, J = 56.0, 56.0, 5.2 Hz, 1H), 4.18 (ddd, J = 10.2, 5.2, 5.2 Hz, 1H), 2.64–2.24 (m, 4H), 1.46–1.32 (m, 4H), 1.29–1.23 (m, 2H), 0.12 (s, 9H) ppm.

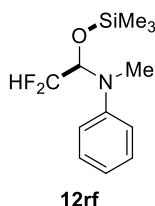
^{13}C NMR (125 MHz, C_6D_6): δ = 114.5 (dd, J = 244.6, 244.6 Hz), 88.3 (dd, J = 27.1, 27.1 Hz), 49.0, 26.4 (3C), 24.9, 0.2 (3C) ppm.

^{19}F NMR (471 MHz, C_6D_6): δ = –124.3 (ddd, J = 283.9, 56.0, 5.2 Hz, 1F), –129.3 (ddd, J = 283.9, 56.0, 10.2 Hz, 1F) ppm.

IR (neat): ν = 2935, 2856, 1442, 1394, 1253, 1107, 1026, 842, 653 cm^{-1} .

HRMS (EI): calculated for $\text{C}_{10}\text{H}_{21}\text{F}_2\text{NO}^{28}\text{Si}^+ = [\text{M}^+]$; m/z = 237.1355, found: m/z = 237.1352.

***N*-Methyl-*N*-phenyl-2,2-difluoro-1-trimethylsiloxy-ethanamine (**12rf**)**



Compound **12rf** was prepared and isolated according to *GP-XII* from $\text{HCF}_2\text{SiMe}_3$ (**1r**; 43.2 mg, 0.36 mmol, 1.8 equiv) and methyl phenyl formamide (**11f**; 27.0 mg, 0.20 mmol, 1.0 equiv) using KO^tBu (2.2 mg, 10 mol%) as the catalyst in dioxane at 25 °C for 18 h. The solvent and the excess amount of **1r** were removed *in vacuo* before adding hexane (500 μL). The potassium salt was filtered off and the hexane was evaporated *in vacuo* to yield the pure compound.

Colorless liquid.

Yield: 43.0 mg (83%).

^1H NMR (500 MHz, C_6D_6): δ = 7.18–7.15 (m, 2H), 6.81–6.76 (m, 1H), 6.75 (dd, J = 8.8, 1.0 Hz, 2H), 5.52 (ddd, J = 55.9, 55.9, 5.4 Hz, 1H), 5.21 (ddd, J = 8.6, 5.4, 5.4 Hz, 1H), 2.52 (s, 3H), 0.05 (s, 9H) ppm.

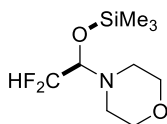
^{13}C NMR (125 MHz, C_6D_6): δ = 149.1, 129.6 (2C), 120.2, 116.1 (2C), 114.3 (dd, J = 246.7, 244.0 Hz), 84.1 (dd, J = 29.2, 29.2 Hz), 31.5, 0.2 (3C) ppm.

^{19}F NMR (471 MHz, C_6D_6): δ = –126.4 (ddd, J = 282.1, 55.9, 5.4 Hz, 1F), –130.2 (ddd, J = 282.1, 55.9, 8.6 Hz, 1F) ppm.

IR (neat): ν = 3061, 2958, 2852, 1597, 1446, 1348, 1253, 1088, 867, 613 cm^{-1} .

HRMS (EI): calculated for $\text{C}_{12}\text{H}_{19}\text{F}_2\text{NO}^{28}\text{Si}^+ = [\text{M}^+]$; m/z = 259.1198, found: m/z = 259.1198.

***N*-(2,2-Difluoro-1-trimethylsilyloxyeth-1-yl)-morpholine (**12rg**)**



12rg

Compound **12rg** was prepared and isolated according to *GP-XII* from $\text{HCF}_2\text{SiMe}_3$ (**1r**; 24.0 mg, 0.20 mmol, 1.0 equiv) and 4-formyl morpholine (**11g**; 23.1 mg, 0.20 mmol, 1.0 equiv) using KO^tBu (2.2 mg, 10 mol%) as the catalyst in THF at 25 °C for 18 h. The solvent and the excess amount of **1r** were removed *in vacuo* before adding hexane (500 μL). The potassium salt was filtered off and the hexane was evaporated *in vacuo* to yield the pure compound.

Colorless liquid.

Yield: 45.4 mg (95%).

^1H NMR (500 MHz, C_6D_6): δ = 5.41 (ddd, J = 55.9, 55.8, 5.0 Hz, 1H), 4.05 (ddd, J = 10.2, 5.0, 5.0 Hz, 1H), 3.54–3.40 (m, 4H), 2.46–2.29 (m, 4H), 0.08 (s, 9H) ppm.

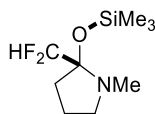
^{13}C NMR (125 MHz, C_6D_6): δ = 114.1 (dd, J = 244.6, 244.6 Hz), 87.5 (dd, J = 26.8, 26.8 Hz), 67.0 (3C), 48.2, 0.1 (3C) ppm.

^{19}F NMR (471 MHz, C_6D_6): δ = –124.3 (ddd, J = 284.9, 55.9, 5.0 Hz, 1F), –130.1 (ddd, J = 284.9, 55.8, 10.2 Hz, 1F) ppm.

IR (neat): ν = 2964, 2931, 1440, 1386, 1205, 1122, 1087, 797, 623 cm^{-1} .

HRMS (EI): calculated for $\text{C}_9\text{H}_{19}\text{F}_2\text{NO}_2^{28}\text{Si}^+ = [\text{M}^+]$: m/z = 239.1148, found: m/z = 239.1144.

***N*-Methyl-(1-difluoromethyl-1-trimethylsilyloxy)-pyrrolidine (**12rh**)**



12rh

Compound **12rh** was prepared and isolated according to *GP-XII* from $\text{HCF}_2\text{SiMe}_3$ (**1r**; 24.0 mg, 0.20 mmol, 1.0 equiv) and *N*-methyl-2-pyrrolidone (**11h**; 19.8 mg, 0.20 mmol, 1.0 equiv) using KO^tBu (2.2 mg, 10 mol%) as the catalyst in THF at 25 °C for 18 h. To this mixture under an inert atmosphere was re-added the corresponding $\text{HCF}_2\text{SiMe}_3$ (**1r**; 4.8 mg, 0.04 mmol, 0.2 equiv), and stirred at 25 °C for another 18 h to ensure full conversion of lactam **11h**. The solvent and the excess amount of **1r** were removed *in vacuo* before adding hexane (500 μL). The potassium salt was filtered off and the hexane was evaporated *in vacuo* to yield the pure compound.

Yellow liquid.

Yield: 37.0 mg (83%).

^1H NMR (500 MHz, C_6D_6): δ = 5.41 (dd, J = 56.6, 55.8 Hz, 1H), 2.72–2.64 (m, 1H), 2.60–2.54 (m, 1H), 2.21 (s, 3H), 2.19–2.12 (m, 1H), 1.74–1.67 (m, 1H), 1.57–1.41 (m, 2H), 0.15 (s, 9H) ppm.

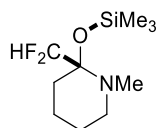
^{13}C NMR (125 MHz, C_6D_6): δ = 115.3 (dd, J = 249.4, 247.0 Hz), 92.6 (dd, J = 24.9, 23.4 Hz), 54.1, 33.6, 32.8, 21.0, 1.4 (3C) ppm.

^{19}F NMR (471 MHz, C_6D_6): δ = –126.2 (dd, J = 277.4, 56.6 Hz, 1F), –131.1 (dd, J = 277.4, 55.8 Hz, 1F) ppm.

IR (neat): ν = 2943, 2875, 1442, 1300, 1112, 1049, 655 cm^{-1} .

HRMS (EI): calculated for $\text{C}_9\text{H}_{19}\text{F}_2\text{NO}^{28}\text{Si}^+ = [\text{M}^+]$: m/z = 223.1198, found: m/z = 223.1217.

***N*-Methyl-(1-difluoromethyl-1-trimethylsilyloxy)-piperidine (**12ri**)**



12ri

Compound **12ri** was prepared and isolated according to *GP-XII* from $\text{HCF}_2\text{SiMe}_3$ (**1r**; 24.0 mg, 0.20 mmol, 1.0 equiv) and *N*-methyl-2-piperidone (**11i**; 22.6 mg, 2.0 mmol, 1.0 equiv) using KO^tBu (2.2 mg, 10 mol%) as the catalyst in THF for 18 h. To this mixture under an inert atmosphere was re-added the corresponding $\text{HCF}_2\text{SiMe}_3$ (**1r**; 2.4 mg, 0.02 mmol, 0.1 equiv), and stirred at at 25 °C for another 18 h to ensure full conversion of lactam **1i**. The solvent and the excess amount of **1r** were removed *in vacuo* before adding hexane (500 μL). The potassium salt was filtered off and the hexane was evaporated *in vacuo* to yield the pure compound.

Yellow liquid.

Yield: 42.7 mg (90%).

¹H NMR (500 MHz, C_6D_6): δ = 5.41 (dd, J = 55.9, 55.9 Hz, 1H), 2.59–2.47 (m, 1H), 2.36–2.25 (m, 1H), 2.09 (s, 3H), 1.86–1.80 (m, 2H), 1.55–1.25 (m, 4H), 0.17 (s, 9H) ppm.

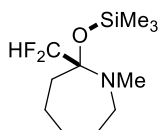
¹³C NMR (125 MHz, C_6D_6): δ = 115.0 (dd, J = 252.2, 245.0 Hz), 88.0 (dd, J = 23.8, 21.5 Hz), 50.4, 37.0, 29.1, 25.2, 19.0, 1.4 (3C) ppm.

¹⁹F NMR (471 MHz, C_6D_6): δ = –127.5 (dd, J = 279.0, 55.9 Hz, 1F), –133.6 (dd, J = 279.0, 55.9 Hz, 1F) ppm.

IR (neat): ν = 2939, 2866, 1448, 1352, 1330, 1117, 1056, 650 cm^{-1} .

HRMS (EI): calculated for $\text{C}_{10}\text{H}_{21}\text{F}_2\text{NO}^{28}\text{Si}^+ = [\text{M}^+]$: m/z = 237.1355, found: m/z = 237.1301.

***N*-Methyl-(1-difluoromethyl-1-trimethylsilyloxy)-azepane (**12rj**)**



12rj

Compound **12rj** was prepared and isolated according to *GP-XII* from $\text{HCF}_2\text{SiMe}_3$ (**1r**; 24.0 mg, 0.20 mmol, 1.0 equiv) and *N*-methyl caprolactam (**11j**; 25.4 mg, 0.20 mmol, 1.0 equiv) using KO^tBu (2.2 mg, 10 mol%) as the catalyst in THF for 20 h. **12rj** was not isolated due to the unremovable amide **11j**, however the product formation was confirmed by ¹H NMR, ¹⁹F NMR, and HRMS analyses.

70% NMR yield.

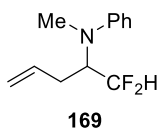
¹H NMR (500 MHz, CDCl_3): δ = 5.65 (dd, J = 56.3, 56.3 Hz, 1H), 2.93–2.90 (m, 1H), 2.71–2.64 (m, 1H), 2.44 (s, 3H), 2.15–2.07 (m, 1H), 1.82–1.76 (m, 3H), 1.61–1.46 (m, 4H), 0.12 (s, 9H) ppm.

¹⁹F NMR (471 MHz, C_6D_6): δ = –126.9 (dd, J = 272.6, 56.3 Hz, 1F), –132.0 (dd, J = 272.6, 56.6 Hz, 1F) ppm.

HRMS (EI): calculated for $\text{C}_{11}\text{H}_{23}\text{F}_2\text{NO}^{28}\text{Si}^+ = [\text{M}^+]$: m/z = 251.1512, found: m/z = 251.1504.

One-Pot Sequence Difluoromethylation/Allylation

N-Methyl-*N*-phenyl-*N*-(1,1-difluoropent-4-en-2-yl)-amine (**169**)



Compound **169** was prepared according to general procedure *GP-XIII* using $\text{HCF}_2\text{SiMe}_3$ (**1r**; 12.0 mg, 0.10 mmol, 1.0 equiv), methyl phenyl formamide (**11f**; 40.5 mg, 0.30 mmol, 3.0 equiv) using KO^tBu (1.1 mg, 0.01 mmol, 10 mol%) as the catalyst in THF at 25 °C for 18 h. The subsequent allylation was carried out according to a literature procedure:^[202] InOTf (2.6 mg, 0.01 mmol, 10 mol%) and allyl boronic acid pinacol ester (**1m**; 16.8 mg, 0.10 mmol, 1.0 equiv) were added to the reaction mixture, which was stirred at 25 °C for 18 h. The solvent was removed *in vacuo*, and **169** was purified by PTLC on silica gel (EtOAc/PE = 1:9; *eluted once*).

Colorless liquid.

Yield: 14.7 mg (70%).

¹H NMR (500 MHz, CDCl_3): δ = 7.26–7.22 (m, 2H), 6.83 (dd, J = 8.8, 1.0 Hz, 2H), 6.81–6.75 (m, 1H), 5.86 (ddd, J = 56.3, 55.4, 3.0 Hz, 1H), 5.75 (ddt, J = 17.1, 10.2, 6.4 Hz, 1H), 5.17 (dd, J = 17.1, 1.6 Hz, 1H), 5.07 (dd, J = 10.2, 1.6 Hz, 1H), 4.13 (ddtd, J = 18.1, 11.1, 5.2, 3.0 Hz, 1H), 3.13 (s, 3H), 2.66–2.52 (m, 2H) ppm.

¹³C NMR (125 MHz, CDCl_3): δ = 150.2, 133.7, 129.2 (2C), 117.8, 117.7, 116.3 (dd, J = 250.3, 250.3 Hz), 113.4 (2C), 60.2 (dd, J = 22.5, 21.6 Hz), 31.9, 29.7 ppm.

¹⁹F NMR (471 MHz, CDCl_3): δ = –120.4 (ddd, J = 283.8, 55.4, 11.1 Hz, 1F), –127.1 (ddd, J = 283.8, 56.3, 18.1 Hz, 1F) ppm.

IR (neat): ν = 2922, 2852, 2833, 2360, 1598, 1504, 1458, 1259, 1022, 798, 692 cm^{-1} .

HRMS (EI): calculated for $\text{C}_{12}\text{H}_{15}\text{F}_2\text{N}^+$ = $[\text{M}^+]$: m/z = 211.1167, found: m/z = 211.1166.

References

- [1] IUPAC *Compendium of Chemical Terminology*, **2012**.
- [2] Kondrashev, D. O.; Kleimenov, A. V.; Gulyaeva, L. A.; Khavkin, V. A.; Krasil'nikova, L. A.; Grudanova, A. I.; Khrapov, D. V.; Panov, A. V. *Catal. Ind.* **2017**, *9*, 128.
- [3] Mierczynski, P.; Ciesielski, R.; Kedziora, A.; Maniukiewicz, W.; Maniecki, T. P. *Catal. Ind.* **2017**, *9*, 99.
- [4] Anastas, P. T. *Chem. Rev.* **2007**, *107*, 2167.
- [5] Brahmachari, G. *RSC Adv.* **2016**, *6*, 64676.
- [6] Pérez, M.; Fañanás-Mastral, M.; Bos, P. H.; Rudolph, A.; Harutyunyan, S. R.; Feringa, B. L. *Nat. Chem.* **2011**, *3*, 377.
- [7] Brown, J. M.; Cooley, N. A. *Chem. Rev.* **1988**, *88*, 1031.
- [8] Giannerini, M.; Fañanás-Mastral, M.; Feringa, B. L. *J. Am. Chem. Soc.* **2012**, *134*, 4108.
- [9] Wang, P.-S.; Lin, H.-C.; Zhai, Y.-J.; Han, Z.-Y.; Gong, L.-Z. *Angew. Chem. Int. Ed.* **2014**, *53*, 12218.
- [10] Miyaura, N.; Suzuki, A. *Chem. Rev.* **1995**, *95*, 2457.
- [11] Penafiel, J.; Maron, L.; Harder, S. *Angew. Chem. Int. Ed.* **2015**, *54*, 201.
- [12] Cherney, A. H.; Kadunce, N. T.; Reisman, S. E. *Chem. Rev.* **2015**, *115*, 9587.
- [13] Pauling, L. *J. Am. Chem. Soc.* **1932**, *54*, 3570.
- [14] Tamaru, Y. in *Handbook of Organopalladium Chemistry for Organic Synthesis*, John Wiley & Sons, Inc., **2003**.
- [15] Ferreira, R. *Trans. Faraday Soc.* **1963**, *59*, 1064.
- [16] Mahrwald, R. *Drug Discov. Today Technol.* **2013**, *10*, e29.
- [17] Scheffler, U.; Mahrwald, R. *Chem. – Eur. J.* **2013**, *19*, 14346.
- [18] Shilov, A. E.; Shul'pin, G. B. *Chem. Rev.* **1997**, *97*, 2879.
- [19] Stuart, D. R.; Fagnou, K. *Science* **2007**, *316*, 1172.
- [20] Labinger, J. A.; Bercaw, J. E. *Nature* **2002**, *417*, 507.
- [21] Chen, M. S.; White, M. C. *J. Am. Chem. Soc.* **2004**, *126*, 1346.
- [22] Reed, S. A.; White, M. C. *J. Am. Chem. Soc.* **2008**, *130*, 3316.
- [23] Reed, S. A.; Mazzotti, A. R.; White, M. C. *J. Am. Chem. Soc.* **2009**, *131*, 11701.
- [24] Lin, S.; Song, C.-X.; Cai, G.-X.; Wang, W.-H.; Shi, Z.-J. *J. Am. Chem. Soc.* **2008**, *130*, 12901.
- [25] Young, A. J.; White, M. C. *J. Am. Chem. Soc.* **2008**, *130*, 14090.
- [26] Trost, B. M.; Thaisrivongs, D. A.; Donckele, E. J. *Angew. Chem. Int. Ed.* **2013**, *52*, 1523.
- [27] Stang, E. M.; White, M. C. *J. Am. Chem. Soc.* **2011**, *133*, 14892.
- [28] Andrus, M. B.; Zhou, Z. *J. Am. Chem. Soc.* **2002**, *124*, 8806.
- [29] Huang, X.-F.; Salman, M.; Huang, Z.-Z. *Chem. – Eur. J.* **2014**, *20*, 6618.
- [30] Sekine, M.; Iliès, L.; Nakamura, E. *Org. Lett.* **2013**, *15*, 714.
- [31] Marshall, J. A. *Chem. Rev.* **2000**, *100*, 3163.
- [32] Masuyama, Y.; Kinugawa, N.; Kurusu, Y. *J. Org. Chem.* **1987**, *52*, 3702.
- [33] Araki, S.; Kamei, T.; Hirashita, T.; Yamamura, H.; Kawai, M. *Org. Lett.* **2000**, *2*, 847.
- [34] Nakamura, H.; Iwama, H.; Yamamoto, Y. *J. Am. Chem. Soc.* **1996**, *118*, 6641.
- [35] Wallner, O. A.; Szabó, K. J. *J. Org. Chem.* **2003**, *68*, 2934.
- [36] Nakamura, H.; Nakamura, K.; Yamamoto, Y. *J. Am. Chem. Soc.* **1998**, *120*, 4242.
- [37] Fernandes, R. A.; Stimac, A.; Yamamoto, Y. *J. Am. Chem. Soc.* **2003**, *125*, 14133.
- [38] Solin, N.; Kjellgren, J.; Szabó, K. J. *Angew. Chem. Int. Ed.* **2003**, *42*, 3656.
- [39] Solin, N.; Szabó, K. J. *Organometallics* **2001**, *20*, 5464.
- [40] Szabó, K. J. *Chem. – Eur. J.* **2004**, *10*, 5268.
- [41] Solin, N.; Kjellgren, J.; Szabó, K. J. *J. Am. Chem. Soc.* **2004**, *126*, 7026.
- [42] Barczak, N. T.; Grote, R. E.; Jarvo, E. R. *Organometallics* **2007**, *26*, 4863.
- [43] Fernandes, R. A.; Yamamoto, Y. *J. Org. Chem.* **2004**, *69*, 735.
- [44] Kiyohara, H.; Nakamura, Y.; Matsubara, R.; Kobayashi, S. *Angew. Chem. Int. Ed.* **2006**, *45*, 1615.
- [45] Naodovic, M.; Wadamoto, M.; Yamamoto, H. *Eur. J. Org. Chem.* **2009**, *2009*, 5129.
- [46] Shaghafi, M. B.; Kohn, B. L.; Jarvo, E. R. *Org. Lett.* **2008**, *10*, 4743.
- [47] Waetzig, J. D.; Swift, E. C.; Jarvo, E. R. *Tetrahedron* **2009**, *65*, 3197.
- [48] Vieira, E. M.; Snapper, M. L.; Hoveyda, A. H. *J. Am. Chem. Soc.* **2011**, *133*, 3332.
- [49] Duong, H. A.; Huleatt, P. B.; Tan, Q.-W.; Shuying, E. L. *Org. Lett.* **2013**, *15*, 4034.
- [50] Wada, R.; Shibuguchi, T.; Makino, S.; Oisaki, K.; Kanai, M.; Shibasaki, M. *J. Am. Chem. Soc.* **2006**, *128*, 7687.
- [51] Luo, Y.; Hepburn, H. B.; Chotsaeng, N.; Lam, H. W. *Angew. Chem. Int. Ed.* **2012**, *51*, 8309.
- [52] Kobayashi, S.; Mori, Y.; Fossey, J. S.; Salter, M. M. *Chem. Rev.* **2011**, *111*, 2626.
- [53] Luo, Y.; Carnell, A. J.; Lam, H. W. *Angew. Chem. Int. Ed.* **2012**, *51*, 6762.
- [54] Bao, W.; Kossen, H.; Schneider, U. *J. Am. Chem. Soc.* **2017**, *139*, 4362.

- [55] Wei, X.-F.; Xie, X.-W.; Shimizu, Y.; Kanai, M. *J. Am. Chem. Soc.* **2017**, *139*, 4647.
- [56] Michigami, K.; Mita, T.; Sato, Y. *J. Am. Chem. Soc.* **2017**, *139*, 6094.
- [57] Yamamoto, Y.; Asao, N. *Chem. Rev.* **1993**, *93*, 2207.
- [58] Schlosser, M.; Stähle, M. *Angew. Chem. Int. Ed.* **1980**, *19*, 487.
- [59] Mauzé, B. *J. Organomet. Chem.* **1980**, *202*, 233.
- [60] Baldwin, J. E. *J. Chem. Soc., Chem. Commun.* **1976**, 734.
- [61] Seyferth, D.; Simon, R. M.; Sepelak, D. J.; Klein, H. A. *J. Am. Chem. Soc.* **1983**, *105*, 4634.
- [62] Hua, D. H.; Miao, S. W.; Chen, J. S.; Iguchi, S. *J. Org. Chem.* **1991**, *56*, 4.
- [63] Kleinman, E. F.; Volkmann, R. A. in *Comprehensive Organic Synthesis* (Ed.: I. Fleming), Pergamon, Oxford, **1991**.
- [64] Bloch, R. *Chem. Rev.* **1998**, *98*, 1407.
- [65] Lu, W.; Chan, T. H. *J. Org. Chem.* **2000**, *65*, 8589.
- [66] Jiang, S.; Agoston, G. E.; Chen, T.; Cabal, M.-P.; Turos, E. *Organometallics* **1995**, *14*, 4697.
- [67] Ipaktschi, J.; Halimehjani, A. Z.; Saidi, M. R. *Organometallics* **2007**, *26*, 201.
- [68] Borzilleri, R. M.; Weinreb, S. M. *Synthesis* **1995**, 1995, 347.
- [69] Drury, W. J., III; Ferraris, D.; Cox, C.; Young, B.; Lectka, T. *J. Am. Chem. Soc.* **1998**, *120*, 11006.
- [70] Haféz, A. M.; Taggi, A. E.; Dudding, T.; Lectka, T. *J. Am. Chem. Soc.* **2001**, *123*, 10853.
- [71] Ferraris, D.; Young, B.; Cox, C.; Drury, W. J., III; Ryzhkov, L.; Taggi, A. E.; Lectka, T. *J. Am. Chem. Soc.* **2002**, *124*, 67.
- [72] Hosomi, A.; Sakurai, H. *Tetrahedron Lett.* **1976**, *17*, 1295.
- [73] Huber, J. D.; Leighton, J. L. *J. Am. Chem. Soc.* **2007**, *129*, 14552.
- [74] Yasuda, M.; Sugawa, Y.; Yamamoto, A.; Shibata, I.; Baba, A. *Tetrahedron Lett.* **1996**, *37*, 5951.
- [75] Diner, C.; Szabó, K. J. *J. Am. Chem. Soc.* **2017**, *139*, 2.
- [76] Rauniyar, V.; Hall, D. G. *Angew. Chem. Int. Ed.* **2006**, *45*, 2426.
- [77] Jain, P.; Antilla, J. C. *J. Am. Chem. Soc.* **2010**, *132*, 11884.
- [78] Lou, S.; Moquist, P. N.; Schaus, S. E. *J. Am. Chem. Soc.* **2007**, *129*, 15398.
- [79] Fujita, M.; Nagano, T.; Schneider, U.; Hamada, T.; Ogawa, C.; Kobayashi, S. *J. Am. Chem. Soc.* **2008**, *130*, 2914.
- [80] Chakrabarti, A.; Konishi, H.; Yamaguchi, M.; Schneider, U.; Kobayashi, S. *Angew. Chem. Int. Ed.* **2010**, *49*, 1838.
- [81] Silverio, D. L.; Torker, S.; Pilyugina, T.; Vieira, E. M.; Snapper, M. L.; Haeffner, F.; Hoveyda, A. H. *Nature* **2013**, *494*, 216.
- [82] van der Mei, F. W.; Miyamoto, H.; Silverio, D. L.; Hoveyda, A. H. *Angew. Chem. Int. Ed.* **2016**, *55*, 4701.
- [83] Takahashi, M.; McLaughlin, M.; Micalizio, G. C. *Angew. Chem. Int. Ed.* **2009**, *48*, 3648.
- [84] Liu, J.; Cao, C.-G.; Sun, H.-B.; Zhang, X.; Niu, D. *J. Am. Chem. Soc.* **2016**, *138*, 13103.
- [85] Yus, M.; González-Gómez, J. C.; Foubelo, F. *Chem. Rev.* **2011**, *111*, 7774.
- [86] Müller, T. E.; Hultsch, K. C.; Yus, M.; Foubelo, F.; Tada, M. *Chem. Rev.* **2008**, *108*, 3795.
- [87] Patel, M.; Saunthwal, R. K.; Verma, A. K. *Acc. Chem. Res.* **2017**, *50*, 240.
- [88] Ogata, T.; Ujihara, A.; Tsuchida, S.; Shimizu, T.; Kaneshige, A.; Tomioka, K. *Tetrahedron Lett.* **2007**, *48*, 6648.
- [89] Horrillo-Martínez, P.; Hultsch, K. C.; Gil, A.; Branchadell, V. *Eur. J. Org. Chem.* **2007**, 2007, 3311.
- [90] Alonso-Moreno, C.; Carrillo-Hermosilla, F.; Romero-Fernández, J.; Rodríguez, A. M.; Otero, A.; Antiñolo, A. *Adv. Synth. Catal.* **2009**, *351*, 881.
- [91] Couce-Rios, A.; Lledós, A.; Ujaque, G. *Chem. – Eur. J.* **2016**, *22*, 9311.
- [92] Ensign, S. C.; Vanable, E. P.; Kortman, G. D.; Weir, L. J.; Hull, K. L. *J. Am. Chem. Soc.* **2015**, *137*, 13748.
- [93] Huang, L.; Arndt, M.; Gooßen, K.; Heydt, H.; Gooßen, L. J. *Chem. Rev.* **2015**, *115*, 2596.
- [94] Kourra, C.; Klotter, F.; Sladojevich, F.; Dixon, D. J. *Org. Lett.* **2012**, *14*, 1016.
- [95] Olmstead, W. N.; Bordwell, F. G. *J. Org. Chem.* **1980**, *45*, 3299.
- [96] Bordwell, F. G.; Fried, H. E. *J. Org. Chem.* **1991**, *56*, 4218.
- [97] Hartrampf, F. W. W.; Furukawa, T.; Trauner, D. *Angew. Chem. Int. Ed.* **2017**, *56*, 893.
- [98] Ong, T.-G.; O'Brien, J. S.; Korobkov, I.; Richeson, D. S. *Organometallics* **2006**, *25*, 4728.
- [99] Matthews, W. S.; Bares, J. E.; Bartmess, J. E.; Bordwell, F. G.; Cornforth, F. J.; Drucker, G. E.; Margolin, Z.; McCallum, R. J.; McCollum, G. J.; Vanier, N. R. *J. Am. Chem. Soc.* **1975**, *97*, 7006.
- [100] Rowley, C. N.; Ong, T.-G.; Priem, J.; Richeson, D. S.; Woo, T. K. *Inorg. Chem.* **2008**, *47*, 12024.
- [101] Hill, N. J.; Findlater, M.; Cowley, A. H. *Dalton Trans.* **2005**, 3229.
- [102] Harada, T.; Muramatsu, K.; Fujiwara, T.; Kataoka, H.; Oku, A. *Org. Lett.* **2005**, *7*, 779.
- [103] Harada, T.; Fujiwara, T.; Iwazaki, K.; Oku, A. *Org. Lett.* **2000**, *2*, 1855.
- [104] Takeda, T.; Terada, M. *J. Am. Chem. Soc.* **2013**, *135*, 15306.

- [105] Takeda, T.; Kondoh, A.; Terada, M. *Angew. Chem. Int. Ed.* **2016**, *55*, 4734.
- [106] Nitabaru, T.; Nojiri, A.; Kobayashi, M.; Kumagai, N.; Shibasaki, M. *J. Am. Chem. Soc.* **2009**, *131*, 13860.
- [107] Hashimoto, K.; Kumagai, N.; Shibasaki, M. *Org. Lett.* **2014**, *16*, 3496.
- [108] Yamashita, Y.; Guo, X.-X.; Takashita, R.; Kobayashi, S. *J. Am. Chem. Soc.* **2010**, *132*, 3262.
- [109] Naodovic, M.; Yamamoto, H. *Chem. Rev.* **2008**, *108*, 3132.
- [110] Bordwell, F. G. *Acc. Chem. Res.* **1988**, *21*, 456.
- [111] Yazaki, R.; Kumagai, N.; Shibasaki, M. *Chem. – Asian J.* **2011**, *6*, 1778.
- [112] Suzuki, H.; Sato, I.; Yamashita, Y.; Kobayashi, S. *J. Am. Chem. Soc.* **2015**, *137*, 4336.
- [113] Bordwell, F. G.; Fried, H. E. *J. Org. Chem.* **1981**, *46*, 4327.
- [114] Yamashita, Y.; Sato, I.; Suzuki, H.; Kobayashi, S. *Chem. – Asian J.* **2015**, *10*, 2143.
- [115] Suzuki, H.; Igarashi, R.; Yamashita, Y.; Kobayashi, S. *Angew. Chem. Int. Ed.* **2017**, *56*, 4520.
- [116] Lloyd-Jones, G. C.; Alder, R. W.; Owen-Smith, G. J. *J. Chem. – Eur. J.* **2006**, *12*, 5361.
- [117] Bordwell, F. G.; Algrim, D.; Vanier, N. R. *J. Org. Chem.* **1977**, *42*, 1817.
- [118] Guo, Z.; Wei, X.; Tong, H.; Chao, J.; Liu, D. *J. Organomet. Chem.* **2015**, *783*, 73.
- [119] Rajesh, K.; Berke, H. *Adv. Synth. Catal.* **2013**, *355*, 901.
- [120] Tabassum, S.; Sereda, O.; Reddy, P. V. G.; Wilhelm, R. *Org. Biomol. Chem.* **2009**, *7*, 4009.
- [121] Itoh, M.; Inoue, K.; Ishikawa, J.-i.; Iwata, K. *J. Organomet. Chem.* **2001**, *629*, 1.
- [122] Gillis, E. P.; Eastman, K. J.; Hill, M. D.; Donnelly, D. J.; Meanwell, N. A. *J. Med. Chem.* **2015**, *58*, 8315.
- [123] Bowden, K.; Cook, R. S. *J. Chem. Soc., Perkin Trans. 2.* **1972**, 1407.
- [124] Corbelin, S.; Kopf, J.; Lorenzen, N. P.; Weiss, E. *Angew. Chem. Int. Ed.* **1991**, *30*, 825.
- [125] Braun, M.-G.; Doyle, A. G. *J. Am. Chem. Soc.* **2013**, *135*, 12990.
- [126] Gauthier, D.; Lindhardt, A. T.; Olsen, E. P. K.; Overgaard, J.; Skrydstrup, T. *J. Am. Chem. Soc.* **2010**, *132*, 7998.
- [127] Abdur-Rashid, K.; Fong, T. P.; Greaves, B.; Gusev, D. G.; Hinman, J. G.; Landau, S. E.; Lough, A. J.; Morris, R. H. *J. Am. Chem. Soc.* **2000**, *122*, 9155.
- [128] Brunner, E. *J. Chem. Eng. Data.* **1985**, *30*, 269.
- [129] Fraser, R. R.; Mansour, T. S.; Savard, S. *J. Org. Chem.* **1985**, *50*, 3232.
- [130] Westerhausen, M. *Inorg. Chem.* **1991**, *30*, 96.
- [131] Hussain, N.; Frensch, G.; Zhang, J.; Walsh, P. J. *Angew. Chem. Int. Ed.* **2014**, *53*, 3693.
- [132] Crimmin, M. R.; Casely, I. J.; Hill, M. S. *J. Am. Chem. Soc.* **2005**, *127*, 2042.
- [133] Shu, K.; Miyuki, Y.; Magno, A.; Uwe, S. *Chem. Lett.* **2009**, *38*, 296.
- [134] Imaizumi, T.; Yamashita, Y.; Kobayashi, S. *J. Am. Chem. Soc.* **2012**, *134*, 20049.
- [135] Nagae, H.; Shibata, Y.; Tsurugi, H.; Mashima, K. *J. Am. Chem. Soc.* **2015**, *137*, 640.
- [136] Clayden, J.; Greeves, N.; Warren, S.; Wothers, P. *Organic Chemistry (1st ed.)*, Oxford University Press, Oxford, **2001**.
- [137] Mulvey, R. E.; Robertson, S. D. *Angew. Chem. Int. Ed.* **2013**, *52*, 11470.
- [138] Yu, Z.; Yan, S.; Zhang, G.; He, W.; Wang, L.; Li, Y.; Zeng, F. *Adv. Synth. Catal.* **2006**, *348*, 111.
- [139] Gordillo, A.; Ortuño, M. A.; López-Mardomingo, C.; Lledós, A.; Ujaque, G.; de Jesús, E. *J. Am. Chem. Soc.* **2013**, *135*, 13749.
- [140] Bordwell, F. G.; Algrim, D. J. *J. Am. Chem. Soc.* **1988**, *110*, 2964.
- [141] Streitwieser, A.; Vorpagel, E. A.; Chen, C. C. *J. Am. Chem. Soc.* **1985**, *107*, 6970.
- [142] Stasch, A. *Chem. Commun.* **2015**, *51*, 5056.
- [143] Pearson, R. G. *J. Am. Chem. Soc.* **1963**, *85*, 3533.
- [144] Sandel, V. R.; McKinley, S. V.; Freedman, H. H. *J. Am. Chem. Soc.* **1968**, *90*, 495.
- [145] Hancock, R. D. *J. Chem. Educ.* **1992**, *69*, 615.
- [146] Rasappan, R.; Laventine, D.; Reiser, O. *Coord. Chem. Rev.* **2008**, *252*, 702.
- [147] Hoppe, D.; Hense, T. *Angew. Chem. Int. Ed.* **1997**, *36*, 2282.
- [148] Peterson, D. J. *J. Organomet. Chem.* **1967**, *9*, 373.
- [149] Eabonr, C.; Eidenschink, R.; Jackson, P. M.; Walton, D. R. M. *J. Organomet. Chem.* **1975**, *101*, C40.
- [150] Solomon, S. A.; Layfield, R. A. *Dalton Trans.* **2010**, *39*, 2469.
- [151] McMillen, C. H.; Gren, C. K.; Hanusa, T. P.; Rheingold, A. L. *Inorg. Chim. Acta.* **2010**, *364*, 61.
- [152] Yamanaka, M.; Nishida, A.; Nakagawa, M. *Org. Lett.* **2000**, *2*, 159.
- [153] Hong, K.; Liu, X.; Morken, J. P. *J. Am. Chem. Soc.* **2014**, *136*, 10581.
- [154] Bernasconi, C. F.; Kittredge, K. W. *J. Org. Chem.* **1998**, *63*, 1944.
- [155] Block, E.; Thiruvazhi, M.; Toscano, P. J.; Bayer, T.; Grisoni, S.; Zhao, S.-H. *J. Am. Chem. Soc.* **1996**, *118*, 2790.
- [156] Erickson, J. A.; McLoughlin, J. I. *J. Org. Chem.* **1995**, *60*, 1626.
- [157] Schwesinger, R.; Schlemper, H.; Hasenfratz, C.; Willaredt, J.; Dambacher, T.; Breuer, T.; Ottaway, C.; Flutschinger, M.; Boele, J.; Fritz, H.; Putzas, D.; Rotter, H. W.; Bordwell, F. G.; Satish, A. V.; Ji, G.-Z.; Peters, E.-M.; Peters, K.; von Schnering, H. G.; Walz, L. *Liebigs Ann.* **1996**, *1996*, 1055.

- [158] Kisanga, P. B.; Verkade, J. G.; Schwesinger, R. *J. Org. Chem.* **2000**, *65*, 5431.
- [159] Kim, H. W.; Rossi, P.; Shoemaker, R. K.; DiMagno, S. G. *J. Am. Chem. Soc.* **1998**, *120*, 9082.
- [160] Meanwell, N. A. *J. Med. Chem.* **2011**, *54*, 2529.
- [161] Zafrani, Y.; Yeffet, D.; Sod-Moriah, G.; Berliner, A.; Amir, D.; Marciano, D.; Gershonov, E.; Saphier, S. *J. Med. Chem.* **2017**, *60*, 797.
- [162] Du, G.-F.; Wang, Y.; Gu, C.-Z.; Dai, B.; He, L. *RSC Adv.* **2015**, *5*, 35421.
- [163] Zhao, Y.; Huang, W.; Zheng, J.; Hu, J. *Org. Lett.* **2011**, *13*, 5342.
- [164] Chen, D.; Ni, C.; Zhao, Y.; Cai, X.; Li, X.; Xiao, P.; Hu, J. *Angew. Chem. Int. Ed.* **2016**, *55*, 12632.
- [165] Obijalska, E.; Utecht, G.; Kowalski, M. K.; Mlostoń, G.; Rachwalski, M. *Tetrahedron Lett.* **2015**, *56*, 4701.
- [166] Aikawa, K.; Yoshida, S.; Kondo, D.; Asai, Y.; Mikami, K. *Org. Lett.* **2015**, *17*, 5108.
- [167] Volodin, A. D.; Zemtsov, A. A.; Levin, V. V.; Struchkova, M. I.; Dilman, A. D. *J. Fluor. Chem.* **2015**, *176*, 57.
- [168] Bayarmagnai, B.; Matheis, C.; Jouvin, K.; Goossen, L. J. *Angew. Chem. Int. Ed.* **2015**, *54*, 5753.
- [169] Brahms, D. L. S.; Dailey, W. P. *Chem. Rev.* **1996**, *96*, 1585.
- [170] Zafrani, Y.; Sod-Moriah, G.; Segall, Y. *Tetrahedron* **2009**, *65*, 5278.
- [171] Wang, F.; Luo, T.; Hu, J.; Wang, Y.; Krishnan, H. S.; Jog, P. V.; Ganesh, S. K.; Prakash, G. K. S.; Olah, G. A. *Angew. Chem. Int. Ed.* **2011**, *50*, 7153.
- [172] Honda, K.; Harris, T. V.; Hatanaka, M.; Morokuma, K.; Mikami, K. *Chem. – Eur. J.* **2016**, *22*, 8796.
- [173] Prakash, G. K. S.; Wang, F.; Zhang, Z.; Haiges, R.; Rahm, M.; Christe, K. O.; Mathew, T.; Olah, G. A. *Angew. Chem. Int. Ed.* **2014**, *53*, 11575.
- [174] Schwesinger, R.; Schlemper, H.; Hasenfratz, C.; Willaredt, J.; Dambacher, T.; Breuer, T.; Ottaway, C.; Fletschinger, M.; Boele, J.; Fritz, H.; Putzas, D.; Rotter, H. W.; Bordwell, F. G.; Satish, A. V.; Ji, G.-Z.; Peters, E.-M.; Peters, K.; von Schnering, H. G.; Walz, L. *Liebigs Ann.* **1996**, *1996*, 1055.
- [175] Agami, C.; Comesse, S.; Kadouri-Puchot, C. *J. Org. Chem.* **2002**, *67*, 1496.
- [176] Bryantsev, V. S. *Chem. Phys. Lett.* **2013**, *558*, 42.
- [177] Kost, D.; Kalikhman, I. in *The Chemistry of Organic Silicon Compounds*, John Wiley & Sons, Ltd, **2003**, pp. 1339.
- [178] Rendler, S.; Oestreich, M. *Synthesis* **2005**, *2005*, 1727.
- [179] Denmark, S. E.; Beutner, G. L. *Angew. Chem. Int. Ed.* **2008**, *47*, 1560.
- [180] Lelais, G.; MacMillan, D. W. C. in *New Frontiers in Asymmetric Catalysis*, John Wiley & Sons, Inc., **2006**.
- [181] Gawronski, J.; Wascinska, N.; Gajewy, J. *Chem. Rev.* **2008**, *108*, 5227.
- [182] Couzijn, E. P. A.; Slootweg, J. C.; Ehlers, A. W.; Lammertsma, K. Z. *Anorg. Allg. Chem.* **2009**, *635*, 1273.
- [183] Hiyama, T. in *Organometallics in Synthesis*, John Wiley & Sons, Inc., **2013**.
- [184] Holmes, R. R. *Chem. Rev.* **1996**, *96*, 927.
- [185] Pauling, L. *The Nature of the Chemical Bond*; 3rd ed., Cornell University Press: Ithaca, New York **1960**.
- [186] Magnusson, E. *J. Am. Chem. Soc.* **1990**, *112*, 7940.
- [187] Bent, H. A. *Chem. Rev.* **1961**, *61*, 275.
- [188] Staemmler, V. *Angew. Chem.* **1979**, *91*, 595.
- [189] Jensen, W. B. *The Lewis Acid-Base Concepts*; Wiley-Interscience: New York, **1980**.
- [190] Kobayashi, S.; Nishio, K. *Tetrahedron Lett.* **1993**, *34*, 3453.
- [191] Nakajima, M.; Saito, M.; Shiro, M.; Hashimoto, S.-i. *J. Am. Chem. Soc.* **1998**, *120*, 6419.
- [192] Denmark, S. E.; Wynn, T. *J. Am. Chem. Soc.* **2001**, *123*, 6199.
- [193] Denmark, S. E.; Wynn, T.; Beutner, G. L. *J. Am. Chem. Soc.* **2002**, *124*, 13405.
- [194] Denmark, S. E.; Heemstra, J. R. *Org. Lett.* **2003**, *5*, 2303.
- [195] Denmark, S. E.; Beutner, G. L.; Wynn, T.; Eastgate, M. D. *J. Am. Chem. Soc.* **2005**, *127*, 3774.
- [196] Denmark, S. E.; Coe, D. M.; Pratt, N. E.; Griedel, B. D. *J. Org. Chem.* **1994**, *59*, 6161.
- [197] Szarek, W. A.; Hay, G. W.; Doboszewski, B. *J. Chem. Soc., Chem. Commun.* **1985**, 663.
- [198] Kolomeitsev, A.; Movchun, V.; Rusanov, E.; Bissky, G.; Lork, E.; Roschenthaler, G.-V.; Kirsch, P. *Chem. Commun.* **1999**, 1017.
- [199] Prakash, G. K. S.; Krishnamurti, R.; Olah, G. A. *J. Am. Chem. Soc.* **1989**, *111*, 393.
- [200] Maggiorosa, N.; Tyrra, W.; Naumann, D.; Kirij, N. V.; Yagupolskii, Y. L. *Angew. Chem. Int. Ed.* **1999**, *38*, 2252.
- [201] Antonchick, A. P.; Gerding-Reimers, C.; Catarinella, M.; Schürmann, M.; Preut, H.; Ziegler, S.; Rauh, D.; Waldmann, H. *Nat. Chem.* **2010**, *2*, 735.
- [202] Schneider, U.; Dao, H. T.; Kobayashi, S. *Org. Lett.* **2010**, *12*, 2488.
- [203] Wang, D.-K.; Zhou, Y.-G.; Tang, Y.; Hou, X.-L.; Dai, L.-X. *J. Org. Chem.* **1999**, *64*, 4233.
- [204] Large, S.; Roques, N.; Langlois, B. R. *J. Org. Chem.* **2000**, *65*, 8848.

- [205] Yamashita, Y.; Imaizumi, T.; Guo, X.-X.; Kobayashi, S. *Chem. – Asian J.* **2011**, *6*, 2550.
- [206] Yamashita, Y.; Yoshimoto, S.; Masuda, K.; Kobayashi, S. *Asian J. Org. Chem.* **2012**, *1*, 327.
- [207] Mayer, M.; Czaplik, W. M.; Jacobi von Wangelin, A. *Adv. Synth. Catal.* **2010**, *352*, 2147.
- [208] Hong, X.; Wang, H.; Liu, B.; Xu, B. *Chem. Commun.* **2014**, *50*, 14129.
- [209] Pirovano, V.; Facoetti, D.; Dell'Acqua, M.; Della Fontana, E.; Abbiati, G.; Rossi, E. *Org. Lett.* **2013**, *15*, 3812.
- [210] Ahlbrecht, H.; Zimmermann, K.; Boche, G.; Decher, G. *J. Organomet. Chem.* **1984**, *262*, 1.
- [211] Mayer, M.; Czaplik, W. M.; von Wangelin, A. J. *Adv. Synth. Catal.* **2010**, *352*, 2147.
- [212] Too, P. C.; Chan, G. H.; Tnay, Y. L.; Hirao, H.; Chiba, S. *Angew. Chem. Int. Ed.* **2016**, *55*, 3719.
- [213] Yamada, K.-i.; Konishi, T.; Nakano, M.; Fujii, S.; Cadou, R.; Yamamoto, Y.; Tomioka, K. *J. Org. Chem.* **2012**, *77*, 1547.
- [214] Seayad, A. M.; Ramalingam, B.; Yoshinaga, K.; Nagata, T.; Chai, C. L. L. *Org. Lett.* **2010**, *12*, 264.
- [215] Grote, R. E.; Jarvo, E. R. *Org. Lett.* **2009**, *11*, 485.
- [216] Zhang, Y.-F.; Wu, B.; Shi, Z.-J. *Chem. – Eur. J.* **2016**, *22*, 17808.
- [217] Wang, L.; Cao, C.; Cao, C. J. *Phys. Org. Chem.* **2014**, *27*, 818.
- [218] Anderson, J. C.; Howell, G. P.; Lawrence, R. M.; Wilson, C. S. *J. Org. Chem.* **2005**, *70*, 5665.
- [219] Pagadala, R.; Meshram, J. S.; Chopde, H. N.; Jetti, V.; Udayini, V. *J. Heterocycl. Chem.* **2011**, *48*, 1067.
- [220] Denmark, S. E.; Nakajima, N.; Stiff, C. M.; Nicaise, O. J. C.; Kranz, M. *Adv. Synth. Catal.* **2008**, *350*, 1023.
- [221] Jarrahpour, A.; Ebrahimi, E. *Molecules* **2010**, *15*, 515.
- [222] Tomaszewski, M.; Warkentin, J.; Werstiuk, N. *Aust. J. Chem.* **1995**, *48*, 291.
- [223] Patel, M.; Chhasatia, M.; Bhatt, B. *Med. Chem. Res.* **2011**, *20*, 220.
- [224] Bengharez, Z.; El Bahri, Z.; Mesli, A. *Int. J. Chem. Kinet.* **2013**, *45*, 404.
- [225] Tobisu, M.; Yamaguchi, S.; Chatani, N. *Org. Lett.* **2007**, *9*, 3351.
- [226] Lee, P.-S.; Yoshikai, N. *Org. Lett.* **2015**, *17*, 22.
- [227] Simon, R. C.; Busto, E.; Schrittwieser, J. H.; Sattler, J. H.; Pietruszka, J.; Faber, K.; Kroutil, W. *Chem. Commun.* **2014**, *50*, 15669.
- [228] Enders, D.; Rembiak, A.; Stöckel, B. A. *Adv. Synth. Catal.* **2013**, *355*, 1937.
- [229] Wei, Y.; Deb, I.; Yoshikai, N. *J. Am. Chem. Soc.* **2012**, *134*, 9098.
- [230] Wu, J.; Yoshikai, N. *Angew. Chem. Int. Ed.* **2015**, *54*, 11107.
- [231] Lundgren, R. J.; Sappong-Kumankumah, A.; Stradiotto, M. *Chem. – Eur. J.* **2010**, *16*, 1983.
- [232] Henseler, A.; Kato, M.; Mori, K.; Akiyama, T. *Angew. Chem. Int. Ed.* **2011**, *50*, 8180.
- [233] Jiang, Q.; Wang, J.-Y.; Guo, C. J. *J. Org. Chem.* **2014**, *79*, 8768.
- [234] Wong, W.-Y.; Wong, W.-T. *J. Organomet. Chem.* **1999**, *584*, 48.
- [235] Hirashita, T.; Hayashi, Y.; Mitsui, K.; Araki, S. *J. Org. Chem.* **2003**, *68*, 1309.
- [236] Saha, S.; Roy, S. C. *J. Org. Chem.* **2011**, *76*, 7229.
- [237] Soderquist, J. A.; Lee, S.-J. H. *Tetrahedron* **1988**, *44*, 4033.
- [238] Seyferth, D.; G. Vaughan, L. *J. Organomet. Chem.* **1963**, *1*, 138.
- [239] Hopper, S. P.; Tremelling, M. J.; Goldman, E. W. *J. Organomet. Chem.* **1980**, *191*, 363.
- [240] Weber, F.; Schmidt, A.; Röse, P.; Fischer, M.; Burghaus, O.; Hilt, G. *Org. Lett.* **2015**, *17*, 2952.
- [241] Matteson, D. S.; Majumdar, D. *Organometallics* **1983**, *2*, 230.
- [242] Althaus, M.; Mahmood, A.; Suárez, J. R.; Thomas, S. P.; Aggarwal, V. K. *J. Am. Chem. Soc.* **2010**, *132*, 4025.